GRI-94/0456

GEOLOGIC CHARACTERIZATION AND COALBED METHANE OCCURRENCE: WILLIAMS FORK FORMATION, PICEANCE BASIN, NORTHWEST COLORADO

Annual Report

(December 1, 1993–November 30, 1994)

Prepared by

Roger Tyler, William R. Kaiser, Ronald G. McMurry, H. Seay Nance, Andrew R. Scott, and Naijiang Zhou

Bureau of Economic Geology
Noel Tyler, Director
The University of Texas at Austin
Austin, Texas 78713-8924

Carol M. Tremain

Colorado Geological Survey

for

Gas Research Institute
Contract No. 5091-214-2261
John Hansen, Technology Manager

March 1995

QAe7763

DISCLAIMER

LEGAL NOTICE This work was prepared by the Bureau of Economic Geology as an account of work sponsored by the Gas Research Institute (GRI). GRI, nor members of GRI, nor any person acting on behalf of either:

a. Makes any warranty or representation, expressed or implied, with respect to the accuracy, completeness, or usefulness of the information contained in this report, or that the use of any apparatus, method, or process disclosed in this report may not infringe privately owned rights; or

b. Assumes any liability with respect to the use of, or for damages resulting from the use of, any information, apparatus, method, or process disclosed in this report.

50272-101

REPORT DOCUMENTATION PAGE	1. REPORT NO. GRI-94/0456	2.	3. Recipient's Accession No.

4. Title and Subtitle

Geologic Characterization and Coalbed Methane Occurrence: Williams Fork Formation, Piceance Basin, Northwest Colorado

5. Report Date March 1995

6.

7. Author(s) Roger Tyler, W. R. Kaiser, R. G. McMurry, H. S. Nance, C. M. Tremain, A. R. Scott, and Naijiang Zhou

8. Performing Organization Rept. No.

9. Performing Organization Name and Address

Bureau of Economic Geology
The University of Texas at Austin
University Station, Box X
Austin, TX 78713-8924

10. Project/Task/Work Unit No.

11. Contract(C) or Grant(G) No.

(C) 5091-214-2261

(G)

12. Sponsoring Organization Name and Address

Gas Research Institute
8600 West Bryn Mawr Avenue
Chicago, IL 60631-3562

Technology Manager: John T. Hansen

13. Type of Report & Period Covered Annual Report 12/1/93–11/30/94

14.

15. Supplementary Notes

16. Abstract (Limit: 200 words)

The coal-bearing Upper Cretaceous Williams Fork Formation, 1,200 to 2,500 ft thick, is operationally defined on the basis of correlation with the Sand Wash Basin. Net coal thickness is typically 80 to 120 ft and is thickest in a north-south belt west of the Divide Creek Anticline. Depositional setting and thrust faults cause coals along the Grand Hogback and in the subsurface to be in modest to poor hydraulic communication. Thus, meteoric recharge and flow basinward is restricted. Face cleats of Late Cretaceous age strike east-northeast and west-northwest in the southern and northern parts of the basin, respectively, normal to the Hogback thrust front. Parallelism between face-cleat strike and present-day maximum horizontal stress direction may enhance coal permeability in the north. Lineament azimuths lie between 20 to 40° and 280 to 310°; they are not a reliable indicator of subsurface fracture attributes nor of gas production. In the Grand Valley/Rulison and White River/Pinyon Ridge areas, structure and sandstone development control gas production from Cameo coals and/or sandstones. The most productive wells are on structural terraces and anticlines or correspond to Cameo sandstone development, reflecting fracture-enhanced permeability. As predicted, from an evolving coalbed methane producibility model, extraordinary coal-gas production is precluded by the absence of dynamic ground-water flow. The best potential for coal-gas production may lie in conventional traps basinward of where outcrop and subsurface coals are in good hydraulic communication.

17. Document Analysis a. Descriptors

coal occurrence, coalbed methane, Colorado, depositional fabric, gas production, Grand Valley field, horizontal stress, lineaments, Mesaverde Group, natural fractures, Parachute field, Piceance Basin, Pinyon Ridge field, Rulison field, stratigraphy, structure, Upper Cretaceous, White River field, Williams Fork Formation

b. Identifiers/Open-Ended Terms

basin-scale producibility model, coal and sandstone mapping, coal occurrence, coal-gas production, fracture stratigraphy, methane from coal beds, regional and field-scale genetic stratigraphy, regional tectonics, stress rotation

c. COSATI Field/Group

18. Availability Statement	19. Security Class (This Report)	21. No. of Pages 218
	20. Security Class (This Page)	22. Price

(See ANSI–Z39.18) *See Instructions on Reverse*

OPTIONAL FORM 272 (4-77)
(Formerly NTIS–35)
Department of Commerce

RESEARCH SUMMARY

Title	Geologic Characterization and Coalbed Methane Occurrence: Williams Fork Formation, Piceance Basin, Northwest Colorado
Contractor	Bureau of Economic Geology, The University of Texas at Austin, GRI Contract No. 5091-214-2261
Principal Investigator	W. R. Kaiser
Report Period	December 1, 1993–November 30, 1994
Objectives	To further evaluate the interplay of geologic and hydrologic controls on coalbed methane production and to refine and validate our basin-scale coalbed methane producibility model (Kaiser and others, 1994).
Technical Perspective	No validated basin-scale model is currently available for evaluating coalbed methane potential in frontier basins or for finding "sweet spots" in basins with established production. Coalbed methane exploration typically proceeds without benefit of a unifying concept or strategy and is heavily dependent on drilling and mine records, with little understanding of geologic and hydrologic controls unique to coalbed methane producibility. Our conceptual model identifies critical controls and integrates them to show how they interact for commercial production. A synergistic interplay between these controls determines high productivity, as shown in earlier studies of the San Juan and Sand Wash Basins (GRI-91/0072 and GRI-92/0420). Our model evolved out of a comparison between those two basins and will be refined and validated in the Piceance Basin, the nation's third most productive coal-gas basin. Refinement and validation of the model in the Piceance Basin is critical because it is a low-permeability basin. At this time, the model is built on analysis of coal basins with highly dynamic ground-water flow systems. The critical research issue is whether or not dynamic flow is required for extraordinary coal-gas production.
Results	An operational Williams Fork Formation is defined on the basis of correlation with the Sand Wash Basin; it ranges in thickness from 2,500 ft (760 m) in the east to approximately 1,500 ft (~460 m) in the west. Overlying undifferentiated Upper Cretaceous strata, traditionally assigned to the Williams Fork, are assigned here to the Lance/Lewis Formation. Coals immediately above the Rollins Sandstone are the thickest and most laterally continuous. Some extend for up to 30 mi. Net coal thickness is typically 80 to 120 ft and is thickest in a north-south belt west of the Divide Creek Anticline. Lower Williams Fork coals in the subsurface reach outcrop along the Grand Hogback but are reduced in number and total thickness, whereas upper Williams Fork coals are abundant but thinner, discontinuous, and collectively less extensive basinward. Modest to poor hydraulic communication between coals at outcrop and in the subsurface limits meteoric recharge and flow basinward. Flow is further restricted by offset of coals along thrust faults. Face cleats of Late Cretaceous age strike east-northeast and west-northwest in the southern and northern parts of the basin, respectively, normal to the basin-fold axis and Hogback thrust front, and parallel to the ancient horizontal compressive stress directions. Face cleats strike obliquely to present-day maximum stress direction in the south and parallel to it in the north. Face-cleat and stress parallelism in the north may cause fracture-

enhanced permeability. Lineament azimuths are strongly bimodal and lie between 20 to 40° and 280 to 310°; lineaments are not a reliable indicator of subsurface fracture attributes or gas production.

In the Grand Valley/Rulison area, greater structural complexity in the Williams Fork reflects folds and faults above thrust detachment zones in the Mancos Shale. Structure and sandstone development are controls on gas production from Cameo coals and/or sandstones. The most productive wells are on structural terraces and anticlines or correspond to Cameo maximum sandstone trends. Higher production is attributed to fracture-enhanced permeability associated with tectonic flexure and/or differential compaction. In the White River/Pinyon Ridge area, fracture-enhanced permeability controls gas production on associated anticlines. Migrated and conventionally trapped coal gases account for approximately 65 to 80 percent of the production. In both areas, consistent with the producibility model, the absence of dynamic ground-water flow precludes extraordinary coal-gas production. Predictably, the parts of the basin with the best potential for coal-gas production should be those basinward of where outcrop and subsurface coals are in good hydraulic communication for consequent generation of secondary biogenic gas, advective gathering and transport of gas, and subsequent basinward resorption and conventional trapping, which promote fully gas-saturated coals and high productivity.

Technical Approach

This study was conducted using traditional subsurface geologic techniques and emphasized geologic aspects in its first year. Approximately 250 geophysical logs were used to evaluate Williams Fork genetic stratigraphy, coal occurrence, and structure. On the basis of correlation with the Sand Wash Basin, an operational Williams Fork Formation was defined by a maximum flooding surface at the base of the Rollins shale (Mancos Tongue) and a change in sandstone stacking pattern and associated high-conductivity interval at the top. Williams Fork genetic units 1, 2, and 3/4 of the Sand Wash Basin are easily recognized in the Piceance Basin. These units were defined by marine-shale marker beds and provided the foundation for subsurface correlation and mapping. They were carried westward to establish lithostratigraphic units in the fluvial dominated Williams Fork.

In the absence of density or sonic logs, coals were operationally identified by very high resistivity, low natural gamma-ray response, and shalelike SP response. Individual coals were correlated on the basis of their gamma-ray and density profiles, log signatures sensitive to fluctuations in the coal lithotypes. Coal packages, or groups of individual coals, are correlated regionally on stratigraphic position.

In field-scale studies, sandstone-dispersal patterns were delineated in maximum sandstone maps. Log response defines the maximum sandstone as the single thickest sandstone in the interval of interest without regard to correlatability. Experience has shown that maximum sandstone maps are similar in appearance to net sandstone maps in that both depict the depositional fabric, the former accentuating the framework elements of the depositional system.

Fracture attributes and structural elements were evaluated on the basis of published data and new data collected at 33 stations in Williams Fork coals. Outcrop work was supplemented with low-altitude aerial reconnaissance and photography, which provided information on the orientation and continuity of fractures between outcrops, spacing, changes in style along strike and upsection, and on the structure of the Grand Hogback. Concepts

of fracture stratigraphy were used to evaluate fractures and stresses through time. Face-cleat genesis and orientation were interpreted in terms of the Hogback thrust front and ancient horizontal compressive stresses. Lineaments were mapped on 1:250,000-scale Landsat Thematic Mapper and 1:100,000-scale Side-Looking Airborne Radar images and compared with those of published data. Lineament length and azimuth were statistically analyzed.

Coal occurrence, sandstone, and structure maps were compared with gas-productivity trends to identify possible geologic controls on production. To compare productivity between wells and to minimize the time variable inherent in cumulative production data, we examined maximum annual or monthly production, or that of the well's most productive year or month. Maximum production measures a well's highest capacity to produce gas.

Project Implications

This report describes the development of the third portion of a coalbed methane producibility model that GRI has researched over the last several years. Previous coalbed methane work in the San Juan and Sand Wash Basins has documented the interdependence of geologic and hydrologic variables on gas occurrence and production. The models developed in these studies will be further investigated and confirmed in this new regime, the Piceance Basin. Research results should aid producers in the evaluation of coalbed methane potential of the Piceance and other basins and help identify favorable well sites within regions containing significant coalbed methane resources.

John T. Hansen
GRI Technology Manager

CONTENTS

Research Summary vii

Tectonic Evolution and Stratigraphic Setting of the Piceance Basin, Colorado: A Review
Roger Tyler 1

Abstract 1

Geologic Overview 1

Tectonic Evolution and Stratigraphic Setting 6

Basin Margin and Intrabasin Uplifts 10

Stratigraphic and Depositional Settings of Coal-Bearing Formations 13

Iles Formation (Black Diamond Coal Zone) 22

Williams Fork Formation (Cameo-Wheeler-Fairfield, South Canyon, and Coal Ridge Coal Zones) 23

Rollins-Trout Creek Shale and Sandstone Member 26

Cameo-Wheeler-Fairfield Coal Zone (Bowie Shale Member) 27

South Canyon Coal Zone (Bowie Shale Member) 29

Coal Ridge Coal Zone (Paonia Shale Member) 29

"Undifferentiated" Upper Cretaceous Strata (Undifferentiated Mesaverde Formation); Upper Williams Fork Formation 30

Conclusions 31

Natural Fracture Attributes and Stress Patterns in the Piceance Basin, Colorado: Controls on Coal Permeability and Coalbed Methane Producibility
Carol M. Tremain and Roger Tyler 32

Abstract 32

Introduction 33

Natural Fracture Patterns and Cleat Attributes in the Piceance Basin 35

Cleat Strike Domains in Mesaverde Group and Wasatch Formation Coal Beds: A Review 35

Joint Strikes in the Wasatch Formation and Green River Formation Sandstones: A Review 40

Cleat Domains and Joint Strikes and Attributes of the Mesaverde Group and Wasatch and Green River Formations: A Comparison 40

Timing of Cleat and Sandstone Fracture Development: A Discussion 45

New Perspective 47
Cleat Spacing 54
Cleat Mineralization 54
Faults and Folds 57
Tectonic Stress History 58
Current Stress State 64
Conclusions 68
Future Work and Remaining Questions 70
Lineament Analysis of the Piceance Basin: Relationships Between Lineament Attributes and Coalbed Methane Production
Roger Tyler, Ronald G. McMurry, and Naijiang Zhou 73
Abstract 73
Introduction 73
Approach 74
Review of Previous Lineament Studies in the Piceance Basin 74
Brief Summary of Natural Fracture Studies and Stresses in the Piceance Basin 89
Stress Orientation 92
Lineament Data Sources and Procedures 94
Landsat Imagery 94
Lineament Mapping Procedures 94
Preliminary Results 95
Graphical Display of Results 96
Lineament Azimuth and Polar Graphs 96
Future Work 103
Length-Weighted Frequency of Lineament Azimuths 103
Graphical Display of Results 104
Selection of Polar Graphs 104
Statistical Significance of Lineament Azimuths 104

Definition and validity of peak values 105

Vector sums of greater-than-average peaks 105

Lineament Density 106

Production Data Versus Lineament Attributes 106

Conclusions 106

Preliminary Assessment of the Regional Genetic Stratigraphy and Coal Occurrence of the Upper Cretaceous Mesaverde Group, Williams Fork Formation, Piceance Basin, Colorado
Roger Tyler and Ronald G. McMurry 107

Abstract 107

Introduction 108

Operationally Defined Williams Fork Formation and Undifferentiated Upper Cretaceous Strata 109

Regional Correlation of the Williams Fork Genetic Depositional Sequences 112

Comparison with Traditional Stratigraphy 112

Regionally Correlatable Williams Fork Genetic Sequences 115

Genetic Unit 1 (Coal Package 1) 115

Genetic Unit 2 (Coal Package 2) 116

Genetic Unit 3 (Coal Package 3) 118

Coal Occurrence of the Williams Fork Formation 120

Coal Identification and Mapping 120

Net Coal Occurrence 122

Coal Seam Continuity 124

Depositional Systems 128

Geologic Controls on Coal Seam Occurrence 129

Conclusions 130

Geologic Characterization and Gas Production: Cameo Coal Group, Grand Valley/ Rulison Area, Garfield County, Colorado
H. Seay Nance and William R. Kaiser 133

Abstract 133

Introduction 134
Methods 134
Stratigraphy 136
Structure 139
Coal/Sandstone Relations 141
Coalbed Continuity and Configuration 141
Coal Distribution 144
Sandstone Continuity 145
Depositional Systems 146
Regional Setting 146
Fluvial Deposition and Sandstone Geometry 151
Sandstone and Coal Trends: Implications for Paleogeography 152
Cameo Production 154
Statistics 154
Controls on Production 156
Producibility Model 157
Future Work 158
Conclusions 158
Coalbed Methane Producibility in the Williams Fork Formation, White River and Pinyon Ridge Fields, Northern Piceance Basin
Andrew R. Scott 161
Abstract 161
Introduction 162
Methods 164
Structural Features 164
Coal Depositional Patterns 168
Composition and Origins of Coal Gases 173
Gas and Water Production 180

Hydrogeologic Factors Affecting Coalbed Methane Producibility 185

Conclusions 190

Future Work 191

Conclusions
Roger Tyler, William R. Kaiser, Carol M. Tremain, Andrew R. Scott, H. Seay Nance, Ronald G. McMurry, and Naijiang Zhou 192

Genetic Stratigraphy 192

Fractures 193

Lineaments 193

Grand Valley, Parachute, and Rulison Field Studies 194

White River and Pinyon Ridge Field Studies 194

Producibility Model 195

Future Work 197

Acknowledgments 198

Conversion Chart 198

References 199

Figures

1. Western United States coal basins and coal gas resources 2

2. Basins and uplifts created during the Laramide Orogeny in northeastern Utah, northwestern Colorado, and southwestern Wyoming 3

3. Locality map of the Piceance Basin, northwestern Colorado 4

4. Structure map contoured on top of the Rollins-Trout Creek sandstone members, Piceance Basin 5

5. Northwest-southeast cross section A–A′ through Piceance Basin 7

6. Coal-bearing stratigraphic and confining units in the Piceance Basin 8

7. Structural complexity of the Piceance Basin, showing northwestern alignment of the structural fabric 11

8. Location of published studies and cross sections used in this report 14

9. Location of the Piceance Basin relative to the Western Interior Seaway 15

10. Regressive limits of the sandstone members of the Mancos Tongue and Iles Formation, Mesaverde Group 17

11. Transgressive limits of the Mancos Shale tongues (flooding surfaces), Iles and Williams Fork Formations, Mesaverde Group 18

12. Traditionally defined stratigraphic column of principal coal-bearing zones, depositional environments, and sandstone reservoir characteristics in the Piceance Basin 19

13. Schematic section and characteristics of coal beds and sandstones in major coal-bearing units in the Piceance Basin 20

14. Cross section of east end of Grand Valley field to southeast of New Castle, showing stratigraphic relationships and changes in the coal zones 21

15. Shoreline trends of the Corcoran and Cozzette Sandstones in the southeast part of the Piceance Basin 24

16. Net coal thickness and depth to base of the Iles Formation (Black Diamond coal zone) 25

17. Net coal thickness of the Cameo-Wheeler-Fairfield coal zone. 28

18. Face-cleat strikes and domains in the Mesaverde Group and Wasatch Formation coal beds, Piceance Basin 36

19. Butt-cleat strikes and domains in the Mesaverde Group and Wasatch Formation coal beds, Piceance Basin 39

20. Regional distribution and orientations of F_1 joint sets in the Piceance Basin 41

21. Regional distribution and orientations of F_2 joint sets in the Piceance Basin 42

22. Regional distribution and orientations of F_3 joint sets in the Piceance Basin 43

23. Regional distribution and orientations of F_4 joint sets in the Piceance Basin 44

24. Measured array of natural fracture strikes of F_2 and F_3 in Mesaverde and Tertiary strata around the Piceance Basin and analytical stress trajectories 53

25. Regional west-east alignment of intrusive Tertiary basalts and dikes in the Piceance Basin 59

26. Fracture density from core descriptions in the Piceance Basin 60

27. Restored section of Pennsylvanian–Permian rocks, Eagle Basin, Colorado, showing block faulting in the Piceance Basin 62

28. Two stages of the Laramide orogeny showing uplifts and direction of compressional forces 63

29. Maximum horizontal stress orientations in the Piceance Basin area 66

30. Lineament data sources and previous lineament studies in the vicinity of the Piceance Basin 75

31. Landsat lineaments in the northern Piceance Basin and enlargement of study area 76

32. Landsat lineaments in the southern Piceance Basin and enlargement of study area 78

33. SLAR lineaments in the southeastern Piceance Basin and enlargement of study area 80

34. SLAR lineaments in the southwestern Piceance Basin and enlargement of study area 82

35. Aerial photolineaments in southwestern Piceance Basin and enlargement of study area 84

36. Aerial photolineament joint sets from outcrop in the Green River and Wasatch Formations, northern Piceance Basin 86

37. Composite of all lineaments in the Piceance Basin mapped in this and previous studies 88

38. Stress province map showing major stress province boundaries in the vicinity of the Piceance Basin 93

39. Polar graphs of Landsat lineaments in the northern Piceance Basin 97

40. Polar graphs of Landsat lineaments in the southern Piceance Basin 97

41. Polar graphs of SLAR lineaments in the southeastern Piceance Basin 98

42. Polar graphs of SLAR lineaments in the southwestern Piceance Basin 98

43. Polar graphs of aerial photolineaments in southwestern Piceance Basin 99

44. Polar graphs of aerial photolineament joint sets from outcrop in the Green River and Wasatch Formations, northern Piceance Basin 99

45. Polar graph composite of all lineaments in the Piceance Basin mapped in this and previous studies 100

46. Genetic stratigraphy and type log of the upper Mesaverde Group in the southeastern Piceance Basin 110

47. Comparison between the genetic stratigraphy and a type log of the Williams Fork Formation in the southeastern Piceance Basin and southeastern Sand Wash Basin 111

48. Nomenclature used in this study and by various previous authors for the Upper Cretaceous and early Tertiary rocks in the eastern and southeastern Piceance Basin 114

49. Areal extent of genetic unit 1 coals 117

50. Westward limit of genetic unit 2 coals, indicating a north to northwest orientation of coal thickness trends 119

51. Westward limit of genetic unit 3 coals, indicating a north to northwest orientation of coal thickness trends 121

52. Net coal thickness map of genetic units 1 through 3, Williams Fork Formation 123

53. Detailed stratigraphic cross section showing lateral continuity of genetic unit 1 coal beds 125

54. Detailed west-east cross section through T9S showing the genetic sequence stratigraphy, Rollins-Trout Creek progradation, and coal occurrence of unit 1 126

55. Base map of the Grand Valley/Rulison study area showing well locations, field names, and locations of cross sections 135

56. Type log showing stratigraphy and the occurrence of coal at Grand Valley field 138

57. Structure-contour map on the base of the Mancos Tongue 140

58. Structure-contour map on the top of the lower Williams Fork Formation 140

59. West-east stratigraphic cross section of lower Williams Fork Formation (units 1 and 2) 142

60. North-south stratigraphic cross section of lower Williams Fork Formation 143

61. Maximum sandstone map of the interval from the top of the Rollins to the top of the lower Williams Fork Formation 147

62. Maximum sandstone map of the upper Williams Fork Formation 148

63. Maximum sandstone map of the undifferentiated Upper Cretaceous above the upper Williams Fork Formation 149

64. Maximum coal map of Cameo Coal Group 150

65. Net coal map of Cameo Coal Group 153

66. Map of maximum annual production (MAP), Cameo wells, Grand Valley/Rulison area 155

67. Map showing location of study area and coalbed methane fields in the northern Piceance Basin 163

68. Structure map, top of the Rollins-Trout Creek sandstone 166

69. Seismic line across the northeastern part of the study area 167

70. Type logs from the White River Dome and Pinyon Ridge fields in the northern Piceance Basin and from Sand Wash Basin 169

71. Net coal trends for the lower coal-bearing interval (units 1 and 2) of the Williams Fork Formation in the northern Piceance and Sand Wash Basins 171

72. Net coal map for the lower coal-bearing interval (units 1 and 2) of the Williams Fork Formation in the northern Piceance Basin 172

73. Relation between the coal-gas-generation rate and vitrinite reflectance 174

74. Carbon dioxide content of coal gases in the northern Piceance Basin 176

75. Correlation of coal thickness and carbon dioxide content 177

76. Cross section showing the variability of carbon dioxide and gas content in the Sand Wash Basin 179

77. Maximum monthly coal gas production in the study area 182

78. Maximum monthly water production in the study area 183

79. Maximum monthly condensate production in the study area 184

80. Mean annual precipitation for the northern Piceance and Sand Wash Basins 187

81. Schematic diagram showing the importance of thrust faulting to regional hydrogeology... 188

Tables

1. Natural fracture sets in the southern Piceance Basin 49

2. Natural fracture sets in the southern Piceance Basin (stratigraphically ordered) 50

3. Average coal cleat orientation in upper Cretaceous Mesaverde Group and Paleocene and Eocene Wasatch Formation, southern Piceance Basin 51

4. Average coal cleat orientation in upper Cretaceous Mesaverde Group and Paleocene and Eocene Wasatch Formation, southern Piceance Basin (stratigraphically ordered) 52

5. Mineralization in cleats 55

6. Current stress data 67

Tectonic Evolution and Stratigraphic Setting of the Piceance Basin, Colorado: A Review

Roger Tyler

ABSTRACT

The Piceance Basin, bounded by the Uinta Mountain Uplift, Axial Arch, White River Uplift, and Elk Mountains, forms part of the Rocky Mountain foreland. Coals in the Cameo-Wheeler-Fairfield coal zone (Williams Fork Formation, Mesaverde Group) are the major coalbed methane targets. The Cameo-Wheeler-Fairfield coal zone occurs at an average depth of approximately 6,000 ft (1,830 m). Maximum thickness of individual Cameo-Wheeler-Fairfield coal beds is 20 to 35 ft (6 to 11 m), and net coal thickness ranges from less than 20 ft (<6 m) to more than 80 ft (>24 m). The most continuous Cameo-Wheeler-Fairfield coal beds formed landward (northwestward) of the Rollins-Trout Creek progradational shoreline sandstone and have extended northeast- to north-northeastward along depositional strike for at least 5 to 10 mi (8 to 16 km) in the southeastern Piceance Basin. Less continuous, fluvial Williams Fork coal beds occur up the paleoslope to the northwest. In the vicinity of the Danforth Hills coal area, north of Meeker, Cameo-Wheeler-Fairfield coals are in excess of 100 ft (>30 m) thick and they are major coalbed methane targets.

GEOLOGIC OVERVIEW

The Piceance Basin in northwestern Colorado (figs. 1, 2, and 3) is an asymmetric, northwest-trending elongate structural basin of Late Cretaceous to early Tertiary age. The basin is bounded by the Uinta Mountain Uplift on the northwest, Axial Arch on the north, White River Uplift on the east, Elk Mountains and Sawatch Uplift to the southeast, Gunnison Uplift and San Juan volcanic field to the south, and Uncompahgre Uplift to the southwest (fig. 4). It is

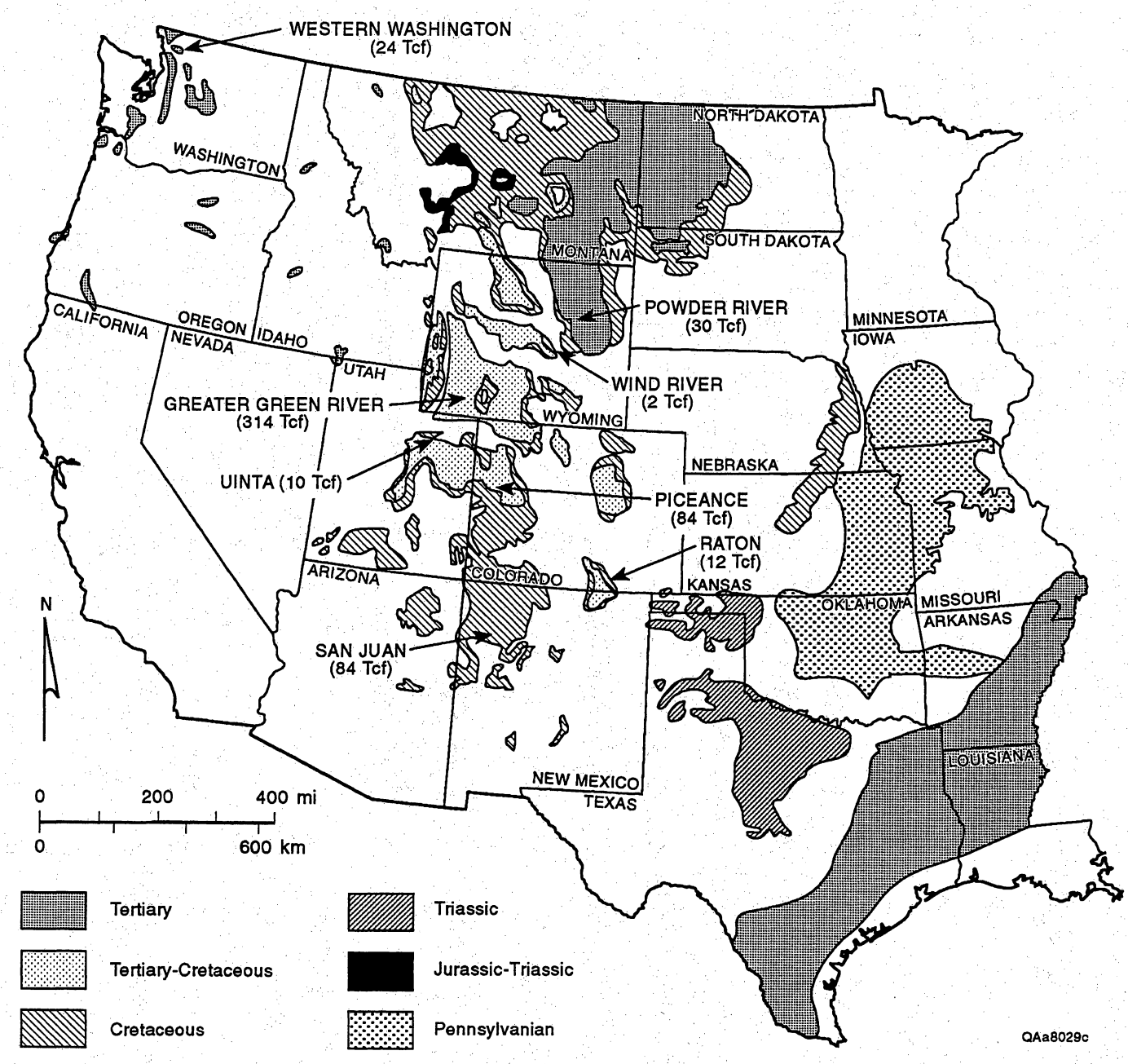

Figure 1. Western United States coal basins and coal gas resources. Modified from Wood and Bour (1988) and Scott and others (1994).

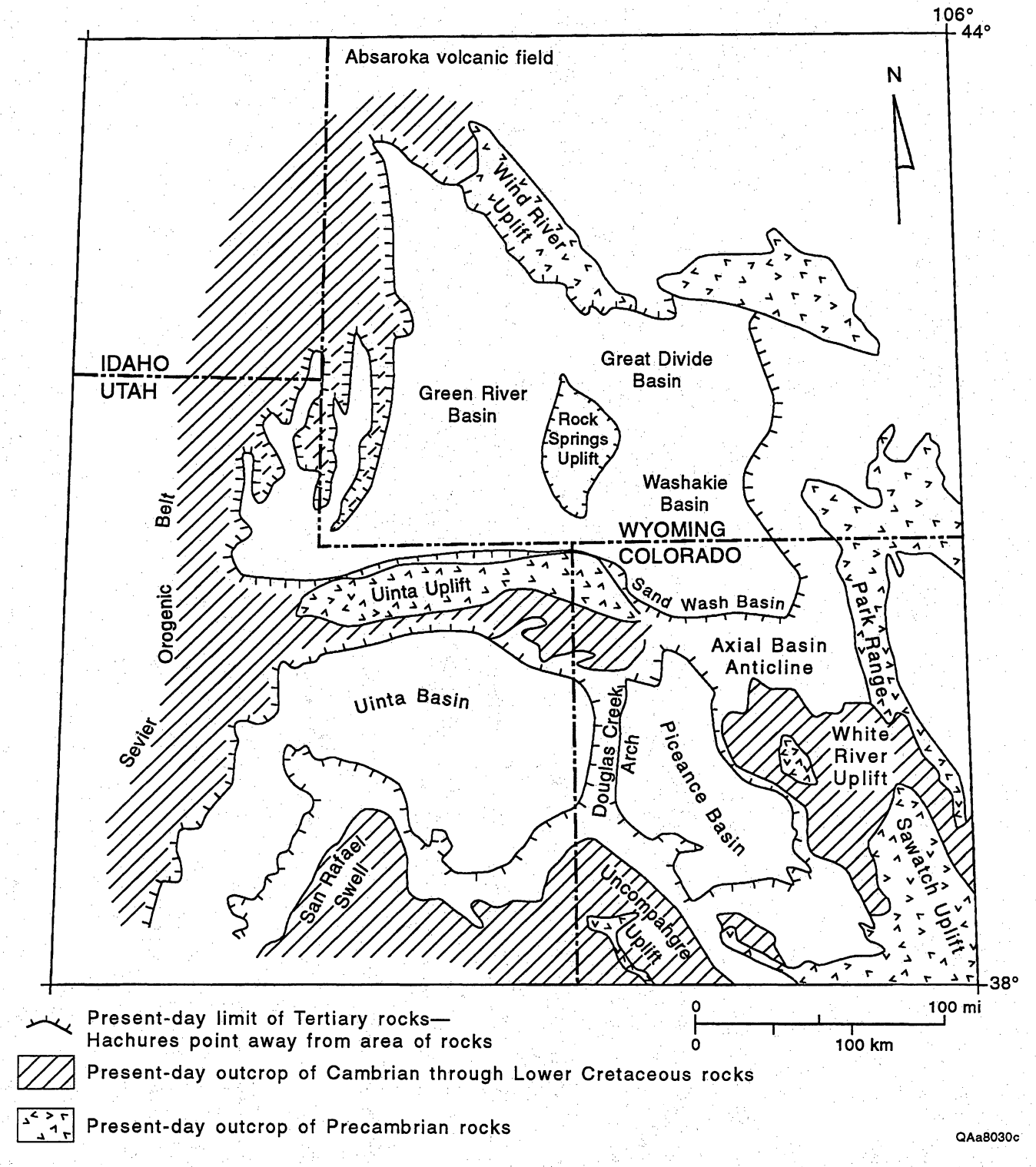

Figure 2. Basins and uplifts created during the Laramide Orogeny in northeastern Utah, northwestern Colorado, and southwestern Wyoming. Modified from Johnson (1989).

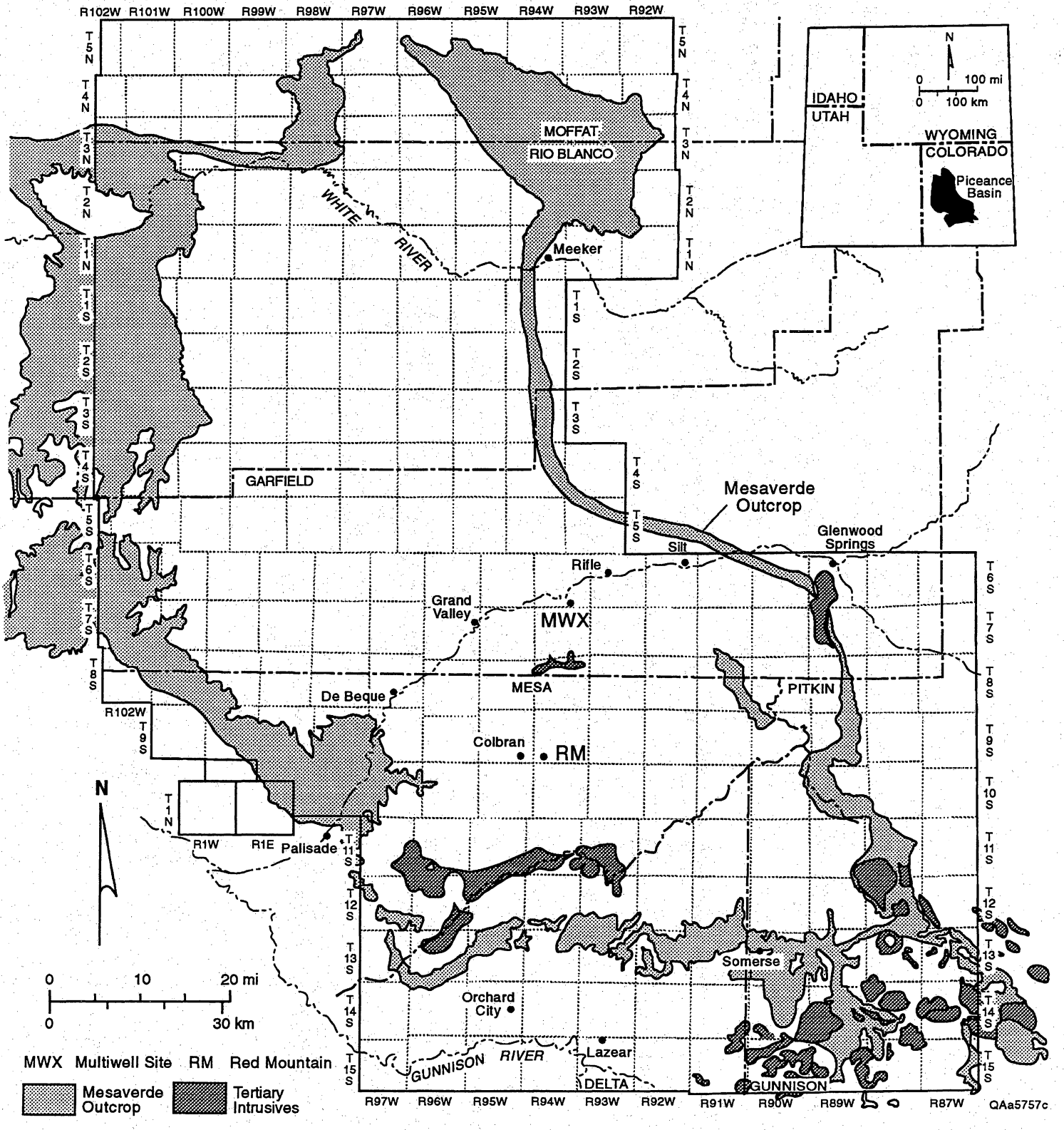

Figure 3. Locality map of the Piceance Basin, northwestern Colorado.

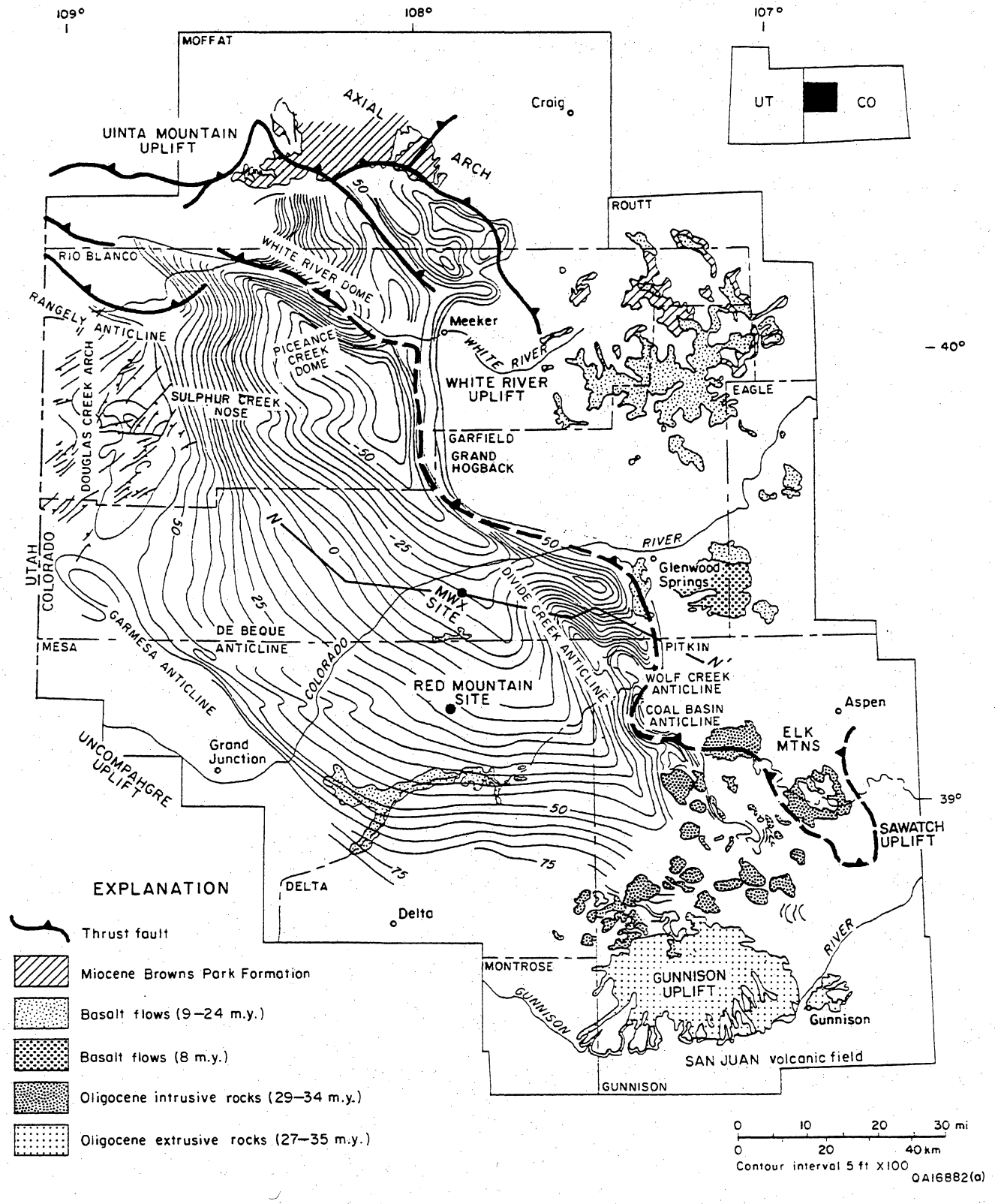

Figure 4. Structure map contoured on top of the Rollins-Trout Creek Sandstone Members, Piceance Basin. Contour interval 500 ft (152 m). Cross section A–A′ shown in figure 5. Modified from Johnson and Nuccio (1986).

separated from the Uinta Basin to the west by the Douglas Creek Arch. The structural axis is on the northeast side of the basin, adjacent to the Grand Hogback, where it extends for about 150 mi (240 km) northwestward (fig. 4). Width of the basin ranges from 90 mi (145 km) in the north to 20 mi (32 km) in the south. Dips of the strata are gentle (5°-10°) on the west and southwest flanks of the basin, but steep (>60° to overturned) along the sharply upturned east flank, adjacent to the Grand Hogback (figs. 4 and 5). The potential coalbed methane reservoirs are contained in Upper Cretaceous (Mesaverde Group) deposits, which cover an area of about 7,225 mi^2 (18,720 km^2). Depth of the coal-bearing Iles and Williams Fork Formations (fig. 6) varies from outcrop along the basin margin to more than 12,000 ft (3,660 m) along the structural axis of the basin (fig. 4). The Cameo-Wheeler-Fairfield coal is less than 6,000 ft (<1,830 m) deep in approximately 50 to 60 percent of the Piceance Basin.

TECTONIC EVOLUTION AND STRATIGRAPHIC SETTING

The following review of the regional structural and stratigraphic setting of the Piceance Basin is adapted from Johnson (1987, 1989, and references therein). In the northeast part of the Colorado Plateau, the Sevier Orogeny (160 to 72 mya) caused east-west horizontal compression during deposition of the Upper Cretaceous and lower Tertiary sediments (Baars and others, 1988). East-west folding, contemporary with the orogeny, is marked by a low-amplitude, north-south-trending flexure in the area of the present–day Douglas Creek Arch (Quigley, 1965) (fig. 4). Intermittently during the early Cenozoic, the Douglas Creek Arch divided the Uinta and Piceance Basins into two separate basins. At other times (Cretaceous), there was little relief on the Douglas Creek Arch and sediments buried the arch, creating one large basin (Johnson, 1985, 1986, 1987, 1989; Johnson and Finn, 1986). Rapid subsidence at the beginning of the Late Cretaceous caused a major marine invasion (Mancos Shale) (fig. 6), and the Western Interior Seaway covered much of the Rocky Mountain foreland basin. Pulses of orogenic activity in the Overthrust Belt throughout much of the Late Cretaceous caused

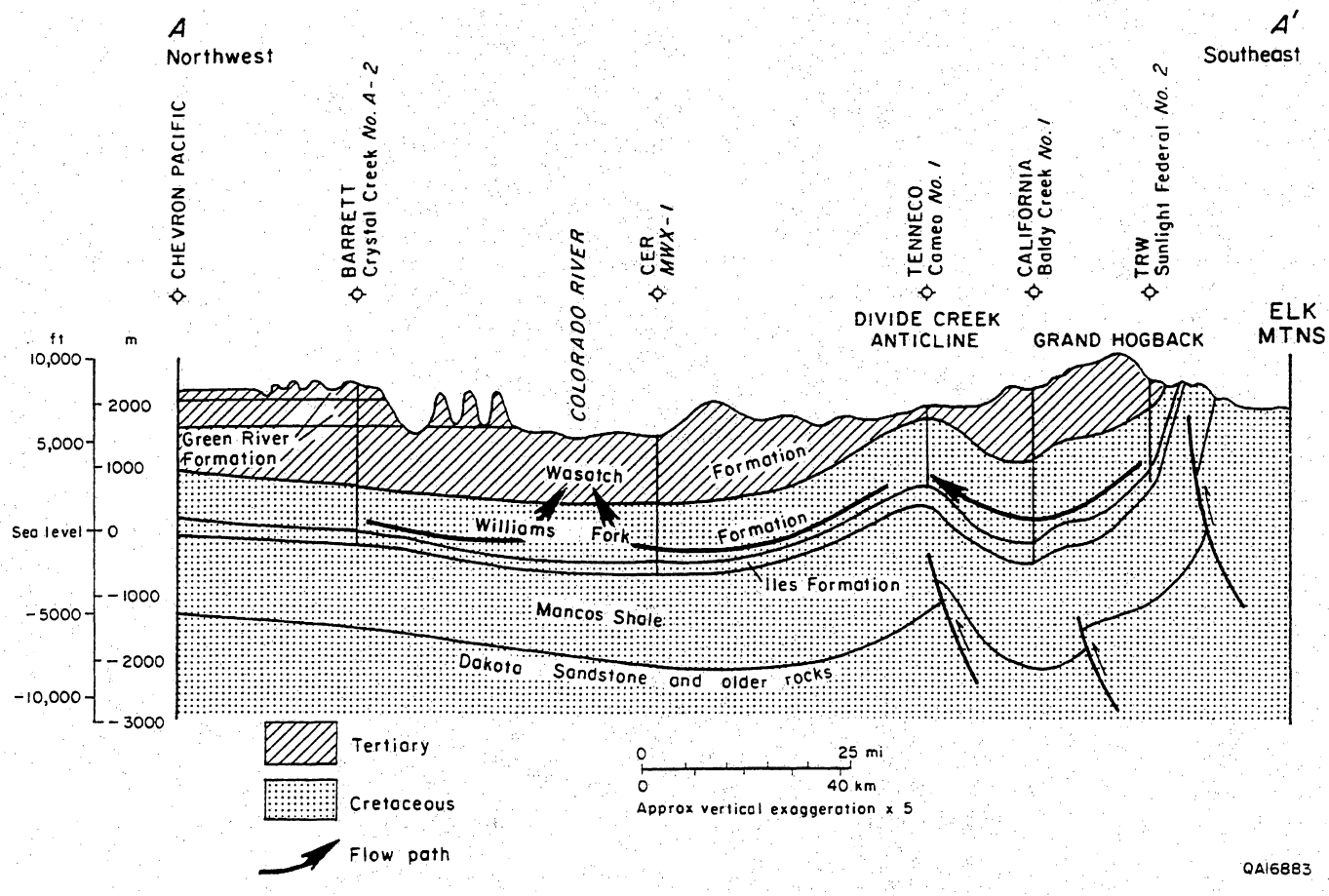

Figure 5. Northwest-southeast cross section A–A' through Piceance Basin. Modified from Law and Johnson (1989). The Fort Union Formation is undifferentiated. Mesaverde Group receives recharge along wet, elevated Grand Hogback. Ground water flows northwestward, down hydraulic gradient, converging on the Colorado River valley. Line of section shown in figure 4.

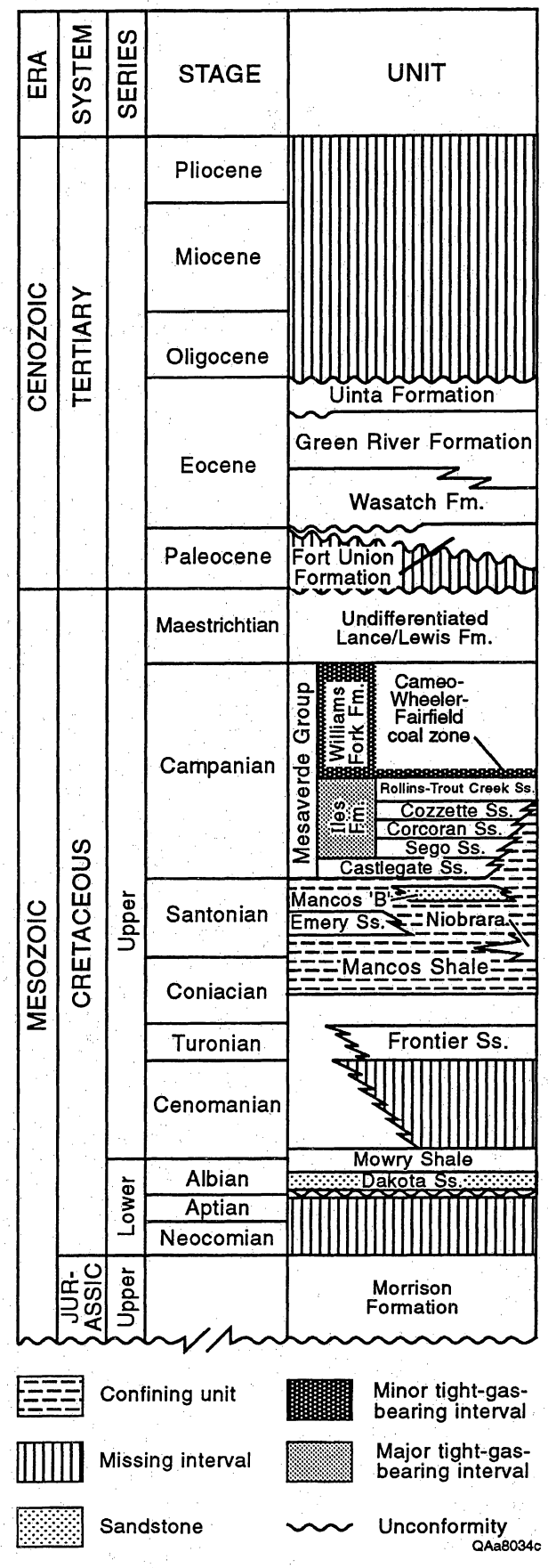

Figure 6. Coal-bearing stratigraphic and confining units in the Piceance Basin. Modified from Rocky Mountain Association of Geologists (1977) and Finley (1984).

sediment to be shed eastward into the epeiric sea, resulting in episodic transgression and regression along a fairly narrow area adjacent to the Orogenic Belt (Frontier and Emery Sandstones and Niobrara Formation) (fig. 6). By Campanian time, tectonically induced pulses of clastic sediment had begun to advance the shoreline of the interior seaway farther to the east (Mesaverde Group; Fouch and others, 1983), and by the beginning of the Maestrichtian, the shoreline had prograded beyond the present-day east margin of the basin, and the Piceance Basin was the site of coastal-plain sedimentation (Lance Formation) (fig. 6).

The Piceance Basin was subsequently bounded by uplifts that formed in the Rocky Mountain foreland region during the Laramide Orogeny, approximately 72 to 40 mya (Dickinson and Snyder, 1978; Tweto, 1980). The onset of the Laramide Orogeny is recorded by an unconformity at the top of the Upper Cretaceous (Johnson and Nuccio, 1986) (fig. 6). Local relief on the unconformity is slight, but thousands of feet of Upper Cretaceous rocks may have been removed (Johnson and Nuccio, 1986). Subsidence continued through the Paleocene to near the end of the Eocene in the Piceance Basin, during which time as much as 12,000 ft (3,600 m) of Paleocene and Eocene sediments was deposited. During late Eocene to early Oligocene time, an erosion surface developed across the basin. This surface is similar to late Eocene erosion surfaces that developed in other parts of the Rocky Mountain foreland basins (Epis and Chapin, 1975). In the Piceance Basin, remnants of this surface are still preserved beneath 9.7-million-year-old basalts at a present-day elevation of about 10,000 ft (3,050 m) (Marvin and others, 1966). The amount of section removed is clearly a function of basin subsidence trends and varies from little or no section removed in the basin center to 2,000 to 3,000 ft (610 to 910 m) removed along the slowly subsiding margins of the basin. The erosional surface probably started to develop around the margins of the basin during the latest stages of basin subsidence (late Eocene) and then spread to cover the entire basin after subsidence ceased (Johnson and Nuccio, 1986). Below the erosional surface, the thick sequence of lower Tertiary rocks provided the thermal blanket that led to large quantities of methane being generated from source rocks in the Mesaverde Group.

At the end of the Laramide Orogeny, about 40 mya, basin subsidence ceased and little structural movement or sedimentation occurred in the basin until the Colorado River system began to cut deep canyons, about 10 mya. The late Cenozoic tectonism that affected many areas in Colorado and Utah apparently did not greatly affect the Piceance Basin. Probably the most significant post-Laramide tectonism in the basin was faulting on the Douglas Creek Arch and along the White River Dome (Johnson and Nuccio, 1986).

By 24 mya, the White River Uplift east of the basin had become beveled to about the same level as the erosion surface in the Piceance Basin surface. The erosion surface on the uplift is covered by basalts that are from 24 to 8 m.y. old (Larsen and others, 1975). Because basalts probably intercepted recharge, the artesian system that existed earlier along the flank of the uplift was probably destroyed, and Mesaverde outcrops along the Uncompahgre, Uinta, and Sawatch Uplifts were probably reduced to about the same elevation as that of the adjacent basin (Johnson and Nuccio, 1986). Only along the south margin of the basin is there evidence that during this period Mesaverde outcrops were significantly higher than the erosion surface beneath the basalts in the Piceance Basin. Even today the Mesaverde is exposed at elevations of almost 12,000 ft (~3,660 m) adjacent to Oligocene-age plutons, and even higher outcrops were present before the Recent period of erosion, so an artesian system may have been maintained in the southern Piceance Basin.

Basin Margin and Intrabasin Uplifts

The northernmost part of the Piceance Basin is almost isolated from the rest of the basin by the White River Dome, a southeast-plunging anticline (fig. 4). Another southeast-plunging anticline, the Rangely Anticline, to the southwest of the White River Dome, forms the northern terminus of the Douglas Creek Arch (fig. 7). Both the Rangely Anticline and the White River Dome are probably subsidiary anticlines related to the eastern terminus of the Uinta Mountain Uplift (Johnson, 1987). These uplifts and anticlines are underlain by west- and southwest-vergent thrust faults (Gries, 1983; Lorenz, 1985). The regional stress regime during

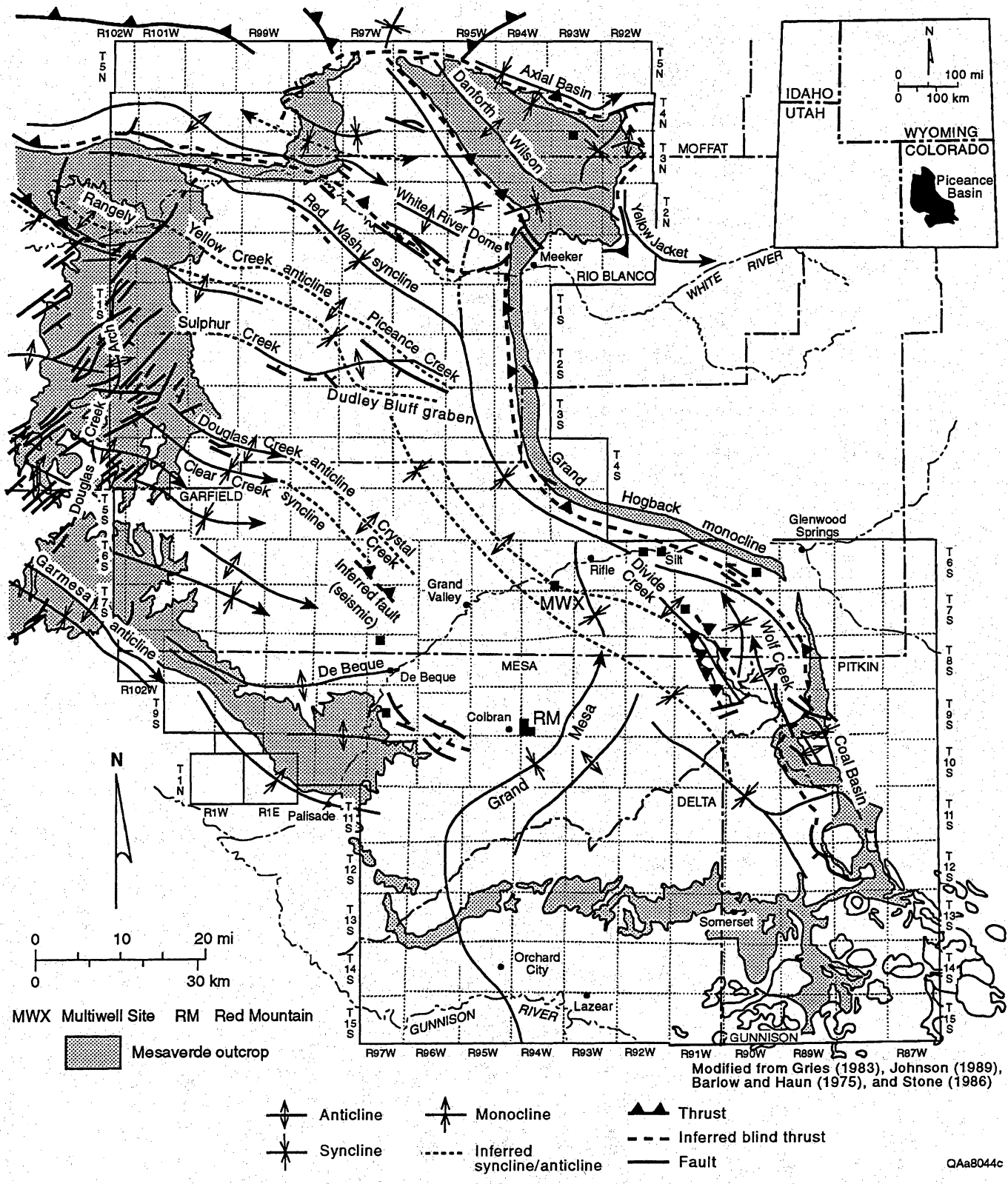

Figure 7. Structural complexity of the Piceance Basin, showing northwestern alignment of the structural fabric.

the Laramide Orogeny was primarily one of east-west compression (Lorenz, 1985), but the northwest trend of the White River Dome, Rangely Anticline, and some folds and naturally occurring fractures in coal in the Piceance Basin suggest that either an episode of northeast-oriented compression occurred during part of the Laramide Orogeny (Tyler and others, 1991a, b, 1994), such as the late Laramide reorientation of stresses proposed by Chapin and Cather (1981), or the fold trends resulted from reactivation of northwest-trending anisotropy in the crystalline Precambrian basement (Tweto, 1980; Lorenz, 1985).

In the southeast part of the basin, three large closed anticlines, the Divide Creek, Wolf Creek, and Coal Basin Anticlines (fig. 7), are underlain by deep-seated west- and southwest-vergent thrust faults, extending beneath the Grand Hogback (Grout and others, 1991). The Divide Creek Anticline is cut by several normal faults transverse to the fold trend (Berry, 1959; Grout and others, 1991). The geometry of the Coal Basin Anticline has been altered by intrusions of plutons during the Oligocene (Johnson, 1987). Several relatively minor east- and southeast-trending anticlines within the central and north-central Piceance Basin include the Piceance Creek Dome–Sulphur Creek Nose, the De Beque Anticline, and the Garmesa Anticline (fig. 7). These anticlines may have formed as a result of reactivation of faults during the Laramide Orogeny (Stone, 1977). The north part and center of the basin were apparently not intruded by Oligocene plutons (Larsen and others, 1975). The asymmetry of the Rangely and Piceance Creek domes suggests that reverse and thrust faults also underlie these anticlines at depth (Gries, 1983; Lorenz, 1985). Traditionally, with the exception of faults that have minor displacement (100 ft [30 m]) along the Grand Hogback, thrust faults were thought not to cut the Upper Cretaceous through Eocene rocks (Johnson and Nuccio, 1983, 1986). More recent investigations have found that the thrust faults do penetrate close to surface along the Divide Creek Anticline (Michael S. Wilson, Advanced Resources International, personal communication, 1994).

STRATIGRAPHIC AND DEPOSITIONAL SETTINGS OF COAL-BEARING FORMATIONS

The following section, relating the stratigraphic and depositional settings of coal-bearing formations, Mesaverde Group, Colorado, relies heavily on published studies and cross sections (fig. 8), although they were interpreted with new insight gained in this study. The Mesaverde Group was first named by Holmes (1877) for Upper Cretaceous outcrop exposures of interbedded sandstone, shale, and coal in the San Juan Basin of the Four Corners area. Mesaverde strata exposed in the Piceance Basin, northwest Colorado, are lithologically similar to but younger than the Mesaverde at its type section (Weimer, 1960; Collins, 1976). The Mesaverde in northwest Colorado was deposited in the Eagle Basin of Utah and Colorado. The Eagle Basin was destroyed by the Late Cretaceous–early Tertiary Laramide Orogeny that formed the Uinta, White River, Sawatch, and Uncompahgre Uplifts, and the Douglas Creek Arch, which define the margins of the Piceance Basin (Quigley, 1965; Kauffman, 1977; Johnson and Keighin, 1981).

During the Cretaceous Period, the region now occupied by the Piceance Basin was covered by the Cretaceous Interior Seaway (Quigley, 1965; Kauffman, 1977) (fig. 9). More than 5,000 ft (>1,525 m) of intertonguing marine (shoreface and shelf) and nonmarine (deltaic and fluvial) sediments was deposited in the Piceance Basin during the Late Cretaceous. Intertonguing of these deposits resulted from southeastward progradation of the shoreline, which was interrupted by northwestward shoreline retreat during periods of relative sea-level rise (Spieker, 1949; Young, 1955; Weimer, 1960; Gunter, 1962; Warner, 1964), resulting in the fluvial, paludal, strandplain/deltaic, and paralic depositional systems (Young, 1955; Warner, 1964; Quigley, 1965; Collins, 1976; Lorenz and Rutledge, 1985; Johnson, 1987, 1989). The coal-bearing sequences have been interpreted as ancient wave-dominated linear clastic shoreline (Young, 1966) or as deltaic deposits (Collins, 1970, 1976).

Collins (1976), Johnson (1987, 1989), Lorenz (1989), and Sandia National Laboratories and CER Corporation (1987–1990) divide the Mesaverde Group into the two formations first

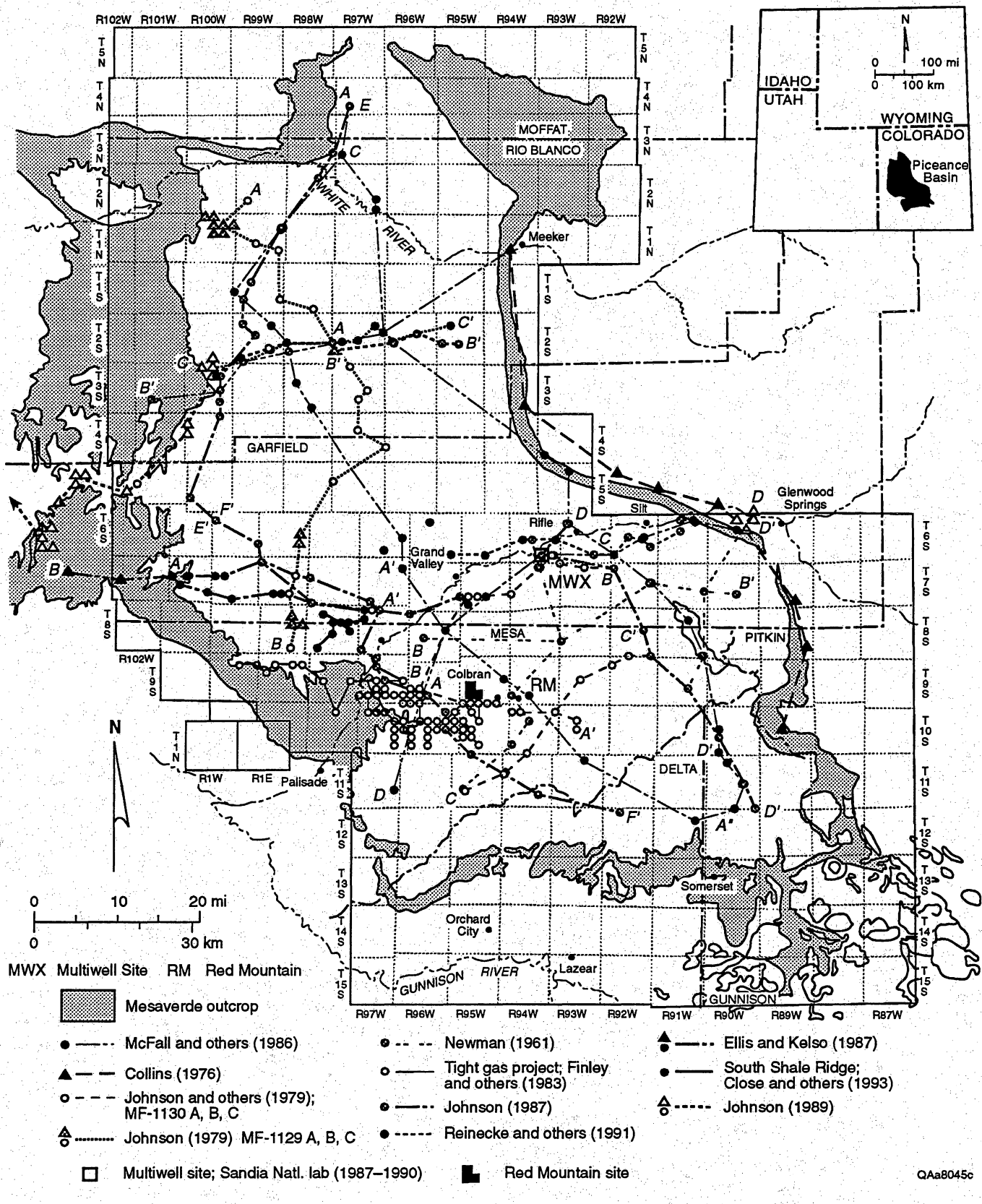

Figure 8. Location of published studies and cross sections used in this report.

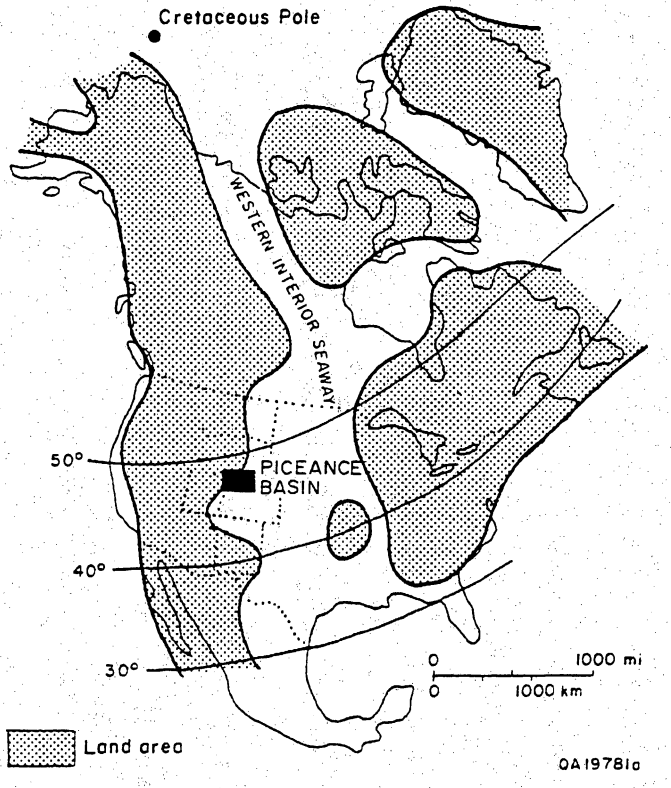

Figure 9. Location of the Piceance Basin relative to the Western Interior Seaway. Modified from Kauffman (1977).

proposed by Hancock (1925), the basal Iles Formation and the overlying Williams Fork Formation (fig. 5). Collins (1976) and Johnson (1987, 1989) have demonstrated the regressive and transgressive interfingering relationships between the Mancos Shale and the Morapos, Castlegate, Lloyd, Sego, Corcoran, Cozzette, and Rollins-Trout Creek sandstones (figs. 6, 10, and 11). In the southern Piceance Basin, Johnson (1987), Lorenz (1989), Nowak (1990, 1991), Reinecke and others (1991), and other authors have further subdivided the Williams Fork Formation into the Bowie Shale Member (Cameo-Wheeler-Fairfield and South Canyon coal zones), the Paonia Shale Member (Coal Ridge coal zone), and the "undifferentiated" Williams Fork Formation (Lorenz, 1983b; Johnson, 1989) or fluvial Mesaverde (Reinecke and others, 1991) (figs. 12 through 14). The traditionally defined Williams Fork Formation ranges from 4,600 to 6,400 ft (1,400 to 2,000 m) thick and is overlain by conglomerates of the Ohio Creek Conglomerate and sandstone member (Collins, 1976; Dunn and Irwin, 1977; Boyles and others, 1981; Lorenz, 1989). This traditional thickness of the Williams Fork Formation is most certainly too thick. Palynological data and correlation at outcrop between the Sand Wash Basin and the northern Piceance Basin confirm the presence of equivalent Lewis and Lance sediments (Newman, 1964). The Williams Fork, as defined in the Sand Wash Basin (Kaiser and others, 1994b), has been traced southward in the subsurface throughout the Piceance Basin. Along the Grand Hogback, coal-bearing strata extend upsection above the Rollins Sandstone for approximately 1,500 to 2,000 ft (460 to 600 m) and are divided into three coal packages (Cameo-Wheeler-Fairfield, South Canyon, and Coal Ridge) by Mancos Tongues, corresponding to units 1, 2, and 3/4 of the Sand Wash Basin (Hamilton, 1993, 1994). In the absence of the Lewis Shale, the top of the Williams Fork coal-bearing zone is operationally defined above package 3 coals and below a thick sequence of fluvial "undifferentiated" Upper Cretaceous strata. The undifferentiated Upper Cretaceous strata above the operationally defined Williams Fork coals are 1,500 to 2,000 ft (460 to 600 m) thick and locally contain thin discontinuous coals. The "undifferentiated" Upper Cretaceous strata are tentatively assigned Lewis/Lance Formation status.

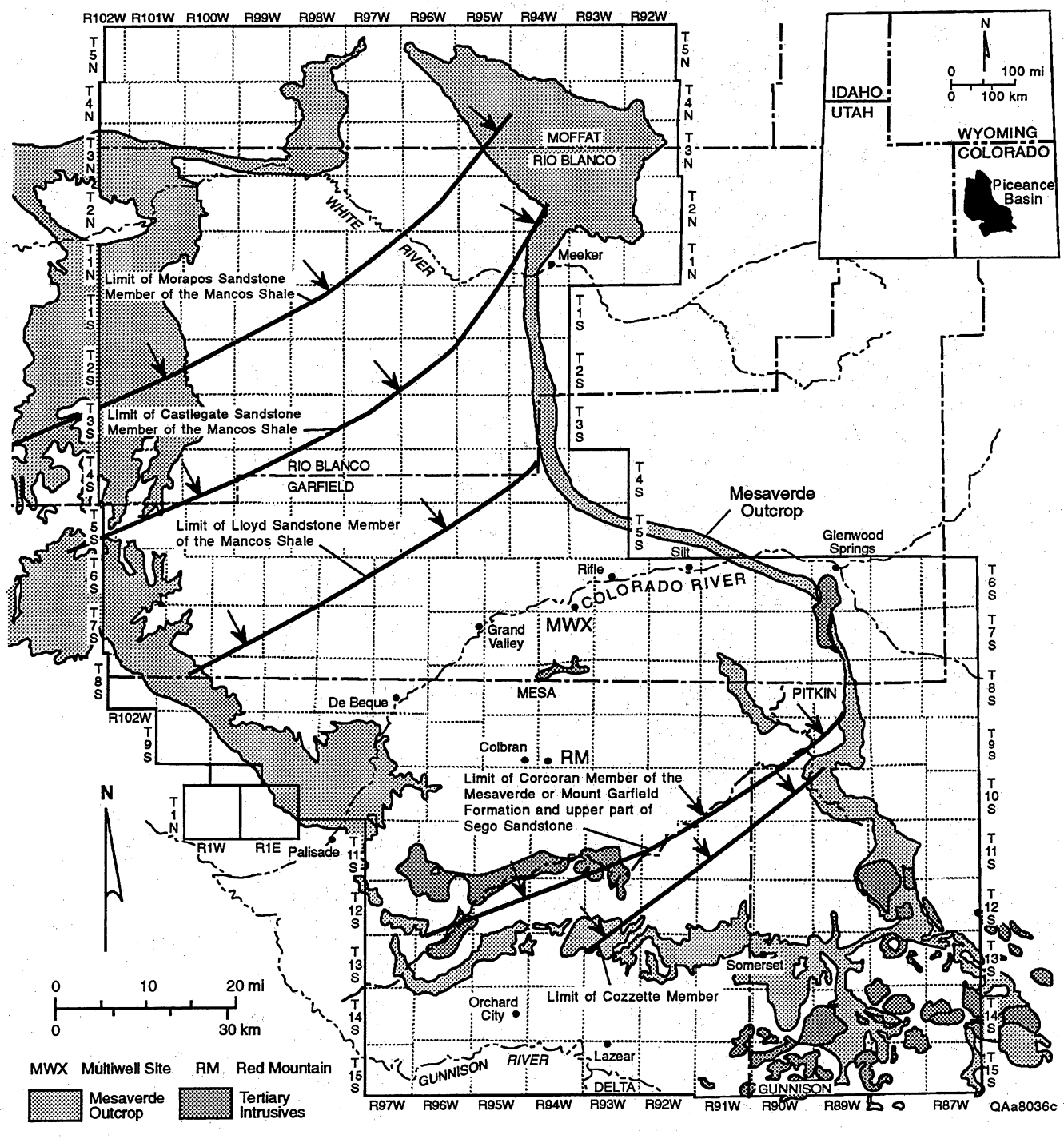

Figure 10. Regressive limits of the sandstone members of the Mancos Tongue and Iles Formation, Mesaverde Group. Limits of the Sego Sandstone cannot be determined with certainty. Seaward limit of the Rollins-Trout Creek progradational sequence is beyond the southeastern corner of the Piceance Basin and the mapped area. Arrows indicate direction of regression. Modified from Zapp and Cobban (1960), Warner (1964), Gill and Cobban (1969), Gill and Hail (1975), and Johnson (1989).

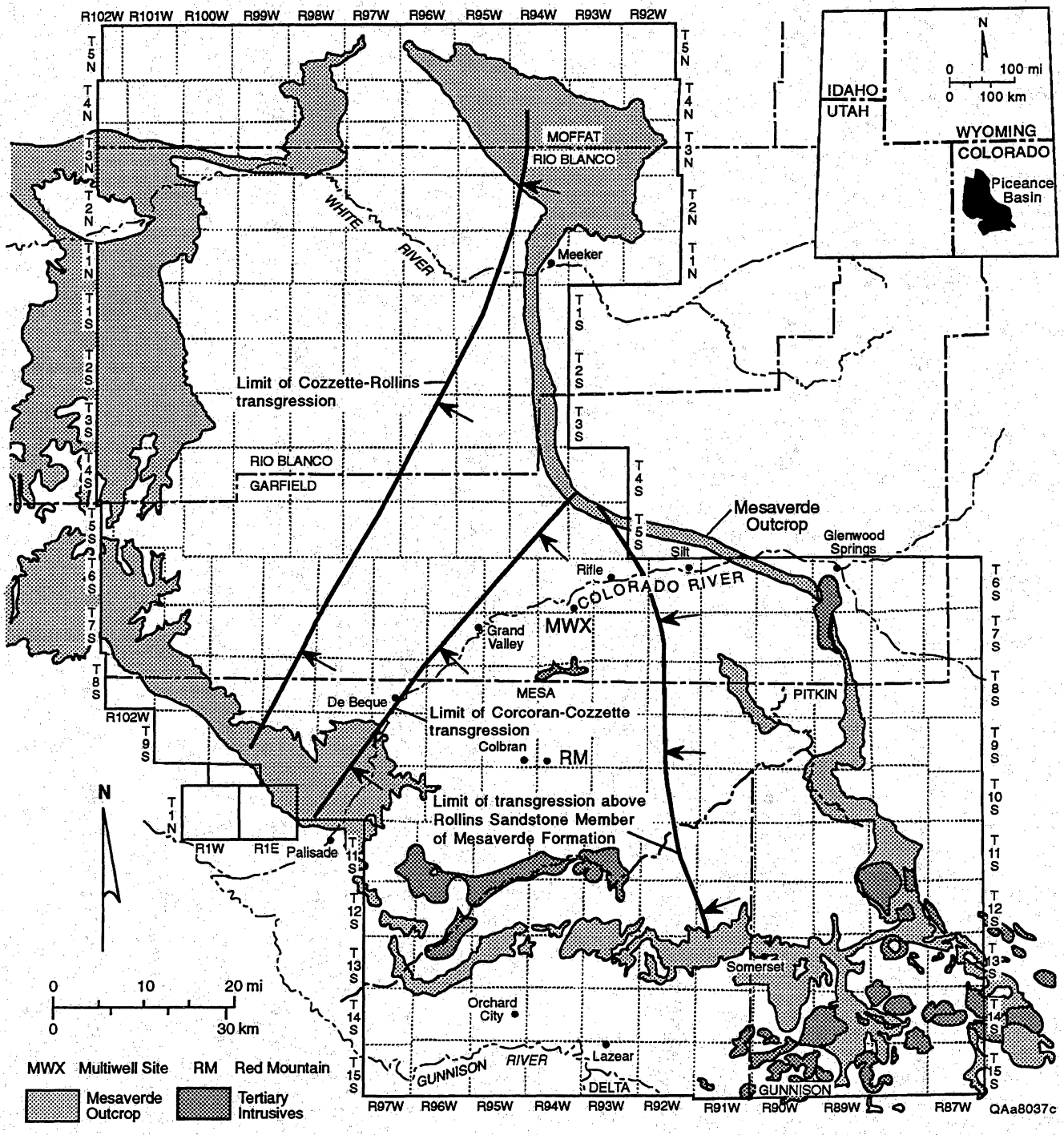

Figure 11. Transgressive limits of the Mancos Shale tongues (flooding surfaces), Iles and Williams Fork Formations, Mesaverde Group. Arrows indicate direction of transgression. Modified from Zapp and Cobban (1960), Warner (1964), Gill and Cobban (1969), Gill and Hail (1975), and Johnson (1989). Note the north-south orientation in post-Rollins and Trout Creek strata.

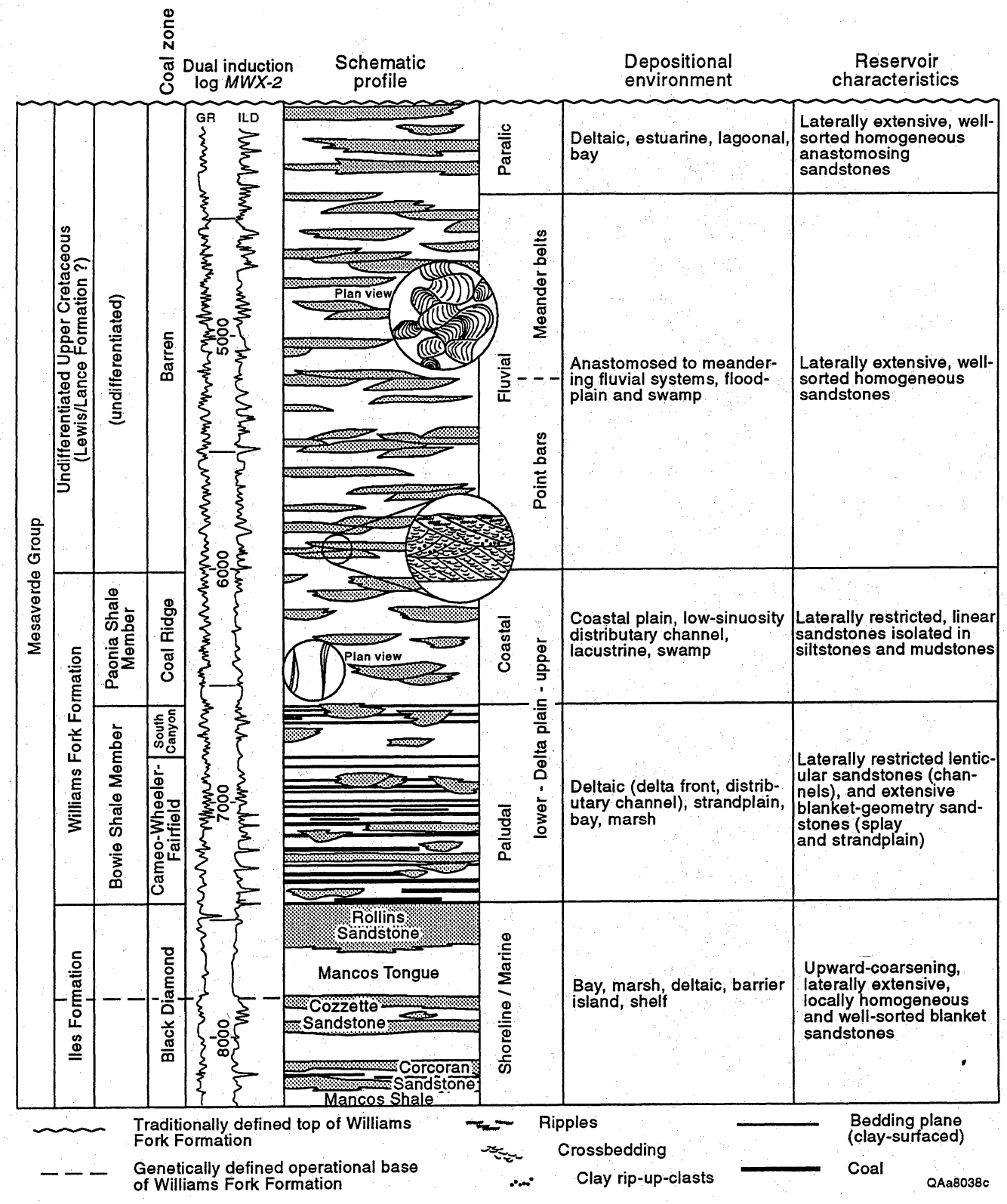

Figure 12. Traditionally defined stratigraphic column of principal coal-bearing zones, depositional environments, and sandstone reservoir characteristics in the Piceance Basin, showing inferred depositional environments and reservoir characteristics in Rulison field. Modified from Lorenz (1983b).

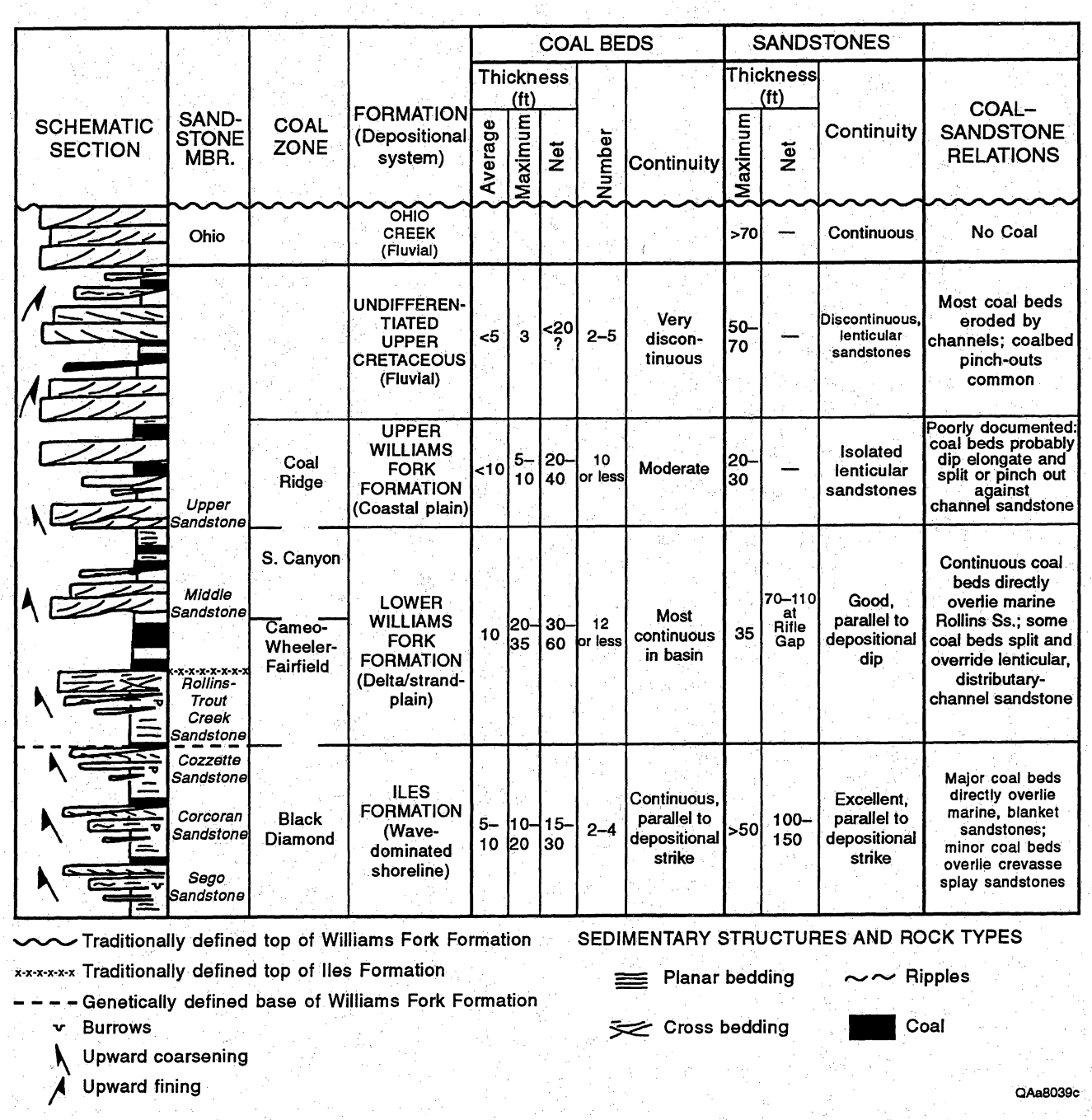

Figure 13. Schematic section and characteristics of coal beds and sandstones in major coal-bearing units in the Piceance Basin. Modified from Tyler and others (1991a, 1994).

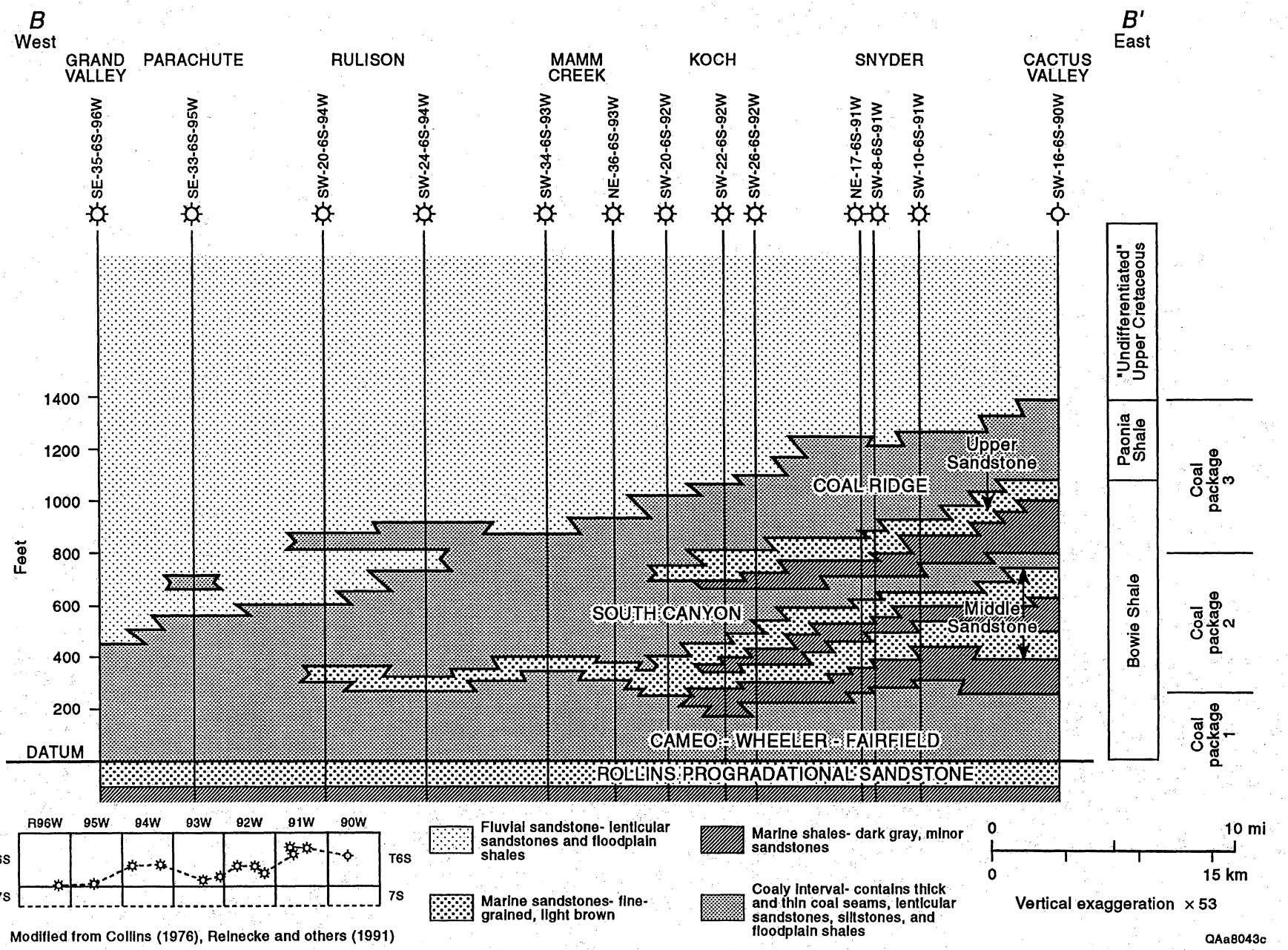

Figure 14. Cross section of east end of Grand Valley field to southeast of New Castle, showing stratigraphic relationships and changes in the coal zones. Modified from Reinecke and others (1991).

The principal coal-bearing zones in the Mesaverde Group are associated with regressive shoreline sequences (figs. 13 and 14). Thin coal beds in the Iles Formation (Black Diamond coal zone) overlie the regressive Sego, Corcoran, and Cozzette sandstones. However, the thickest coal beds in the basin occur in the Williams Fork Formation (Bowie Shale Member, Cameo-Wheeler-Fairfield coal zone; Reinecke and others, 1991), which overlies the Rollins-Trout Creek progradational shale and sandstone sequence. We have operationally defined the base of the Williams Fork Formation as the base of the progradational Rollins-Trout Creek shale (maximum flooding surface), to be consistent with the sequence stratigraphy defined in the Sand Wash Basin study (figs. 12 and 13) (Kaiser and others, 1993). Other coal beds are found in the South Canyon coal zone (Bowie Shale Member, Williams Fork Formation; Reinecke and others, 1991), the Coal Ridge coal zone (Paonia Shale Member, Williams Fork Formation; Reinecke and others, 1991) and in the upper, undifferentiated Upper Cretaceous strata (Williams Fork Formation; McFall and others, 1986; Lorenz, 1989). This overall regressive package overlies and intertongues with the Mancos Shale and is probably overlain by the Lance Formation, the Ohio Creek Conglomerate, and/or the Lewis Shale in various parts of the basin (Collins, 1976; Boyles and others, 1981; Lorenz, 1989). Detailed descriptions of the coal-bearing formations and their component members follow.

Iles Formation (Black Diamond Coal Zone)

Interbedded sandstones, siltstones, coals, and shales, having a combined thickness ranging from 890 to 1,600 ft (270 to 487 m), compose the Iles Formation (Collins, 1976) (figs. 12 and 13). Sandstones and coalbeds of the Iles Formation were deposited in a regressive, wave-dominated coastal setting (Young, 1966; Collins, 1976; Finley and Ladwig, 1985; Madden, 1985; Johnson, 1987, 1989; Lorenz, 1989). Marine deposits (shelf, shoreface, barrier-island, strandplain, delta-front, bay-lagoon, and tidal-inlet) in the Iles Formation grade northwestward (paleoslope) into nonmarine deposits (coastal plain marsh and swamp, fluvial, and floodplain). Thickest coal beds occur landward (northwestward) of thick, northeast-trending barrier-

strandplain sequences (fig. 15) (Finley and others, 1983). These coal beds override the barrier-strandplain sandstones and pinch out seaward (southeastward) into transgressive mudstones (Finley, 1985).

Black Diamond coal zone. Coal beds in the Black Diamond coal zone overlie progradational sandstones in the Iles Formation (fig. 13). These sandstones (Sego, Corcoran, and Cozzette Members) are each 0 to 220 ft (0 to 67 m) thick and contain individual sandstone units that range from 0 to 100 ft (0 to 30 m) thick (fig. 13). Iles sandstones exhibit excellent continuity (50 by 75 mi [80 by 120 km]) and are described as blanket sandstones (Lorenz, 1983a). They trend northeastward and intertongue to the southeast with marine Mancos Shale wedges and to the northwest with the terrestrial coal-bearing deposits (Young, 1955; Warner, 1964; Finley, 1985) (figs. 10 and 11). Iles paleoshorelines advanced to the southeast; the greatest advance of the shoreline was approximately 15 mi (24 km) northwest of the present southeast margin of the basin (fig. 10). Black Diamond coal beds are interbedded with carbonaceous mudstones or thin sandstones (Madden, 1985). Two to four Black Diamond coal beds typically occur in the 300-ft (90-m) thick interval (McFall and others, 1986). Individual coal beds are commonly less than 3 ft (<1 m) thick, although some are as thick as 10 ft (3 m) (fig. 13) (Madden, 1985). Net coal thickness is also commonly less than 10 ft (<3 m), but in the northeast part of the basin it is more than 30 ft (>9 m). Black Diamond coal beds are thin or absent in the far west and southeast parts of the basin (fig. 16a) (McFall and others, 1986; Johnson, 1989). Black Diamond net coal thickness trends contain both strike- and dip-parallel elements (McFall and others, 1986). The Black Diamond coal zone contains the most deeply buried Mesaverde coal beds in the Piceance Basin; in Rio Blanco and Garfield Counties, these coal beds are more than 12,000 ft (>3,660 m) deep (fig. 16b).

Williams Fork Formation (Cameo-Wheeler-Fairfield, South Canyon, and Coal Ridge Coal Zones)

The Williams Fork Formation overlies the Iles Formation and consists of a series of marine and nonmarine conglomerates, sandstones, siltstones, mudstones, claystones, and rare fresh-

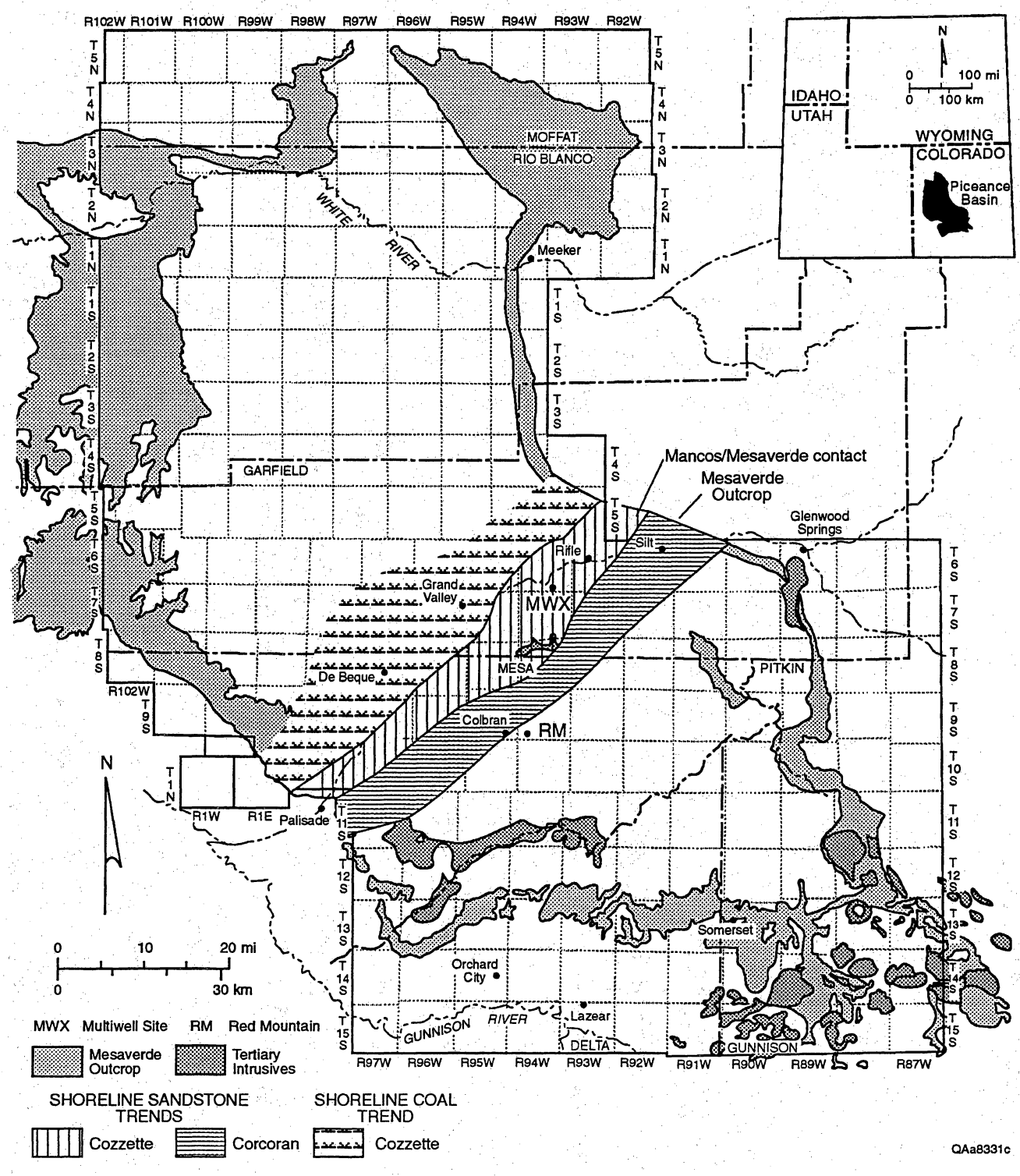

Figure 15. Shoreline trends of the Corcoran and Cozzette Sandstones in the southeast part of the Piceance Basin. Thick northeast-trending coal beds formed landward (northwest) of these shoreline trends. Modified from Finley and others (1983).

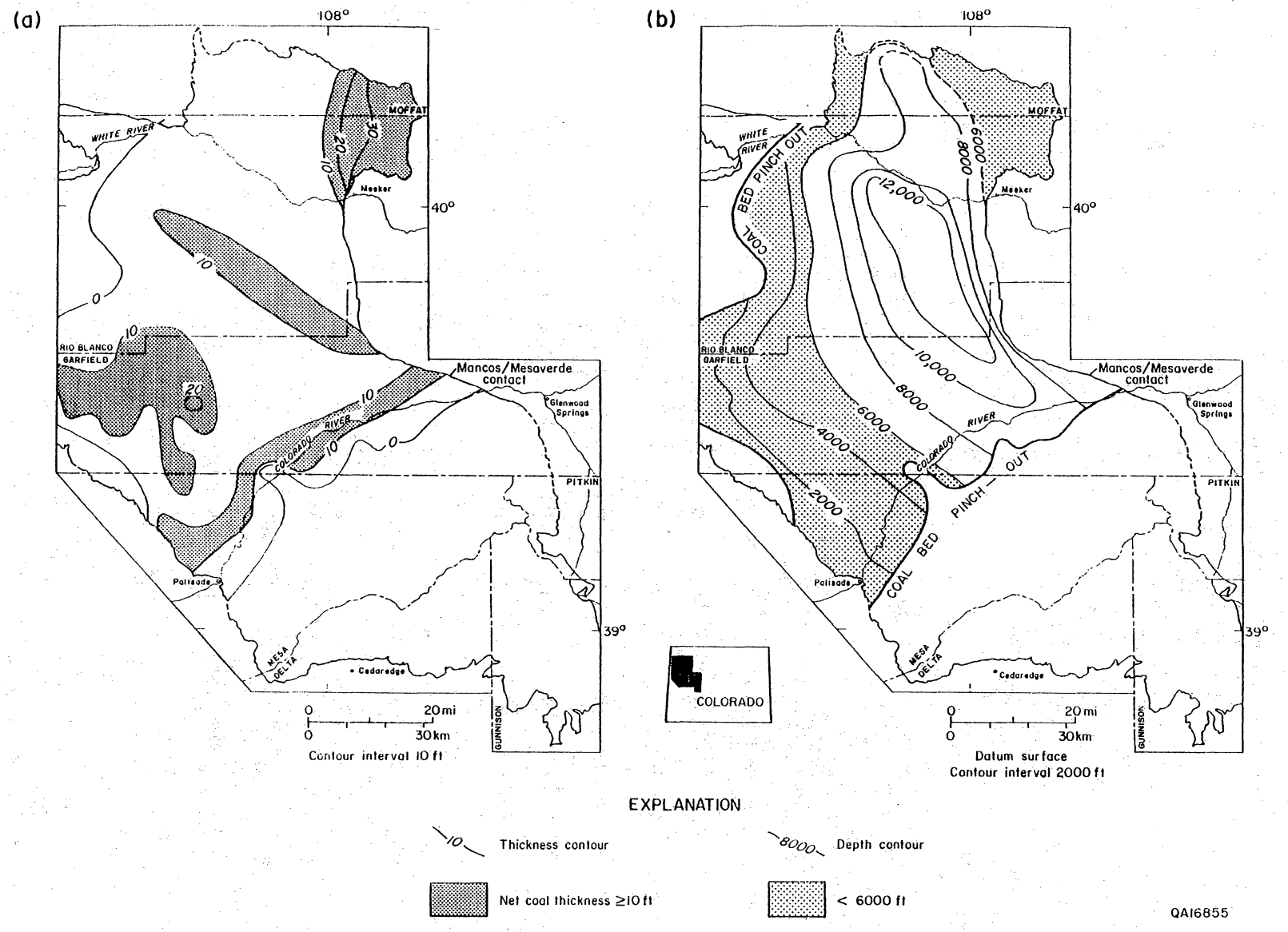

Figure 16. (a) Net coal thickness of the Iles Formation (Black Diamond coal zone) and (b) depth to base of the Iles Formation (Black Diamond coal zone). Modified from McFall and others (1986).

water algal limestones (Collins, 1976). The Williams Fork Formation, as defined here, varies from the traditional stratigraphy of Collins (1976), Johnson (1987, 1989), and Lorenz (1989) (figs. 12 through 14). In this study, the Rollins-Trout Creek shale and overlying sandstone member, which are traditionally assigned to the uppermost part of the underlying Iles Formation, are included with the Williams Fork Formation. Depositionally, the Rollins-Trout Creek shale/sandstone couplet records an episode of marine transgression and subsequent progradation. Thus the progradational Rollins/Trout Creek sequence is genetically coupled with the Williams Fork to define progradational/aggradational couplets. Above the Rollins-Trout Creek, in the southeastern Piceance Basin, the Williams Fork has been divided into major coal-bearing packages: coal package 1, the Cameo-Wheeler-Fairfield coal zone (Bowie Shale Member); coal package 2, the South Canyon coal zone (Bowie Shale Member); coal package 3, the Coal Ridge coal zone (Paonia Shale Member), and finally an upper (very minor) coal package of undifferentiated fluvial sediments (fig. 14). The Cameo-Wheeler-Fairfield and Coal Ridge coal zone intervals are separated by marine tongues of the Mancos Shale and progradational shoreline sandstones of the Middle and Upper Sandstone Members (Reinecke and others, 1991) (fig. 14). Each sequence consists of a basal marine shale and sandstone that is overlain by nonmarine coal-bearing rocks.

Rollins-Trout Creek Shale and Sandstone Member

The Rollins-Trout Creek shale and sandstone member consists of a major transgressive tongue of the Mancos Shale (Young, 1955) and a thick progradational shoreline sandstone, which Collins (1976) interpreted as a prograding bar–beach–delta-front sand complex. This member is less than 100 ft (<30 m) thick in northwestern Mesa County (Dunn and Irwin, 1977), and the sandstone (Rollins-Trout Creek) can reach 125 ft (38 m) in thickness (Warner, 1964). In the Southeastern Piceance Basin (T10S, R89W) the Rollins-Trout Creek shale and sandstone member is greater than 900 ft (>270 m) thick.

Cameo-Wheeler-Fairfield Coal Zone (Bowie Shale Member)

The Cameo-Wheeler-Fairfield coal zone is the major coal-bearing horizon in the Mesaverde Group and composes the lowermost 680 ft (207 m) of the Williams Fork Formation above the Rollins-Trout Creek sandstone member (figs. 12 and 13). It generally consists mostly of shale, interbedded with sandstone and coal beds. Fresh-water swamps in the coal zone formed landward of wave-dominated shoreline deposits of the Rollins-Trout Creek sandstone (Lorenz, 1983b, 1989). These swamp deposits overrode the Rollins-Trout Creek sandstone and with continued progradation of the shoreline, resulted in thick, somewhat continuous coal beds (Collins, 1976). Peat formation was periodically interrupted by transgressions; some lower coal beds are overlain by nearshore-marine and distributary-mouth-bar sandstones that formed the platform for subsequent peat swamps (Bell and Wiman, 1985). These sandstones in the Cameo-Wheeler-Fairfield coal zone are thin, averaging less than 20 ft (<6 m), and occur in strike-elongate sheets crosscut by lenticular sandstone pods, 370 to 520 ft (113 to 159 m) wide (fig. 13) (Lorenz, 1989). Maximum sandstone thickness is 35 ft (11 m), and net sandstone thickness is 70 to 110 ft (21 to 34 m) in the eastern part of the Piceance Basin (Madden, 1985; Lorenz, 1989). Coal beds compose 10 to 15 percent of the Cameo-Wheeler-Fairfield coal zone (Lorenz, 1989). Thickness of individual seams is as great as 35 ft (11 m) on the eastern margin of the basin (Collins, 1976). Net coal thickness ranges from less than 20 ft (<6 m) in the southeast part of the basin to more than 60 ft (>18 m) in the east-central part of the basin (fig. 17) (Johnson 1987, 1989). At the Red Mountain site in northeastern Mesa County, at least five coal beds have a net thickness of more than 50 ft (>15 m). The thickest coal bed (D coal seam, 16 to 20 ft [4.9 to 6.1 m] thick) at the Red Mountain site is in the lower part of the group, 50 to 150 ft (15 to 46 m) above the A coal seam (12 ft [3.7 m] thick) that directly overlies the Rollins Sandstone (Bell and Wiman, 1985). Lower coal beds at the Red Mountain site extend for more than 4 mi (>6.4 km) parallel to depositional strike (Bell and Wiman, 1985). However, these coal beds are locally truncated by crosscutting channel-sandstone deposits (Lorenz, 1983b). Coal-

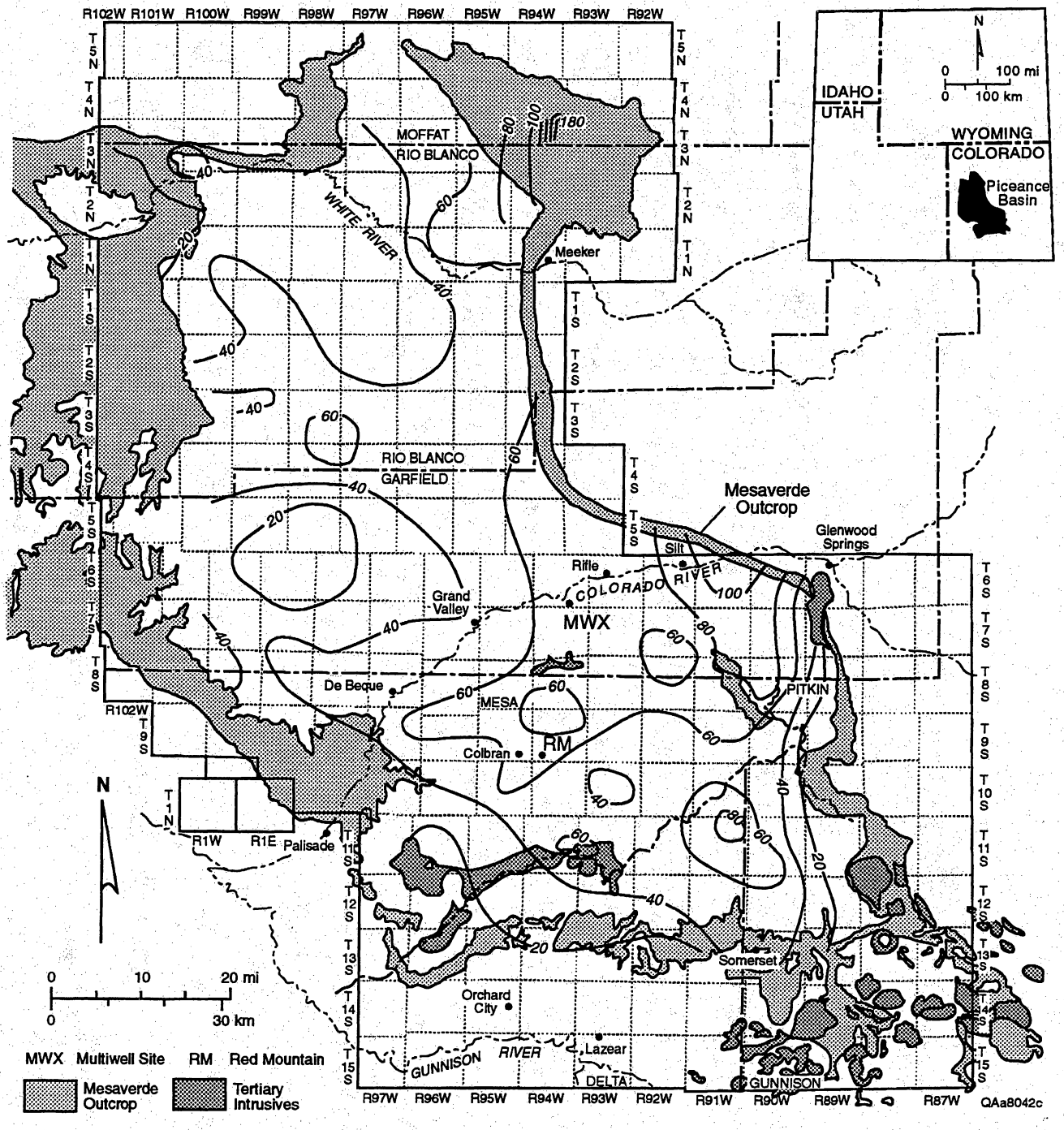

Figure 17. Net coal thickness of the Cameo-Wheeler-Fairfield coal zone. Contour interval 20 ft. Modified from Johnson (1989).

seam splits also occur along margins of channel sandstones. Collins (1976), for example, reported a 35-ft-thick (11-m) coal seam in the east part of the basin splitting into four thinner coal seams over a distance of less than 3,000 ft (<1,200 m). Cameo-Wheeler-Fairfield net coal thickness decreases to less than 20 ft (<6 m) in the southeast part of the Piceance Basin because of seaward (southeastward) pinch-out of the underlying Rollins Sandstone platform into the marine Mancos Shale (Murray and others, 1977).

Although coal beds in the Cameo-Wheeler-Fairfield coal zone are thickest and most continuous in the Piceance Basin, they are more than 6,000 ft (>1,800 m) deep throughout much of the basin, and as much as 10,000 ft (3,050 m) deep in the northeast part of the basin. However, Cameo-Wheeler-Fairfield net coal thickness of more than 40 ft (>12 m) is present in the center and southeast part of the basin, where these coal beds are less than 6,000 ft (<1,800 m) deep (McFall and others, 1986).

South Canyon Coal Zone (Bowie Shale Member)

The South Canyon coal zone occurs directly above the first persistent sandstone outcrop within the Bowie Shale Member (Collins, 1976), locally known as the middle sandstone. Collins (1976) separated the South Canyon coal zone from the Cameo-Wheeler-Fairfield coal zone because of the thick development of coals in that area. Two major coal seams occur in the basal 100 ft (31 m) of the South Canyon coal zone. However, coals in the South Canyon are much less persistent than those in the Cameo-Wheeler-Fairfield, varying widely in thickness from 3 to more than 20 ft (>1 to 6 m) (Collins, 1976).

Coal Ridge Coal Zone (Paonia Shale Member)

The Coal Ridge Group consists of basal marine shale and sandstone that grade upward into nonmarine sandstone, siltstone, shale, and coal (fig. 13) (Lorenz, 1983a). This group has a

gradational upper contact with the overlying, undifferentiated sediments and averages 560 ft (170 m) in thickness in the east part of the basin (Collins, 1976).

Sandstone bedding is variable; the thickest sandstones (12 to 60 ft [3.7 to 18 m] thick, 400 to 600 ft [120 to 180 m] wide) are lenticular in cross section, linear in plan view (Lorenz, 1989) (fig. 13), and are associated laterally with thin-bedded sandstone and siltstone. Coal beds in the Coal Ridge Group vary greatly in thickness over relatively small distances (Collins, 1976). Individual coal beds are commonly less than 5 ft (<1.5 m) thick (Lorenz, 1983b) and occur only in the southeast part of the basin, where as many as 10 coal seams have a net thickness of as much as 40 ft (12 m) (McFall and others, 1986). The coal beds are also discontinuous as a result of having formed in restricted swamps between low-sinuosity distributaries on a low-gradient coastal plain (Lorenz, 1989). These coal beds commonly contain siltstone partings of overbank (levee and splay) origin.

"Undifferentiated" Upper Cretaceous Strata (Undifferentiated Mesaverde Formation [Collins, 1976]; Upper Williams Fork Formation [McFall and others, 1986; Lorenz, 1989])

Upper Cretaceous strata consist of lithologically variable sediments (conglomerate, sandstone, siltstone, shale, coal) that range from 1,500 to 2,000 ft (460 to 610 m) in thickness. Lenticular sandstones and thin-bedded coals are common. Regionally, we tentatively correlated the undifferentiated upper Cretaceous strata with the Lewis/Lance Formation in the Sand Wash Basin. Although this correlation is still to be examined, on the basis of thickness relationships it appears entirely plausible.

Thin, minor coal beds are present in the upper strata, but they are discontinuous and commonly grade into carbonaceous shales interbedded with mudstones and lenticular sandstones (fig. 13). Thickest coal beds (as much as 3 ft [1 m] thick) occur in the east part of the basin (Horn and Gere, 1959). Upper Cretaceous coal beds were deposited in stable floodplains between laterally restricted, anastomosing rivers (Payne and Scott, 1982) or in unstable,

restricted floodplains between meandering streams (Lorenz, 1983a). These coal beds are minor coalbed methane targets.

CONCLUSIONS

The Piceance Basin has a single major coalbed methane target, the Cameo-Wheeler-Fairfield coal zone (Williams Fork Formation, Mesaverde Group), that ranges from 300 to 600 ft (91 to 183 m) thick and lies at an average depth of approximately 6,000 ft (~1,800 m). The most continuous and thickest Cameo coal beds (individual seams from 20 to 35 ft [6 to 11 m] thick) formed in coastal plain environments landward (northwestward) of the progradational delta-front and/or strandplain deposits of the Rollins-Trout Creek sandstone. A more detailed description of the regional genetic stratigraphy and coal occurrence of the Williams Fork Formation follows in the chapter by Tyler and McMurry.

Natural Fracture Attributes and Stress Patterns in the Piceance Basin, Colorado: Controls on Coal Permeability and Coalbed Methane Producibility

Carol M. Tremain and Roger Tyler

ABSTRACT

Regional mapping of natural fracture and cleat sets in sandstones and coal beds of the Upper Cretaceous Mesaverde Group and Tertiary Wasatch and Green River Formations in the Piceance Basin, Colorado, shows that domains of uniformly oriented natural fracture and cleat strike exist. Upper Cretaceous face-cleat domains whose strikes are east-northeast in the southern Piceance Basin and west-northwest in the northern part of the basin are oriented normal to the basin-fold axis and the Grand Hogback thrust front and parallel to the ancient maximum horizontal compressive stresses. Generally, east-northeast-trending face-cleat domains in the southeast part of the basin are oblique to current maximum stress directions, whereas face-cleat domains in the northern half of the basin are parallel to current maximum stress directions. Face cleats in the northern half of the basin, therefore, may provide more permeable pathways for gas production.

Younger and sequentially developed Tertiary (Wasatch and Green River Formations) regional joint sets, termed F_1 (oldest) through F_5 (youngest), also show consistent style and orientation throughout the basin (Grout, 1991; Grout and others, 1991; Grout and Verbeek, 1992). Grout (1991) found that a correlation existed between Tertiary joints in clastic beds and face and butt cleats in Upper Cretaceous coal beds. Most face and butt cleats in the Upper Cretaceous coal beds are of an orientation and fracture style similar to that of the Tertiary F_3 and F_4 joint sets, respectively, and their ages are bracketed at 43 to 10 mya (Grout, 1991c). Further, Lorenz and Finley (1991) found that northwest-trending face cleats measured in the northern basin are consistent with west-northwest regional systematic fractures, to which they

assigned an age of 40 to 36 mya. Thus, according to various studies by both Grout and Lorenz, two opening-mode fracture sets formed at about the same time (~40 mya), suggesting that Upper Cretaceous Mesaverde coals remained unfractured for at least 30 my. It is stressed, however, that similar style and orientation of fractures in different stratigraphic intervals does not imply equivalent age of formation or corresponding genesis. More recent stratigraphic and structural evidence suggests that the Upper Cretaceous face-cleat strike domains are sequential products of the same period of compression (~72–40 mya) that gave rise to the Grand Hogback and associated intrabasin folds. The relative age of Upper Cretaceous and Tertiary fracture sets indicates that the maximum horizontal compressive stress (stress parallel to fracture strike) rotated with time during and following Laramide compressive events. Vertical and lateral extrapolation and lateral correlation of joints and face cleats, therefore, cannot be randomly applied throughout the Piceance Basin to infer similarity of age because differences in lithology, diagenesis, coalification, and burial and thermal histories may cause fractures of different orientation to form in adjacent and overlying strata.

INTRODUCTION

The importance of natural fractures in coal reservoirs is well known. Natural fractures (cleats) are the primary control on coalbed permeability and coalbed methane producibility, and they include regional and local tectonic fracture sets. Locally, cleat sets may be affected by faults, folds, and compactional folding. Cleats in coal are orthogonal fractures that occur normal to bedding and that form during the coalification process; the orientation of cleats is influenced by the maximum horizontal compressive stresses existing during coalification. Coal cleats may be one of the easier regional fracture sets to study because they usually form a single orthogonal fracture set of face and butt cleats, having only rare third- and fourth-order cleat directions. Face cleats are the first formed and usually most prominent joints in coal; other, less planar joints, called butt or end cleats, frequently abut the face cleats at an approximately 90-degree angle. Both types of cleats are normal to bedding.

To study the natural fracture and cleat attributes in the Piceance Basin coals and adjacent sandstones, we compiled data from the literature and made field observations in the basin. Numerous fracture studies have been undertaken in the Piceance Basin (Murray, 1967; Amuedo and Ivey, 1978; Smith and Whitney, 1979; Smith, 1980; Jamison and Stearns, 1982; Grout and Verbeek, 1983; Verbeek and Grout, 1983, 1984a, b; Grout, 1991; Grout and others, 1991; Lorenz and Finley, 1987a, 1991; Lorenz and Hill, 1991, 1994; Tyler and others, 1991a, b, 1993; Tremain and Tyler, this volume and references therein). However, observations of cleat characteristics are dependent on the quality of coal exposures. Easily accessible coal mines and coal outcrops in the Mesaverde Group are concentrated in the southern part of the basin, as are cleat observations. Only two operating mines are located in the northern half of the basin, the Deserado (T2N-T3N, R101W), in the northwest corner of the Piceance Basin, near Rangely, and the Colowyo (T2N-T3N, R93W), in the northeast corner, near Meeker. Coals on the steeply dipping Grand Hogback on the eastern edge of the basin are at high elevation and are not well exposed nor readily accessible. Coals are also less accessible on the northern and western basin margins.

Recently, natural fracture systems in the sandstones and coal beds have also been studied in order to aid tight gas and coalbed methane exploration in this and other western basins (Lorenz and Laubach, 1994; Laubach and others, 1992a, b). The value of this research is indicated by the number of public and private investigations that have been or are currently being undertaken in the area. Much of the publicly available fracture work has been performed with U.S. Department of Energy (DOE; Multiwell and Slant Hole Completion Test Sites) and Gas Research Institute (GRI; Red Mountain Site) funding during tight gas sandstone and coalbed methane research. The DOE is currently funding a fracture-detection and modeling project by Advanced Resources International and a proprietary cleat study (Small Business Innovation Research Grant) on the northern margin of the basin. In addition, a Denver consulting group has recently made a public offering of fracture and basement structure analyses for various sections of the basin. Two general types of natural fracture systems have been documented:

regional fracture sets and fracture sets associated with specific folds or faults (Kelley and Clinton, 1960; Lorenz and Finley, 1987a). The following is a summary of some of the observations of natural fracture and cleat attributes in the Piceance Basin.

NATURAL FRACTURE PATTERNS AND CLEAT ATTRIBUTES IN THE PICEANCE BASIN

Cleat Strike Domains in Mesaverde Group and Wasatch Formation Coal Beds: A Review

The accumulated fracture data set for the Mesaverde Group suggests that face cleats in the Piceance Basin form two broad regional fracture domains—an east-northeast-trending fracture domain in the southern part of the basin and a west-northwest-trending fracture domain in the northern part of the basin (fig. 18). Richardson (1909) may have made the earliest reported face-cleat orientation observation when he noted trends of N65-75°E at the Book Cliff mine (sec. 8, T10S, R99W) about 12 mi north of Grand Junction. Lee (1912) did extensive work in numerous small mines in the southern Piceance Basin. He reported generally northeast-trending face cleats in the Book Cliffs (T7S-T10S, R102W-R98W), Grand Mesa (T12S-T13S, R97W-R93W), and Somerset (T13S, R92W-R89W) fields along the southern margin of the basin and in the Crested Butte coal field (T14S-T15S, R86W) in the extreme southeast corner of the basin (fig. 18). Lee (1912) also noted one mine in the Crested Butte field in which the face-cleat trend changed from N55°W to N50°E. He observed disturbances in the cleat near faults such as those at the Bulkley mine (sec. 11, T14S, R86W), where the faulted area contained "contorted laminae, warped cleat faces, and crushed coal." Boreck and Strever (1980) did a cleat and joint study at the Hawk's Nest mine (T13S, R90W) and found a mean face-cleat trend of N70-90°E and butt-cleat trend of N10-20°W. Surface joints they measured at the mine trend N80-90°E and N20-30°W. Hucka and others (1990) made a cleat and joint study at the Dutch Creek mine (T10S, R89W) and reported a face cleat of N15°W and major surface sandstone joints of N75°E. Khalsa and Ladwig (1981) also reported both northeast and northwest face-cleat strikes in several mines in the southeast corner of the basin. Geological Services of Tulsa,

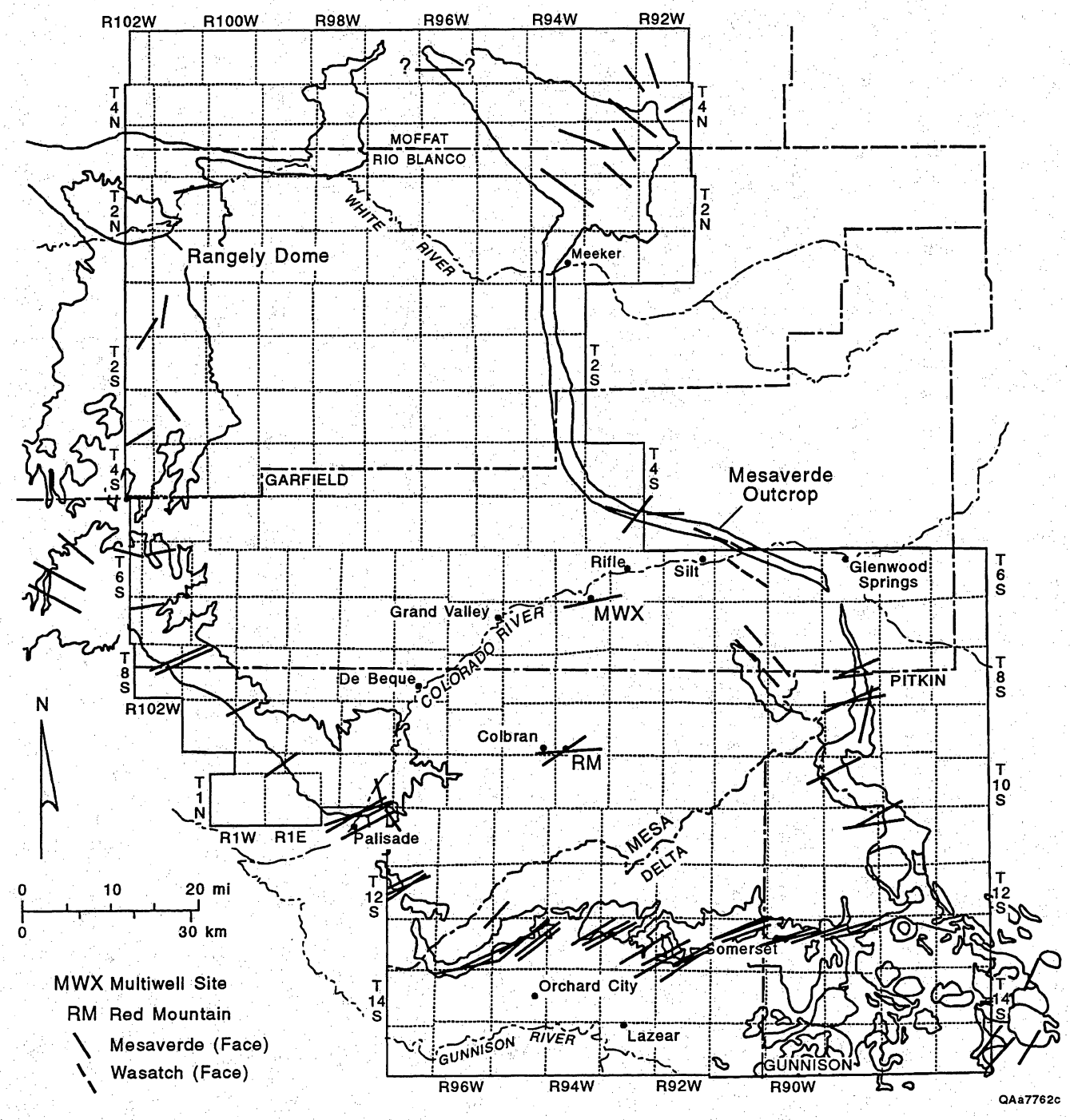

Figure 18. Face-cleat strikes and domains in the Mesaverde Group and Wasatch Formation coal beds, Piceance Basin. Cleat orientations were obtained during field work by the authors and from studies by Richardson (1909), Lee (1912), Boreck and Strever (1980), Geological Services of Tulsa (1980), Khalsa and Ladwig (1981), Logan and others (1986), Finley and Lorenz (1988), Jeu and others (1988), and Grout (1991).

Inc. (1980) performed a cleat study along the margin of the southern half of the basin and found a "relatively uniform" east-northeast trend to the face cleat. Recent studies of cleat and fracture trends in the southern part of the basin have been published by Grout (1991), Grout and others (1991), and Grout and Verbeek (1992). A brief summary of their conclusions follows.

Cleat sets in Upper Cretaceous Mesaverde Group and lower Tertiary Wasatch coal beds, both in the Piceance Basin and in the bounding Grand Hogback monocline, can be correlated on the basis of joint style, relative age, and orientation with sets of regional extension fractures in the enclosing clastic rocks (Grout, 1991; Grout and others, 1991; Grout and Verbeek, 1992). Two to three of the joint sets (the Hogback system) predate Laramide thrust-fold events and are exposed in the monocline and along a narrow basinward strip adjacent to it. Face-cleat sets in the monocline correlate with two prominent joint sets in clastic rocks whose strikes are east-northeast (older set) (Grout, unpub. data) and west-northwest (younger set) (Grout, 1991; Grout and others, 1991; Grout and Verbeek, 1992). Butt cleats correlate with a younger set of joints whose strikes average north-northwest. The rocks that contain these three sets were passively rotated on the basinward flank of the monocline above the Laramide fold-thrust system. Stratigraphic and structural evidence summarized in Grout and Verbeek (1992) suggests that at least two of these fracture sets are sequential products of the same period of compression that later gave rise to the Grand Hogback and associated intrabasin folds. Grout and others (1991) concluded that these cleat sets should not be found much farther than about 12 mi (20 km) into the basin, the limit of Laramide thrust and splay faulting. However, recent seismic data indicate that thrust faulting is more regionally extensive than previously thought (Gunneson and others, 1994) and face-cleat orientation and paleostresses may have extended, or influenced cleat genesis, across the basin. Face cleats in angled core recovered from correlative-age strata at the MWX site (Lorenz and Hill, 1991), 10 mi (16 km) southwest of the monocline (fig. 18), probably correspond in part to one or both of the face-cleat sets in the monocline.

We measured cleat orientations at 33 stations in the Piceance Basin in coals of the Williams Fork Formation (figs. 18 and 19). Most face-cleat orientations that we observed in the northern half of the basin trend northwest. This fracture domain parallels the current maximum stress direction (Tyler and others, 1991a, b) and corresponds to the northwesterly Williams Fork face-cleat domain as seen in the Sand Wash Basin (Tyler and others, 1994). In the southern half of the basin, most of the face-cleat trends are oriented east-northeast, forming a southern fracture domain. There is also evidence of an east-west face-cleat domain (or overlapping, crosscutting face-cleat domain) along the Grand Hogback monocline, near Rifle Gap (T5S, R93W) that extends into the basin toward the Multiwell and Red Mountain sites (fig. 18). Regionally it is proposed that these face-cleat domains are oriented orthogonal to the thrust front along the Grand Hogback, parallel to the maximum horizontal compressive stresses that existed at the time of cleat formation (Tyler and others, 1992, 1993, 1994).

Further, some northwest-trending face cleats were found on the southwestern margin of the basin, on the western flank of the Douglas Creek Arch (fig. 18). The northwest orientation of the face-cleat strike has been correlated into the Book Cliffs of Utah. Other variations to the dominant regional trends occur in areas of local structural disturbance such as (a) in the folded, faulted, and intruded Crested Butte coal field (T14S-T15S, R86W), (b) at Rifle Gap (T5S, R93W) near the flexure or strike slip zone in the Grand Hogback, (c) at Coal Basin Anticline (T10S, R89W), and (d) at Divide Creek Anticline (T8S, R91W).

Locally, on outcrop scale, correlation between face-cleat trends and the systematic or major joint trends in surrounding rock varies. For instance, at an outcrop in Coal Canyon near the Cameo mine, face and butt cleats did correlate with systematic and nonsystematic joint directions in an overlying sandstone. However, at the Deserado mine in the northwest part of the basin, the face-cleat trend was N80°E to N100°E, whereas the systematic trend in the overlying sandstone was N60°W. One cleat direction from oriented core in the MWX 3 well also had a east-northeast trend (N85°E), different from the predominant west-northwest trend of the other fractures measured in the hole. This may just be an example of what Hancock (1985)

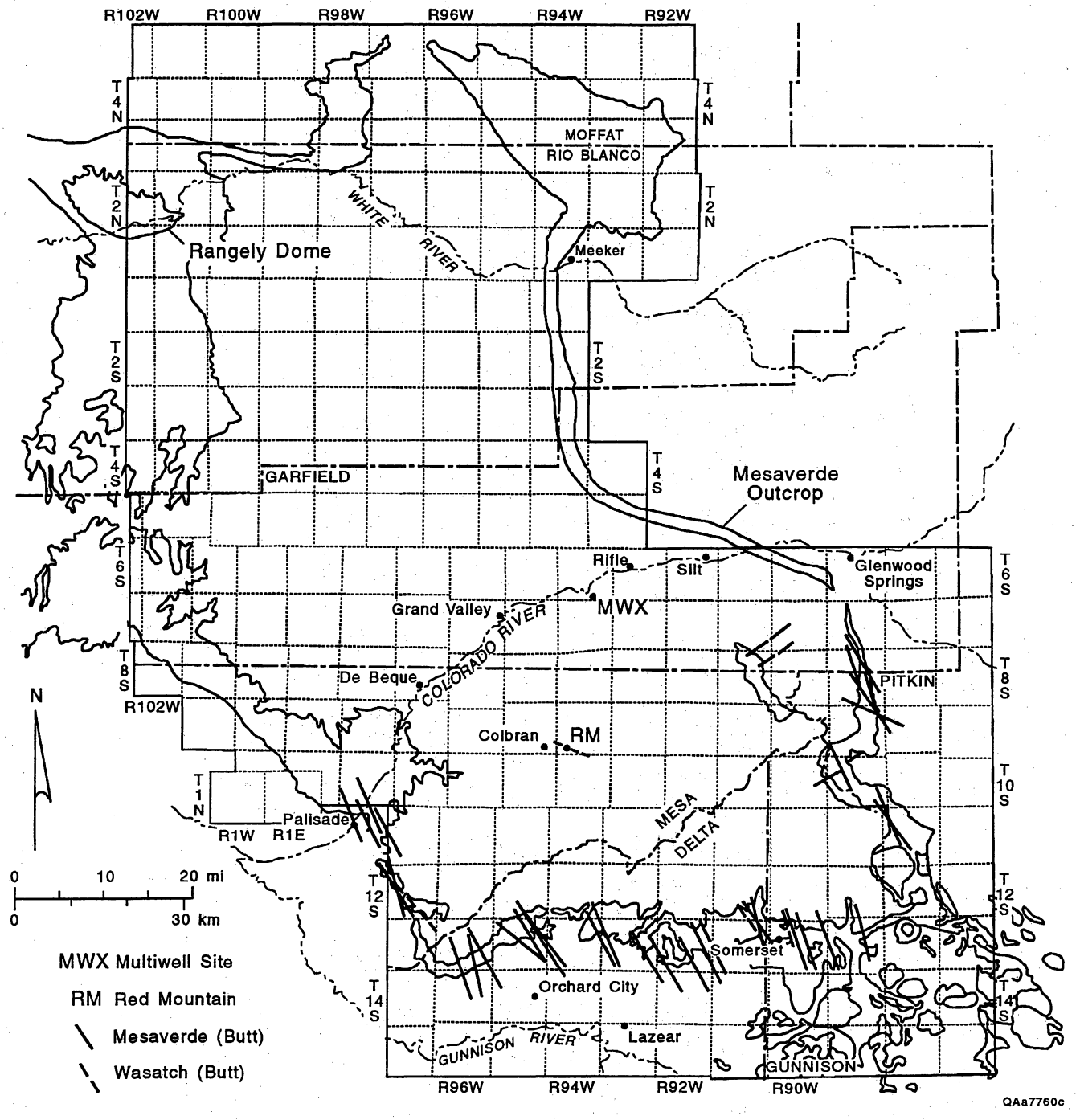

Figure 19. Butt-cleat strikes and domains in the Mesaverde Group and Wasatch Formation coal beds, Piceance Basin. Cleat orientations were obtained during field work by the authors and from studies by Boreck and Strever (1980), Geological Services of Tulsa (1980), Khalsa and Ladwig (1981), and Grout (1991).

calls "lithologically controlled refraction" of joint trends, or it may have other stress shifting significance; overlapping cleat and fracture domains still must be defined.

Joint Strikes in the Wasatch Formation and Green River Formation Sandstones: A Review

Younger and sequentially developed Tertiary (Wasatch and Green River Formations) sandstone joint sets, termed F_1 (oldest) through F_5 (youngest), show consistent style throughout the basin (Grout, 1991; Grout and others, 1991; Grout and Verbeek, 1992). Early-formed F_1 (north-northwest-striking; fig. 20) and F_2 (west-northwest-striking; fig. 21) joint sets are present chiefly in the northern two-thirds of the basin, whereas the intermediate-age F_3 (east-northeast-striking; fig. 22) joint set dominates the fracture network in the south half of the basin (Grout, 1991; Grout and others, 1991; Grout and Verbeek, 1992). The F_4 joints (north-northwest-striking; fig. 23) are abundant throughout the basin, but the F_5 joints are sparse, occurring only in Eocene oil shales. The age of Tertiary fractures is constrained by structural, stratigraphic, and geomorphic evidence and is bracketed at 43 to 10 m.y. old (Grout, 1991; Grout and others, 1991; Grout and Verbeek, 1992).

Cleat Domains and Joint Strikes and Attributes of the Mesaverde Group and Wasatch and Green River Formations: A Comparison

A correlation exists between the orientation of Tertiary joints in clastic beds and the orientation of face and butt cleat domains in Upper Cretaceous and lower Tertiary coal beds in the Piceance Basin. Most face and butt cleats in the Upper Cretaceous and lower Tertiary coal beds are of an orientation and fracture style similar to that of the Tertiary F_3 and F_4 joint sets, respectively (Grout, 1991; Grout and others, 1991; Grout and Verbeek, 1992). For example, in the southeastern Piceance Basin, Mesaverde and Wasatch face-cleat domains trend east-northeastward (N50°E-N86°E; Grout, 1991, and references therein; fig. 18) and are correlated in orientation with the Tertiary F_3 joint set (fig. 22) that is both prominent and abundant in the sandstones in this area (Grout, 1991; Grout and others, 1991; Grout and Verbeek, 1992).

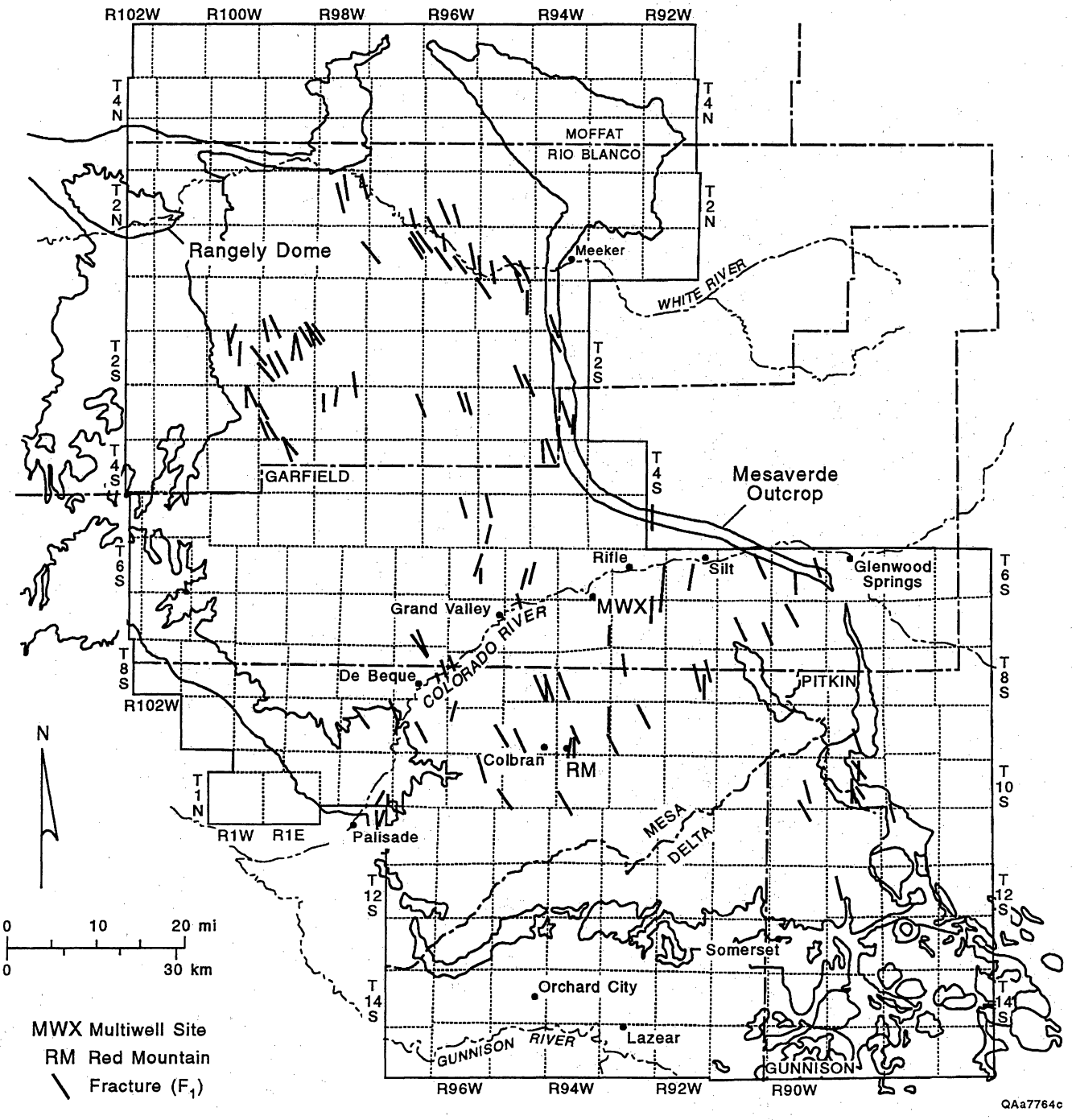

Figure 20. Regional distribution and orientations of F_1 joint sets in the Piceance Basin. F_1 joints occur predominantly in the Green River and Wasatch Formations. After Grout and Verbeek (1992).

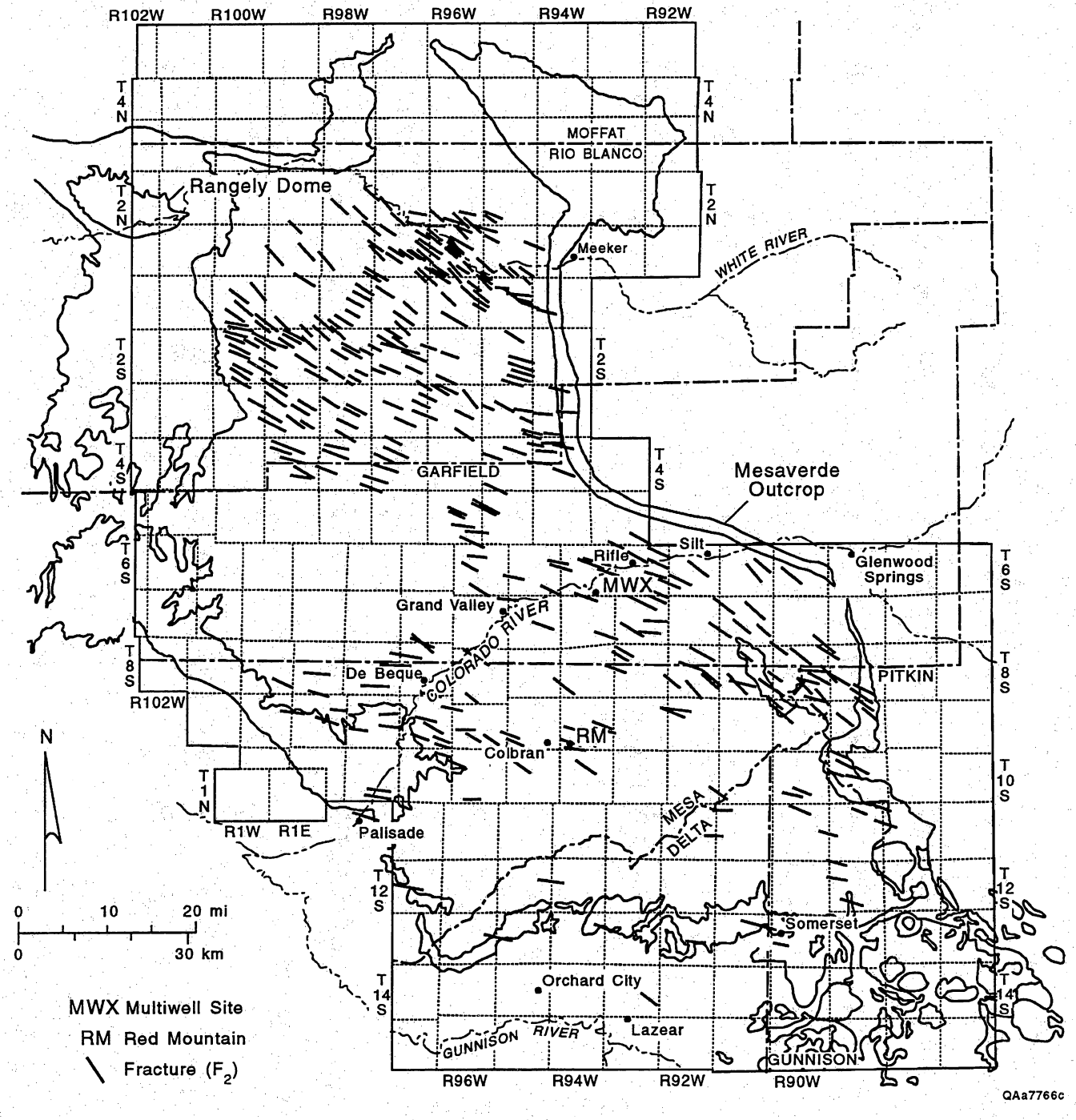

Figure 21. Regional distribution and orientations of F_2 joint sets in the Piceance Basin. F_2 joints occur predominantly in the Green River and Wasatch Formations. After Grout and Verbeek (1992).

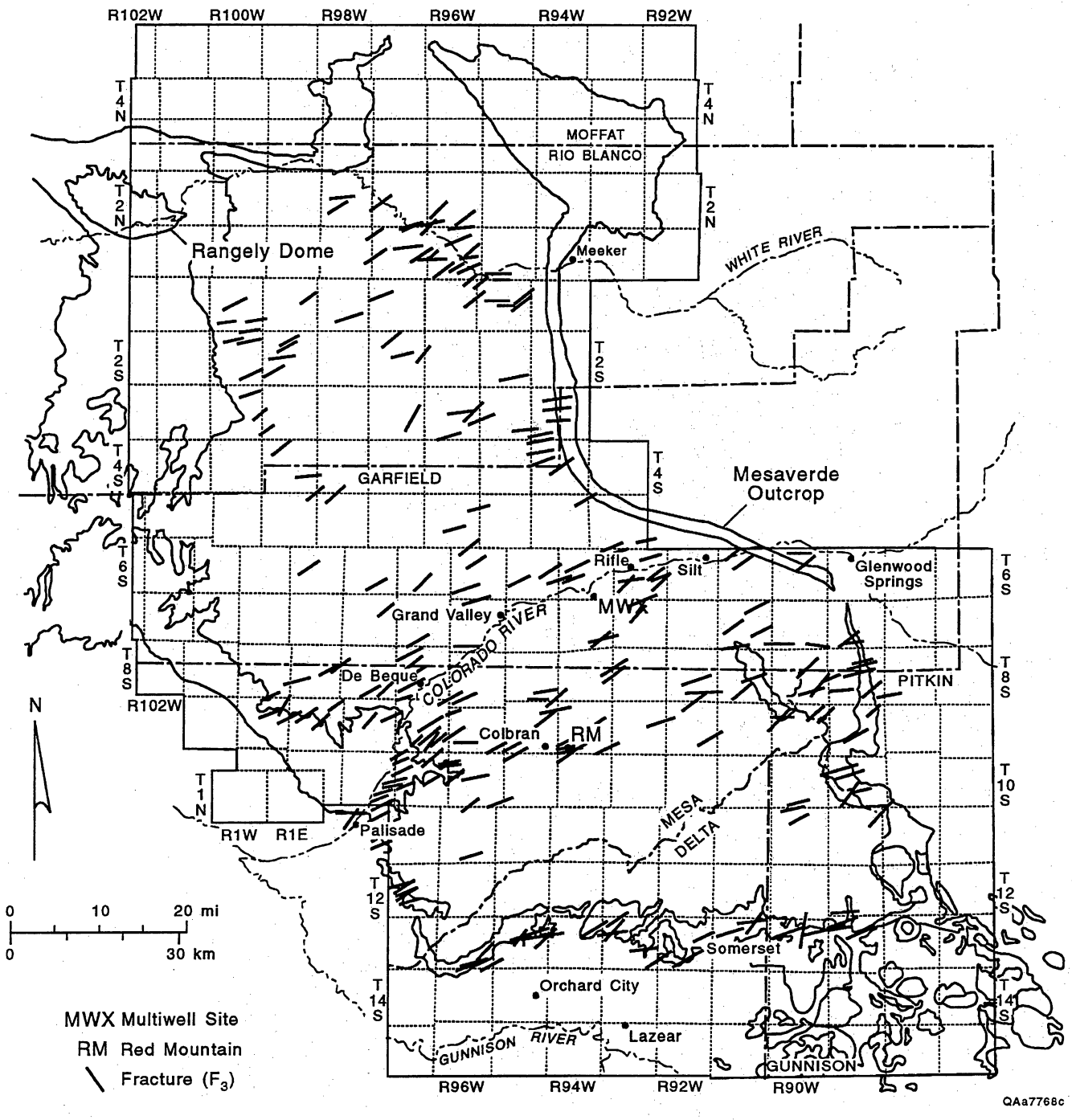

Figure 22. Regional distribution and orientations of F_3 joint sets in the Piceance Basin. F_3 joints occur predominantly in the Green River and Wasatch Formations. After Grout and Verbeek (1992).

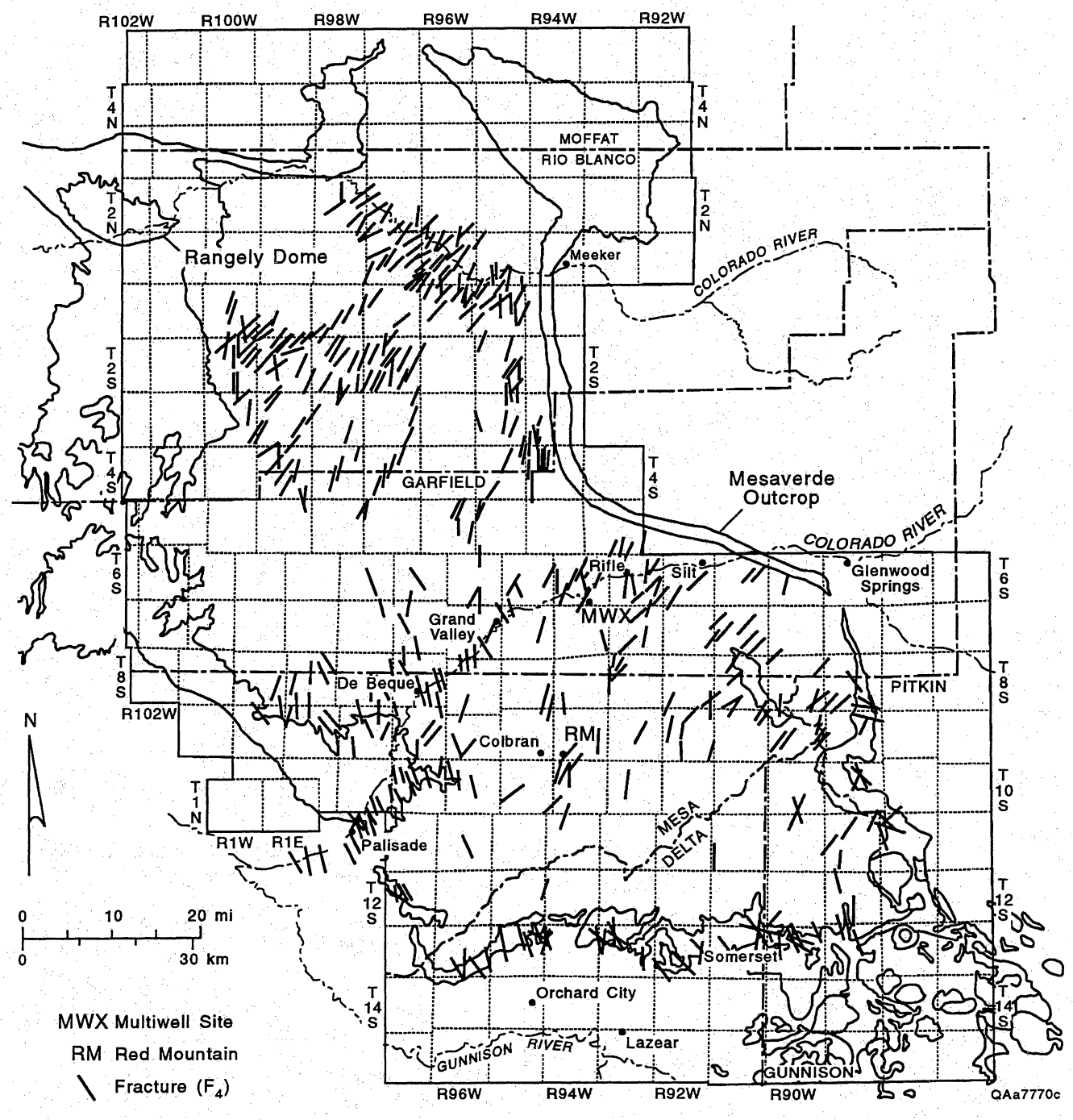

Figure 23. Regional distribution and orientations of F_4 joint sets in the Piceance Basin. F_4 joints occur predominantly in the Green River and Wasatch Formations. After Grout and Verbeek (1992).

Butt-cleat domains strike between N10°W and N30°W (fig. 19) and correlate with the fourth-formed (F_4; fig. 23) regional joint set in the Piceance Basin. Locally, abutting relations confirm the presence of older face cleats that strike N50-70°W and N5-20°W, which correlate with the second- (F_2; fig. 21) and first-formed (F_1; fig. 20) regional basin sets, respectively. Face cleats in Wasatch coal stringers on the Divide Creek Anticline are younger than those along the monocline; they are vertical and strike N38°-47°W (Grout, 1991; Grout and others, 1991). The relative age of these fracture sets, established by abutting relations, indicates that the maximum horizontal compressive stress (stress parallel to fracture strike) rotated counterclockwise with time from N50°W to N10°W, following Laramide compressive events (Verbeek and Grout, 1986). The age of coal cleat and sandstone fracture sets is also bracketed at 43 to 10 mya ago (Grout and Verbeek, 1992).

Timing of Cleat and Sandstone Fracture Development: A Discussion

In describing the timing of cleat formation in the southern half of the basin, Grout (1991) correlated cleats with similar trending joints in the area and concluded that cleats and adjacent joint sets were formed at the same time. Grout and Verbeek found five separate joint sets in the basin (figs. 20–23). Younger and sequentially developed Cretaceous and Tertiary regional joint sets, termed F_1 (oldest) through F_5 (youngest), show consistent style throughout the basin. Grout found a correlation between the orientation of Tertiary joints in clastic beds and the orientation of Upper Cretaceous face and butt cleats in coal beds in the Piceance Basin. Fracture (cleat) sets in Upper Cretaceous Mesaverde Group and lower Tertiary prefold face cleats in the Grand Hogback monocline in the south half of the basin strike east-northeastward (M. A. Grout, unpub. data) and west-northwestward. Prefold butt cleats strike north-northwestward. Grout found that most of the cleats in the Upper Cretaceous coal beds are of an orientation and fracture style similar to that of the Tertiary F_3 and F_4 joint sets.

On the eastern side of the basin, Grout and other authors (Boreck and Strever, 1980; Kent and Arndt, 1980) found that the rocks that contain the cleats were passively rotated on the

basinward flank of the monocline above the Laramide fold-thrust system. Stratigraphic and structural evidence suggests that the face-cleat sets are sequential products of the same period of compression that later gave rise to the Grand Hogback monocline and associated intrabasin folds (Grout and Verbeek, 1992). Face cleats in angled core recovered from correlative-age strata at the U.S. Department of Energy and Gas Research Institute Multiwell (MWX) site, 5 mi (8 km) southwest of the monocline, probably correspond in part to one of the east-northeast face-cleat sets in the monocline.

In the southeastern Upper Cretaceous outcrop, the face cleats trend east-northeastward and are correlated in style and orientation with the Tertiary F_3 joint set that is both prominent and abundant in the sandstones in this area (Grout, 1991; Grout and others, 1991). In the De Beque Canyon and Grand Mesa areas, most of the Upper Cretaceous face cleats strike from 060° to 066°, and at the Red Mountain site and along the south rim of the basin from 050° to 086°. In the center of the basin, these face cleats correlate with the F_3 fractures exposed in the Wasatch Formation (Grout, 1991). However, face cleats in lower Tertiary coaly stringers on the Divide Creek Anticline are subvertical and strike 313°-322° (Grout, 1991). The age of these fractures is bracketed at 43 to 10 m.y. old (Grout, 1991).

Further, Grout and Verbeek (1992) found that fractures trend northwesterly in the northern two-thirds of the basin and northeasterly in the southern half of the basin. In the southern part of the basin, face-cleats trend east-northeast and are no older than 43 mya and postdate northwest-trending fractures (Grout and Verbeek, 1992). Northwest-trending face cleats measured in the northern basin are consistent with west-northwest regional, systematic fractures assigned an age of 40 to 36 mya by Lorenz and Finley (1991). Thus, according to various studies by both Grout and Lorenz, two of the oldest opening-mode fracture sets of different orientation formed at about the same time (~40 mya) in response to ancient maximum horizontal compressive stresses (Hancock and Bevan, 1987; Pollard and Aydin, 1988), implying that the coal beds lay uncleated for at least 30 m.y. Experience in the Rocky Mountain foreland indicates that cleating of coal begins early in the coalification process. Coals

are cleated in the Texas Gulf Coast lignites. The formation of these fractures implies either (1) different ages of formation, (2) rotation parallel to maximum horizontal compressive stresses, or (3) cleat formation at similar times but different orientations. All of these conditions could possibly result in overlapping and interfering cleat domains.

New Perspective

Cleat forms early in coalification as peat undergoes metamorphism to coal and is a function of the coal's maturity; cleat occurs in coal as low rank as lignite. Furthermore, face-cleat trends in superposed beds are usually similar (Tremain and others, 1991). Sandstone fracturing, however, depends less on the age of the strata than on the degree of cementation and lithification and consequent competence for fracturing. As Lorenz and Laubach (1994) found in studies of Cretaceous Frontier sandstones, "adjacent sandstone beds . . . may contain dissimilar fracture sets . . . dependent on the petrophysical properties of the rocks, properties which controlled the susceptibility of the rock to fracturing over time, and which are in turn a product of its composition and diagenetic history." The authors noted similar varying fracture trends in Mesaverde sandstones along the northern part of the Grand Hogback. In addition, the influence of surficial stress relief fractures on prevailing fracture patterns has yet to be addressed. As early as 1909, Richardson observed that in the orthogonal joints he observed in the Book Cliffs, one set of joints "is parallel to the face of the cliffs" and "the escarpment is gradually being worn back by blocks of sandstone breaking along these cracks." Indeed, Lorenz and others (1993) suggested Grout's F_4 set, which has not been documented in the subsurface, may consist solely of surficial stress-release fractures that formed normal to the F_2 regional fracture set. They also found a "related phenomena" of microcrack development in MWX core normal to the maximum horizontal stress direction after the core was brought to the surface.

Grout's interpretation that the timing of cleat formation correlates with the timing of adjacent sandstone fracturing (F_3 and F_4) in the basin interior suggests that Mesaverde coals had to have remained "unfractured for tens of millions of years" (Grout, 1991). Grout (1991),

who ordered the relative age of formation of cleat sets in coal with joint sets in clastic rock, as confirmed by consistent abutting relations in the southern Piceance Basin, disregarded stratigraphic formational constraints (tables 1 and 3), coal rank or maturity, and evidence of how early cleat can form in coalification. When the authors added geologic formational constraints to Grout's cleat table (tables 1 and 3) and then rearranged the table by formation age (tables 2 and 4), we found a general sequential east-northeast trend to face cleats in lower Williams Fork coals in the southern Piceance Basin, shifting to northwesterly trending face cleats in the uppermost Tertiary coals and sandstones. We would like to stress that similar style and orientation of fractures in different stratigraphic intervals does not imply equivalent age of formation or corresponding genesis. Therefore, the Mesaverde fractures of Grout and Verbeek (1992) need not be of Eocene and younger age. Importantly, the relative age of Upper Cretaceous and Tertiary fracture sets, established by abutting relations, indicates that the maximum horizontal compressive stress (stress parallel to fracture strike) shifted with time during and following Laramide compressive events. Vertical and lateral extrapolation and lateral correlation of joints and face cleats, therefore, cannot be randomly applied throughout the Piceance Basin because differences in lithology, diagenesis, coalification, burial, and thermal histories may cause fractures of different orientation to form in adjacent and overlying strata.

Further, Lorenz and Finley (1991), who have modeled fracture patterns within the Piceance Basin and along the Grand Back Hogback monocline, show a fan-shaped fracture pattern radiating across the Piceance Basin in front of the White River Uplift thrust fault, which acts as a point source (fig. 24a). The measured array of F_2 (predominantly Green River Formation) and F_3 (predominantly Wasatch Formation) strikes were taken together with fracture strikes from the Mesaverde Group sandstone and coal beds and plotted on figure 24a. These fracture patterns were then duplicated using analytical models of localized indentors, where superimposed stresses from westward indentation of (1) the northern and (2) the southern segments of the White River Uplift onto (3) a regional west-northwest compressive stress, with a stress ratio of 8:6:1, respectively (Lorenz and Finley, 1991) (fig. 24b). However,

TABLE 1
NATURAL FRACTURE SETS IN THE SOUTHERN PICEANCE BASIN

Relative Age and Orientation	Fracture and Location	Relative Abundance	Group/ Formation
OLDEST			
N. 28°–55° W.	Local fold–parallel sets in sandstones (Divide Creek Anticline)	moderate	WTCH
N .38°–47° W.	Face cleats (Divide Creek Anticline)	abundant	WTCH
N. 37°–40° W.	Face cleats (Coal Basin area)	sparse	MVRD/WTCH
N. 6°–36° W.	F_1 in sandstones (Divide Creek Anticline)	sparse	WTCH
N. 5°–20° W.	F_1 in sandstones (southern basin)	sparse	WTCH
N. 14° W.	Face cleats (Colorado River area)	sparse	WTCH
N. 46°–74° W.	F_2 in sandstones (Divide Creek Anticline)	abundant	WTCH
N. 60°–85° W.	F_2 in sandstones (southern basin)	moderate	MVRD/WTCH
N. 51°–70° W.	Face cleats (Colorado River and Coal Basin areas)	sparse	MVRD/WTCH
N. 74° W.	Butt cleats (Red Mountain site cores) (Horner, 1986)	sparse	MVRD
N. 70°–90° E.	Face cleats (southern basin rim) (Borek and Strever, 1981)	abundant	MVRD
N. 51°–87° E.	Face cleats (southern basin rim) (Geological Services of Tulsa, 1980)	abundant	MVRD
N. 62°–73° E.	Face cleats (Colorado River and Coal Basin areas)	abundant	MVRD/TERT
N. 50°–86° E.	Face cleats (Red Mountain site cores) (Seccombe and Decker, 1986; Horner, 1986)	abundant	MVRD
N. 50°–90° E.	F_3 in sandstones (southern basin)	very abundant	WTCH/TERT
N. 54°–88° E.	F_3 in sandstones (Divide Creek Anticline)	abundant	WTCH/TERT
N. 40°–57° E.	Butt cleat (Divide Creek Anticline)	few measured	WTCH
N. 35° W.–N. 44° E.	F_4 in sandstones (southern basin)	abundant	WTCH
N. 10°–20° W.	Butt cleats (Borek and Strever, 1980)	abundant	MVRD
N. 19°–31° W.	Butt cleats (Colorado River and Coal Basin areas)	abundant	MVRD
N. 11°–55° W.	Butt cleats (southern basin rim) (Geological Services of Tulsa, 1980)	abundant	MVRD
N. 55°–80° W.	F_5 in sandstones (southern basin)	sparse	GREEN RIVER
YOUNGEST			

SOURCE: Modified from Grout (1991). MVRD–Mesaverde; WTCH–Wasatch; TERT–Tertiary.
*Note that even through the fracture and cleat sets formed sequentially, they formed in a rotational stress field (Verbeek and Grout, 1986); some fracture and cleat orientations of one set, therefore, may be nearly coincident with some of those of another set.

TABLE 2
NATURAL FRACTURE SETS IN THE SOUTHERN PICEANCE BASIN (STRATIGRAPHICALLY ORDERED)

Relative Age and Orientation	Fracture and Location	Relative Abundance	Group/ Formation
OLDEST			
N. 70°–90° E.	Face cleats (southern basin rim) (Borek and Strever, 1981)	abundant	MVRD
N. 51°–87° E.	Face cleats (southern basin rim) (Geological Services of Tulsa, 1980)	abundant	MVRD
N. 50°–86° E.	Face cleats (Red Mountain site cores) (Seccombe and Decker, 1986; Horner, 1986)	abundant	MVRD
N. 62°–73° E.	Face cleats (Colorado River and Coal Basin areas)	abundant	MVRD
N. 10°–20° W.	Butt cleats (Borek and Strever, 1980)	abundant	MVRD
N. 19°–31° W.	Butt cleats (Colorado River and Coal Basin areas)	abundant	MVRD
N. 11°–55° W.	Butt cleats (southern basin rim) (Geological Services of Tulsa, 1980)	abundant	MVRD
N. 74° W.	Butt cleats (Red Mountain site cores) (Horner, 1986)	sparse	MVRD
N. 37°–40° W.	Face cleats (Coal Basin area)	sparse	MVRD/WTCH
N. 51°–70° W.	Face cleats (Colorado River and Coal Basin areas)	sparse	MVRD/WTCH
N. 38°–47° W.	Face cleats (Divide Creek Anticline)	abundant	WTCH
N. 6°–36° W.	F_1 in sandstones (Divide Creek Anticline)	sparse	WTCH
N. 5°–20° W.	F_1 in sandstones (southern basin)	sparse	WTCH
N. 14° W.	Face cleats (Colorado River area)	sparse	WTCH
N. 28°–55° W.	Local fold-parallel sets in sandstones (Divide Creek Anticline)	moderate	WTCH
N. 46°–74° W.	F_2 in sandstones (Divide Creek Anticline)	abundant	WTCH
N. 60°–85° W.	F_2 in sandstones (southern basin)	moderate	MVRD/WTCH
N. 50°–90° E.	F_3 in sandstones (southern basin)	very abundant	WTCH/TERT
N. 54°–88° E.	F_3 in sandstones (Divide Creek Anticline)	abundant	WTCH/TERT
N. 40°–57° E.	Butt cleat (Divide Creek Anticline)	few measured	WTCH
N. 35° W.–N. 44° E.	F_4 in sandstones (southern basin)	abundant	WTCH
N. 55°–80° W.	F_5 in sandstones (southern basin)	sparse	GREEN RIVER
YOUNGEST			

SOURCE: Modified from Grout (1991). MVRD–Mesaverde; WTCH–Wasatch; TERT–Tertiary.

TABLE 3
AVERAGE COAL CLEAT ORIENTATION IN UPPER CRETACEOUS MESAVERDE GROUP AND PALEOCENE AND EOCENE WASATCH FORMATION, SOUTHERN PICEANCE BASIN, COLORADO

Location	Average Orientation		Group/ Formation
	Face Cleats	Butt Cleats	
Divide Creek Anticline (Grout, 1988)	N. 38°–47° W.	N. 40°–57° E.	WTCH
DeBeque Canyon, Colorado River area (Grout and Verbeek, 1985)		N. 14° W.	MVRD
		N. 70° W.	MVRD
	N. 62°–66° E.	N. 19°–31° W.	MVRD
Colorado River area, eastern Piceance Basin (Grout, 1988)	N. 51°–65° W.		WTCH
Red Mountain site cores (Seccombe and Decker, 1986; Horner, 1986)		(N. 74° W.?)	MVRD
	N. 69°–86° E.		MVRD
	N. 50°–63° E.		MVRD
Coal Basin area (Grout, 1991)	N. 37°–40° W.		WTCH/MVRD
	N. 56° W.	N. 35° E.	WTCH/MVRD
	N. 73°E.	N. 19° W.	MVRD
Grand Mesa and Gunnison River area (Grout, 1991)	N. 60°–86° E.	N. 19°–30° W.	MVRD
Gunnison River area mines (Boreck and Strever, 1980)	N. 70°–90° E.	N. 10°–20° W.	MVRD
Southern Piceance Basin (Geological Services of Tulsa, 1980)	N. 51°–87° E.	N. 11°–55° W.	MVRD

SOURCE: Modified from Grout (1991). MVRD–Mesaverde; WTCH–Wasatch.

TABLE 4
AVERAGE COAL CLEAT ORIENTATION IN UPPER CRETACEOUS MESAVERDE GROUP AND PALEOCENE AND EOCENE WASATCH FORMATION, SOUTHERN PICEANCE BASIN, COLORADO (STRATIGRAPHICALLY ORDERED)

Location	Average Orientation		Group/ Formation
	Face Cleats	Butt Cleats	
Grand Mesa and Gunnison River area (Grout, 1991)	N. 60°–86° E.	N. 19°–30° W.	MVRD
Gunnison River area mines (Boreck and Strever, 1980)	N. 70°–90° E.	N. 10°–20° W.	MVRD
Southern Piceance Basin (Geological Services of Tulsa, 1980)	N. 51°–87° E.	N. 11°–55° W.	MVRD
Red Mountain site cores		(N. 74° W.?)	MVRD
Seccombe and Decker, 1986;	N. 69°–86° E.		MVRD
Horner, 1986)	N. 50°–63° E.		MVRD
DeBeque Canyon, Colorado River		N. 14° W.	MVRD
area (Grout and Verbeek, 1985)		N. 70° W.	MVRD
	N. 62°–66° E.	N. 19°–31° W.	MVRD
Coal Basin area (Grout, 1991)	N. 73°E.	N. 19° W.	MVRD
	N. 56° W.	N. 35° E.	WTCH/MVRD
	N. 37°–40° W.		WTCH/MVRD
Divide Creek Anticline (Grout, 1988)	N. 38°–47° W.	N. 40°–57° E.	WTCH
Colorado River area, eastern Piceance Basin (Grout, 1988)	N. 51°–65° W.		WTCH

SOURCE: Modified from Grout (1991). MVRD–Mesaverde; WTCH–Wasatch.

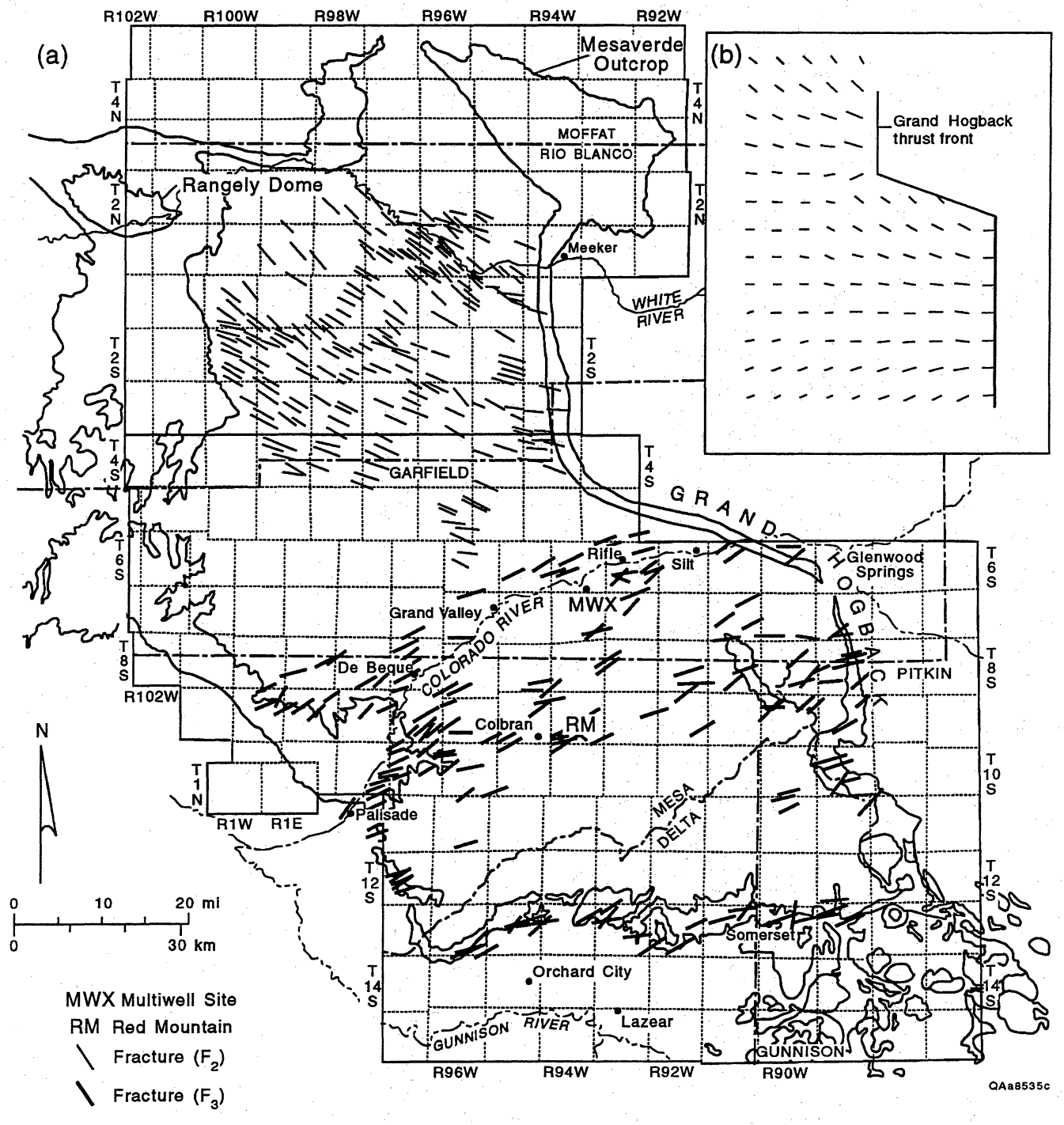

Figure 24. (a) Measured array of natural fracture strikes of F_2 (northern half of the basin) and F_3 (southern half of the basin) in Mesaverde and Tertiary strata around the Piceance Basin (from TRW, 1980; Verbeek and Grout, 1983). (b) Analytical stress trajectories produced by superimposing stresses from westward indentation of the (1) northern and (2) southern segments of the White River Uplift onto (3) a regional west-northwest compressive stress, with a stress ratio of 8:6:1, respectively; line length represents stress magnitude and line trend represents orientation of maximum horizontal stress. After Lorenz and others (1991). Analysis performed by N. R. Warpinski.

the model is based on the assumption that similar orientation of fractures in different stratigraphic intervals does infer equivalent age of formation or corresponding genesis. The authors stress again that extrapolation and lateral correlation of natural fractures cannot be randomly applied throughout the Piceance Basin because of differences in lithology, age, and burial and thermal histories. Any modeling or subsurface fracture prediction must be accomplished using genetically equivalent surface exposures.

Cleat Spacing

Cleat spacing is a significant parameter in coal reservoir and permeability modeling and, in some coal beds, has been reported to correlate with bedding thickness, lithotype, and coal rank (Ammosov and Eremin, 1960; Tremain and others, 1991a, b; Law, 1993). In other coal beds, there is no correlation of spacing with thickness. In field studies, our findings corresponded to those of Grout (1991), who found most Upper Cretaceous face cleats to be unmineralized, orthogonal to bedding, and spaced from 0.5 inch (1.27 cm) to more than 12 inches (>30.5 cm) apart, depending on the coal rank. The butt cleats had spacing ranging from less than 0.5 inch (1.27 cm) to more than 8 inches (>20.3 cm), depending on the coal rank.

Cleat Mineralization

Although Grout (1991a) and other authors observed that cleats in many Piceance Basin coals lack cleat-filling minerals, we have compiled several instances of cleat mineralization (table 5). Minor amounts of pyrite are frequently reported in coal mines and cores. The pyrite occurs as isolated rosettes on cleat surfaces in fresh coal samples. Reddish-brown staining in outcropping coals and associated sandstones may reflect pyrite formerly present in the cleats and joints. Calcite and gypsum have also been reported. Calcite fills some cleats at the Dutch Creek mine (table 5) near Redstone, Colorado. Calcite and pyrite were noted in a number of USGS coal core holes around the basin and in desorption samples of deeper coals. Calcite-filled

TABLE 5
MINERALIZATION IN CLEATS

Well Name	Location Sec	Twp	Rge	Coal Depth (ft) Top	Bottom	Mineralization	References
USGS D-38-EG	18	4 N	94 W	146.5	157.1	sparse pyrite	Tremain and Toomey, 1983
				163.5	183.0	part pyritic	Reheis, 1978
				202.5	205.5	pyritic	
				226.5	229.0	pyritic	
				418.6	420.6	pyritic	
W.F.Moon Lake #310129-4	29	3 N	101 W	904.3	912.0	pyrite	Tremain and Toomey
W.F.Moon Lake #310135-4	35	3 N	101 W	1198.3	1206.7	calcite	Tremain and Toomey, 1983
N.N.G. 22C	16	2 N	93 W	2224.1	2231.1	calcite	Tremain and Toomey, 1983
N.N.G. 77-21C	21	2 N	93 W	2106.0	2118.8	calcite	Tremain and Toomey, 1983
Twin Arrow C&K 4-14	14	3 S	101 W	808.1	809.7	calcite and pyrite	Tremain and Toomey, 1983
				801.9	804.4	some pyrite	
				989.0	990.5	some pyrite	
Fuelco D-26-3-101-S	26	3 S	101 W	1148.9	1151.9	gypsum on cleat faces	Tremain and Toomey, 1983
				1148.9	1159.0	gypsum in slickensides, calcite in cleats	
				1209.1	1217.8	gypsum on slickensides	
Fuelco 0-28-3-101-S	28	3 S	101 W	1582.0	1584.0	occasional pyrite	Tremain and Toomey, 1983
MWX-1	34	6 S	94 W	6603.4	6606.0	calcite filled cleats	Finley and Lorenz, 1988
MWX-3	34	6 S	94 W	6897.4	6894.5	calcite filled cleats	Finley and Lorenz, 1988
USGS Carbonera 1-C	10	7 S	104 W	154.6	155.7	white, non-calcareous mineral	Hobbs et al., 1982
				292.0	294.5	gypsum, pyrite	Tremain and Toomey, 1983
				299.9	304.5	gypsum rosettes	Hobbs et al., 1982
				303.9	310.7	gypsum, pyrite	Tremain and Toomey, 1983
				375.7	376.5	pyrite scale	Hobbs et al., 1982
				631.7	632.4	white, filmy mineral	Hobbs et al., 1982

TABLE 5 (cont.)

Well Name	Location Sec	Twp	Rge	Coal Depth (ft) Top	Bottom	Mineralization	References
USGS C.B.B.C. 1	17	7 S	104 W	84.5	85.5	sparse non-calcitic mineral	J.L. Gualtieri, 1979
				147.3	148.3	sparse, white mineral	
				190.9	196.1	abdt., non-calc. scale	
				204.0	205.2	white, scaley mineral	
				239.1	240.2	sparse, scaley mineral	
				513.4	516.0	sparse pyrite, scaley calcite	
				528.7	529.2	calcite scale	
Dutch Creek No. 2 Mine	5	10 S	89 W	1500.0	1508.7	trace calcite	Khalsa and Ladwig, 1981
WSC#8	1	13 S	90 W	80.3	92.3	some pyrite on cleat	Tremain and Toomey, 1983
				147.4	155.3	some gypsum on cleat	
				346.6	358.6	flake pyrite in cleat	
				393.8	397.0	calcite, flake pyrite	
				418.1	424.8	some calcite in cleat	
WSC#5	11	13 S	90 W	81.4	86.2	vit.streaks, pyrite	Tremain and Toomey, 1983
				110.5	114.1	calcite, minor pyrite	
				155.5	158.4	calcite in cleats	
				341.25	347.8	some pyrite in fracs. gypsum, trace calcite	
				395.0	409.0	pyrite, calcite	
				415.3	422.1	trace gypsum	
WSC#6	11	13 S	90 W	337.4	342.0	calcite in cleats	Tremain and Toomey, 1983
				399.6	412.8	flake pyrite	
WSC#7	11	13 S	90 W	339.1	346.0	gypsum on cleats	Tremain and Toomey, 1983
				392.8	397.1	calcite, some gypsum	

cleats were reported at depths of over 6,000 ft in two of the MWX wells. The presence of secondary mineralization in cleats is important for several reasons. Minerals deposited in cleats can obstruct the permeability of coal seams, and studies of cleat mineralization and mineralization of fractures in adjoining strata may also provide clues to the timing of cleat and joint development. Moreover, a mineralized cleat implies that the fracture was open to ground-water flow.

FAULTS AND FOLDS

The Piceance Basin is an asymmetric, northwest-trending basin of Laramide age in the Rocky Mountain foreland. Bounded by uplifts, it is separated from the Uinta Basin on the west by the Douglas Creek Arch and from the White River Uplift on the northeast by the Grand Hogback monocline. The monocline overlies a late Laramide, southwest- and west-southwest-directed blind thrust system accompanied by decollement and splay faults that extend more than 12 mi (20 km) into the basin (Gunneson and others, 1994). The decollement cuts through Pennsylvanian evaporites and extends upsection as imbricate splay and thrust faults into the Mancos Shale and younger rocks beneath at least one of the folds in the southeastern basin, the Divide Creek Anticline. Detailed genetic stratigraphy has defined duplication of the Williams Fork coal-bearing section along the Divide Creek Anticline. Additional seismic data across the Grand Hogback monocline is needed to adequately define the vertical extent of the thrust system.

The structural axis of the basin is on the east side, adjacent to the Grand Hogback monocline, where Mesaverde Group strata dip steeply and are locally overturned. Strata dip gently on the west and southwest flanks of the basin. Numerous predominantly northwest-trending anticlines are present, including the Divide Creek, Coal Basin, Wolf Creek, Douglas Creek, Crystal Creek, Rangely, Piceance Creek, White River, and Danforth and Wilson Creek Anticlines (Tyler, this volume, fig. 7). Northwest-trending normal faults are also prominent in the interior of the basin. The Douglas Creek Arch contains numerous northeast-trending faults,

and northeast- and east-trending folds and faults also occur along the southwest margin of the basin in Mesaverde and Mancos strata (Tweto, 1979). Tertiary east-west-trending dikes up to 5 mi long occur in the southern half of the basin (fig. 25).

Faults and folds in the Piceance Basin should enhance fracture connectivity and permeability in coal beds as well as in sandstones. Kent and Arndt (1980) noted reports of high "friability," or extensive cleating and fracturing, in Dutch Creek mine coals associated with the Coal Basin Anticline. These structures could also form conventional traps. A small anticline at the Bear mine (T13S, R90W) apparently formed such a trap. Sudden increases in the rate of methane emissions were reported whenever mining crossed the northwest-trending structure. According to a United States Bureau of Mines memorandum (1965), "fracturing of the roof as well as of the coal at the crest of the anticline provides the reservoir and the trap necessary for the accumulation of methane." In tight Mesaverde sandstone studies in the southern half of the basin, Myal and others (1989) found enhanced permeability and production in naturally fractured wells. Through log analyses of natural fractures they found the highest density of natural fractures in the southeast uplift area, followed by the central basin, and then the southwest flank. In an unpublished Mesaverde sandstone study, Tremain (1989) reviewed core descriptions and found densely fractured cores along anticlinal structures; however, moderately fractured cores were also found in several unfolded areas of the basin (fig. 26).

TECTONIC STRESS HISTORY

The Piceance Basin has a complicated tectonic history that goes back to Precambrian times. Apparently, the Precambrian basement faulted into a pattern that influenced later structural trends and Stone (1975) envisioned that northeast-southwest compression was probably initiated at this time. According to Pearson, DeRidder and Johnson, Inc., and LSSI, in association with Waechter (written communication, 1994), "late Paleozoic block fault trends follow the strong magnetic signatures of the underlying Precambrian Basement." Subsequently, in Pennsylvanian-Permian times, the Ancestral Rocky Mountains arose. This orogeny included

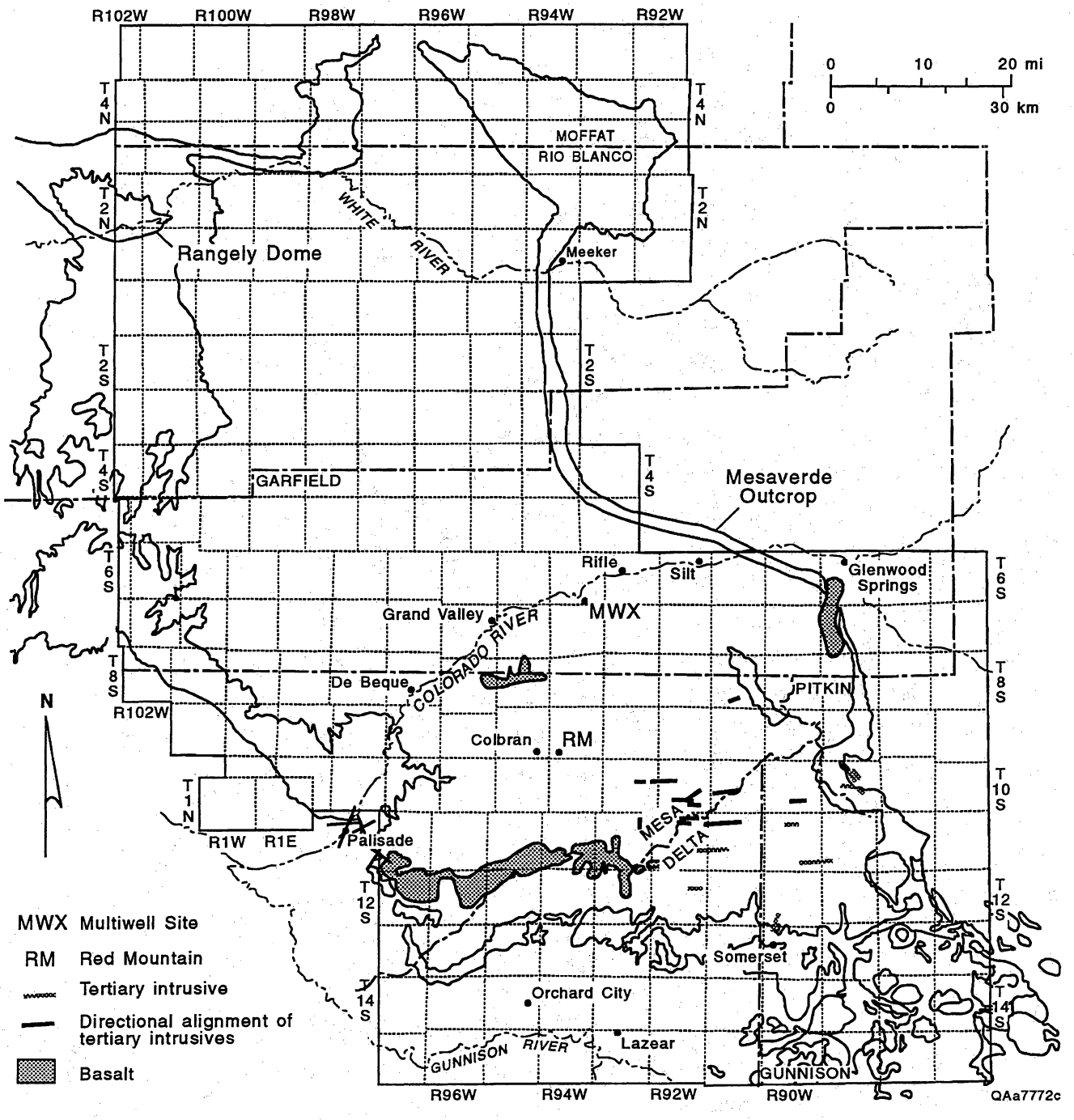

Figure 25. Regional west-east alignment of intrusive Tertiary basalts and dikes in the Piceance Basin may reflect east-west compression during the Laramide Orogeny.

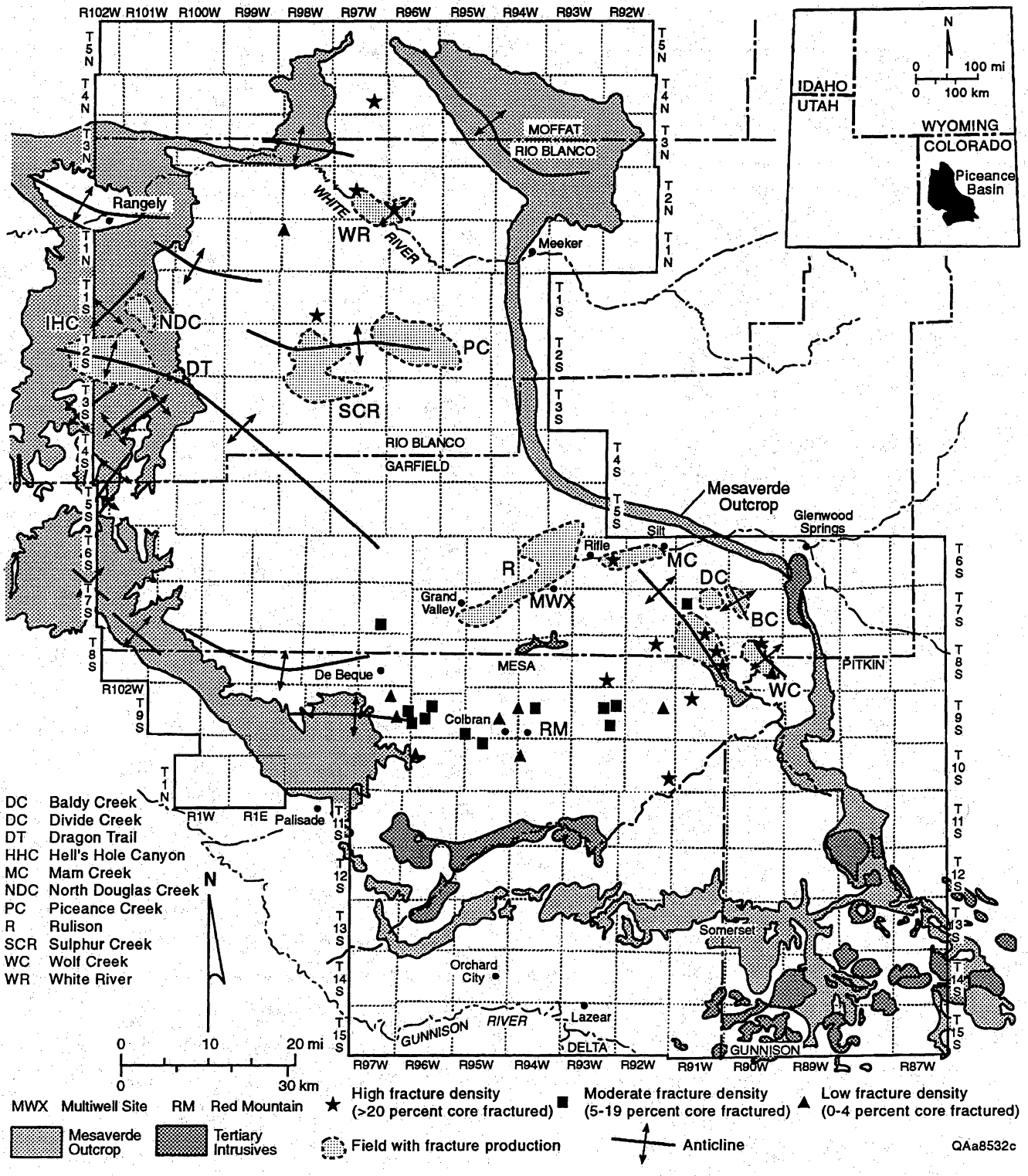

Figure 26. Fracture density from core descriptions in the Piceance Basin. After Tremain (1989). Note occurrence of densely fractured cores near anticlines.

elevation of the Uncompahgre Uplift and the Ancestral Front Range and creation of the Central Colorado trough between the two (De Voto, 1980). Block faulting also occurred north of the Uncompahgre Uplift (Waechter and De Voto, 1989) (fig. 27). Block faulting of the same age has also been identified by Stone (1977) along the Douglas Creek Arch and has been inferred to control the occurrence of younger structures.

The Sevier Orogeny (160 to 72 mya), in the northeast part of the Colorado Plateau, caused east-west horizontal compression during deposition of the Upper Cretaceous and lower Tertiary sediments (Johnson, 1987, 1989). Folding, contemporary with the orogeny, is marked by a low-amplitude north-south-trending flexure in the area of the present-day Douglas Creek Arch (Quigley, 1965; Gries, 1983) (fig. 28a). Intermittently during the early Cenozoic, the Douglas Creek Arch divided the Uinta and Piceance Basins into two separate basins. At other times (Cretaceous), there was little relief on the Douglas Creek Arch, and sediments buried the arch, creating one large basin, the Eagle Basin (Johnson, 1985, 1986, 1987, 1989; Johnson and Finn, 1986).

The Piceance Basin was subsequently bounded by uplifts that formed in the Rocky Mountain foreland during the Laramide Orogeny approximately 72 to 40 mya (Dickinson and Snyder, 1978; Tweto, 1980). Original east-west compression of the early Laramide shifted to north-south compression (Gries, 1983; fig. 28b) or northeast compression, according to Chapin and Cather (1983), in the late Paleocene to early Eocene. From 60 to 40 mya (mid-Paleocene to Late Eocene), east-west-trending uplifts such as the Uinta-Axial Uplift, and possibly the De Beque Anticline and similar folds within the Piceance Basin, formed perpendicular to the earlier north-south-trending Douglas Creek Arch–Rock Springs Uplift trend. Stone (1986) also defined a period of west-east strike slip motion along the Grand Hogback thrust front (Tyler, this volume, fig. 7). Stone (1975) also inferred that left lateral wrench faulting in northwestern Colorado was probably produced by east-northeast–west-southwest compression and lateral shearing at depth.

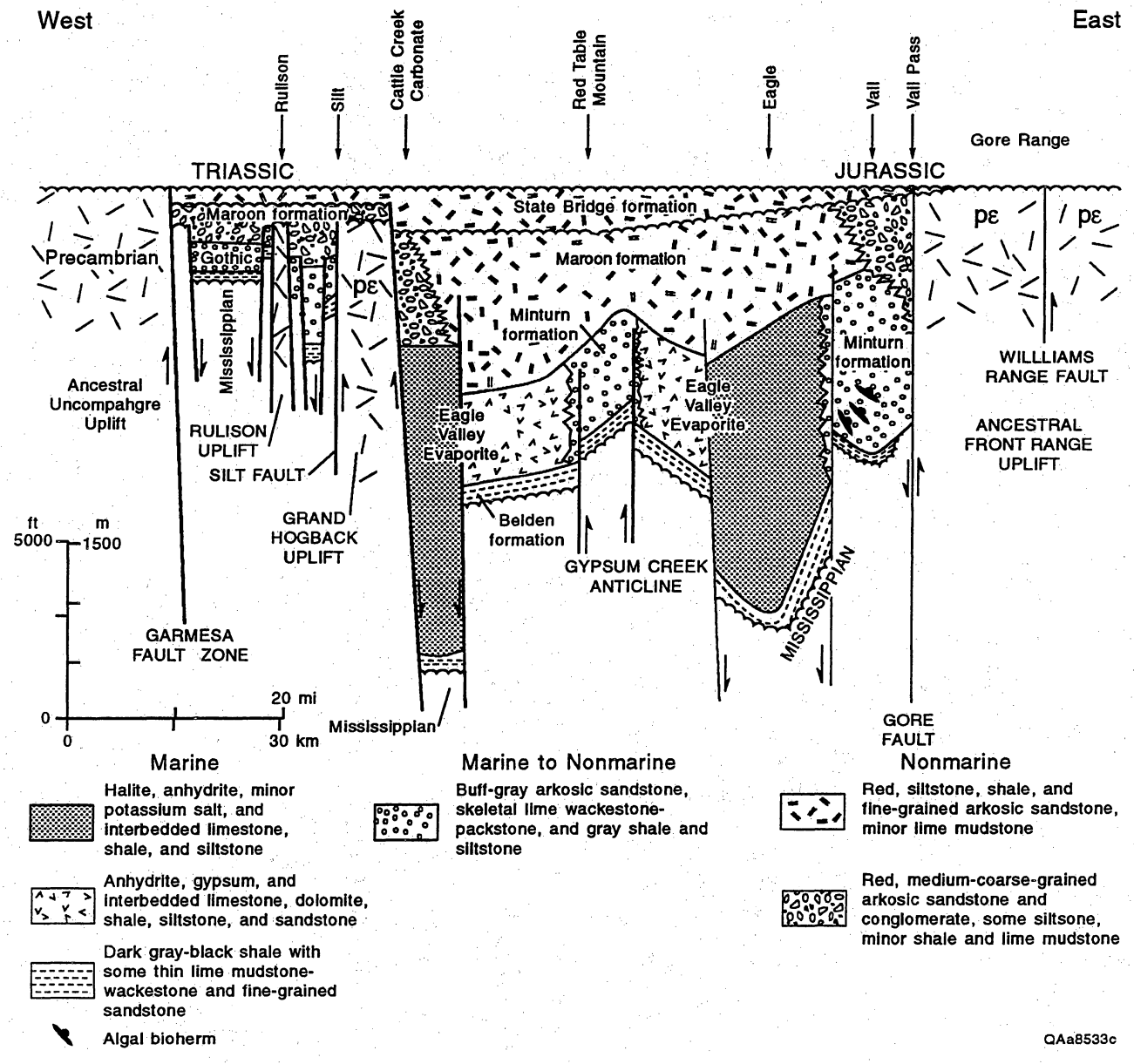

Figure 27. Restored section of Pennsylvanian–Permian rocks, Eagle Basin, Colorado, showing block faulting in the Piceance Basin. From Waechter and De Voto (1989). Basement faulting is inferred as a contol on the occurrence and alignment of younger structures in the basin, as well as being a control on gas producibility.

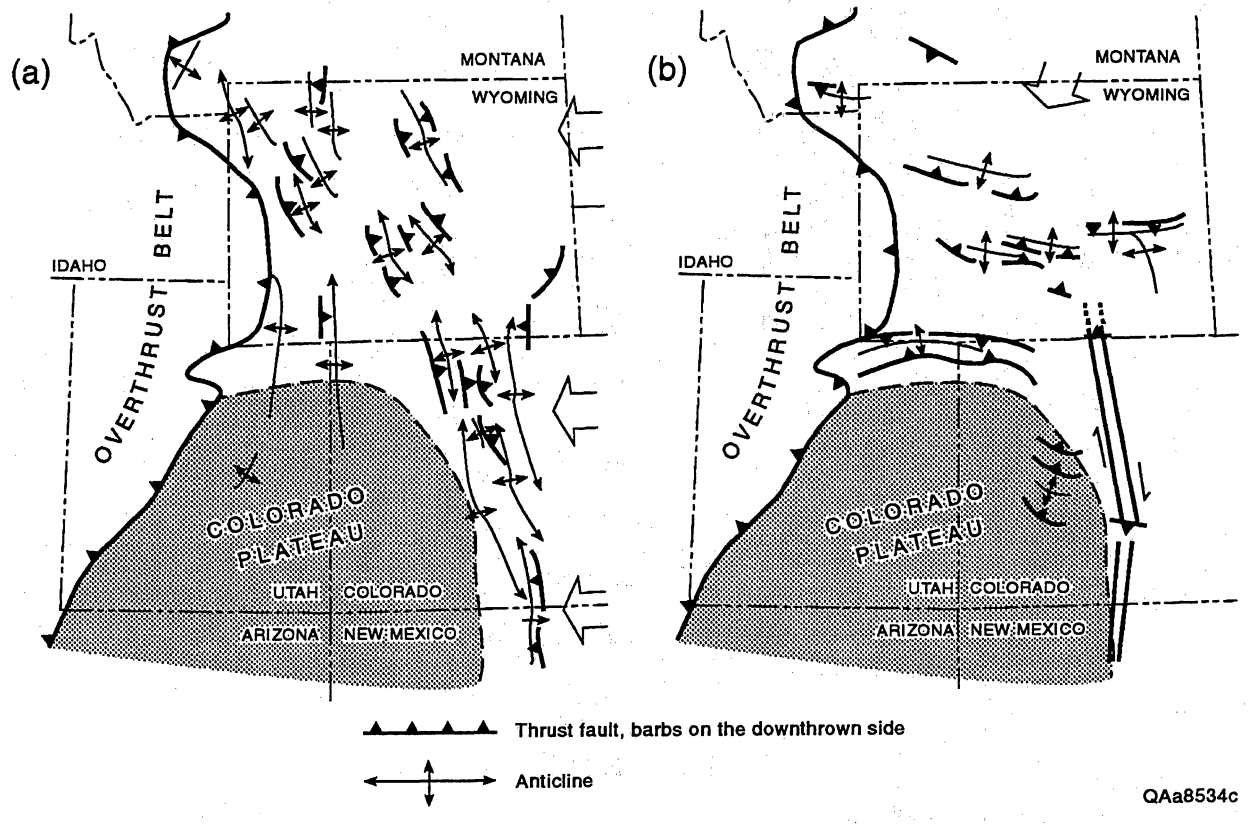

Figure 28. Two stages of the Laramide orogeny showing uplifts and direction of compressional forces. (a) Early Laramide and the formation of north trending uplifts. (b) Late Laramide and the formation of east-west-trending uplifts. After Gries (1983).

At the end of the Laramide Orogeny, about 40 mya, basin subsidence ceased. "During late Eocene to early Oligocene time, an erosion surface developed across the basin possibly in response to the rejuvenation of the White River Uplift and emplacement of the Axial Arch Uplift" (Johnson, 1987, 1989). Little structural movement or sedimentation occurred in the basin until the Colorado River system began to cut deep canyons, about 10 mya. The late Cenozoic tectonism that affected many areas in Colorado and Utah apparently did not greatly affect the Piceance Basin. Probably the most significant post-Laramide tectonism in the basin was faulting on the Douglas Creek Arch and along the White River Dome (Johnson and Nuccio, 1986). By 24 mya, the White River Uplift east of the basin was beveled to about the same level as the erosion surface in the Piceance Basin. The erosion surface on the uplift is covered by basalts that are from 24 to 8 mya (Larsen and others, 1975). Basalts on the Grand Mesa and overlying the Grand Hogback near Glenwood Springs are dated at 14 to 9 mya. The West Elk Mountains intruded the southeast part of basin approximately 12 mya. The late Pliocene to Recent is marked by epeirogenic uplift and downcutting by the Colorado River and its tributaries. Normal faulting of Miocene basalts overlying the Grand Hogback also occurred.

CURRENT STRESS STATE

The Piceance Basin is in the Colorado Plateau interior stress province (Zoback and Zoback, 1980, 1989), which is surrounded by the Cordilleran Extension stress province. Until recently, the Colorado Plateau stress province was described as a compressional regime having a west-northwest-trending regional maximum horizontal stress orientation—nearly perpendicular to the surrounding stress direction in the Cordilleran Extension stress province (Zoback and Zoback, 1980). However, focal mechanisms (normal and strike-slip faulting) from the Colorado Plateau interior suggest that the current stress regime is actually extensional (Wong and Humphrey, 1989; Zoback and Zoback, 1989).

Lorenz and others (1993) listed a number of different tools used to measure current stress states in oriented core, including anelastic strain recovery, circumferential velocity anisotropy,

and drilling-induced fractures. In the borehole itself, borehole breakouts and drilling- or stimulation-induced fracture directions can be measured by well log tools such as the Formation Micro Scanner, borehole televiewers, or 4-arm dipmeters. Lorenz and Finley (1991) and Lorenz and others (1993) constructed a stress map of the Piceance Basin based on current and paleostress indicators; this map demonstrates a current northwest-trending horizontal stress state in the Piceance Basin approximately orthogonal to that in surrounding regions (Zoback and Zoback, 1989). Horizontal stress orientations determined at the Multiwell (MWX) site where the maximum horizontal stress and high-permeability anisotropy is west-northwestward (Clark, 1983; Towse and Heuze, 1983; Johnson, 1985; Lorenz and others, 1986; Branagan and others, 1987; Lin and Heuze, 1987; Lorenz and Finley, 1987a, b; Lorenz, 1991) are consistent with a northwest regional stress pattern. However, local deviations of minifrac strikes from the expected average regional fracture azimuth have been reported from the Piceance Basin (Towse and Heuze, 1983; Lorenz, 1991). Lorenz (1991) documented mean strike and dip of measured fractures in Mesaverde sediments between N81°W and N84°W, from oriented cores at the Slant Hole Completion Test site (SHCT-1; located about 600 ft [185 m] south of the MWX site). Warpinski (1986, 1989), who modeled the stress history of the Piceance Basin, obtained results that compare favorably with present-day stress data at the MWX site. These results suggest that the geologic history of the basin had an influence on current stress magnitude and orientation. For instance, variations in present-day in situ stress may reflect remnant strains from the Sevier and Laramide east-west compressive stress fields (Wolff and others, 1974; Warpinski and Teufel, 1987).

Kukal and others (1992) also constructed a stress map in the Piceance based on current stress measurements from several Mesaverde tight gas wells. When we combined data shown on both the Lorenz and Kukal maps and other data reported in table 6, a trend of northeast-trending stress indicators from Grand Valley to Colbran (nos. 5, 6, 7, 8, and 14; fig. 29) seems to emerge. However, even within the same well, Kukal and others (1992) found variations in stress orientation (table 6; no. 14). The difficulty in interpreting the tectonic stress fields in this

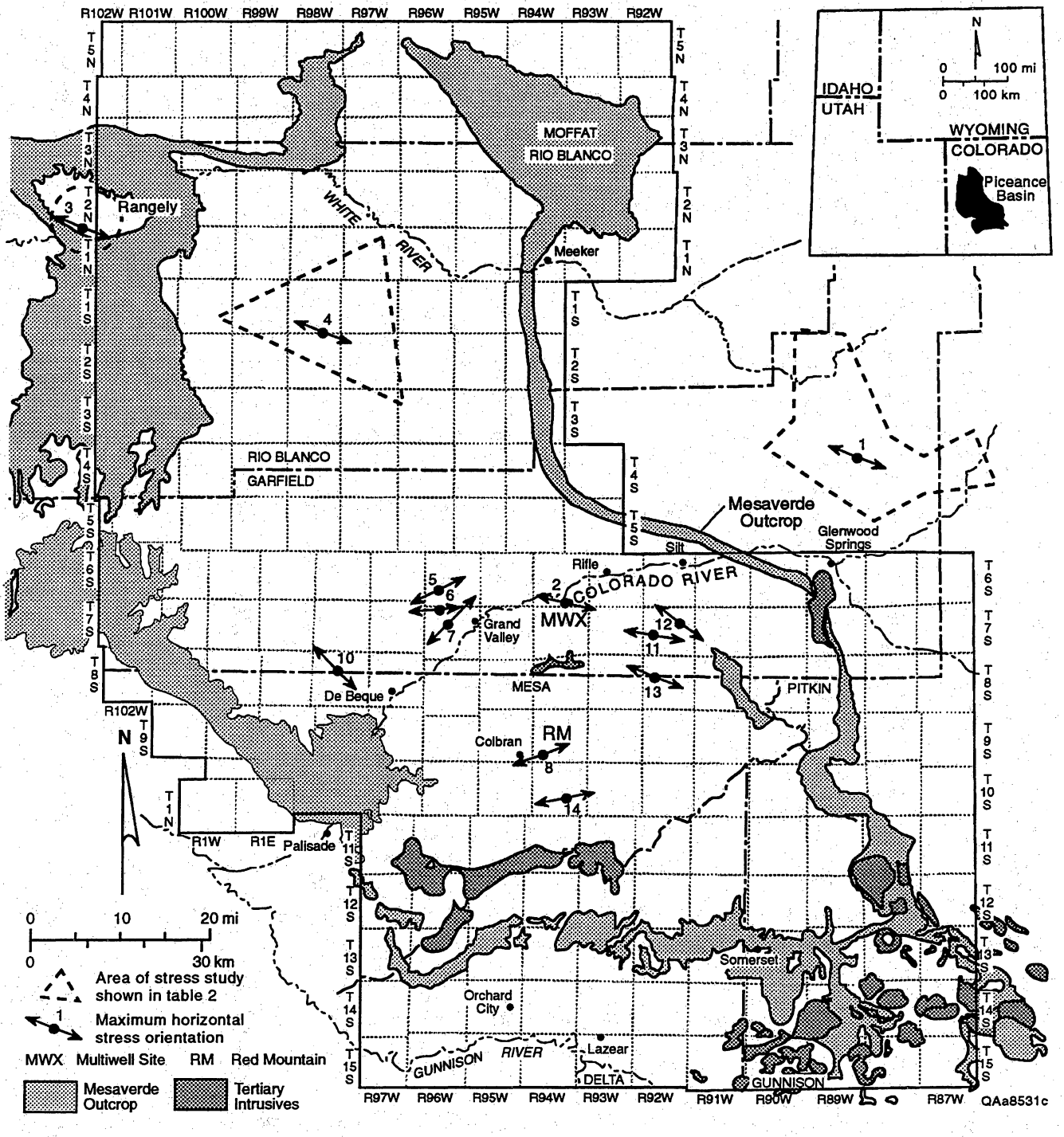

Figure 29. Maximum horizontal stress orientations in the Piceance Basin area. Numbers correspond to data in table 6.

TABLE 6
CURRENT STRESS DATA

AREA	LOCATION	REFERENCE	FORMATIONS	METHODS	MAXIMUM HORIZONTAL STRESS ORIENTATION
1	White River Uplift	Dula, 1981	Paleozoic Quartzites, Cambrian Sawatch Fm., and Devonian Parting Fm.	Microfractures, deformation lamellae, and surface joints	N70°W primary set, parallel to faults; NNE secondary set, both normal to bedding
2	MWX site - three wells, Sec. 34, T6S, R94W	Teufel et al., 1983	Cretaceous Mesaverde Group	Anelastic strain recovery from 26 oriented cores	Maximum principal horizontal in situ stress of N80°W, acoustic velocity anistropies N60-90°W, differential strain analysis-N82W
3	Rangely Field Area	Raleigh et al., 1972	Cretaceous Mancos to Permo-Penn. Weber Fms.	Stresses from 3 surface locations, one hydraulic fracture, and focal plane solutions from series of earthquakes	WNW
4	N. Central Piceance Basin, west of Meeker	Wolff et al., 1974	Eocene Green River Fm.	Borehole televiewer logged 7 shallow holes after hydraulic fracturing. Induced fractures observed in 5 of 6 holes where logging successful	Fracs below 400' within 12° of vertical & N70°W main trend
5	Grand Valley 22-9, Sec. 29, T6S, R96W	Reinecke et al., 1991	Cretaceous Mesaverde Group -- Williams Fork Fm.	Borehole breakout	Long axis N60°E, short axis N30°W
6	MV-8-4, Sec. 4, T7S, R96W	Reinecke et al., 1991	Cretaceous Mesaverde Group -- Williams Fork Fm.	Acoustic-velocity anisotropy	N74-83°E
7	Barrett Energy Grand Valley No. 2 Federal, Sec. 10, T7S, R96W	C.E.R. Corp, 1985	Cretaceous Mesaverde Group -- Cozzette and Corcoran Mbrs. of Iles Fm.	Drilling induced fractures in oriented core	N39°E
8	(Red Mountain) REI 1 Deep Seam 32-2, Sec. 32, T9S, R94W	Seccombe et al., 1986	Cretaceous Mesaverde Group -- Cameo coal zone of Williams Fork Fm.	4-arm caliper log	N69-86°E
9	Chandler & Assoc. SW Rangely Federal 1-7-1-2, Sec. 7, T1S, R102W	Branagan et al., 1992	Cretaceous Mancos Fm. -- Mancos B sandstone	Borehole breakout from FMS log, induced hydraulic fracture.	N73-80°E
10	Conquest Oil S. Shale Ridge #11-15, Sec. 15, T8S, R98W	Close et al., 1993	Cretaceous Mesaverde Group -- Williams Fork Fm. Cameo zone coals	Coal cavity elongation	NW
11	Mobil T45-20P, Sec. 20, T7S, R92W	Kukal et al., 1992	Cretaceous Mesaverde Group -- paludal zone of Williams Fork	Induced fractures identified on FMS log	N60-90°W
12	Meridian 12-14 Lyons, Sec. 14, T7S, R92W	Kukal et al., 1992	Mesaverde Group -- fluvial and paludal zones of Williams Fork Fm.	Induced fractures identified on FMS log	N51°W
13	Oryx Acapulco Fed. #1, Sec. 16, 8S, 92W	Kukal et al., 1992	Mesaverde Group -- Cozzette and Corcoran Mbrs. of Iles Fm.	Induced fractures identified on FMS log	N70°W ±20°
14	Fuelco E-22-10-94-S, Sec. 22, T10S, 94W	Kukal et al., 1992	Mesaverde Group -- a) Cozzette and Corcoran Mbrs. of Iles Fm., b) fluvial zone of Williams Fork Fm.	a) 8 oriented core induced fractures b) borehole breakout from FMS log	a) N80°E b) N34°W

region and in understanding their apparent variations may be related to low differential horizontal stresses, or small differences between maximum and minimum stresses, as suggested by limited thrust faulting within the Colorado Plateau interior (Zoback and Zoback, 1980). This interpretation is consistent with in situ stress measurements in the Piceance Basin that indicate all three principal stresses are approximately equal to lithostatic pressure (Wolff and others, 1974; Bredehoeft and others, 1976). Such a pattern of low differential horizontal stresses complicates the prediction of fluid flow pathways and anisotropy in cleats in coal beds. Furthermore, Lorenz and others (1993) point out an additional complicating factor to calculating current stress directions—the presence of extreme topography can cause local stresses to rotate because of unloading. Lorenz uses this to explain 20- to 40-degree stress differences between the MWX site and some Barrett Resources' wells to the north near the Anvil Point escarpment.

CONCLUSIONS

Coal beds commonly contain pervasive, closely spaced natural fractures (cleats) that are the primary control on coal permeability and coalbed methane producibility. The oldest, and generally most prominent systematic fracture in coal, the face cleat, typically has a preferred orientation, greater along strike interconnectivity, and higher permeabilities than other fractures. Regional mapping of fracture (cleat) sets in coal beds and sandstones of the Upper Cretaceous Mesaverde Group and Tertiary Wasatch and Green River Formations, both in the Piceance Basin and along the Grand Hogback monocline, shows that domains of uniformly oriented natural fracture and face-cleat strike exist. Face cleats within the domains are oriented normal to the basin-fold axis and the Grand Hogback thrust front and parallel to the maximum horizontal compressive paleostresses. Face-cleat attributes can also be correlated on the basis of joint style and orientation with regional systematic fracture sets in the enclosing clastic rocks. Locally, Upper Cretaceous face-cleat domains correlate with prominent joints in clastic rocks whose strikes are east-northeast in the southern Piceance Basin and west-northwest in the

northern part of the basin. Butt cleats correlate with a younger set of joints whose strikes average northwest in the southern Piceance Basin. Stratigraphic and structural evidence suggests that the face-cleat strike domains are sequential products of the same period of compression (~72–40 mya) that gave rise to the Grand Hogback and associated intrabasin folds. Generally, the east-northeast-trending face-cleat domain in the southeast part of the basin are oblique to current maximum stress directions, whereas the face-cleat domain in the northern half of the basin are parallel to current maximum stress directions. Therefore, face cleats in the northern half of the basin may provide more permeable pathways for gas production. Further, faults and folds may also enhance cleat permeability, creating the potential for conventional traps; high permeabilities and rates of gas production have been associated with the highly fractured White River Dome in the northern part of the basin and high rates of water production are associated with the intensely fractured and faulted Divide Creek Anticline in the southern half of the basin.

Younger and sequentially developed Tertiary (Wasatch and Green River Formations) regional joint sets, termed F_1 (oldest) through F_5 (youngest), show consistent style throughout the basin (Grout, 1991; Grout and others, 1991; Grout and Verbeek, 1992). Early-formed F_1 (north-northwest-striking) and F_2 (west-northwest-striking) joint sets are present chiefly in the northern two-thirds of the basin, whereas the intermediate-age F_3 (east-northeast-striking) joint set dominates the fracture network in the south half of the basin. The F_4 joints (north-northwest-striking) are abundant throughout the basin, but the F_5 joints are sparse, occurring only in Eocene oil shales. The age of Tertiary fractures is constrained by structural, stratigraphic, and geomorphic evidence and is bracketed at 43 to 10 mya by Grout (1991), Grout and others (1991), and Grout and Verbeek (1992).

A correlation exists between the orientation of Tertiary joints in clastic beds and the orientation of face and butt cleats in Upper Cretaceous coal beds in the Piceance Basin. Most face and butt cleats in the Upper Cretaceous coal beds are of an orientation and fracture style similar to that of the Tertiary F_3 and F_4 joint sets, respectively (Grout, 1991; Grout and others,

1991; Grout and Verbeek, 1992). For example, in the southeastern Mesaverde outcrop, the face cleats trend east-northeastward and are correlated in orientation with the Tertiary F_3 joint set that is both prominent and abundant in the sandstones in this area. It is stressed that a similar style and orientation of fractures in different stratigraphic intervals does not infer equivalent age of formation or corresponding genesis. Importantly, the relative age of Upper Cretaceous and Tertiary fracture sets, established by abutting relations, indicates that the maximum horizontal compressive stress (stress parallel to fracture strike) rotated with time during and following Laramide compressive events. Vertical and lateral extrapolation and lateral correlation of joints and face cleats, therefore, cannot be randomly applied throughout the Piceance Basin to infer similarity of age because differences in lithology, diagenesis, burial, coalification, and thermal histories may cause fractures of different orientation to form in adjacent and overlying strata.

FUTURE WORK AND REMAINING QUESTIONS

The authors are currently compiling additional field data. Future work will include access and interpretation of geophysical seismic lines, additional field study, and interpretation and description of Mesaverde Group coalbed cores. Future work will also include compilation of fault and fold data from larger scale geologic maps, mine permits, published descriptions of gas fields in the basin, and numerous maps of abandoned mines. Remaining questions to be resolved include (a) Does a northwest-trending face-cleat domain predominate in the northern part of the basin and an east-northeast-trending face-cleat domain predominate in the southern half of the basin, as preliminary data seem to indicate? Are these domains separated by a domain boundary region that might have overlapping, crossing face cleats (Tremain and others, 1991a, b, 1994), or is there a gradual rotation in cleat pattern, as occurs in the Raton Basin (Tyler and others, 1992, 1993, 1994)? Are the cleats in these domains the same age? (b) If areas of crosscutting and mutually abutting face cleats and fracture swarms observed in other basins exist in the Piceance, are these areas of increased cleat connectedness and permeability where

cavity completions might be successful, as in the San Juan Basin (Tremain and others, 1991a, b, 1994; Laubach and Tremain, 1994)? (c) What is the timing of cleat development? Is it highly variable throughout the basin, corresponding to fracture development in adjacent rocks? Or is it more related to coalification? (d) Can we confirm the relationship between face cleat and current stress directions? Current stress directions will determine whether face cleats should be open and permeable. (e) Do faults and anticlines act as conventional traps in the basin to augment basin-centered trapping of gas? And do these structures consistently cause deviation in regional cleat patterns?

We believe the data presented to date have begun to answer some of these questions. However, additional data will be obtained from core, logs, outcrops, the literature, and more detailed mapping should help clarify the fracture and stress history of the basin. The compilation, analyses, and integration of this data will be the focus of future work.

Lineament Analysis of the Piceance Basin: Relationships Between Lineament Attributes and Coalbed Methane Production

Roger Tyler, Ronald G. McMurry, and Naijiang Zhou

ABSTRACT

Coal beds are fractured reservoirs for natural gas. Anomalously high production of coalbed methane is commonly attributed to fracture permeability that formed during and/or subsequent to coalification. This study tests the utility of lineaments for identifying coalbed methane productivity trends in the Williams Fork Formation, Mesaverde Group of the Piceance Basin. The lineament azimuth for the entire Piceance Basin shows a strong bimodal occurrence to lineaments of between 280°–310° and 20°–40°, similar to natural fracture orientations. Production trends are associated with fractures, which presumably may be represented at the surface as lineaments. Preliminary results, however, indicate that Landsat- and Side-Looking-Airborne-Radar (SLAR) -based lineament analysis is neither a reliable indicator of subsurface fracture attributes nor a predictor of production from coalbed methane and/or sandstone gas wells in the Mesaverde Group.

INTRODUCTION

The purpose of this study is to map lineaments and to assess their relationships with Mesaverde Group coalbed methane production. Depth to the gas-producing intervals in the Mesaverde Group varies from surface near the basin margins to 12,000 ft (3,600 m) near the center of the basin. Permeability in conventional reservoirs is enhanced by fractures in many areas of the Piceance Basin (Close and others, 1993; Lorenz and Hill, 1991, 1994; Tyler and others, 1991a, b, 1993, 1994). Lineaments may be spatially correlated with fractures in the subsurface. If a correspondence between lineaments and subsurface fractures can be demonstrated, then the location and orientation of these surface features can be used to assist

selection of drilling sites for enhanced production of coalbed methane from fractured reservoirs.

APPROACH

The approach taken is to test the relationship between lineament data and production data. Some empirical studies regard spatial coincidence between lineaments and highly productive wells as proof that the lineaments or their subsurface counterparts are enhancing production. However, in this study strict statistical criteria will be applied to determine whether lineament attributes have a statistically significant correlation with production data.

Lineaments were mapped on 1:250,000-scale Landsat Thematic Mapper (TM) images (figs. 30–32) and 1:100,000-scale Side-Looking-Airborne-Radar (SLAR) images (figs. 30, 33, and 34). Landsat and SLAR lineaments were compared with lineaments derived from different scales of imagery that were published in three previous studies (figs. 30, 35, and 36). Lineaments from other studies that covered selected areas in the Piceance Basin have also been digitized directly from published maps (figs. 30, 35, and 36). No judgment was made regarding the "validity" of the lineaments in previous studies. Their occurrence will be analyzed, just as those from this study were, using the procedures described below. Subsequently, all lineaments in this study and previous studies were digitized onto a base map for lineament regression analysis (fig. 37). Further, lineament azimuth, length, and density (length/area) from the Landsat and SLAR images will be compared with initial Mesaverde low-permeability sandstone (tight-gas), coalbed methane, and water production data from wells in the Piceance Basin. Linear regression analysis will be used to quantify the relationship between lineament attributes and production data.

REVIEW OF PREVIOUS LINEAMENT STUDIES IN THE PICEANCE BASIN

Previous studies used imagery at scales different from that used in the present study (fig. 30). Kelley and Clinton (1960) produced a fracture map of the southwestern Piceance

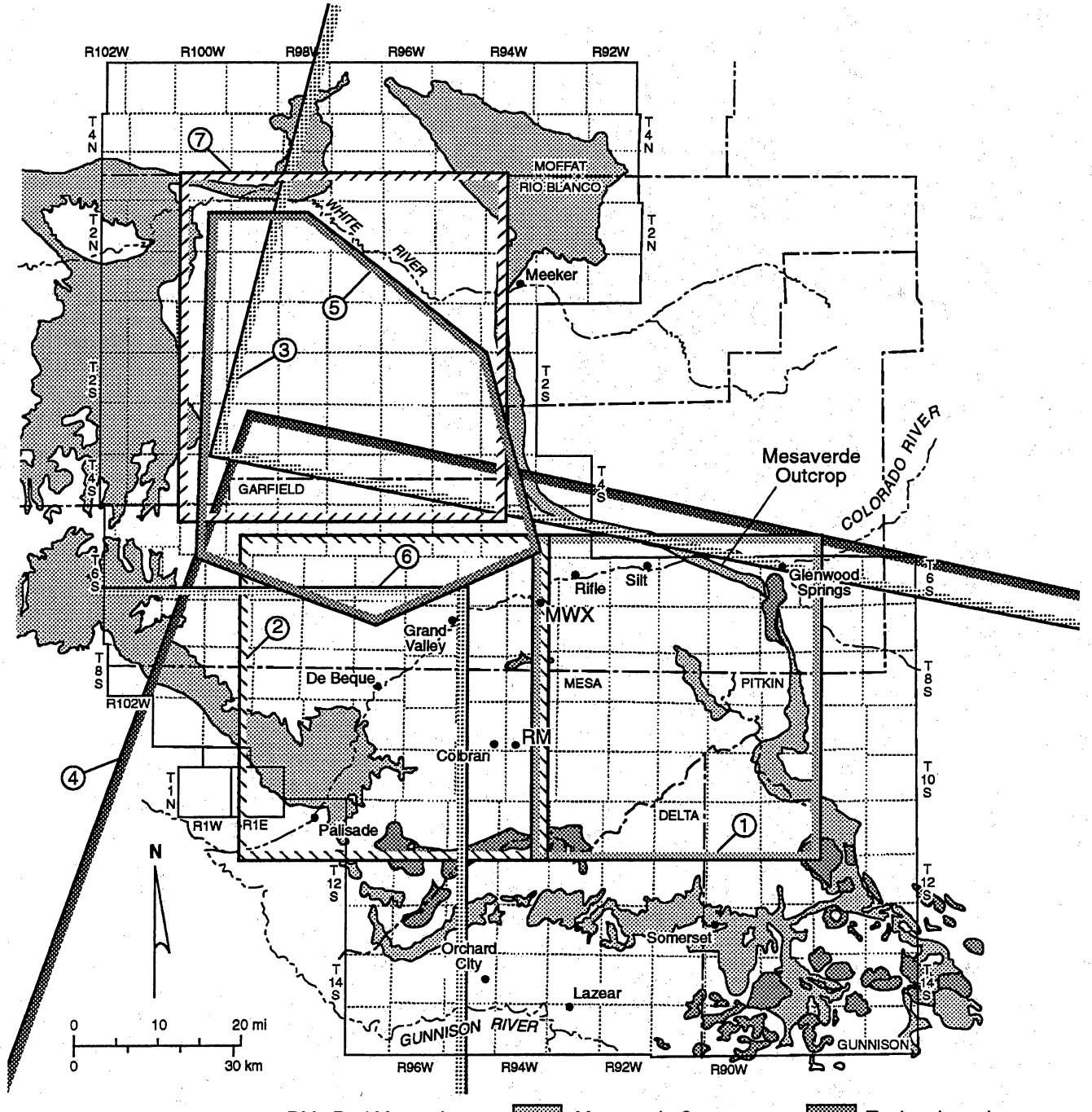

Figure 30. Lineament data sources and previous lineament studies in the vicinity of the Piceance Basin.

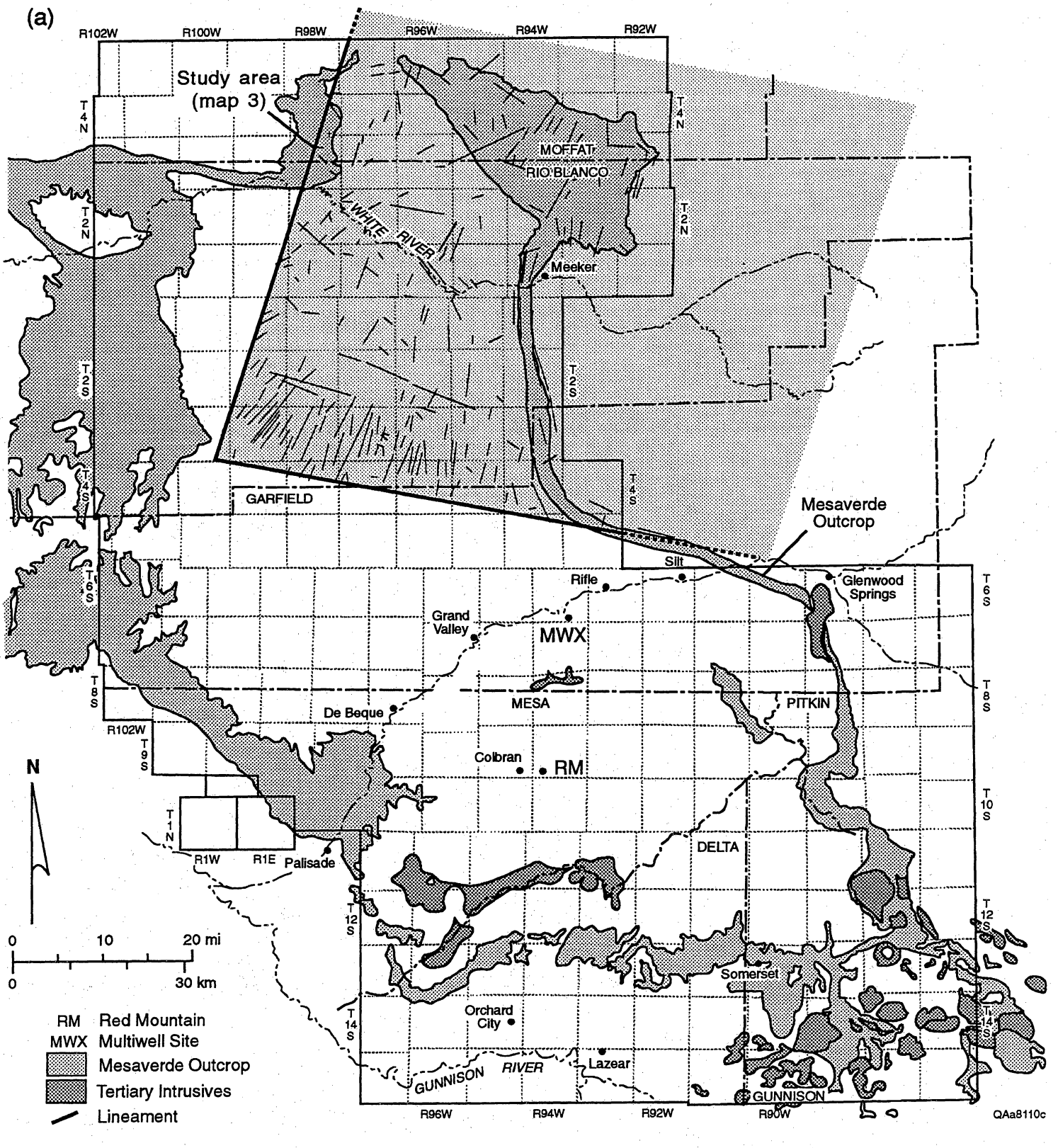

Figure 31. (a) Landsat lineaments in the northern Piceance Basin mapped in this study (map 3) and (b) enlargement of study area.

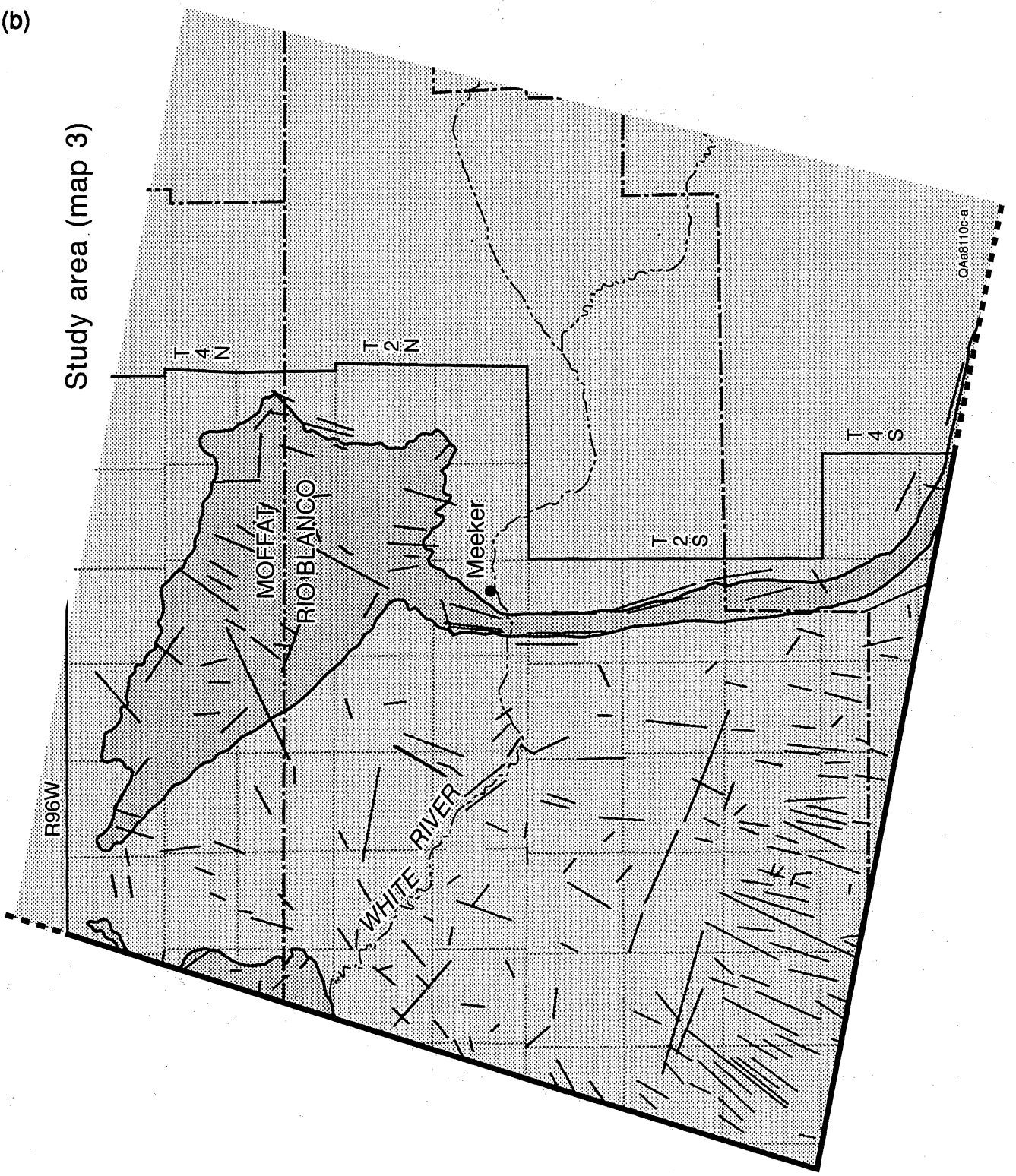
(b)
Study area (map 3)
T 4 N
T 2 N
T 2 S
T 4 S
R96W
MOFFAT
RIO BLANCO
Meeker
WHITE RIVER
QAa8110c-a

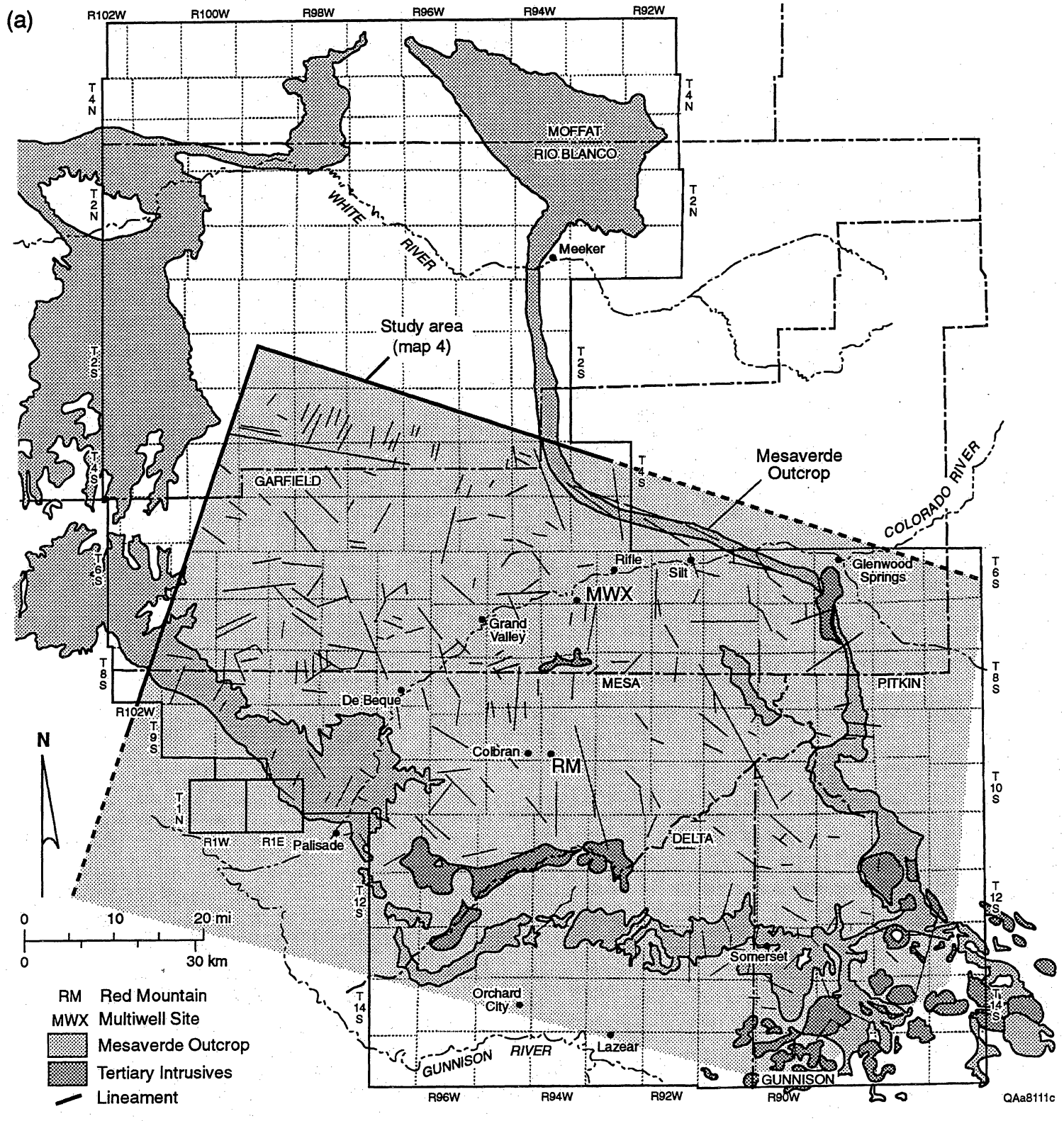

Figure 32. (a) Landsat lineaments in the southern Piceance Basin mapped in this study (map 4) and (b) enlargement of study area.

Study area
(map 4)
GARFIELD
Rifle
Silt
Glenwood
Springs
MWX
Grand
Valley
MESA
PITKIN
De Beque
2W
T
9
S
Colbran
RM
Mesaverde
Outcrop
T
1
N
R1W
R1E
Palisade
DELTA
T
12
S
Somerset
Orchard
City
QAa8111c-a

(a)

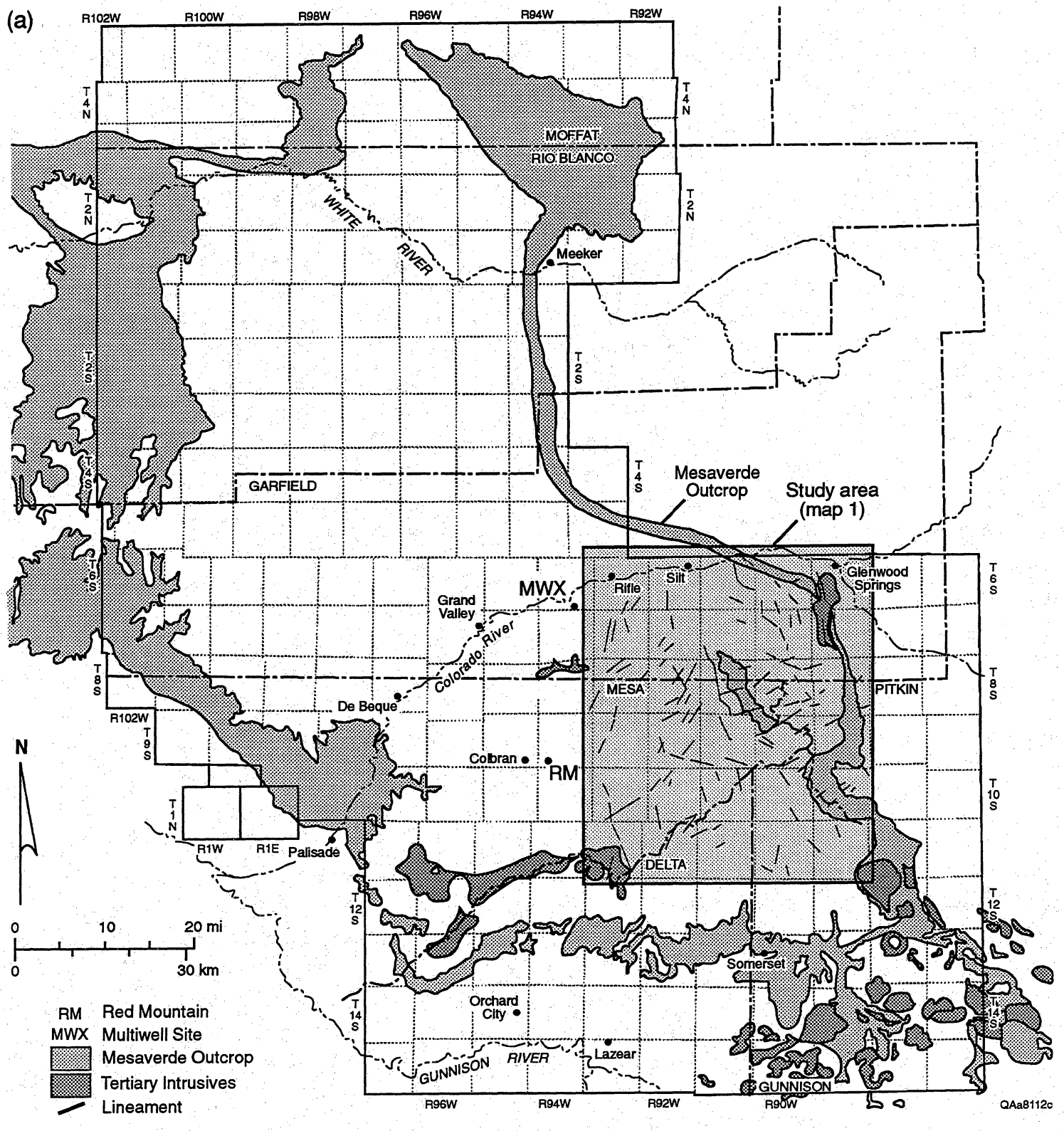

Figure 33. (a) SLAR lineaments in the southeastern Piceance Basin mapped in this study (map 1) and (b) enlargement of study area.

Study area (map 1)

(b)

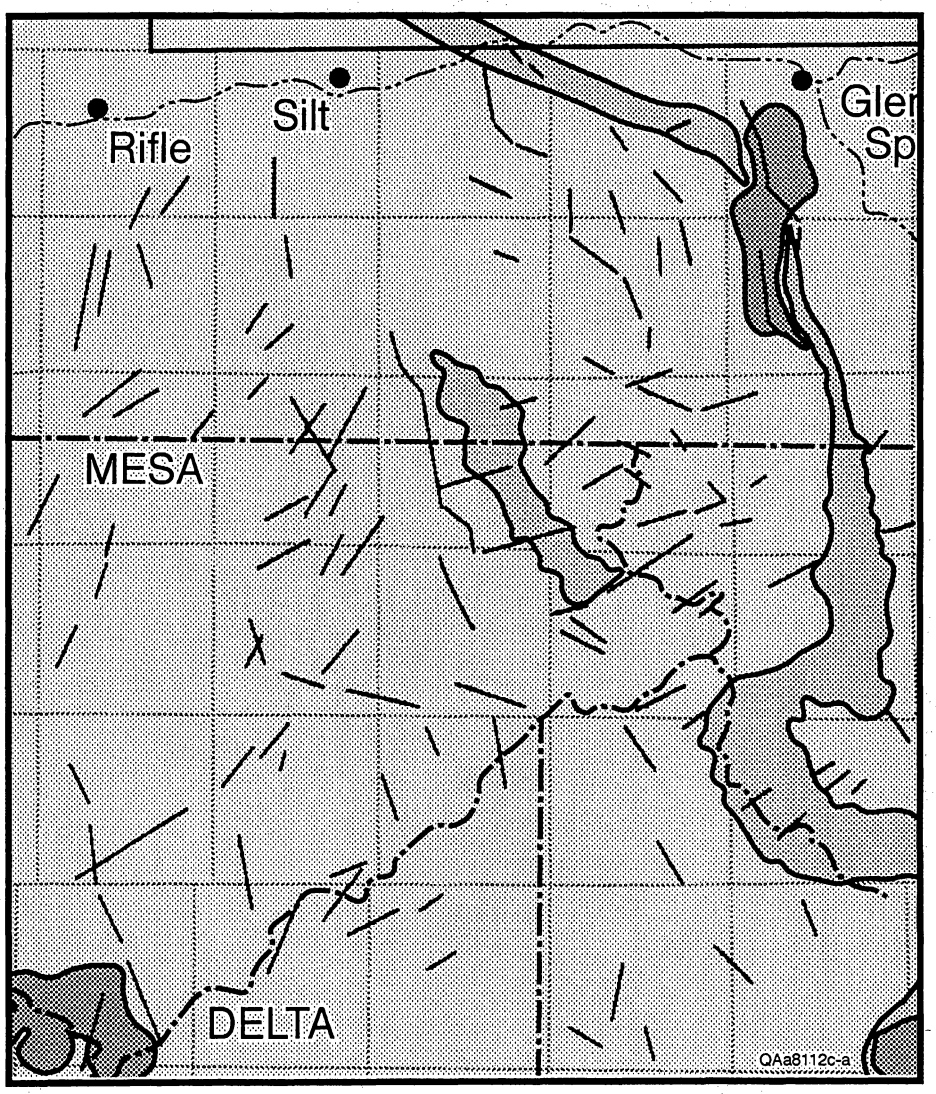

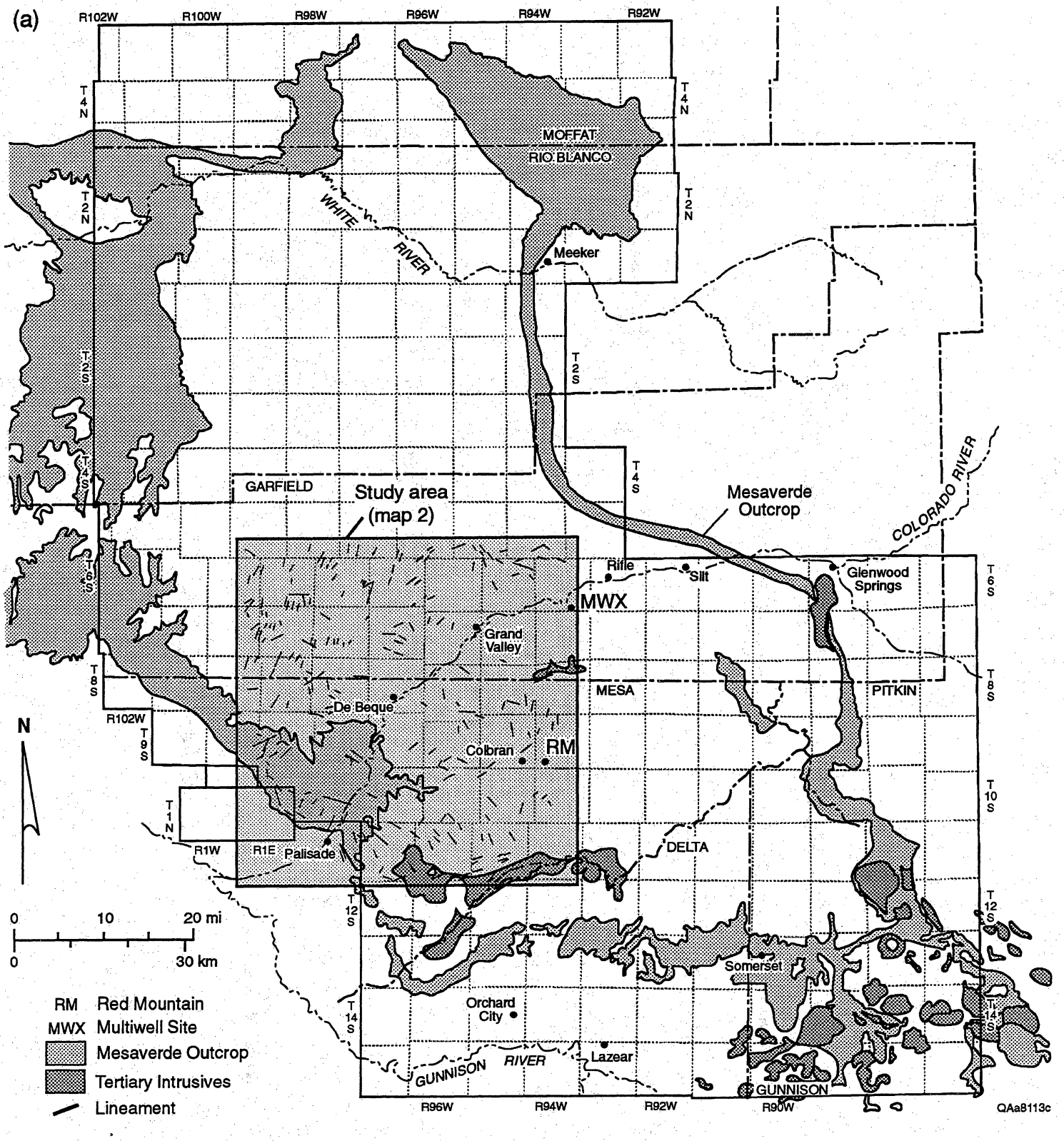

Figure 34. (a) SLAR lineaments in the southwestern Piceance Basin mapped in this study (map 2) and (b) enlargement of study area.

Study area (map 2)

(b)

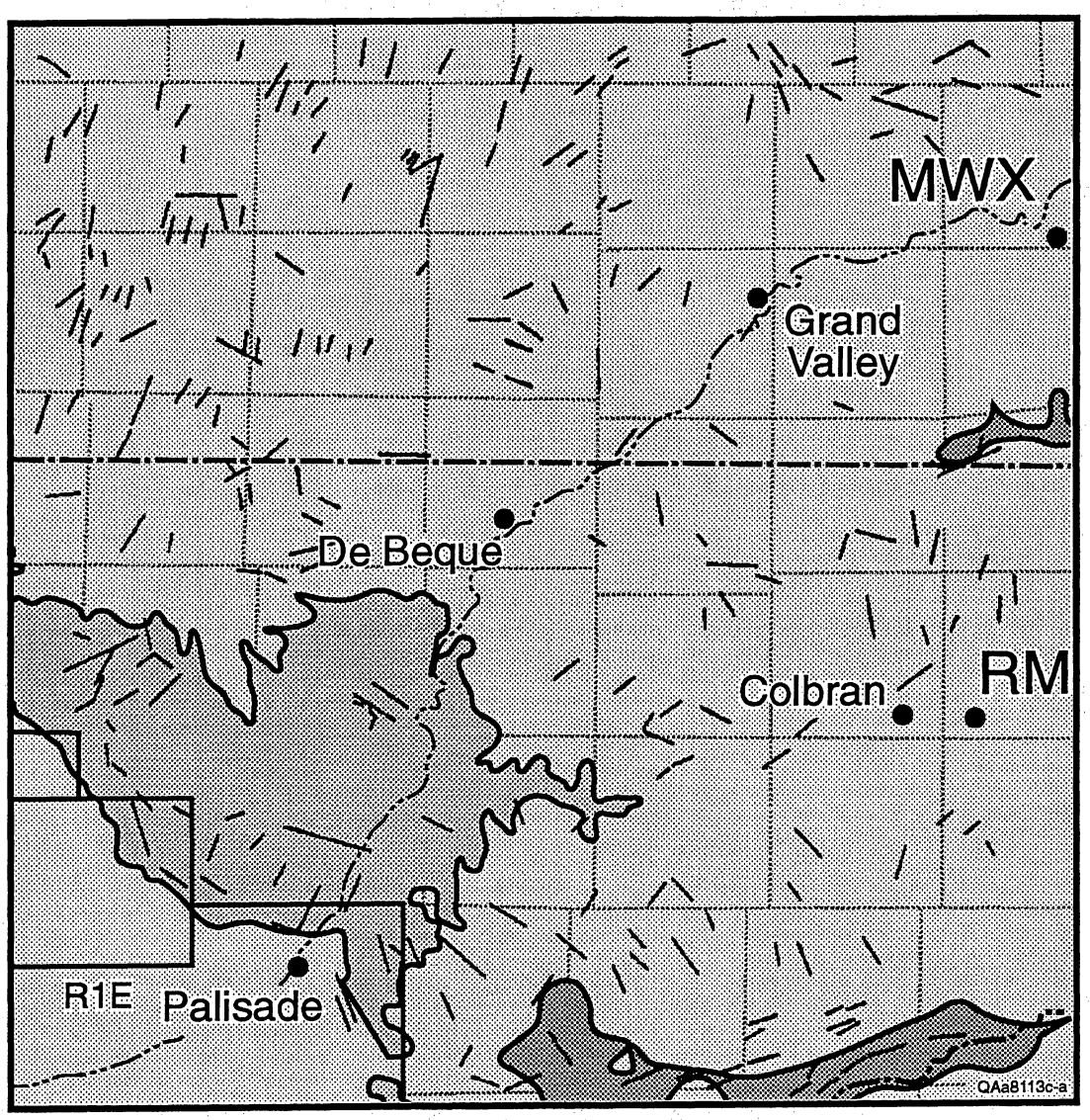

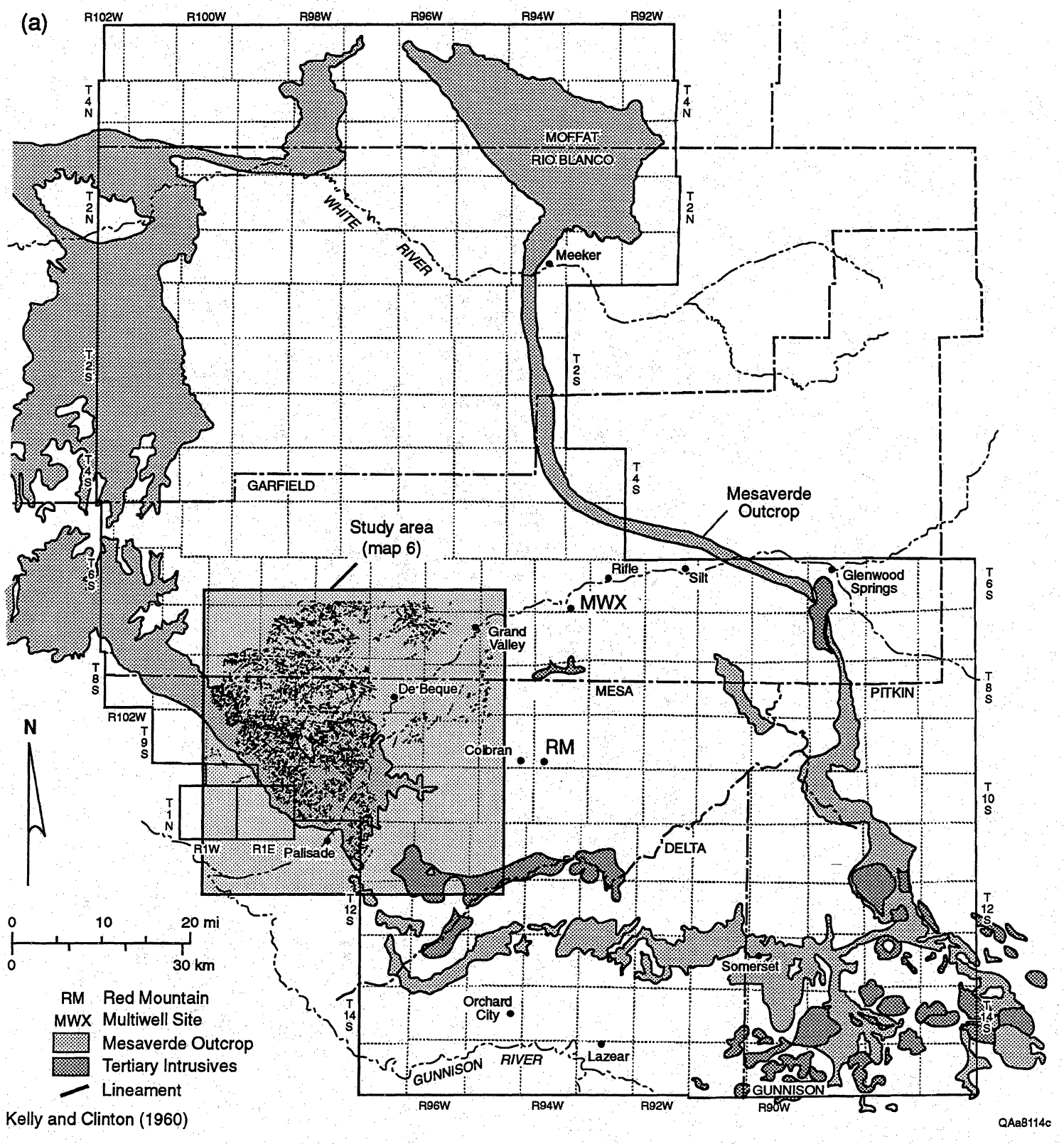

Figure 35. (a) Aerial photolineaments in southwestern Piceance Basin mapped by Kelley and Clinton (1960) (map 6) and (b) enlargement of study area.

(b)

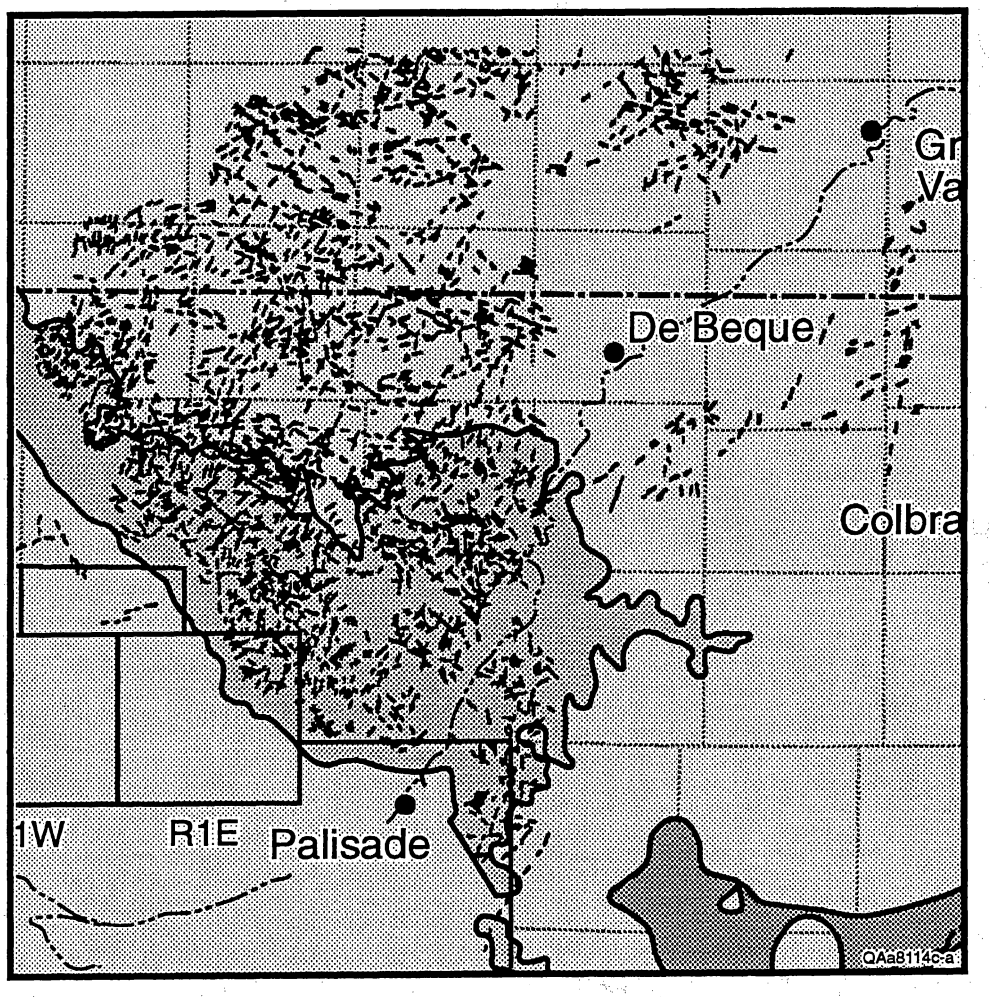

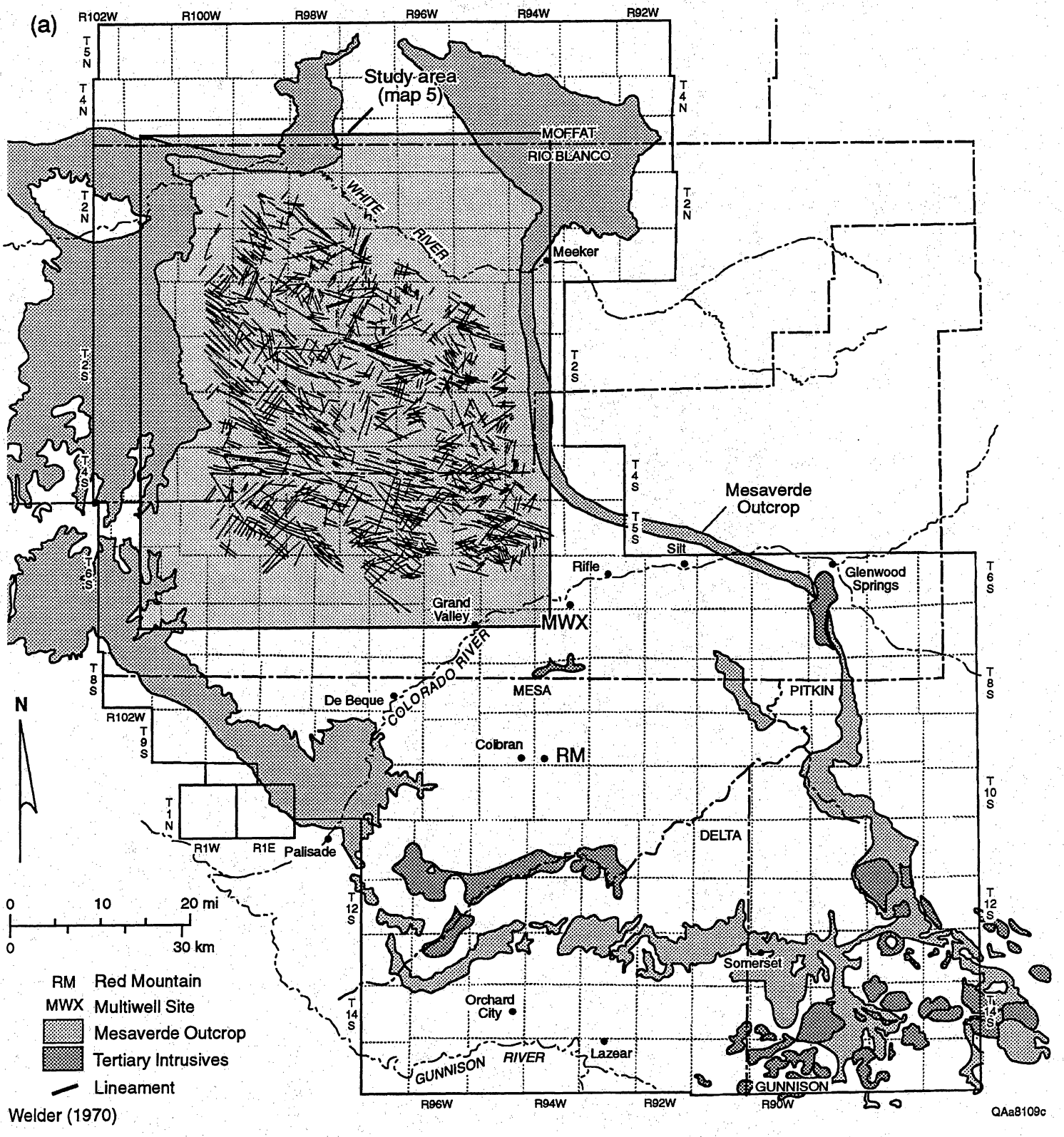

Figure 36. (a) Aerial photolineament joint sets from outcrop in the Green River and Wasatch Formations, northern Piceance Basin, mapped by Welder (1970) and modified from Smith and Whitney (1979) (map 5), and (b) enlargement of study area.

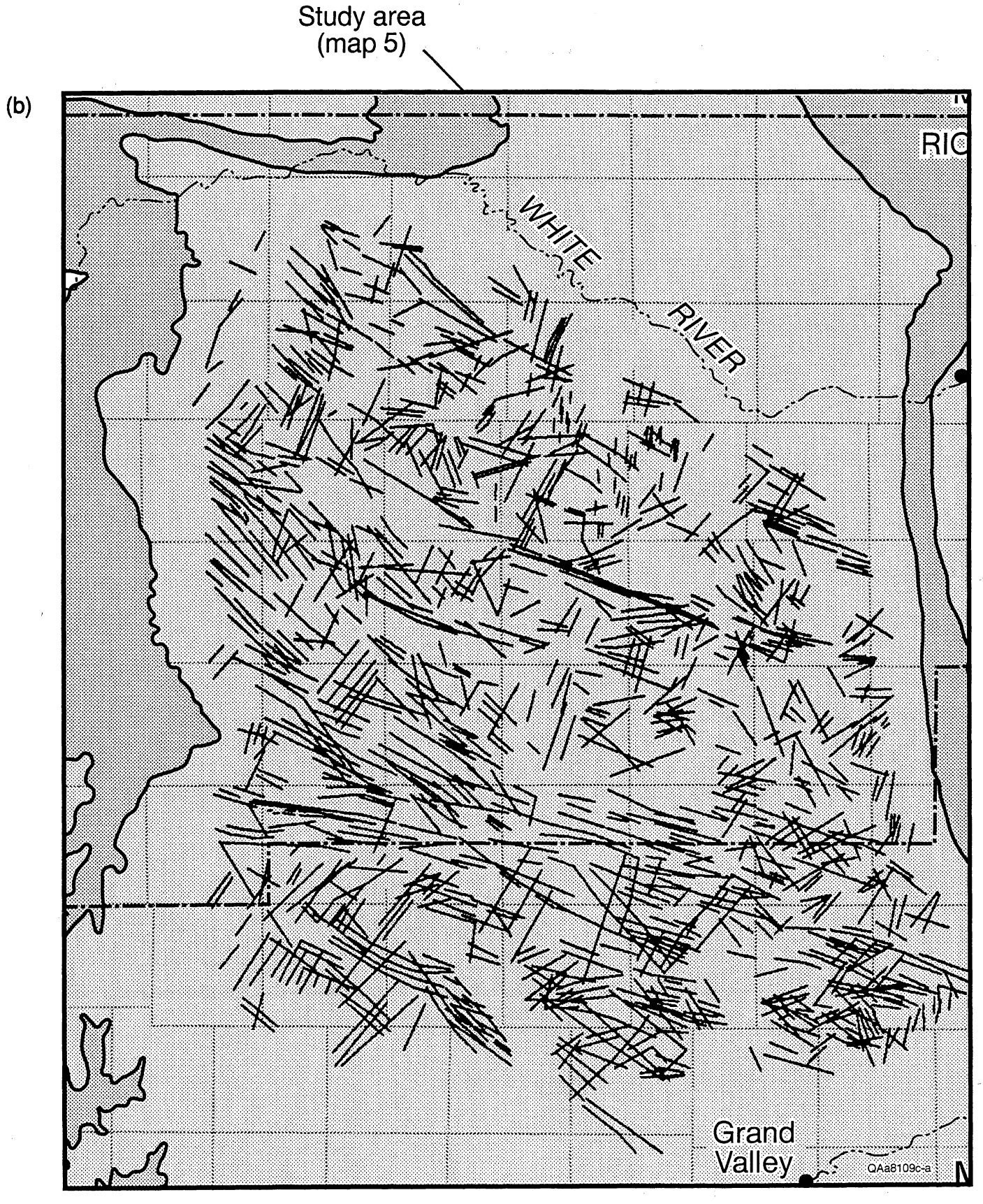
Study area
(map 5)
(b)
WHITE
RIVER
Grand
Valley
QAa8109c-a

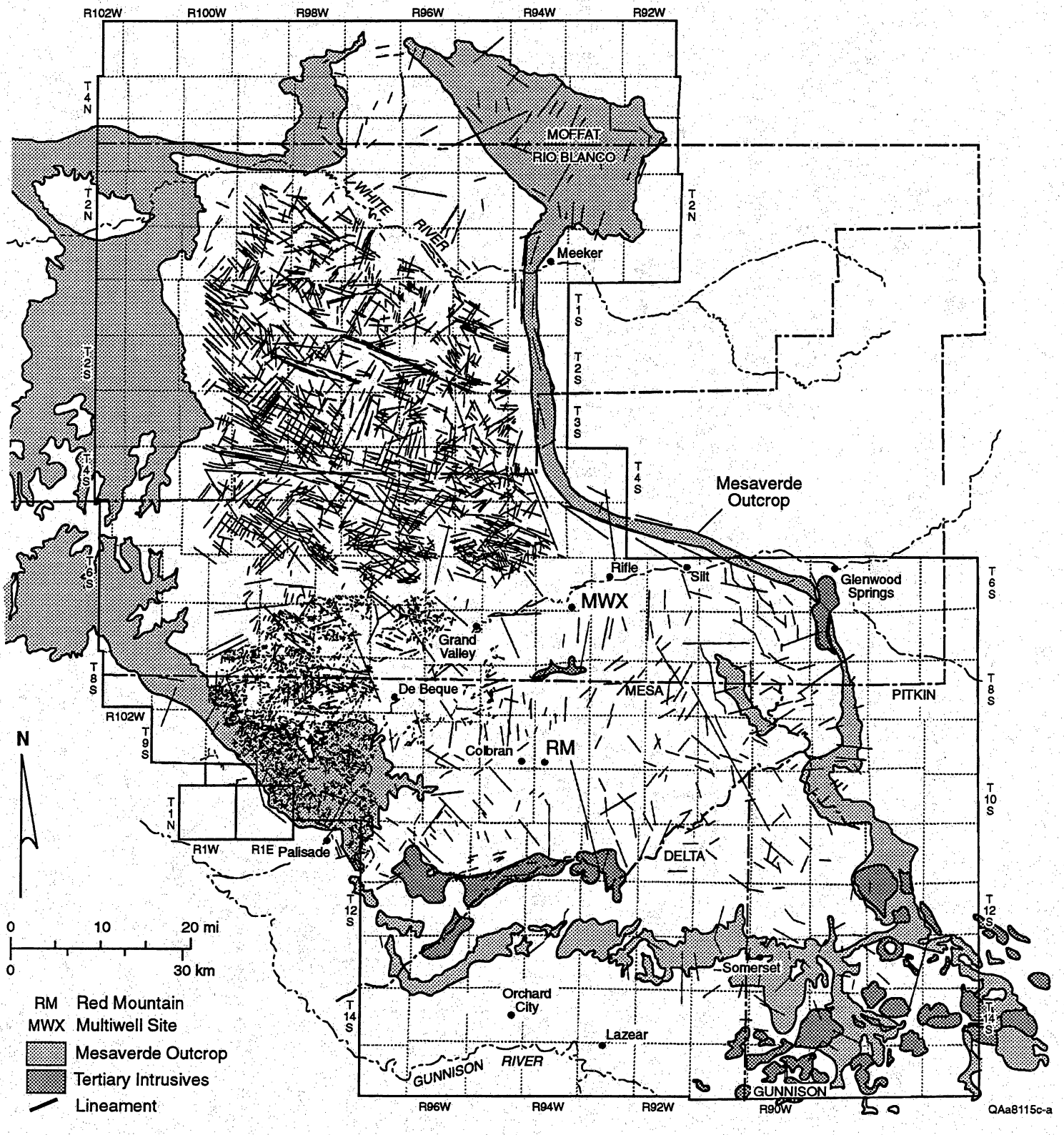

Figure 37. Composite of all lineaments in the Piceance Basin mapped in this and previous studies. See figure 30 for location of study areas (combined maps).

Basin (figs. 30 and 35) based on aerial photographs and photoindices. They concluded that a considerable diversity of joint sets appears to exist, but trends of N30°–40°E and N60°–65°W are probably most abundant. In addition, there are sets trending about N70°E and east-west, but north-south joints are essentially absent (Kelley and Clinton, 1960). The fracture trends are not much at variance with those of the Uncompaghre Uplift to the south, where the "dominant" fracture trend ranges from N40°–55°E. Little significant relationship between mapped fracture sets and local folds is apparent (Kelley and Clinton, 1960).

Welder (1970) published a map showing joint patterns inferred from aerial photographs within the Green River and Wasatch Formations (figs. 30 and 36). Generally, fractures trend northeasterly and northwesterly (figs. 30 and 36). Smith and Whitney (1979), using airphoto lineaments, covered a region similar to that of Welder (1970) (fig. 30) and concluded that the most prominent joint sets in the Green River and Wasatch Formations strike north-northwest. The second most prominent direction is north-northeast. Along Cathedral Bluffs, at the western edge of the basin, major subvertical joint sets have developed parallel to the cliff face, probably in response to unloading (Smith and Whitney, 1979). Smith and Whitney (1979) noted a strong parallelism between the strike of the major joint trend and the principal normal faults in the Green River Formation. This indicates that both faults and natural fractures may have formed in a stress environment in which the maximum horizontal compressive stresses were oriented east-northeast, reflecting epeirogenic movements which took place in Late Tertiary and possibly early Quaternary (Smith and Whitney, 1979). The age of jointing, however, remains uncertain (Smith and Whitney, 1979). A brief summary of additional natural fracture studies and stresses recorded in the Piceance Basin follows below, and for a more detailed description of the natural fracture attributes in the Piceance Basin, see Tremain and Tyler, herein.

BRIEF SUMMARY OF NATURAL FRACTURE STUDIES AND STRESSES IN THE PICEANCE BASIN

Two types of natural fracture systems are present in the Piceance Basin: regional fracture sets and fracture sets associated with specific folds or faults (Kelley and Clinton, 1960; Lorenz

and Finley, 1987a). Regional fracture sets can be caused by small regional strains in conjunction with high fluid pressures (Warpinski, 1986), and they can occur in flat-lying, unfaulted rocks (Hancock, 1985). Fractures associated with folds and faults may have regular geometric patterns, but they commonly cut across lithologic boundaries (Hancock, 1985). Several regional fracture sets of different ages are present in the Piceance Basin (Murray, 1967; Amuedo and Ivey, 1978; Smith and Whitney, 1979; Smith, 1980; Jamison and Stearns, 1982; Grout and Verbeek, 1983; Verbeek and Grout, 1983, 1984a, b; Finley and Lorenz, 1988; Grout, 1991; Lorenz and Finley, 1987a, b, 1991; Lorenz and Hill, 1991, 1994; Tyler and others, 1991a, b, 1993; Tremain and Tyler, herein; and references therein).

Fracture (cleat) sets in Upper Cretaceous Mesaverde Group and lower Tertiary Wasatch coal beds along the Grand Hogback monocline have been correlated on the basis of style, relative age, and orientation with sets of regional extension joints in enclosing clastic rocks (Grout, 1991; Grout and Verbeek, 1992b). Three of the joint sets (Upper Cretaceous) predate late Laramide thrust-fold events and are exposed along the southern Mesaverde outcrop belt, the Grand Hogback monocline, and along a narrow basinward strip adjacent to the monocline. Additional Tertiary joint sets, which postdate these events, are exposed along the hogback and within the basin. Further, Grout (1991) found local fold-parallel sets developed on the Divide Creek Anticline that are synchronous with splay faulting but predate the Tertiary sets in the basin.

Prefold face cleats in the Grand Hogback monocline strike east-northeastward (M. A. Grout, unpub. data) and west-northwestward. Prefold butt cleats strike north-northeastward to north-northwestward. The rocks that contain these fractures were passively rotated on the basinward flank of the monocline above the Laramide fold-thrust system, and stratigraphic and structural evidence suggests that the face-cleat sets are sequential products of the same period of compression that later gave rise to the Grand Hogback monocline and associated intrabasin folds (Grout and Verbeek, 1992b). Face cleats in angled core recovered from correlative-age strata at the U.S. Department of Energy and the Gas Research Institute Multiwell (MWX) site,

5 mi (18 km) southwest of the monocline, probably correspond in part to one of the east-northeast face-cleat sets in the monocline (Tyler and others, 1993).

In field-related studies in the southern Piceance Basin, Grout (1991) found that most of the Upper Cretaceous face cleats are unmineralized, orthogonal to bedding, and spaced from 0.5 inch (1.27 cm) to more than 12 inches (>30.5 cm) apart, depending on the thickness of the coal layer and the coal rank. The butt cleats are smaller, irregular, curviplanar fractures that commonly abut the face cleats at right angles. Butt cleats strike north-northwestward and their spacing ranges from less than 0.5 inch (<1.27 cm) to more than 8 inches (>20.3 cm), depending on the coal thickness and rank.

Younger and sequentially developed Tertiary regional joint sets, termed F_1 (oldest) through F_5 (youngest), show consistent style throughout the basin. Early-formed F_1 (north-northwest-striking) and F_2 (west-northwest-striking) joint sets are present chiefly in the northern two-thirds of the basin, whereas the intermediate-age F_3 (east-northeast-striking) joint set dominates the fracture network in the south half of the basin (Grout, 1991). The F_4 joints (north-northwest-striking) are abundant throughout the basin, but the F_5 joints are sparse, occurring only in Eocene oil shales. A correlation exists between the orientation of Tertiary joints in clastic beds and the orientation of Upper Cretaceous face and butt cleats in coal beds in the Piceance Basin. Most cleats in the Upper Cretaceous coal beds have an orientation and fracture style similar to that of Tertiary F_3 and F_4 joint sets. In the southeastern Upper Cretaceous exposure, the face cleats trend east-northeastward and are correlated in style and orientation with the Tertiary F_3 joint set that is both prominent and abundant in the sandstones in this area (Grout, 1991). In the De Beque Canyon and Grand Mesa areas, most of the Upper Cretaceous face cleats strike from 060° to 066°, and at the Red Mountain site and along the south rim of the basin from 050° to 086°. In the center of the basin, these face cleats correlate with the F_3 fractures exposed in the Wasatch Formation (Grout, 1991). However, face cleats in lower Tertiary coaly stringers on the Divide Creek Anticline are subvertical and strike

313°–322° (Grout, 1991). The age of Tertiary fractures is constrained by structural, stratigraphic, and geomorphic evidence and is bracketed at 43 to 10 mya (Verbeek and Grout, 1986).

The relative age of Upper Cretaceous and Tertiary fracture sets, established by abutting relations, indicates that the maximum horizontal compressive stress (stress parallel to fracture strike) rotated with time before, during, and following Laramide compressive events (Tyler and others, 1993). Vertical and lateral extrapolation and lateral correlation of joints and face cleats, therefore, cannot be randomly applied throughout the Piceance Basin because differences in lithology, age, and burial and thermal histories may cause fractures of different orientation to form in adjacent and overlying strata (Grout, 1991; Grout and Verbeek, 1985, 1987).

Stress Orientation

The Piceance Basin is in the Colorado Plateau interior stress province (Zoback and Zoback, 1980; 1989), which is surrounded by the Cordilleran Extension stress province (fig. 38). The other stress provinces near the Piceance Basin are the Southern Great Plains stress province and the Mid-Plate stress province. The Colorado Plateau stress province originally was characterized by west-northwest-trending regional maximum horizontal compressive stress orientations—nearly perpendicular to the surrounding stress direction in the Cordilleran Extension stress province (Zoback and Zoback, 1989; fig. 38). However, focal mechanisms (normal and strike-slip faults) from the Colorado Plateau interior suggest that the stress regime is extensional. The difficulty in interpreting the tectonic stress fields in this region and understanding their apparent variations may be related to low differential horizontal stresses, as suggested by the apparent absence of major thrust faulting within the Colorado Plateau interior (Zoback and Zoback, 1980, 1989). This interpretation is consistent with in situ stress measurements in the Piceance Basin that indicate all three principal stresses are approximately equal to lithostatic pressure [1.0 psi/ft; 23 kPa/m) (Wolff and others, 1974; Bredehoeft and others, 1976; Warpinski and others, 1983; Tremain and Tyler, herein). The significance of this

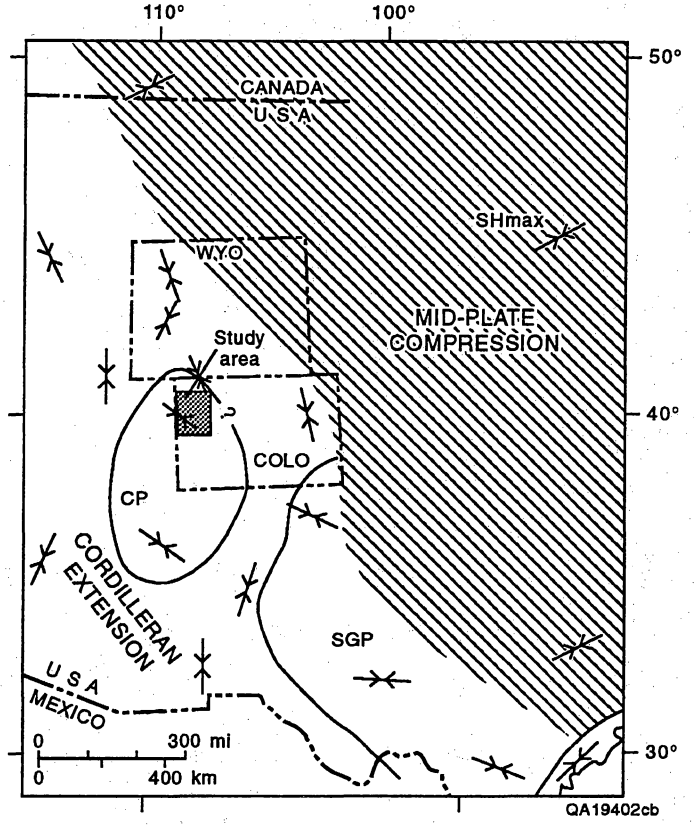

Figure 38. Stress province map showing major stress province boundaries in the vicinity of the Piceance Basin. Inward pointing arrows indicate SHmax direction. CP = Colorado Plateau stress province; SGP = Southern Great Plains stress province. Study area is near the boundary between the Cordilleran Extensional Province and the Midplate Compressional Province. (Modified from Zoback and Zoback, 1989.)

for cleats in coal beds is that prediction of fluid flow pathways and anisotropy may be complicated.

LINEAMENT DATA SOURCES AND PROCEDURES

Landsat Imagery

Two Landsat Thematic Mapper (TM) images (scale 1:250,000) were used for this study (figs. 30–32). These two images provide coverage of most of the Piceance Basin and extend several miles beyond the basin boundary as defined by the outcrop contact between the Mesaverde Group and Mancos Shale. These false-color composite (FCC) images were generated with data from bands 7 (red), 4 (green), and 2 (blue). These bands detect reflective infrared and visible light between wavelengths of 0.52 and 2.35 μm. In bands 4 and 7 the contrast between vegetation and soil is relatively large. Some variations in soil and rock composition, such as might occur along a fault or a formation contact, are more visible in FCC images composed of these three bands. The visibility of lineaments demarcated by vegetation changes, faults, or formation contacts is enhanced by these image characteristics. The resolution of the Thematic Mapper in bands 7, 4, and 2 is approximately 100 ft (~30 m).

Two SLAR images (scale 1:100,000) were used in the southern Piceance Basin (figs. 30, 33, and 34). The SLAR imagery of the southern Piceance Basin, acquired under previous GRI-sponsored tight-gas sandstone programs, provide unique, otherwise unavailable, and highly interpretable imagery of the southern part of the basin. SLAR is a particularly valuable tool for recognizing major fracture patterns and identifying regional structural features.

Lineament Mapping Procedures

The lineament mapping procedures and text herein relies heavily on the work of Baumgardner (1987, 1991, 1994, and unpub. data) in the San Juan Basin. Baumgardner's (1991, 1994) lineament procedures and results have been adapted, and regionally extrapolated, for

use in the Piceance Basin. Lineaments were mapped in a series of steps. The Landsat and SLAR images were placed on a light table and viewed with transmitted light. A transparent sheet of mylar was placed over the image, and the end points of each lineament were marked. To ensure that each image was given equally rigorous inspection, records were kept of time spent per image. Each scene was examined for 5.5 to 7.0 hr. Differences in time spent on each image were caused by differences in complexity of features on each image, but this probably did not significantly affect mapping of the lineaments.

After thorough visual inspection was completed, a second sheet of transparent mylar was placed over the first, and the end points were connected by a line drawn on the second sheet. In this way the image was not obscured during the initial visual inspection by a growing network of lines. Then, the mapped lineaments were checked against U.S. Geological Survey topographic (1:100,000) and geologic (1:500,000) maps to establish the relationship between lineaments, geomorphology, and surface structural features. Lineaments were compared with maps of surface geology to determine whether spatial correspondence existed between lineaments and mapped geologic features, such as faults and formation contacts. At this point, the lineaments are being digitized for computer-assisted statistical analysis.

PRELIMINARY RESULTS

Most linear topographic features probably form as a result of weathering and erosion along linear fractures. Many surface fractures may form in response to stresses in near-surface rocks, which may be different from those in the deep subsurface. Differences in age, thickness, and tectonic history of rocks at the surface and those at depth are likely to produce differences in orientation, length, and location of fractures. As a result, lineaments that form along surface fractures may not be representative of fractures or stress directions at depth in reservoir rocks.

Of the 6,968 lineaments mapped edge to edge in this study, most are within the boundary of the Piceance Basin (fig. 37). Of these, many were checked against geologic maps and some were field checked. More than a third are straight streams or valley axes. Straight formation

contacts account for a small number of the lineaments checked. Some mapped faults were recognized on Landsat and SLAR imagery. More than half of the lineaments checked are straight ridges, tonal anomalies, and other linear features.

Graphical Display of Results

Lineaments from previous studies of the Piceance Basin (figs. 35 and 36) are compared with one another and with lineaments mapped in this study (figs. 31–34); the lineaments also will be correlated with production values from wells in the basin. Because the previous studies were based on imagery at scales different from that in the present study, comparison of the coincidence of lineaments mapped on different images by different observers was possible. Of 6,968 lineaments from all studies, only a few coincided between different studies. Lineaments were considered to coincide if they (1) had the same azimuth within ±5° and (2) overlapped for part of their length.

Lineament Azimuth and Polar Graphs

Lineament azimuths were analyzed to determine (1) if a consistent lineament trend existed for all studies and (2) if a trend exists between lineaments and production. Polar graphs were used in this study to display orientation data because of their familiarity and ease of interpretation. Because lineament data are symmetrical about the axis of a polar diagram, the northern half, from 270° through 360° to 90°, of these diagrams is used (figs. 39–45). These figures and the following results indicate that lineament mapping is strongly dependent upon the interpreter, the type of data base, and the scale of the data base used.

The mean lineament azimuth for Landsat lineaments in the northern Piceance Basin study area (figs. 31 and 39) is between 10° –20° (mean lineament ~18°, with a standard error of 6.65). A bimodal occurrence to lineament azimuth (300°–320°) is observed and is similar in orientation to the F_4 fracture (fig. 23). Most of these lineaments occur within the Green River

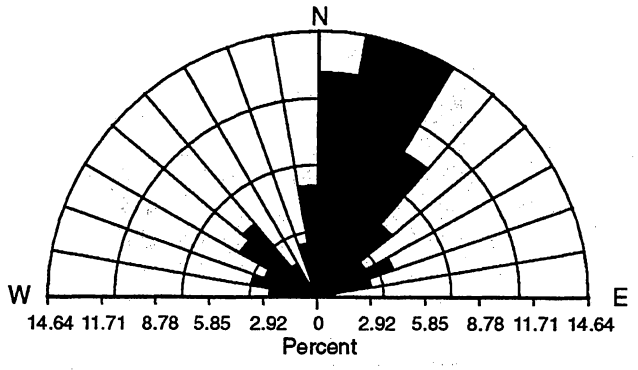

Map 3	Statistics
N = 225	Vector = 18.1°
Class interval = 10°	Std. error = 6.65
Maximum percentage = 14.6	
Mean percentage = 5.55	
(standard deviation = 4.28)	QAa8351c

Figure 39. Polar graphs of Landsat lineaments in the northern Piceance Basin mapped in this study (map 3). The mean lineament azimuth is similar to the dominant F_4 fracture orientation (fig. 23).

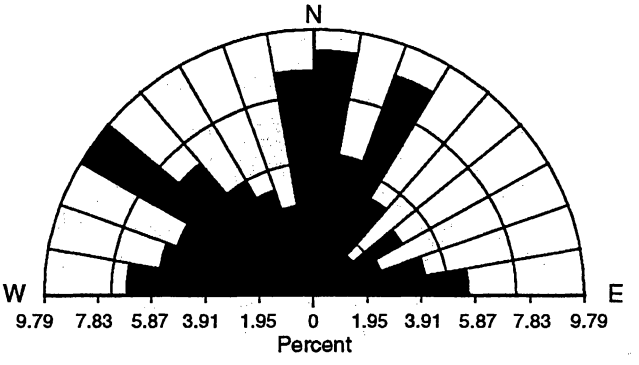

Map 4	Statistics
N = 265	Vector = 330.1°
Class interval = 10°	Std. error = 22.34
Maximum percentage = 9.8	
Mean percentage = 5.55	
(standard deviation = 2.21)	QAa8352c

Figure 40. Polar graphs of Landsat lineaments in the southern Piceance Basin mapped in this study (map 4).

(a)

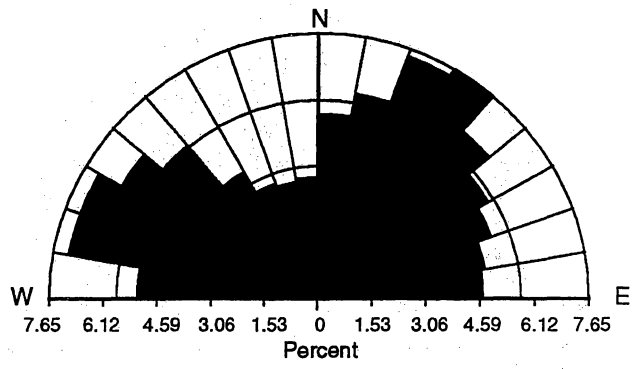

Map all (combined)	Statistics
N = 6968	Vector = 65.5°
Class interval = 10°	Std. error = 7.92
Maximum percentage = 7.6	
Mean percentage = 5.55	
(standard deviation = 1.34)	QAa8357c

(b)

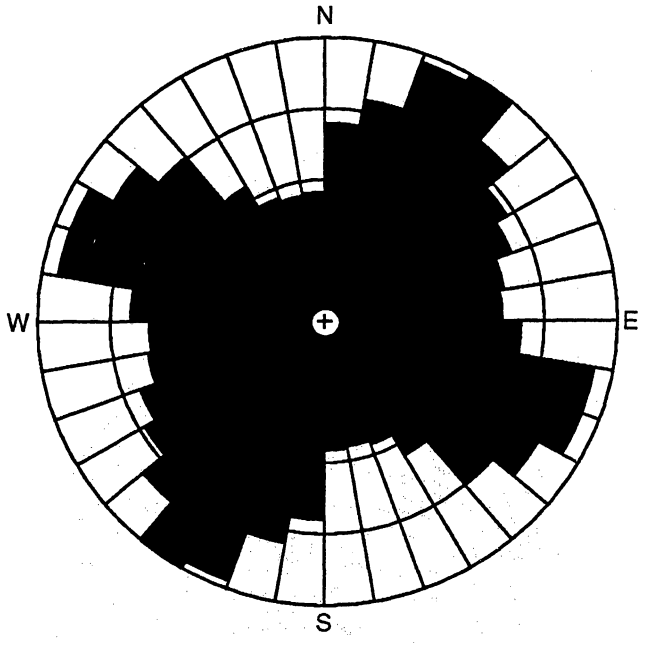

Map all (combined)	Statistics
N = 6968	Vector = 65.5°
Class interval = 10°	Std. error = 7.92
Maximum percentage = 7.6	
Mean percentage = 5.55	
(standard deviation =1.34)	QAa8358c

Figure 45. Polar graph composite of all lineaments in the Piceance Basin mapped in this and previous studies. See figure 1 for location of study areas. (a) Polar graphs used in this study to display orientation data because of their familiarity and ease of interpretation. Because lineament data are symmetrical about the axis of a polar diagram, only the northern half, from 270° through 360° to 90°, of these diagrams will be used. (b) Because of the large data base, the complete polar graph is used. The mean lineament azimuths are similar to F_2 and F_4 fracture trends (figs. 21 and 23).

Formation and parallel stream segments. In the northeastern Piceance Basin, the Landsat lineaments (fig. 31) that occur in the Danforth Hills area are associated with the Mesaverde Group strata. The lineament azimuth for Landsat lineaments in the southern Piceance Basin study area (figs. 32 and 40) is also bimodal (300°–320° and north–30°) with a mean vector of 330°. The lineaments occur in the Mesaverde Group, Wasatch Formation, and the Green River Formation. SLAR lineament azimuth in the southern Piceance Basin (figs. 33, 34, 41, and 42) are also bimodal between 310°–330° and 30°–60°. The mean vector ranged between 10° and 23°, and the standard error was up to 25. The lineaments occur predominantly in the Wasatch and Green River Formations.

In previously published studies, the mean lineament azimuth for the aerial photographic and photoindices study of Kelly and Clinton (1960) in the southwestern Piceance Basin indicated considerable diversity of lineaments, but trends of 20°–50° and 280°–310° are probably most abundant (figs. 35 and 43). In addition, there are sets trending approximately east-west; north-south joints are essentially minor (Kelley and Clinton, 1960). The lineament and fracture trends are not much at variance with those of the Uncompaghre Uplift to the south, where the "dominant" fracture trend ranges from N40°–55°E. Little significant relationship between mapped lineament and fracture sets and local folds is apparent (Kelley and Clinton, 1960).

In Welder's (1970) aerial photography study of lineaments within the Wasatch and Green River Formations of north-central Piceance Basin, the mean lineament azimuth is 295°, although a bimodal trend exists of between 280°–300° and 20°–40° (figs. 36 and 44). Welder (1970) inferred from the study that the fractures trend northeasterly and northwesterly. Smith and Whitney (1979), who covered a region similar to that by Welder (1970) (fig. 30) using airphoto lineaments, concluded that the most prominent joint sets in the Green River and Wasatch Formations strike north-northwest. The second most prominent direction is north-northeast. Smith and Whitney (1979) noted a strong parallelism between the strike of the major joint trend and the principal normal faults in the Green River Formation. This

Regional Correlation of the Williams Fork Genetic Depositional Sequences

Using the genetic stratigraphic framework established in previous studies of the Sand Wash Basin (Hamilton, 1993, 1994), we readily correlated the Williams Fork Formation and its coal-bearing units southward into the Piceance Basin. Identifying the principal bounding surfaces of the Iles and Williams Fork genetic sequences on the basis of log character, including the occurrence of Mancos Shale flooding surfaces, bentonite beds (Yampa), and Foraminifera, is relatively straightforward in the Sand Wash and Piceance Basins (figs. 46 and 47). The Sand Wash and Piceance Basins occupied a marginal marine setting along the western edge of the Western Interior Seaway during Mesaverde deposition (fig. 9, Tyler, herein); the successive clastic wedges are bracketed by transgressive marine flooding surfaces. Defining genetic bounding surfaces in the continental/alluvial plain facies to the west of the coastal plains in these basins was more problematic but still regionally possible.

In the Sand Wash and Piceance Basins, the Williams Fork Formation is divided into at least three to four genetic depositional sequences (coal zones or packages), each bounded by regionally extensive low-resistivity shale markers (Mancos tongues/marine flooding surfaces). Each genetic unit is a progradational-aggradational couplet characterized by fluvial-deltaic sedimentation where a progradational strandplain/delta plain system is flanked landward by a coastal plain system, which is traversed by a fluvial system feeding the advancing shoreline. In the eastern Piceance Basin, the shale markers are easily recognizable, separating aggradational coal-bearing coastal plain facies of one depositional episode from the overlying upward-coarsening progradational sequence of the next. In a landward direction (westward), identification of the shale markers is less precise.

Comparison with Traditional Stratigraphy

In the Piceance Basin the Williams Fork Formation, as operationally defined herein, varies from the traditional stratigraphy in three main ways:

1. The Rollins-Trout Creek shale and overlying sandstone member, which are traditionally assigned to the uppermost part of the underlying Iles Formation (Johnson, 1989, and references therein; Siepman, 1985), are in this study included with the Williams Fork Formation (fig. 48). Depositionally, the Rollins-Trout Creek shale/sandstone couplet records an episode of marine transgression and subsequent progradation and served as a platform for peat accumulation. Thus, the progradational Rollins-Trout Creek sequence belongs genetically with the overlying aggradational Williams Fork Formation (figs. 46–48).

2. The operationally defined Williams Fork Formation is made distinct or is separated from the undifferentiated Upper Cretaceous strata by mapping variations in sandstone and coal stacking patterns. In his published cross sections, Johnson (1989) showed the upper part of the Williams Fork Formation as partly equivalent to the Mesaverde Formation (fig. 48). The upper Williams Fork Formation, as traditionally defined by Johnson (1989) and other authors, is herein separated into a genetic sequence; that is, it is a prominent aggradational sequence of interbedded bed-load and mixed-load fluvial sandstones, together with minor siltstones and coals (figs. 46–48). We also correlate the undifferentiated Upper Cretaceous strata as equivalent to the Lewis/Lance depositional sequence. In the Meeker area the associated rocks contain arenaceous Foraminifera (Newman, 1965). The presence of Foraminifera indicate that nearshore marine deposits of the undifferentiated Upper Cretaceous strata are part of the Lewis transgression and regression (Lewis Shale of the Craig area; Newman, 1964, 1965). Hence, the traditionally defined thick Williams Fork Formation at Meeker can be split into units that are time equivalents of the Williams Fork, Lewis, and Lance Formations of the Craig area (Newman, 1964). Moreover, the coaly sequence above the Lion Canyon Sandstone (the Lion Canyon Sandstone Member is stratigraphically equivalent to the Fox Hills Sandstone; Gill and Cobban, 1966) and below the Fort Union Formation contains the gastropod *Tulotomopos Thompsoni*, which is restricted to the Lance and equivalent formations (Pipiringos and Rosenlund, 1977).

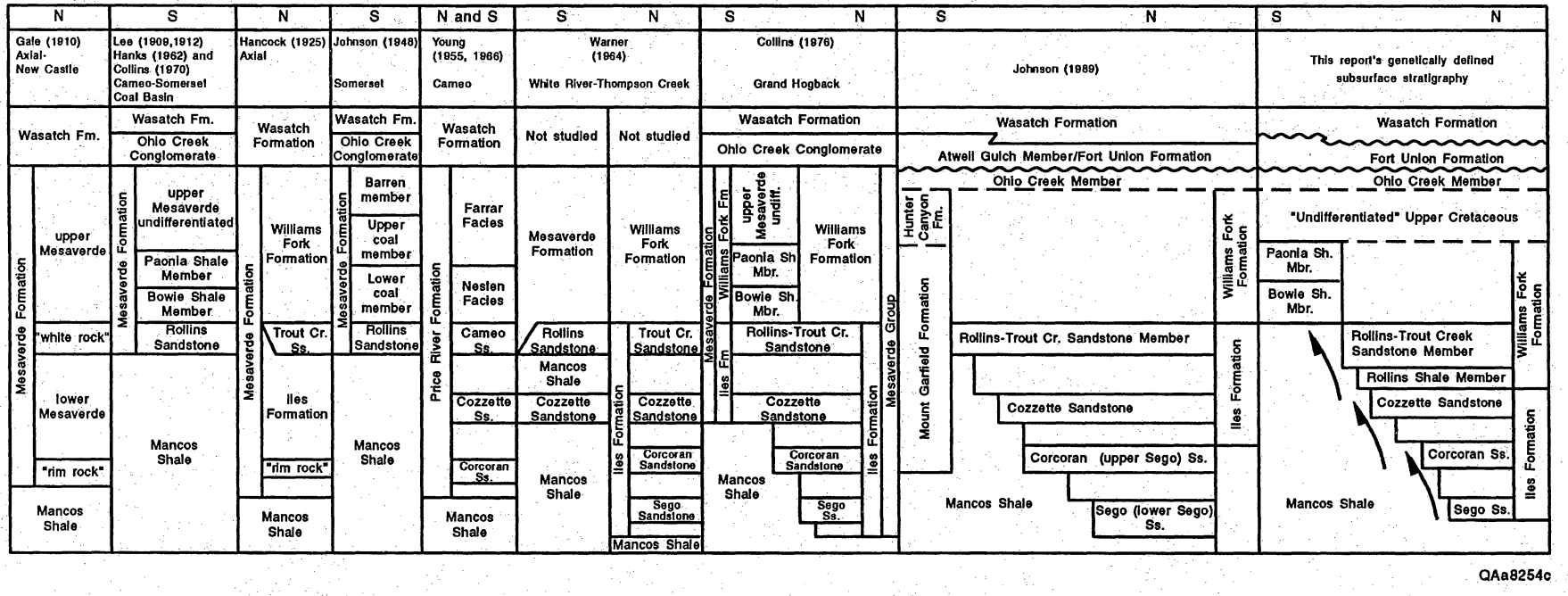

Figure 48. Nomenclature used in this study and by various previous authors for the Upper Cretaceous and early Tertiary rocks in the eastern and southeastern Piceance Basin. Modified after Collins (1976) and Johnson (1989).

3. The genetic depositional sequences of the Williams Fork Formation (genetic units 1, 2, and 3) cut across many of the traditionally defined lithological boundaries. For example, the Cameo coal group in the southwestern part of the basin is not genetically related or stratigraphically equivalent to the South Canyon and Coal Ridge coal groups (see fig. 14, Tyler, herein), as illustrated in Reinecke and others (1991), but is a coal zone that is found directly above the Rollins-Trout Creek progradational shoreline. The Cameo-Wheeler-Fairfield, South Canyon, and Coal Ridge coal zones are genetically separated by progradational/aggradational couplets, bounded by regional flooding surfaces (retrogradational sequences).

REGIONALLY CORRELATABLE WILLIAMS FORK GENETIC SEQUENCES

Genetic Unit 1 (Coal Package 1)

The regionally correlatable lowermost depositional sequence of the Williams Fork Formation, genetic unit 1, is a clastic wedge bounded by regionally extensive, low-resistivity shale markers. The lower bounding surface occurs near the base of the Rollins shale member (Mancos Tongue), where the sequence is characterized by the upward-coarsening, progradational Rollins sandstone member and overlying aggradational coal-bearing rocks (fig. 46). The Rollins shale and sandstone member is depositionally equivalent and homotaxial to the Trout Creek shale and sandstone member in the Sand Wash Basin. The Rollins-Trout Creek shale and sandstone genetic unit is characterized by seaward-stepping progradational sequences extending in a depositional-dip direction for over 60 mi (>100 km) into the basin and containing the thickest and widest linear shoreline (strandplain/delta plain) system in the entire Mesaverde Group. This stacking pattern is best displayed in a regional cross section through T9S and T10S, R97W to R89W in the southern Piceance Basin (plate 1), where at least seven correlatable progradational Rollins-Trout Creek shoreline sequences are recognized (PS-1 through PS-7). Each sequence is bounded by low-resistivity Mancos Shale tongues that represent marine flooding surfaces and consist of upward-coarsening, progradational shoreline

sandstones (plate 1). The youngest regionally correlatable sequences, PS-7 and PS-8, are progradational shoreline sandstones that extended coal-bearing plain deposits beyond the present-day basin margin.

Above each progradational sequence, log facies change into aggradational blocky channel-fill sandstones, interbedded with mudstones and relatively continuous coal beds (Cameo-Wheeler-Fairfield coal zone). The basin's thickest and areally most extensive coals occur in this zone (fig. 49). Maximum thickness of individual Cameo-Wheeler-Fairfield coal beds is 20 to 35 ft (6 to 11 m), and net coal thickness ranges from less than 20 ft (<6 m) to more than 80 ft (>24 m). The most continuous coal beds form just landward (westward) of each Rollins-Trout Creek progradational shoreline sequence. Less continuous, fluvial Williams Fork coal beds occur up the paleoslope to the west, the western limit of coal occurrence being controlled by the transition from coastal plain to alluvial plain deposition. To the east, coal beds pinch out against and/or override the progradational Rollins-Trout Creek shoreline sequences; their ultimate lateral extent is limited by the final shoreline position beyond which marine conditions prevail.

Genetic Unit 2 (Coal Package 2)

The second genetic depositional sequence, unit 2, is a clastic wedge similar to unit 1, except that it did not prograde as far basinward as unit 1. In the southeastern Piceance Basin, unit 2 is subdivided into two genetic units, units 2a and 2b (fig. 46). Unit 2a is bounded by regionally extensive, low-resistivity shale markers. The lower boundary is a flooding surface that terminates the coal-forming conditions of unit 1 (fig. 46). The upper bounding surface is a minor transgressive event (flooding surface), and the log-pattern change above this marker is subtle. Unit 2a is characterized by the upward-coarsening, progradational log patterns of the lower member of the Middle Sandstone (Collins, 1976; Reinecke and others, 1991) in the southeastern parts of the basin and by overlying minor aggradational coal-bearing rocks. Log facies change to the northwest into aggradational blocky channel-fill sandstones, interbedded with mudstones and discontinuous coal beds.

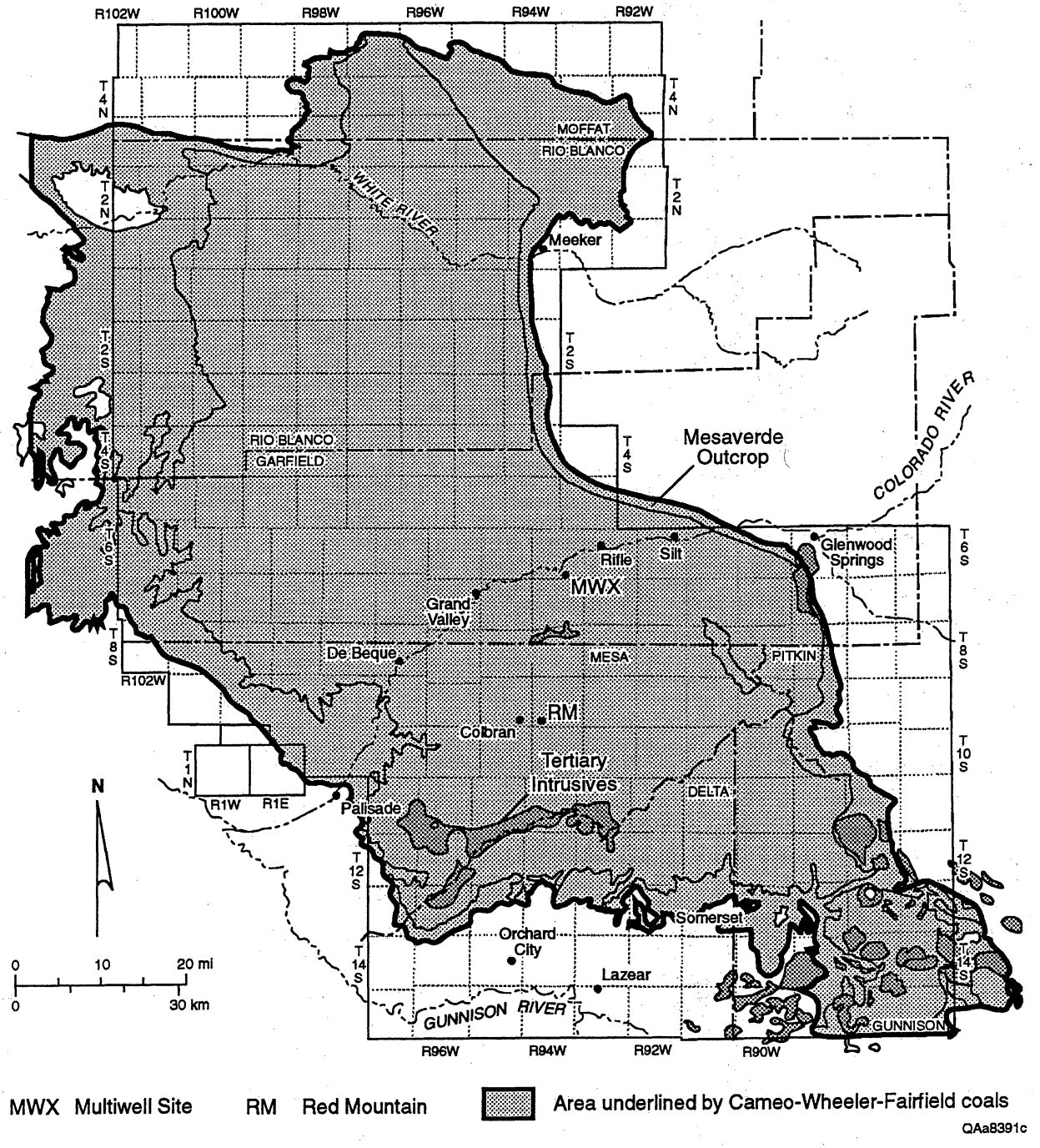

Figure 49. Areal extent of genetic unit 1 coals. Coal-bearing coastal plain deposits extended beyond the present-day margin of the Piceance Basin.

The third genetic depositional sequence of the Williams Fork Formation, unit 2b, is a clastic wedge that possibly extended shoreline and coastal plain deposits farther basinward than unit 2a, but not as far as unit 1. Unit 2b is also bounded by regionally extensive, low-resistivity shale markers (fig. 46). The flooding event that defines the base of unit 2b is minor when compared to other flooding surfaces that punctuate the Williams Fork Formation. Thus, the facies offset from underlying mudstone-rich coal-bearing rocks of unit 2a is subtle. The lower boundary is the maximum flooding surface that precedes the upper member of the Middle Sandstone progradation and the overlying aggradational coal-bearing rocks (South Canyon coal zone). Log facies change to the northwest into aggradational blocky channel-fill sandstones, interbedded with mudstones and discontinuous coal beds. The upper boundary represents another transgressive event, a flooding surface at the base of unit 3.

Recognition of genetic units 2a and 2b is limited to the central and eastern parts of the Piceance Basin (fig. 50), east of R97W. Confident correlation of the maximum flooding surface is possible east of R95W. To the west of R95W, genetic sequence correlation becomes difficult but is still possible.

Genetic Unit 3 (Coal Package 3)

The uppermost genetic depositional sequence of the Williams Fork Formation is genetic unit 3. It is characterized by progradational and aggradational sandstone- and mudstone-rich deposits with minor coal-bearing (Coal Ridge coal zone) horizons. In the southeastern Piceance Basin, unit 3 is dominated by the upward-coarsening and blocky log profiles of the Upper Sandstone progradation (fig. 46), which extended shoreline and coastal plain deposits farther basinward than unit 1. To the northwest, the log facies change to mud-rich aggradational patterns. The upper bounding surface that operationally separates the Williams Fork Formation from the overlying undifferentiated Upper Cretaceous strata is defined on geophysical logs as a change in stacking pattern to blocky, thick fluvial sandstones and accompanying high-

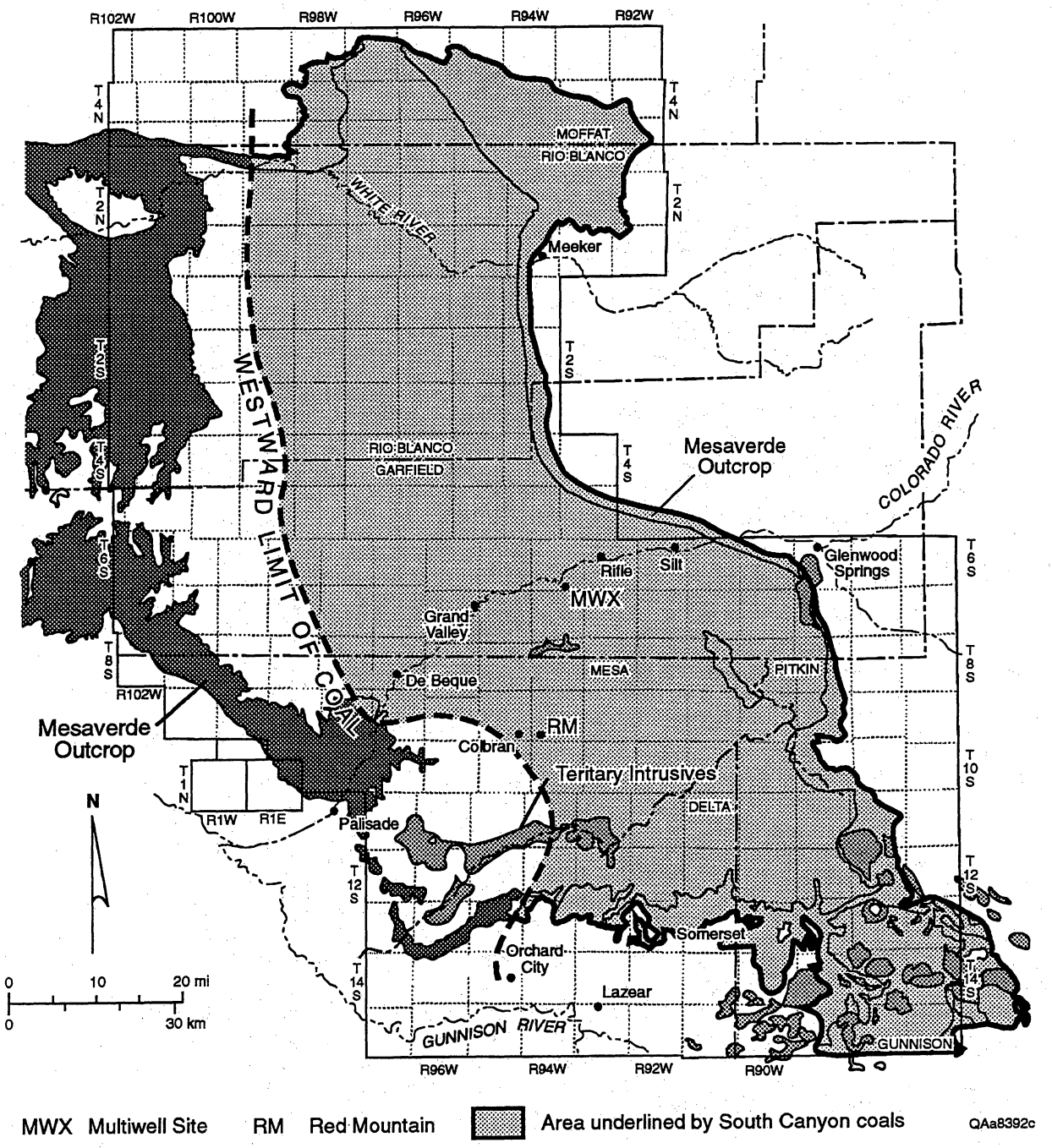

Figure 50. Westward limit of genetic unit 2 coals, indicating a north to northwest orientation of coal thickness trends. Distribution of the coals is intimately related to the depositional systems and basin subsidence trends, indicating an apparent north-south linear shoreline relationship.

conductivity kicks. Coal-bearing strata of genetic unit 3 are limited to the eastern part of the Piceance Basin, east of R95W (fig. 51).

COAL OCCURRENCE OF THE WILLIAMS FORK FORMATION

Coal Identification and Mapping

Coals are identified on geophysical logs by low bulk density, low natural gamma response, very high resistivity, high neutron and density porosities, low sonic velocity, and/or low neutron count. Combinations of these criteria were used because no uniform well log suite was available. Bulk density or sonic logs were run in most wells, and these are the most reliable logs for coal identification. However, natural gamma response was consistently low for all coal beds and was used in conjunction with very high resistivity and shalelike SP response to operationally define coal in some wells.

Regional net coal mapping was undertaken throughout the Piceance Basin. In some areas net coal thickness is inferred because of the lack of data or because of the assimilation of coals by Tertiary intrusive sills. Caution in net coal mapping is advised where thrusting has resulted in the duplication of the coal-bearing section, especially along the Grand Hogback, Divide Creek Anticline, and the Danforth Hills/Wilson Creek area. Unusually thick net coal, in excess of 120 ft, may indicate duplication of the coal section. Confirmation of the thrust duplication of the coal-bearing section will be addressed once access to regional seismic data have been obtained and interpreted. Furthermore, the following discussion of coal depositional systems inferred from coal orientation is based on the use of a net coal map that is an aggregate or average of several genetic sequences and as such is appropriate for regional interpretation. A more detailed description and interpretation of the individual genetic sequences and their net coal thickness is currently ongoing and will be presented in the final report.

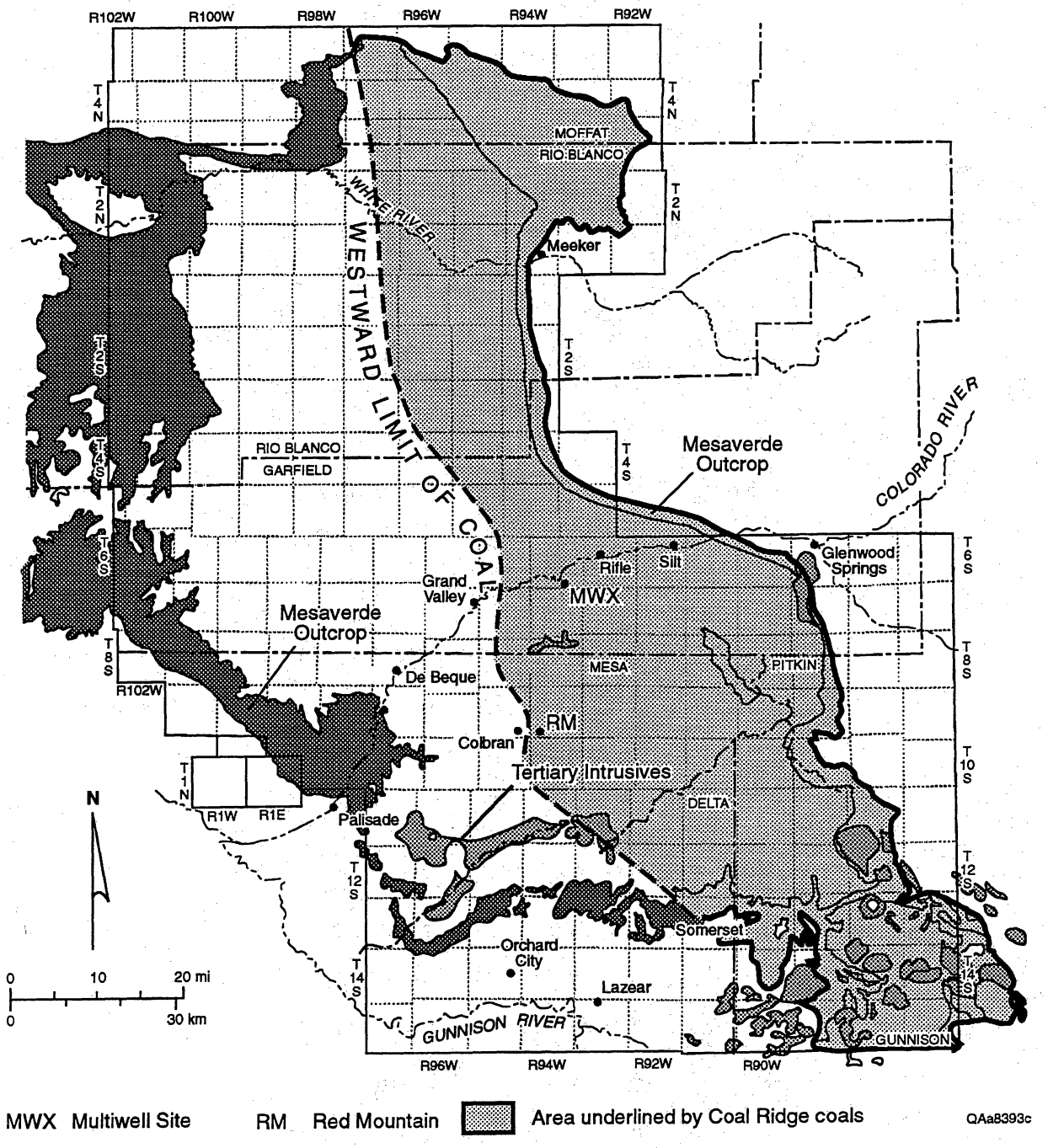

Figure 51. Westward limit of genetic unit 3 coals, indicating a north to northwest orientation of coal thickness trends. Distribution of the coals is intimately related to the depositional systems and basin subsidence trends, indicating an apparent north-south linear shoreline relationship.

Net Coal Occurrence

Conditions for peat accumulation and preservation occur on the coastal plain immediately landward of shoreline (strandplain/delta plain) sandstones (Hamilton, 1993, 1994). Bypassing of coarse clastic sediment, maintenance of high water tables, and optimum subsidence combine in this setting to favor peat accumulation. Gradual westward thinning of coals toward the coastal plain/alluvial plain transition is explained by a lowering water table associated with the rise in surface gradient of the alluvial plain (Hamilton, 1993, 1994). Coals also thin to the east as they pinch out against and override the shoreline sandstones. Marine conditions ultimately limit coal distribution to the east.

In the Piceance Basin coals are thickest in a north-trending belt (fig. 52). Net coal thickness of the Williams Fork Formation is at a maximum thickness in the eastern Piceance Basin, where it is as much as 150 ft (45 m) thick, averaging between 80 and 120 ft (24 and 36 m) (fig. 52). In the southeastern Piceance Basin, coals are thickest in a north-south-trending belt in the vicinity of Divide Creek Anticline. Data are scarce on Williams Fork Formation coal distribution between T5S-T1N, R92W-R97W, north of the Colorado River and in the area approximately 24 mi (38 km) west of the Grand Hogback. Northeast of the White River and east of R98W, net coals of the Williams Fork are oriented northeastward and exceed 150 ft (>45 m) in thickness. Generally the net coal thicknesses average between 80 and 150 ft (24 and 45 m). The thick net coal values may reflect structural duplication of section. Net coal thickness decreases westward to less than 50 ft (<15 m) west of R97W. Thinning also occurs in the southeasternmost part of the basin, where net coal thickness is less than 30 to 40 ft (<9 to 12 m). The thickest and most laterally extensive coals occur in Williams Fork genetic unit 1, the lowermost genetic unit. These coals are generally concentrated in the eastern half of the basin, southeast of the Colorado River and northeast of the White River. Thickness trends, lateral continuity, and sandstone and coal occurrence of genetic unit 1 are currently being evaluated and will be discussed in the final report.

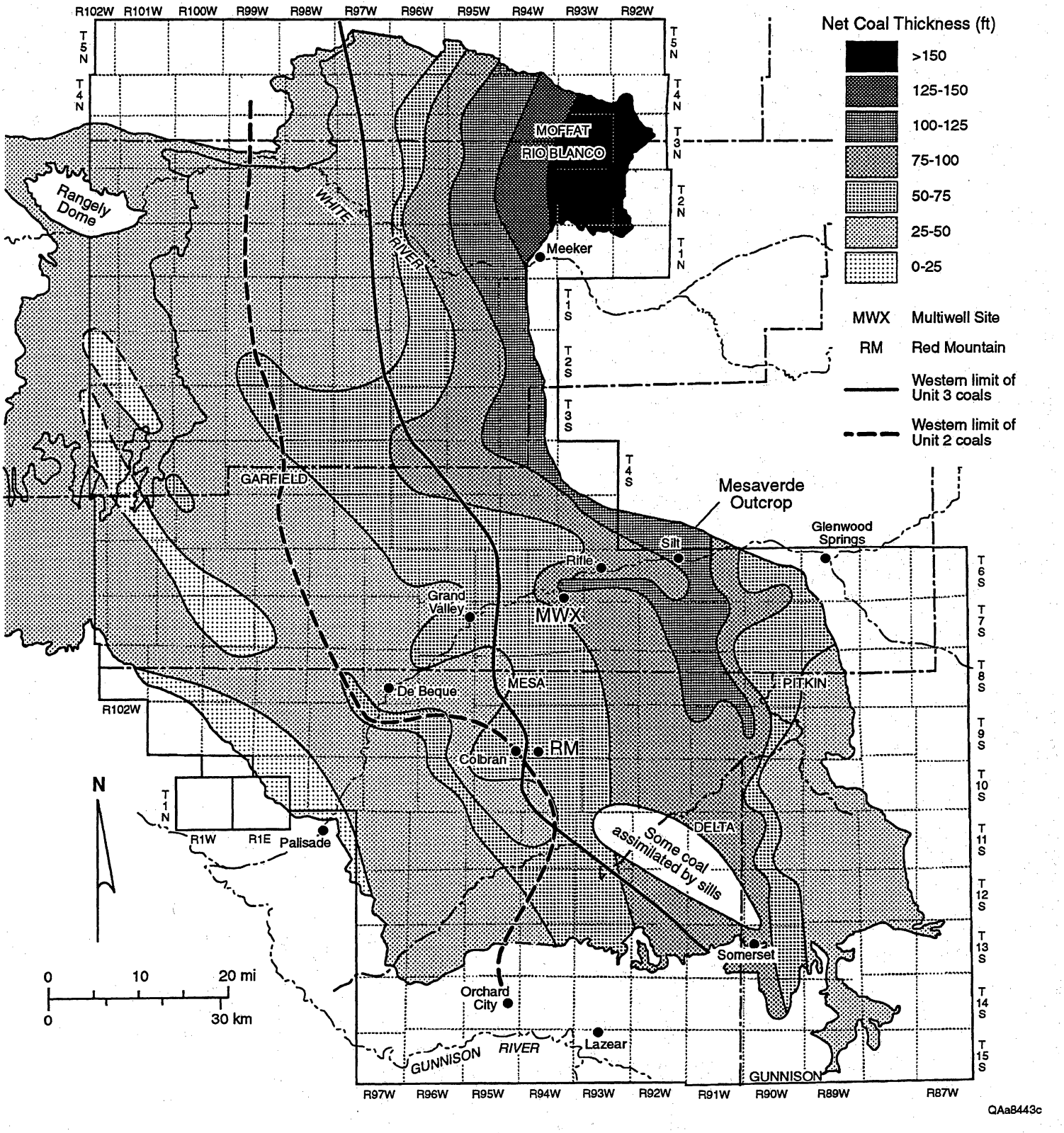

Figure 52. Net coal thickness map of genetic units 1 through 3, Williams Fork Formation. North-northwest to south-southeast net coal thickness trends in the eastern Piceance Basin occur above thick, north-south-oriented progradational shoreline (strandplain/delta plain) systems.

Regionally there is significant coal in the structurally deepest and most thermally mature part of the basin (compare fig. 4, Tyler, herein, with fig. 52). Further, the pronounced north-northwest to south-southeast alignment of coal seam thickness parallels depositional systems and basin subsidence trends (compare figs. 50–52). Moreover, the net coal thickness map indicates that the coal packages are continuous from the subsurface to the eastern, northeastern, and southeastern outcrop belts (figs. 50 and 52). They are thus exposed to meteoric recharge and are potential conduits for basinward flow of ground water and potential coalbed methane targets.

Coal Seam Continuity

Continuity of the Williams Fork coals is variable. Some individual seams were correlatable in the subsurface throughout the eastern half of the Piceance Basin for up to 30 mi (48 km); however, few seams extend to the southern and northeastern outcrop belts. Other seams could be correlated extensively only when grouped together in coal packages. Understanding coal seam continuity is critical to coal gas production and water production because (1) coal seams with considerable continuity provide pathways for diffusion and long-distance migration of coal gases and (2) continuous coals act as major aquifers. Any lack of communication between outcrop and subsurface will influence the hydrodynamics and producibility of coal gases within the basin. Detailed evaluation of individual genetic Williams Fork coals is currently under investigation.

Variability in coal continuity is demonstrated in detailed regional and local genetic stratigraphic cross sections (figs. 53 and 54). Although some coal seams could be traced by their characteristic density and gamma-ray log profiles over most of the southeastern half of the basin, others could be correlated only when grouped within coal packages. Genetic unit 1 coals are somewhat continuous from the subsurface to the outcrop belts in the south and southeast and are thus potential conduits for basinward flow of ground water (figs. 53 and 54). However, where genetic unit 1 coals reach outcrop, they are reduced in number and total thickness

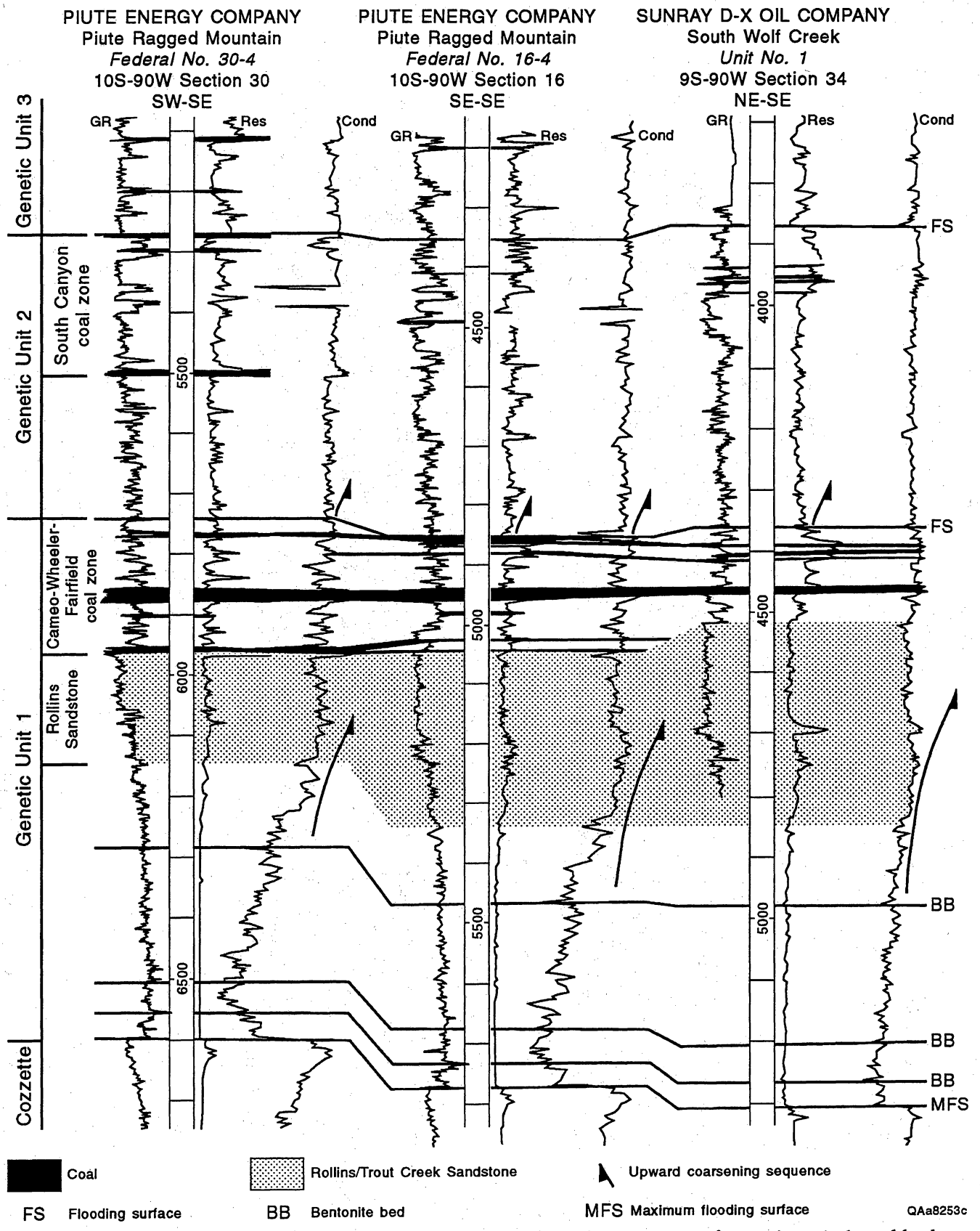

Figure 53. Detailed stratigraphic cross section showing lateral continuity of genetic unit 1 coal beds. Progradation of the Rollins-Trout Creek sandstone and of the coal-bearing horizons to the east is controlled by the depositional systems. Coal beds pinch out against and/or override the shoreline (strandplain/delta plain) sandstones, and their ultimate extent is limited by the final shoreline position beyond which marine conditions prevail.

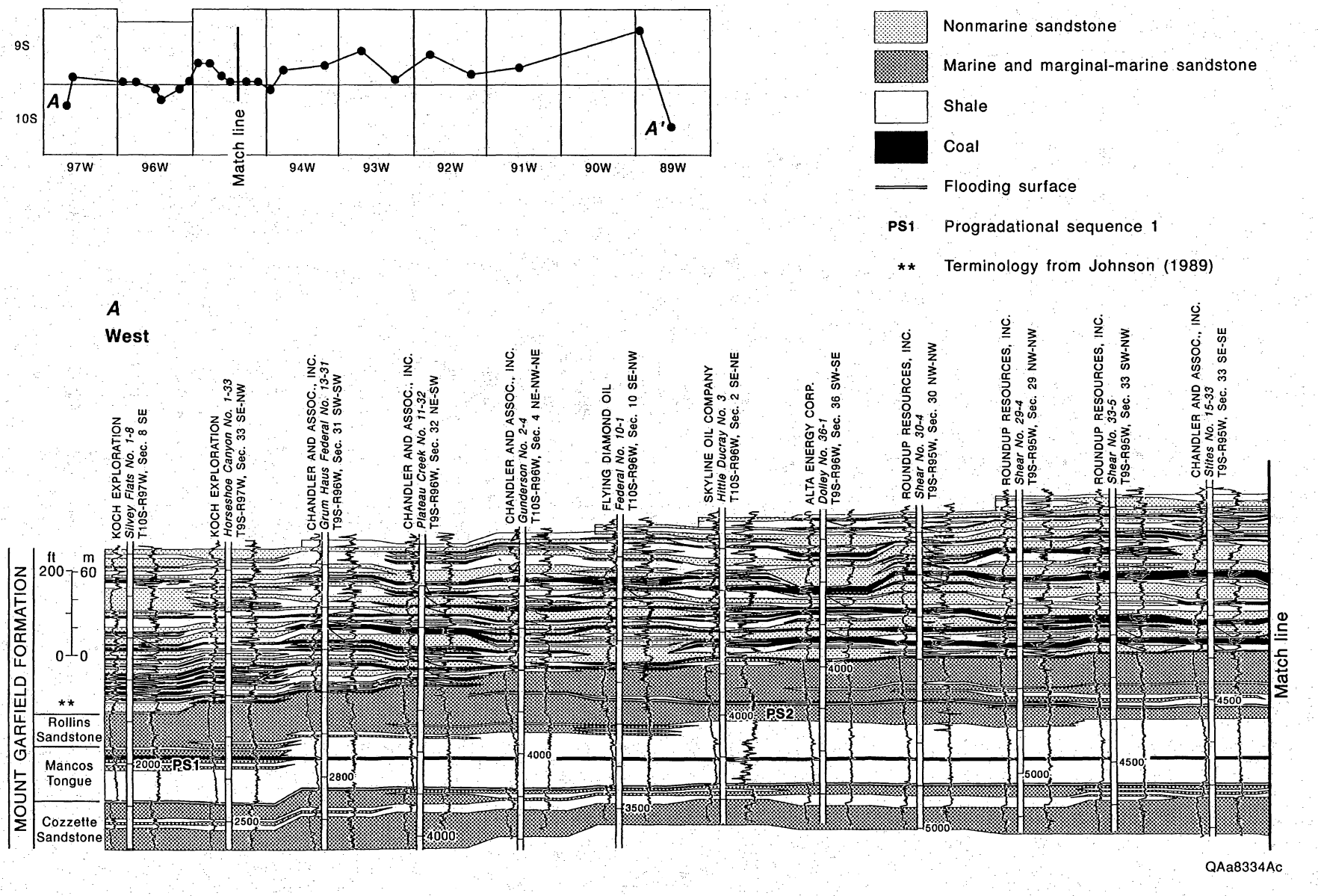

Figure 54. Detailed west-east cross section through T9S showing the genetic sequence stratigraphy, Rollins-Trout Creek progradation, and coal occurrence of unit 1. The western limit of genetic unit 1 coal-bearing horizons is controlled by the transition from coastal plain to alluvial plain deposition. To the east, coal beds pinch out against and/or override the shoreline sandstone, and their ultimate lateral extent is limited by the final shoreline position beyond which marine conditions prevail.

Match line
EXXON COMPANY USA
A. H. Kulp No. 1
T9S-R95W, Sec. 35 SW-SW
TETON ENERGY COMPANY, INC.
Bradshaw Dolley No. 36-3
T9S-R95W, Sec. 36 SW
TETON ENERGY COMPANY, INC.
Dolley No. 6-2
T10S-R94W, Sec. 6 SW-NW
NORRIS OIL COMPANY
Hill No. 29-2
T9S-R94W, Sec. 29 SE-SW
KENAI OIL AND GAS, INC.
Starner No. 26-32
T9S-R94W, Sec. 26 SW-NE
VICTOR DRILLING COMPANY
Gunderson No. 1
T9S-R93W, Sec. 20 NE-NE-NE
EXXON COMPANY USA
Vega No. 4
T9S-R93W, Sec. 35 SW-NE-SW
NORDON CORP. LTD.
Government No. 1
T9S-R92W, Sec. 20 SE-NW
CELERON OIL AND GAS COMPANY
Porter Mountain Federal No. 35-1
T9S-R92W, Sec. 35 NE-NE
MOUNTAIN STATES DRILLING COMPANY
Mountain States - Sun No. 28-1
T9S-R91W, Sec. 28 NE-SW
PRENALTA CORP.
Government No. 12-7-9-89C
T9S-R89W, Sec. 7 SW-NW
Measured section in Coal Basin area*
T10S-R89W
PS1 Progradational sequence 1
Flooding surface
Coal
Shale
Marine and marginal-marine sandstone
Nonmarine sandstone
COAL ZONE
1 Coal Ridge
2 South Canyon
3 Cameo-Wheeler-Fairfield
* Measured section (Collins (1976))
BENTONITE DATUM
QAa8334Bc
A
A'
97W
96W
94W
93W
92W
91W
90W
89W
10S
9S
A' East
Rollins/ Trout Creek Ss
Middle Ss
Up. Ss
Cozzette Ss
Mancos Tongue
Bowie Shale Member
Paonia Shale Member
UNIT 1
UNIT 2
UNIT 3
ILES FM
WILLIAMS FORK FORMATION

relative to the area immediately basinward in R90W-R93W (figs. 53 and 54). Thus, not all coals are positioned to receive recharge; their transmissivity is reduced, and consequently their ability to transmit recharge basinward is reduced.

Genetic unit 2 coals are less continuous in the subsurface and most do not extend to outcrop because their platform of accumulation does not prograde far enough to the east. Genetic unit 2 coals are unlikely to provide potential for interconnected aquifer systems. Genetic unit 3 coals increase in abundance and thickness toward outcrop but have limited westward extent into the basin. Genetic units 2 and 3 are thus minor coalbed methane targets in the Piceance Basin.

The laterally discontinuous coal beds and restricted exposure to the outcrop belt limit the amount of recharge that can be accepted and transmitted basinward from the Grand Hogback and may help explain the presence of mapped underpressure along the basin's eastern margin. Strata that receive too little recharge or are insulated from recharge remain underpressured. Furthermore, limited recharge may have implications for the producibility of coal gas. In the absence of dynamic ground-water flow, less gas is dissolved and swept basinward for eventual resorption and conventional trapping along potential no-flow boundaries. At the same time, the generation of secondary biogenic gases is minimized. Thus, without the additional sources of gas beyond that sorbed on the coal surface, high coal-gas productivity may be precluded. Perhaps the parts of the basin with the best potential for coal-gas production are those basinward of where outcrop and subsurface are in good hydraulic communication.

DEPOSITIONAL SYSTEMS

Three major depositional systems are identified in the coal-bearing Williams Fork Formation from the geometry of framework sandstones and coals and from log facies. A linear shoreline (strandplain/delta plain) system dominates the southeastern part of the basin and is backed landward by a coastal plain system that grades westward into a predominantly fluvial system. Numerous strike-oriented (north to north-northwest) sandstone trends are apparent in

the shoreline system. This, coupled with the strong upward-coarsening log motifs, provides evidence of shoreline progradation. The coastal plain was largely an area of sediment bypass, and the aggradational log patterns that characterize this system reflect thick coals and interbedded mudrocks. The coastal plain passes landward (westward) into alluvial plain and fluvial systems. Log patterns are aggradational and associated with thick, stacked channel sandstones with interbedded floodplain muds.

Geologic Controls on Coal Seam Occurrence

Peat accumulation, metamorphism, and preservation as coal depend on three critical factors: (1) substantial growth of vegetation, (2) maintenance of the water table near the sediment surface, and (3) nondeposition of clastic sediment during peat accumulation. Substantial vegetation growth is determined mostly by climate, and the second two critical factors are controlled by the depositional systems, basin subsidence, and hydrology (Hamilton, 1993, 1994). The depositional systems provide the framework within which the peat swamps are established and, combined with subsidence and hydrologic regime, are important in maintaining optimum water table levels for peat preservation.

The ideal location for preservation of the peat is immediately behind the shoreline system, a regional discharge area where water tables are maintained at optimum levels. Basin subsidence is also an important underlying control on coal occurrence. It determines the location of clastic sedimentation and accommodation space for peat accumulation and preservation. The Williams Fork coals are oriented north-northwest to south-southeast, which parallels the basin subsidence trend. The coals thin to the southeast and are ultimately limited by the final position of the shoreline, beyond which marine conditions existed. The western limit of Williams Fork coal-bearing horizons is controlled by the transition from coastal plain to alluvial plain deposition.

CONCLUSIONS

1. The Williams Fork Formation, the most important coal-bearing unit in the Piceance Basin, can be divided into several genetic depositional sequences. These sequences were deposited during discrete episodes of shoreline advance and retreat and are bounded by regionally extensive, low-resistivity shale markers that represent marine flooding surfaces in the basinward direction and hiatal, nondepositional surfaces in terrestrial facies.

2. The stratigraphically lowest genetic depositional sequence, unit 1, is a clastic wedge that extended coal-bearing coastal plain deposits beyond the present-day basin margin. Three depositional systems are recognized in the genetic unit. A north-oriented linear shoreline system dominated the easternmost part of the basin and was backed landward by a coastal plain system, which in turn graded westward into an alluvial plain system. Genetic units 2 and 3 above are clastic wedges displaying an arrangement of depositional systems similar to that of unit 1, but genetic unit 2 did not prograde as far basinward as unit 1, whereas unit 3 prograded farther basinward than either unit 1 or unit 2.

3. Genetic unit 1 contains the thickest, most laterally extensive coals. Coal occurrence in all units is concentrated in the southeastern and northeastern parts of the basin. Genetic units 1, 2, and 3 coals are concentrated in the eastern half of the basin and are thickest in a north-south-trending belt, west of the Divide Creek Anticline. In the southern Piceance Basin, net coal thickness of the Williams Fork Formation averages 80 to 120 ft (24 to 36 m). Data are scarce on Williams Fork Formation coal distribution between T5S-T1N and R97W-R92W, north of the Colorado River, and for approximately 24 mi (39 km) west of the Grand Hogback. North of the White River and east of R98W, net coals of the Williams Fork exceed 150 ft (>45 m) in thickness but generally average between 80 and 150 ft (24 and 45 m) in thickness.

4. Coal occurrence in all units is intimately related to the depositional systems. The coastal plain immediately landward of the shoreline (strandplain/delta plain) system was the optimum site for peat accumulation and preservation in Williams Fork genetic units 1 through 3. Coalbeds

pinch out against and/or override the shoreline sandstone to the east, and their ultimate lateral extent is limited by the final shoreline position beyond which marine conditions prevailed. In a landward direction, they are limited by rising surface gradient and falling water table, controlled by the transition from coastal plain to alluvial plain.

5. Continuity of the Williams Fork coals is variable. Some individual seams, particularly in genetic unit 1, are correlatable for up to 30 mi (48 km) in the southeastern half of the basin on the basis of their density and gamma-ray profiles. Other seams could be correlated only when grouped within broad coal packages. The coals of unit 1 are only moderately continuous from the subsurface to the southern, southeastern, and northeastern outcrop belts, where they could be exposed for meteoric recharge. However, the genetic unit 1 coals that reach outcrop are reduced in number and total thickness relative to the area immediately basinward in R90-93W. Thus, although positioned to receive recharge, their transmissivity is reduced and, consequently, their ability to transmit recharge basinward is reduced. In the southeastern Piceance Basin, genetic unit 2 coals do not reach outcrop because their platform of accumulation did not prograde far enough to the east. Genetic unit 3 coals increase in abundance and thickness toward outcrop but have limited westward extent into the basin. Further, unit 2 and 3 coals are discontinuous and are unlikely to represent interconnected aquifer systems in the subsurface. Laterally discontinuous coal beds limit, therefore, the amount of recharge that can be accepted and transmitted basinward from the Grand Hogback and may help explain the presence of mapped underpressure along the basin's eastern margin. Strata that receive too little recharge or are insulated from recharge remain underpressured.

6. Limited recharge may have implications for the producibility of coal gas. In the absence of dynamic ground-water flow, less gas is dissolved and swept basinward for eventual resorption and conventional trapping along potential no-flow boundaries. At the same time, the generation of secondary biogenic gases is minimized. Thus, without the additional sources of gas beyond that sorbed on the coal surface, high coal-gas productivity may be precluded. Perhaps

the parts of the basin with the best potential for coal-gas production lie in conventional traps basinward of where outcrop and subsurface are in good hydraulic communication.

7. Caution is advised in net coal and net sandstone mapping and interpretation where duplication or faulting of the section is found along the Grand Hogback, Divide Creek, and Danforth Hills/Wilson Creek areas.

Geologic Characterization and Gas Production: Cameo Coal Group, Grand Valley/Rulison Area, Garfield County, Colorado

H. Seay Nance and William R. Kaiser

ABSTRACT

In the eight-township Grand Valley/Rulison area, the operational Williams Fork Formation is divided into a lower unit dominated by the Cameo Coal Group and an upper coal-barren unit. Strata dip regionally 2.7° northeast and are folded and faulted. The Crystal Creek and Rulison Anticlines are Laramide structures associated with postulated southwest-directed compression. Simpler structure on the base of the Mancos Tongue than on younger strata probably reflects detachment in the Mancos Shale and associated splay faulting into the overlying Williams Fork. Coal anticlines and synclines reflect differential compaction of coals about narrow (0.25 to 1 mi wide) fluvial channel-sandstone belts. At least seven coals extend across the study area. Net coal ranges from 40 to 100 ft in thickness and typically exceeds 50 ft. Coal thicks trend northeast and probably reflect accumulation on a coastal plain behind a northerly trending shoreline to the east. Ancient rivers flowed southeast, east, and northeast across that coastal plain, crossed an inferred syndepositional hingeline, and fed a shoreline that prograded eastward.

In the Grand Valley/Rulison area, Cameo gas wells typically produced less than 100 MMcf in their most productive year. Water production rarely exceeds 1,000 bbl annually. The most productive wells (MPW) are on structural terraces or anticlines, perhaps reflecting fracture-enhanced permeability related to flexure. MPW's follow Cameo maximum sandstone trends west of an inferred hingeline in Parachute field. This is attributed to better sandstone reservoirs and/or differential compaction that folded and fractured the coal beds for enhanced permeability and conventional trapping. MPW's show no relation to coal occurrence.

INTRODUCTION

The Grand Valley/Rulison area is one of major coalbed methane activity in the Piceance Basin. In the eight-township study area (T6-7S, R94-97W) (fig. 55), there are almost 80 gas wells in the Cameo Coal Group. Detailed studies were conducted to investigate geologic controls on production, to determine coal/sandstone relations, structural grain, and depositional fabric for extrapolation into areas of sparse well control, and to support recent drilling by OXY USA, Inc., in western Grand Valley field (T6S, R97W). Closely spaced wells, commonly on quarter-mile centers, allowed detailed investigation of coal stratigraphy, structure, coal occurrence, and coalbed continuity. Coal/sandstone relations were also investigated to yield interpretations of sandstone geometry and compactional structures. Possible geologic controls on production are examined using stratigraphic cross sections in conjunction with coal, sandstone, structure, and production maps.

METHODS

Data used to generate cross sections and maps came from 111 geophysical logs (typically gamma-ray, resistivity, and lithodensity logs). Coals are identified on geophysical logs by their extremely low gamma-ray API values (<60 API units), very high resistivity values (50 to >100 ohm-m), and very low bulk density values (<1.75 gm/cc). They are correlated by two criteria: first, by similarities between log responses, and second, by stratigraphic position. Most of the thicker coal beds produce gamma-ray and density-log responses that reflect internal stratigraphic complexities, such as the inclusion of thin shales or partings. Very often in nearby wells, almost identical responses are observed at approximately the same stratigraphic position. In the absence of evidence to the contrary, such similar log responses are correlated (Hamilton, 1994). The implication is that complexities observed in individually correlated coal beds are at least subregionally extensive. Where log responses become dissimilar but still record coal beds of similar thickness in nearby wells, coal-log responses are correlated according to stratigraphic

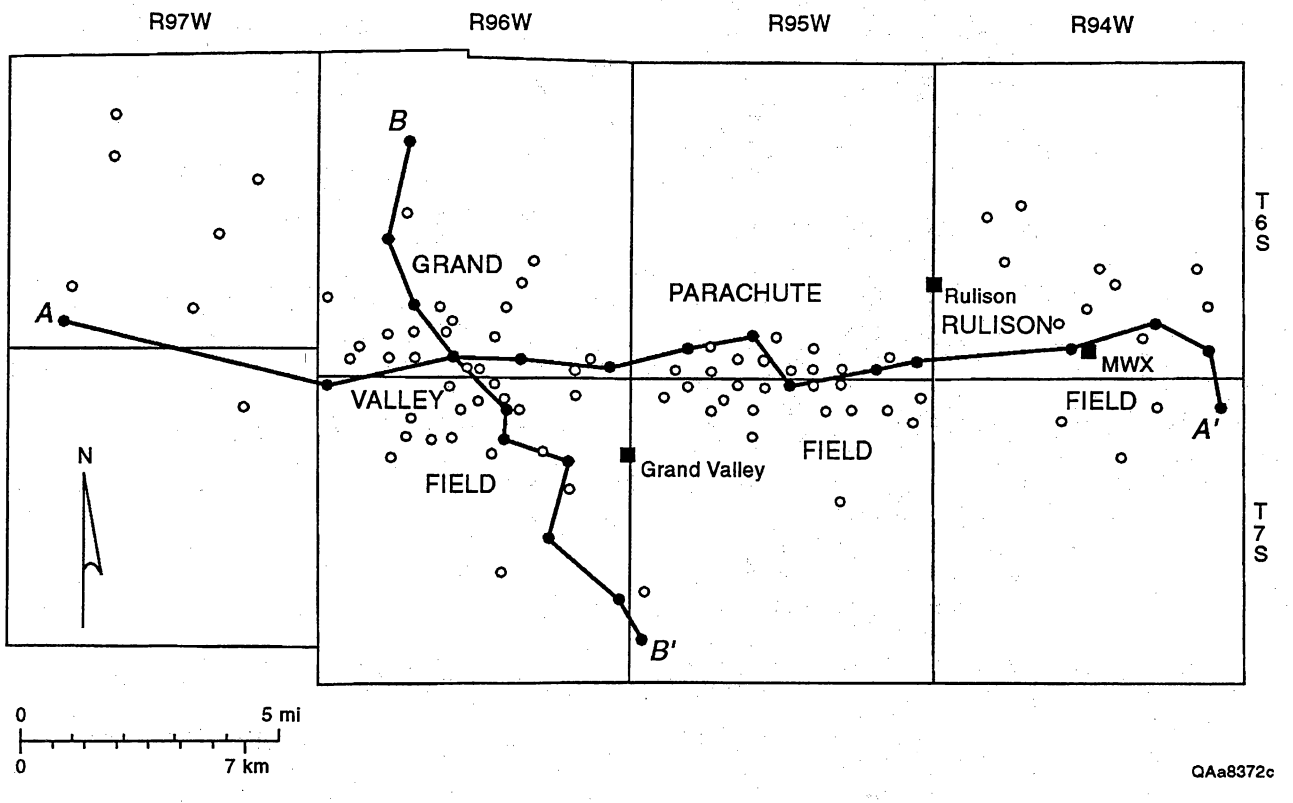

Figure 55. Base map of the Grand Valley/Rulison study area showing well locations, field names, and locations of cross sections (figs. 59 and 60).

position relative to overlying and/or underlying coal beds that do retain log-profile similarities between the wells.

Sandstone is identified by its low gamma-ray values (<75 API units) and by lower resistivity than that of coal (generally, 10 to 50 ohm-m). Extremely high-resistivity sandstones ("hard streaks") are differentiated from coal by coal's much lower bulk density. Shale is identified by gamma-ray values (>75 API units) higher than those of sandstone and by low resistivities (<20 ohm-m). Mudstones (admixtures of sand, silt, and clay) have gamma-ray and resistivity values intermediate to those of sandstone and shale.

Maximum sandstone maps were prepared here because they are a relatively quick method to discern sandstone dispersal patterns without the time-consuming exercise of measuring all the individual sandstone beds, as is required for net sandstone mapping. Log response defines the maximum sandstone as the single thickest sandstone in the interval of interest without regard to correlatability. Experience has shown that maximum-sandstone maps are similar in appearance to net-sandstone maps in that both depict the depositional fabric with the former accentuating the framework elements of the depositional system. For example, in the fluvially dominated section in Grand Valley field, thinner and less extensive splay and overbank sandstones are excluded in maximum sandstone mapping to accentuate the axial elements of the fluvial system.

STRATIGRAPHY

In the Grand Valley/Rulison area the Williams Fork Formation, the major coal-bearing stratigraphic unit, is operationally defined as outlined by Tyler and McMurry (this volume, fig. 6). The base of the Williams Fork is easily defined by a characteristic high-conductivity kick on resistivity logs at the base of the Mancos Tongue (the shale-dominated base of the Rollins progradational sequence) (fig. 56). This marker records a maximum flooding event and is a genetic stratigraphic sequence boundary (terminology of Galloway, 1989). At Grand Valley, the lower Williams Fork (equivalent to units 1 and 2 of Tyler and McMurry, this volume) (fig. 46)

shows a gradual increase in conductivity upward from the top of the Rollins Sandstone, which culminates in a series of high-conductivity kicks over a 100- to 200-ft interval of shales and thin sandstones above the Cameo coals. Within this interval the most prominent conductivity kick, herein informally called the "pound marker," defines the top of the lower Williams Fork (fig. 56). This high-conductivity interval is regionally extensive; it contains marine shale to the east, corresponding to the interval between units 2 and 3 (fig. 53), and may at Grand Valley contain paralic marine, possibly tidally influenced, sediments that reflect marine advance toward the west or sediment starvation on a coastal plain.

In the absence of the Lewis Shale, the top of the Williams Fork is operationally defined on the basis of a change upward to blocky, thick sandstones (change in sandstone stacking patterns) and an accompanying, high-conductivity interval. The operational top is placed at the most conductive spike (herein informally called the "red marker") in the transition to thick sandstone as defined by their blocky, high-resistivity/low gamma-ray response (fig. 56). The red marker defines the top of the operational Williams Fork and separates sandstone-poor rocks below from sandstone-rich rocks above, herein called undifferentiated Upper Cretaceous (probable Lewis/Lance equivalents). This marker is probably not an unconformity (or depositional sequence boundary, in the terminology of Vail, 1987) in the study area, but may be to the south and west.

The operational Williams Fork thins westward from approximately 2,500 ft in the eastern part of the basin (T7S, R89W; fig. 53) to approximately 1,600 ft in Grand Valley field. Coal packages of units 1 and 2 merge into one coal-bearing interval at Grand Valley (Cameo Coal Group), and the coal package of unit 3 is absent, except for a few thin coals in R94W. Coals immediately above the Rollins Sandstone (lower part of unit 1) are generally the thickest and most laterally continuous.

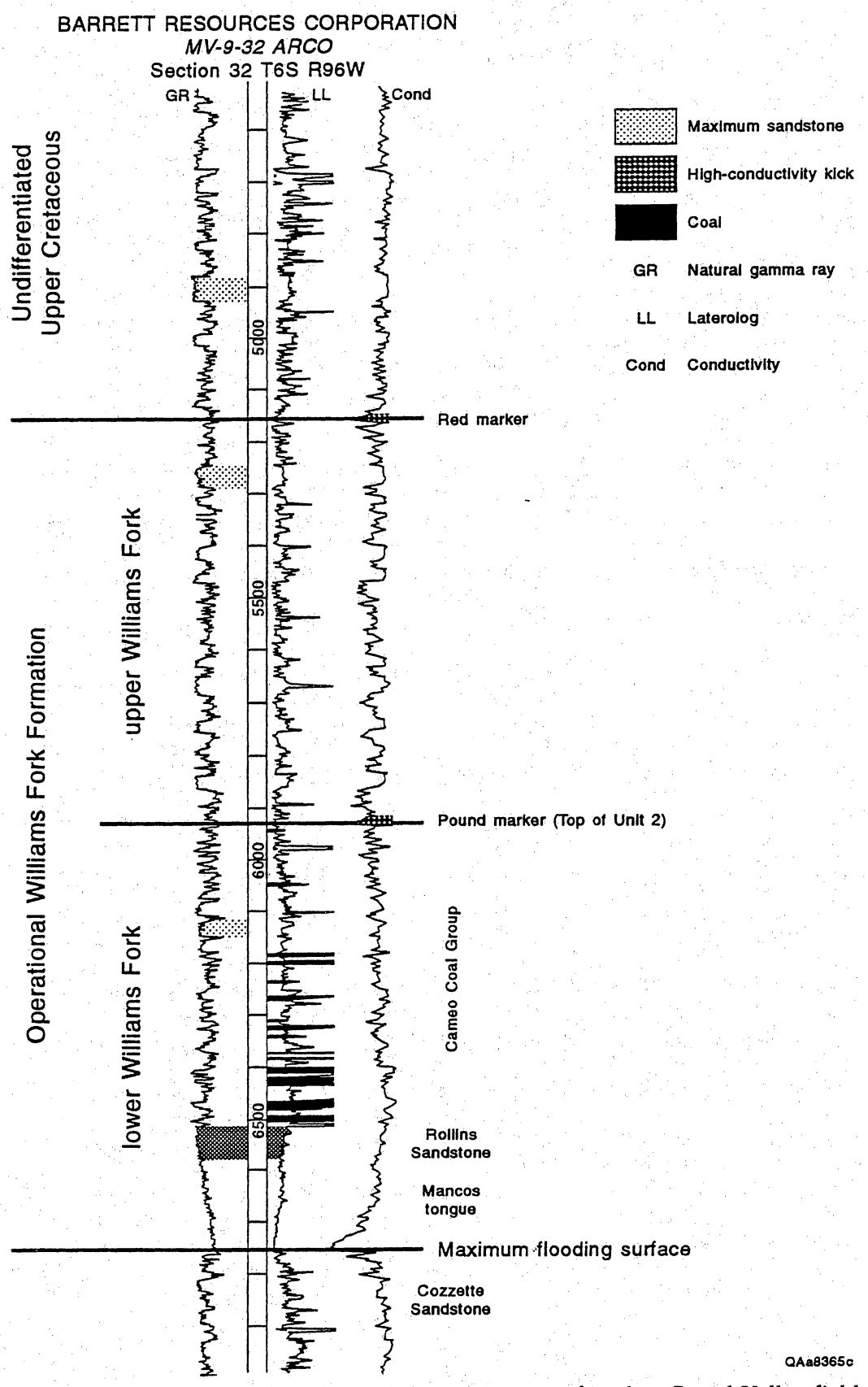

Figure 56. Type log showing stratigraphy and the occurrence of coal at Grand Valley field. Shown are the stratigraphic boundaries, coals, and thickest sandstone beds of the operational Williams Fork Formation and undifferentiated Upper Cretaceous interval. Coals are identified from accompanying density log. The pound marker and red marker are discussed in text.

STRUCTURE

The Grand Valley/Rulison area is located on the western flank of the Piceance Basin and lies mainly west of the MWX site (fig. 4). Strata strike northwest across the area and dip regionally about 2.7° to the northeast (figs. 57 and 58). Structure-contour maps reveal northwest-trending folds and faults of Laramide-age (Johnson, 1989; Tyler, this volume; Tremain and Tyler, this volume). The Crystal Creek Anticline postdates Williams Fork deposition and was not a positive feature during its deposition. Stratigraphic cross sections, hung on the pound marker, show no obvious thinning toward the crest of the anticline, and Cameo coals are present on the crest. Williams Fork deposition is also unrelated to the Rulison Anticline (nose of the Divide Creek Anticline). Isopach trends and the depositional fabric are essentially orthogonal to the anticline's axis.

The Crystal Creek and Rulison Anticlines are related to postulated Laramide thrust and reverse faults associated with southwest-directed compression (Grout and Verbeek, 1992; Gunneson and others, 1994). Structure is simpler on the base of the Mancos Tongue than on the top of the younger lower Williams Fork (fig. 58). Greater structural complexity on the younger horizon is thought to reflect detachment in the Mancos Shale, as reported at the Divide Creek Anticline (Gunneson and others, 1994), and associated splay faulting above the detachment into the overlying Williams Fork Formation. The Crystal Creek and Rulison Anticlines probably formed above the tip lines of these splay faults. One such fault cuts the Crystal Creek Anticline; seismic data indicate a northeast-dipping reverse fault (Reinecke and others, 1991). Other splay faults occur along the crest of the Rulison Anticline and on its southwest flank. Subsurface and seismic data indicate that these northwest-trending faults are reverse faults. Most dip northeast, consistent with southwest-directed compression, but some dip southwest. Those dipping southwest may be backthrusts splaying from the ramp of an eastward-dipping main thrust that flattens into the Mancos Shale. One such fault crosses section

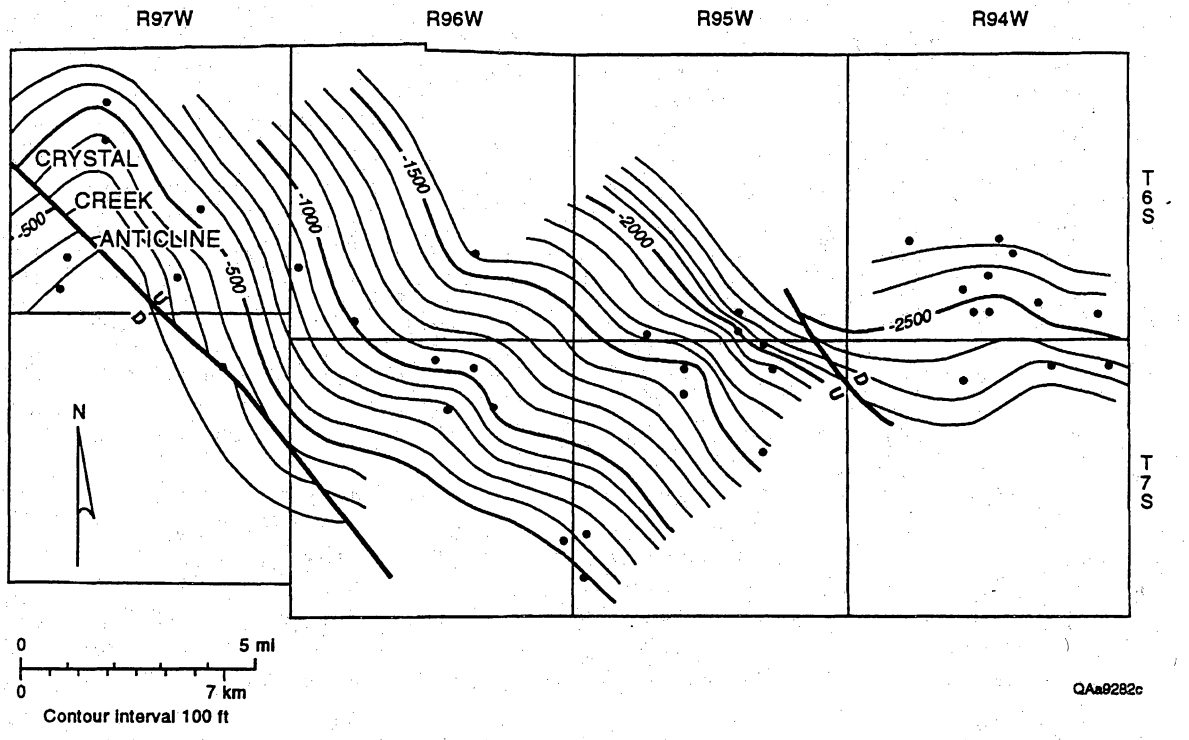

Figure 57. Structure-contour map, base of the Mancos Tongue. Note relative simplicity of this surface compared with that of the pound marker (top unit 2), probably reflecting structural decoupling of rocks below the Mancos from those above it.

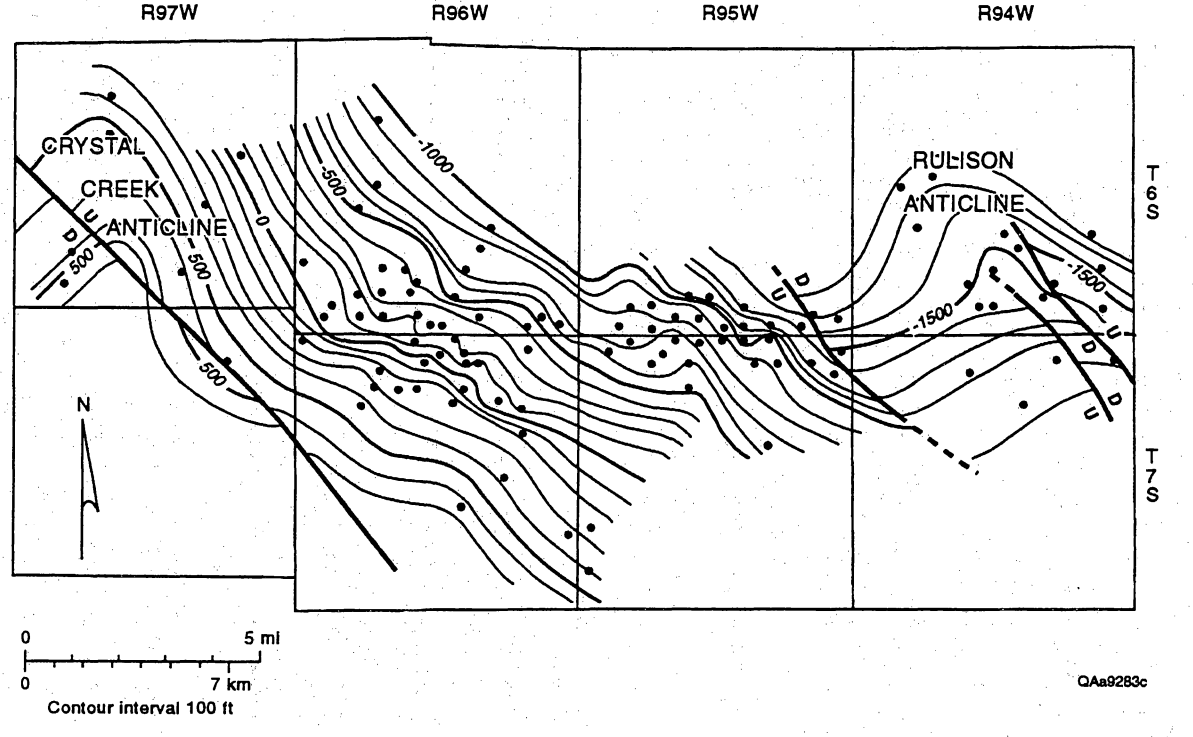

Figure 58. Structure-contour map, top of the lower Williams Fork Formation (top unit 2). Note greater structural complexity of this surface compared with structure on the base of the Mancos Tongue.

1, T7S, R95W (fig. 58). Flattening of dip on fold axes and structural terraces may reflect lateral and vertical termination of faults.

COAL/SANDSTONE RELATIONS

Coalbed Continuity and Configuration

We recognize up to seven regionally extensive coal beds traversing the entire Grand Valley/Rulison study area from west to east (fig. 59). Some beds can be correlated over 30 mi from 6S-94W to 6S-100W. Between regional coal beds, thin, discontinuous coals locally occur that do not extend beyond more than a few wells (figs. 59 and 60). These are laterally adjacent to thick channel sandstones and are limited to the local floodbasins. For example, the uppermost Cameo coal beds appear less extensive in the north-south direction, perhaps recording their pinch-out against west-east-trending channel sandstones, and reflecting the increasing fluvial influence on coal development upward in the Cameo interval (fig. 60).

Thick channel sandstones commonly occur over more compacted floodbasin deposits of immediately underlying sequences, which compact to perhaps 10 to 20 percent of their original thickness. Thus, alteration of floodbasin compaction and channel reoccupation produced a stratigraphic succession of laterally staggered, thick channel sandstones vertically separated by mudstones and regionally extensive coals.

Coal beds are differentially compacted and drape thick channel-fill sandstones to form compactional anticlines and synclines. Differential compaction has produced local relief on individual coal beds up to 50 ft over 1 mi (fig. 59). Compactional high relief on coal beds is generally located immediately over thick, sandstone-rich deposits and lows are immediately over sandstone-poor deposits. In general, each coal bed has its own unique configuration. Anticlines or synclines on one coal bed are not necessarily reflected in the configuration of beds stratigraphically below or above. Where an anticline on one bed immediately underlies

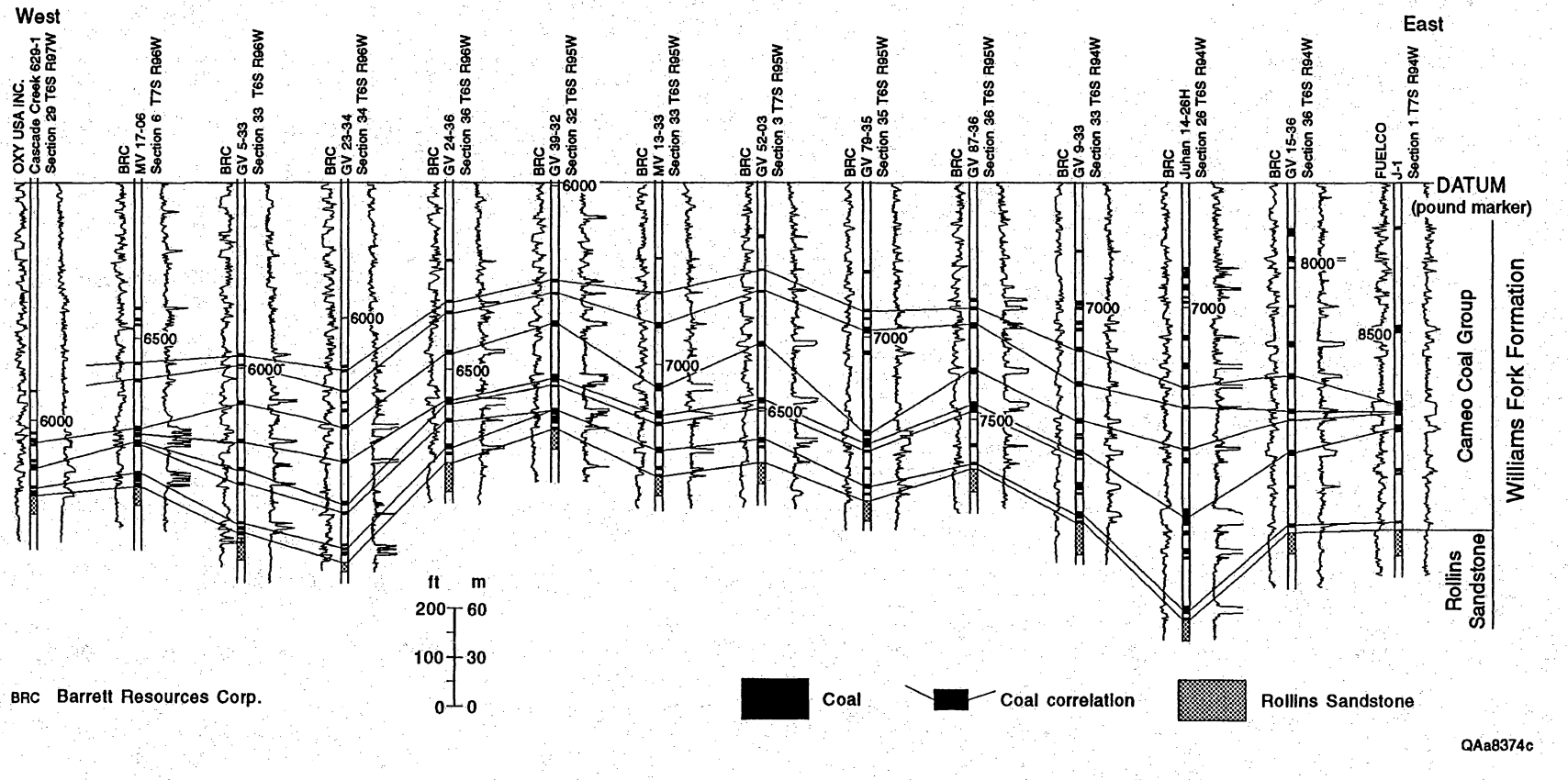

Figure 59. West-east stratigraphic cross section of lower Williams Fork Formation (units 1 and 2). Datum is pound marker at top of unit 2. Individual coals display complex configuration where they drape channel-sandstone bodies. Compactional high at sec. 32, T65, R95W is the approximate location of the syndepositional hingeline described in text.

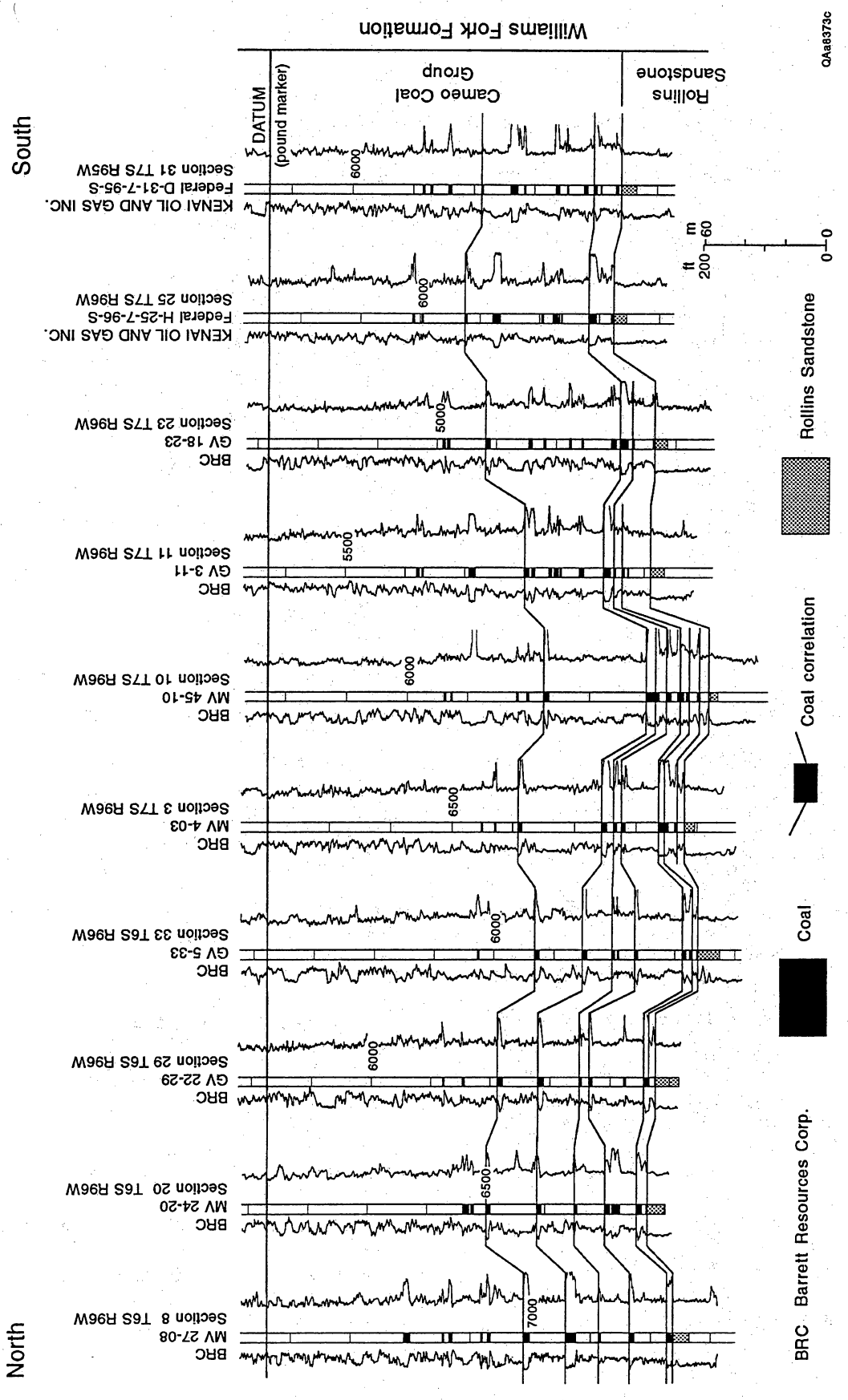

Figure 60. North-south stratigraphic cross section of lower Williams Fork Formation.

the syncline on another bed, beds converge into a single thick coal and associated interbedded mudstones and shales (figs. 59 and 60).

If compactional highs tend to reflect the axial trends of correlative sandstone belts, then measured relief on coal beds actually may be produced over a much shorter distance than 1 mi, perhaps as little as 0.15 mi (half the width of the average fluvial channel belt in the area), because the line of section obliquely crosses the probable trend of the sandstones. In any case, differential compaction may result in the formation of small-scale, southeast- and east-aligned (parallel to fluvial axes) open folds in the coals that may ultimately serve as conventional traps. Among potential sandstone reservoirs, thicker channel sandstones may be better reservoirs because of their greater volumes, textural maturity, and anticlinal drapes (seals) than thinner, dirtier sandstones located away from the channel-belt axes.

Coal Distribution

The net coal map shows that coal deposits are most abundant in Rulison field (up to 115 ft), central Parachute field (up to 72 ft), and southeastern Grand Valley field (up to 87 ft). There is no consistent relationship between net coal thickness and the thickness of the lower Williams Fork Formation. The maximum coal map, or that showing the single thickest coal, indicates that the thickest coal beds are located in northeastern Rulison field (up to 36 ft thick), on the eastern and western flanks of Parachute field (up to 29 ft thick), and on the southern and northeastern flanks of Grand Valley field. The thickest coal beds commonly occur in the lower third of the lower Williams Fork Formation. Although some of the thickest coal beds are located in the thicker portions of the lower Williams Fork Formation, especially in northeastern Rulison field, there is no consistent relation between thicker coal beds and formation thickness. Similarly, although the thicker coal beds occur in northeastern Rulison where net coal values are highest, no consistent relation between the thickest coal beds and the greatest net coal accumulations is evident.

Sandstone Continuity

Laterally extensive coal beds stratigraphically bound siliciclastic sequences (figs. 59 and 60). Siliciclastic sequences comprise sandstone intervals 100 ft or more thick that are interbedded with mudstones and shales 2 to 10 ft thick. Sandstones, especially in the western two-thirds of the Grand Valley/Rulison area, generally comprise one or more upward-fining intervals, as indicated by gamma-ray responses that increase upward through the sandy interval. Thicker sandstones typically rest immediately upon regionally extensive coal beds, documenting the tendency of erosion that precedes sandstone deposition to be arrested when coal beds are contacted. Thin (generally <5 ft thick) sandstones are locally interbedded with thin (<5 ft thick) mudstones, shales, and thin coals.

Net sandstone abundance and bed thickness between wells in the lower Williams Fork, and even within individual coalbed-bounded (coeval) sequences, vary dramatically from well to well. Differences exceeding 400 ft of Williams Fork net sandstone can be observed in wells 0.25 mi apart, reflecting channel-belt or interchannel locations. Within one coal-bounded sequence, for example, net sandstone varies over 0.25 mi from 140 ft (approximately 90 percent of the sequence at sec. 35-T6S-R95) to as little as 14 ft (approximately 20 percent of the sequence at sec. 36-T6S-R95W).

Genetic packages are bounded by laterally extensive coal beds that overlie, underlie, and terminate against sandstones. Correlations are particularly convincing when coal beds are 5 ft or more thick. It now appears that six or more packages may be present. Commonly, these coal-bounded packages are dominated by sandstones that appear to be correlatable (fig. 59). Correlation is apparent here because the cross section used for correlations is generally oriented in the paleoflow direction (west to east from R97W to R94W). Individual channel-fill sandstones are probably amalgamated to form channel-sandstone belts, which may be correlated. However, internal stratigraphic complexities may subdivide such correlative sandstone intervals into numerous compartments and may preclude long-distance pressure

communication. Even in the absence of the diagenetic effects that greatly reduced matrix porosity and permeability in Williams Fork sandstones, permeability continuity at interwell distances between correlative sandstone intervals may never have been good. Commonly, sandstones as close as 1,200 ft are not in pressure communication. Short-distance pressure response reflects very low permeability and/or reservoir compartmentalization.

DEPOSITIONAL SYSTEMS

Regional Setting

Currently, the best model for deposition of laterally continuous coals provides for a regionally extensive, strike-aligned coastal plain that developed landward of a marine shoreline located somewhere east of the Grand Valley/Rulison area, on which vast wetlands (mires) developed to accumulate thick, laterally extensive peats. An eastern shoreline is supported by the maximum sandstone maps (figs. 61–63), which show that ancient rivers trended southeast, east, and northeast across the Grand Valley/Rulison area. These rivers traversed the coastal plain and apparently crossed a syndepositional hingeline to bring sediment to a shoreline that prograded to the east.

The presence of a syndepositional hingeline between Parachute and Rulison fields is inferred from the coincidence of geologic anomalies evident on cross sections and maps. These anomalies include (1) marked thickening of the Cameo Coal Group, (2) increased coal thickness to the east, (3) westward pinch-out or thinning of sandstone-dominated genetic packages, (4) loss of marine flooding surfaces, and (5) increase of bed curvature. The Cameo Coal Group thickens from 450 ft in the vicinity of the hingeline (sec. 32-T6S-R95W) to 600 ft east of it in Rulison field (fig. 59). The single thickest coal thickens from approximately 15 ft at Parachute field to greater than 30 ft at Rulison field (fig. 64). At the same time, thick coals become more numerous and areally extensive eastward. Progressively east of the inferred hingeline, unit 3 coals, uncommon to the west, become more abundant. Thus, the approximately westward limit

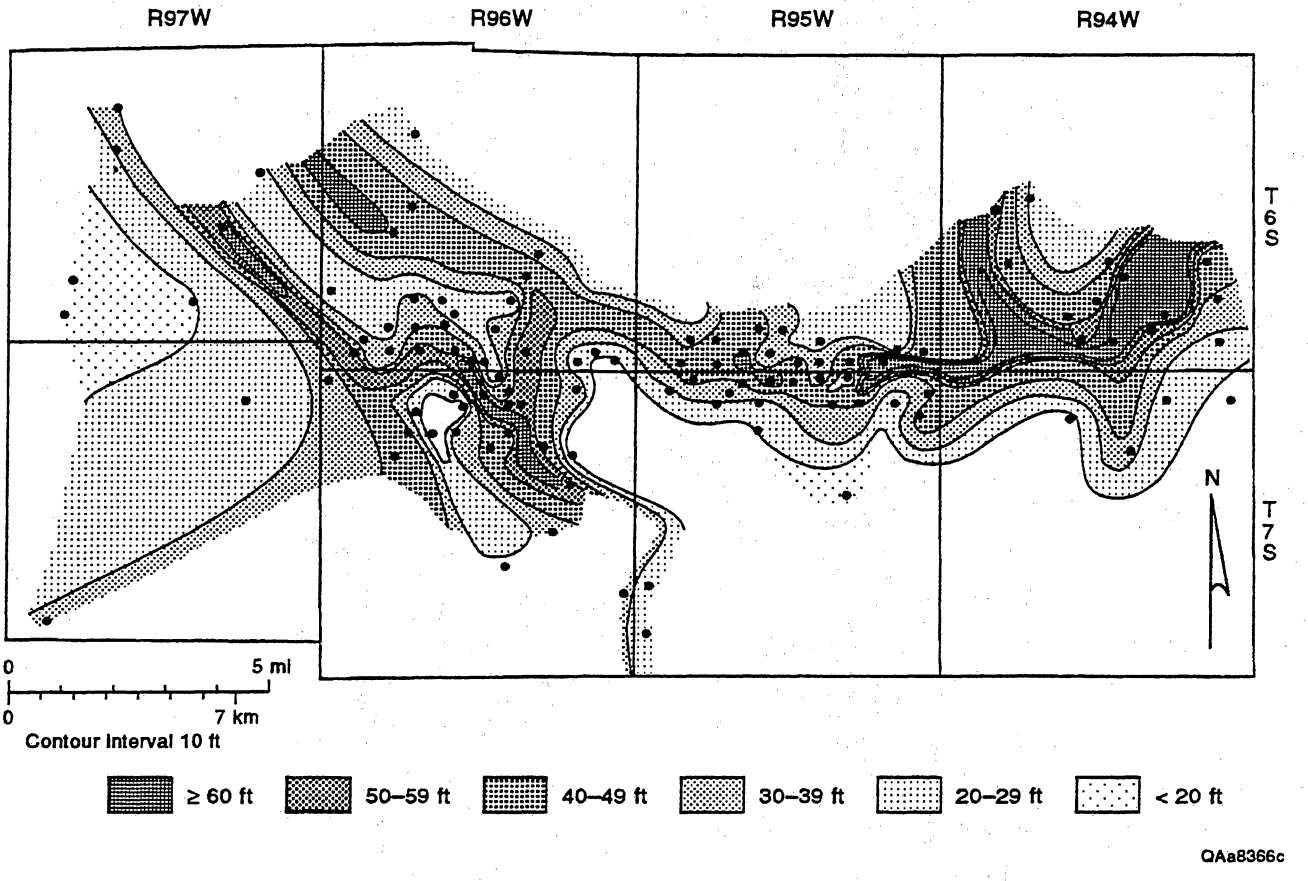

Figure 61. Maximum sandstone map of the interval from the top of the Rollins to the top of the lower Williams Fork Formation. Note similarity to figures 62 and 63.

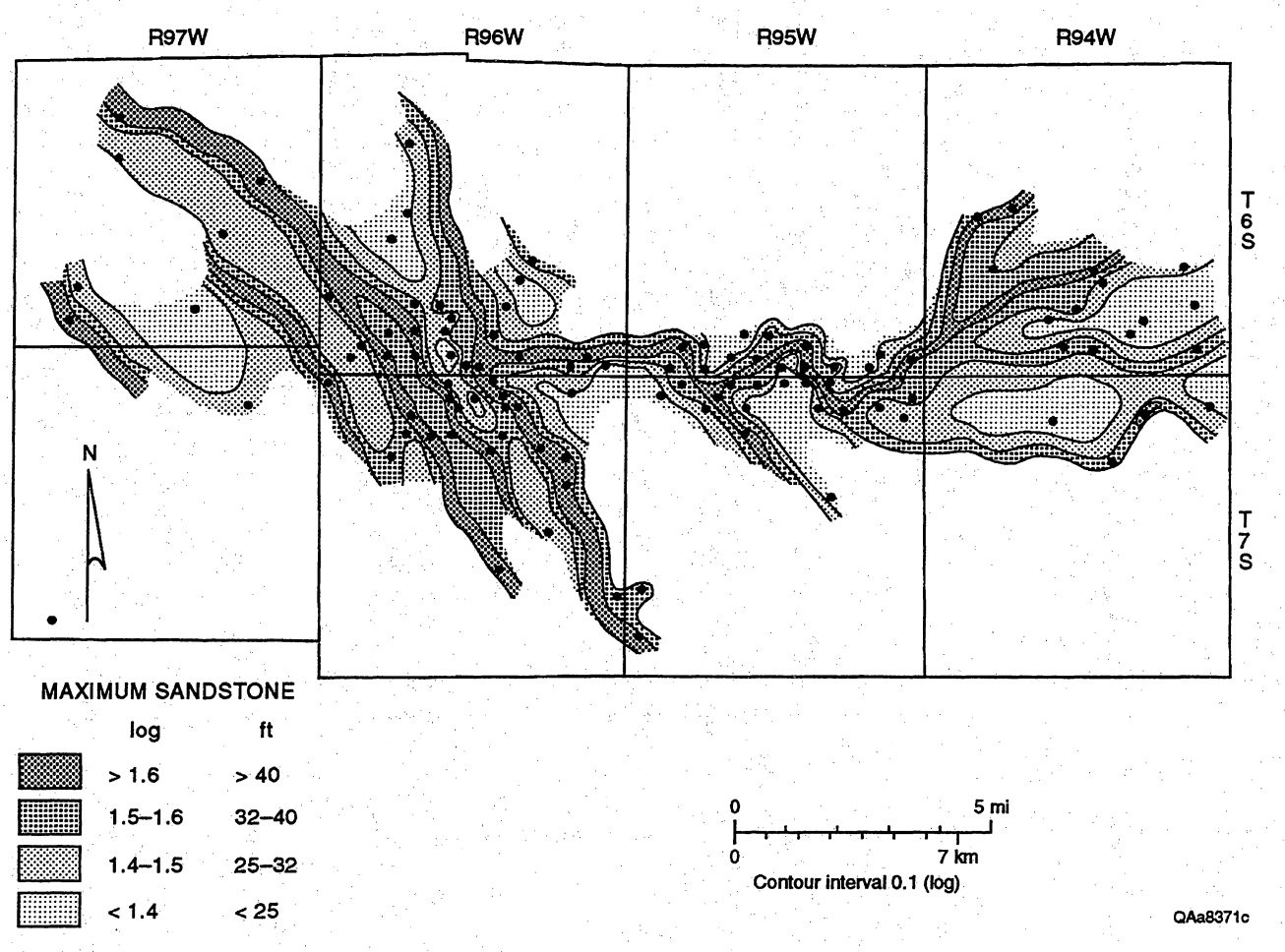

Figure 62. Maximum sandstone map of the upper Williams Fork Formation. Note similarity to other maximum sandstone maps (figs. 61 and 63).

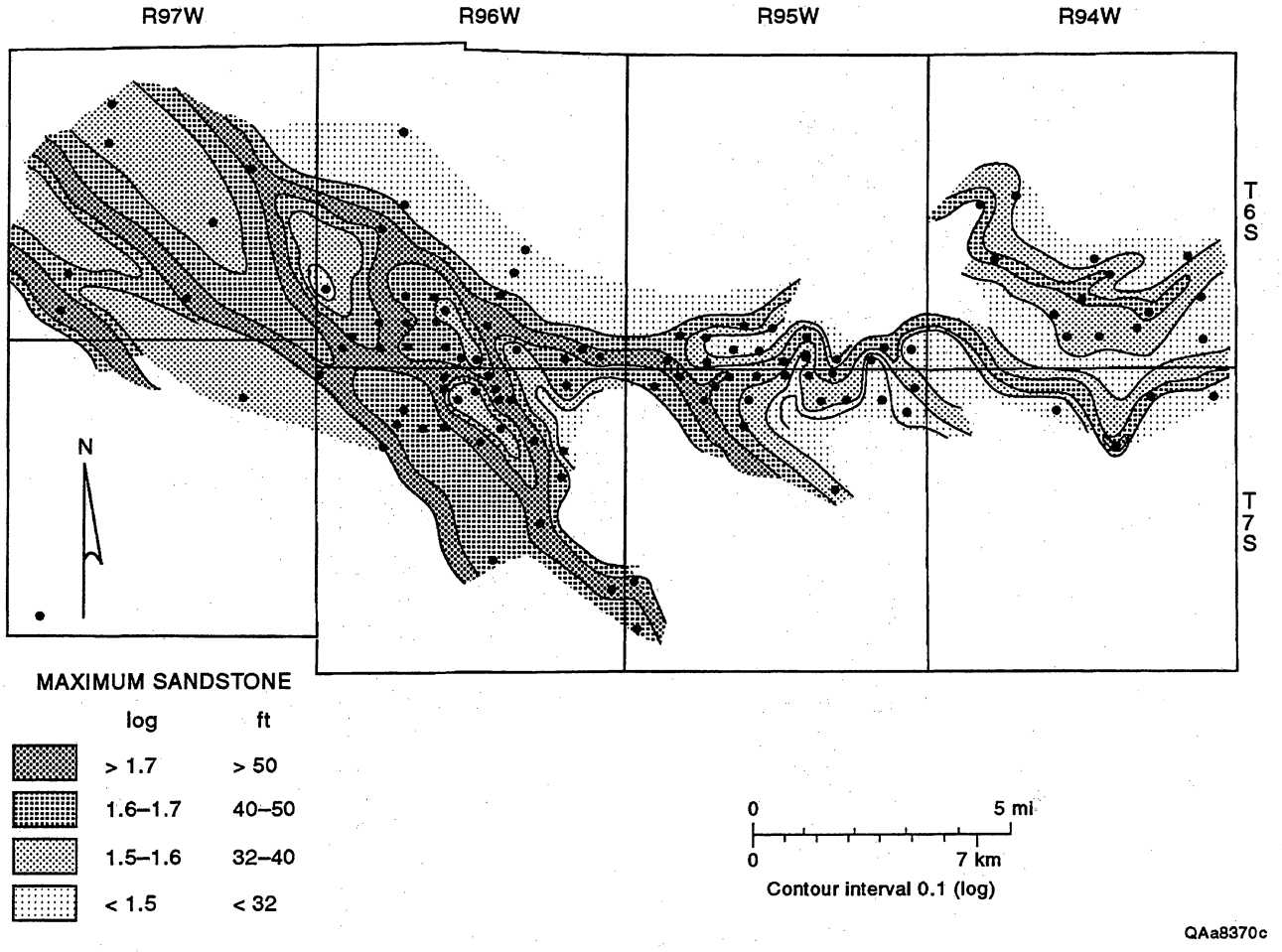

Figure 63. Maximum sandstone map of the undifferentiated Upper Cretaceous above the upper Williams Fork Formation. Note similarity to other maximum sandstone maps (figs. 61 and 62).

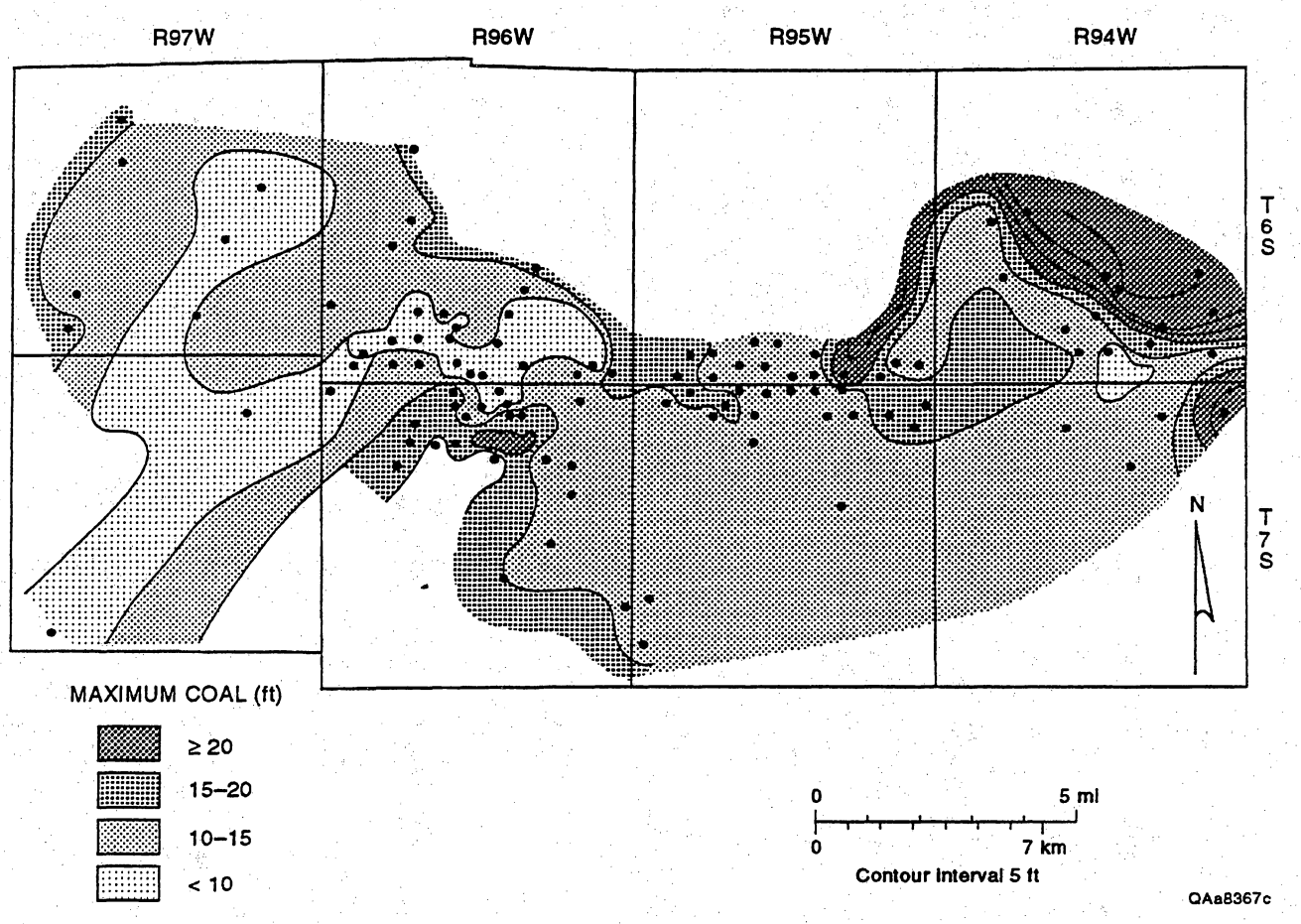

Figure 64. Maximum coal map of Cameo Coal Group. Thickest beds are generally thicker in the east than in the west.

of unit 3 coals corresponds to the hingeline (Tyler and McMurry, this volume, fig. 51). Coal-bounded sandstone intervals thin or pinch out at the hingeline (fig. 59). Moreover, sandstones 10 ft or more thick become thicker and more numerous east of the hingeline, suggesting greater sediment accommodation space. Marine flooding surfaces used to define genetic units in the eastern part of the basin have been traced from near outcrop (R89W) through at least R93W to possibly R95W in Parachute field. Bed curvature calculated on the Rollins Sandstone increases dramatically east of Rulison field (Myal and others, 1989).

Fluvial Deposition and Sandstone Geometry

Most lower Williams Fork sandstones were probably deposited in fluvial systems on a low-relief coastal plain. Fluvial systems are interpreted mostly from the mapped channel geometry. Furthermore, most of the sandstones in the Grand Valley/Rulison area display upward-fining intervals typical of channel abandonment, and sandstone thickness varies dramatically from well to well. Thick channel sandstones are laterally equivalent to thinner sandstones (<5 ft thick), shales, and local coal. These lateral relationships suggest that thicker sandstones are point-bar-channel sequences and that the sandstone-poor areas are laterally adjacent floodbasin deposits. Thin sandstone beds in floodbasin deposits represent overbank or topping events during floods. The low relief of the environment is suggested by the consistent thickness of laterally extensive coal beds that overlie several channel belts and interchannel areas. High local relief is inimical to regionally extensive wetlands.

Fluvial sand bodies are characteristically narrow, dip-elongate belts, generally reflecting the region's depositional slope. In the lower Williams Fork, maximum sandstones range from 20 to 100 ft in thickness and are thickest in Rulison field (>60 ft) (fig. 61). In the upper Williams Fork, maximum thicknesses range from 15 to 60 ft and are thickest to the west (30 to 60 ft), with an eastward decrease in thickness (20 to 45 ft). Channel-sandstone belts range from 0.25 to 1.0 mi in width in the lower Williams Fork and 0.25 to 0.5 mi in width in the upper Williams Fork. This is consistent with Lorenz and others (1985), who calculated the average Williams

Fork channel belt to be 1,500 ft (0.28 mi) wide. Channel belts in the undifferentiated Cretaceous rocks are 0.25 to 0.75 mi wide, maximum sandstones are 25 to 75 ft thick and are thickest in the west (50 to 70 ft), compared with a thickness of 25 to 40 ft in the east.

In eastern Rulison field, well logs indicate several exceptionally thick beds of clean sandstone, some over 100 ft thick, in the lower half of the Cameo Coal Group. The well-developed upward-fining patterns of sandstones located to the west in Parachute and Grand Valley fields are not nearly as common. Some of these sandstones display upward-coarsening characteristics and may record progradation of marine shoreline sands in wave-dominated deltaic environments.

Sandstone and Coal Trends: Implications for Paleogeography

Williams Fork channel-sandstone belts trend southeast, east, and northeast (figs. 61 and 62). Southeast transport is dominant across Grand Valley field; easterly and northeasterly transport is evident in Parachute and Rulison fields. West-east trends seen in Parachute fields undoubtedly reflect the narrow band of data there. Inspection of the maximum sandstone maps and net sandstone values support the presence of southeast trends in this area. Sandstone trends suggest the persistence of an easterly sloping alluvial plain during Williams Fork deposition and the probable downslope presence of a northeast- to north-trending shoreline. Trends of channel-sandstone belts in the undifferentiated Upper Cretaceous are concordant with those in the upper Williams Fork (figs. 62 and 63). Although the boundary between them represents a change in stacking pattern and increased alluviation (change in stream gradient?), it apparently does not signify major basinal reorganization. Thus, the operational top of the Williams Fork is probably conformable in the Grand Valley/Rulison area.

Net coal trends (fig. 65) reflect depositional fabric. Areas characterized by thicker net deposits of coal probably record temporal stability of the mires and reflect episodic southeasterly to easterly progradation of a shoreline that resided east of the study area. If the distance from mire centers to their equivalent marine shorelines is relatively constant, then

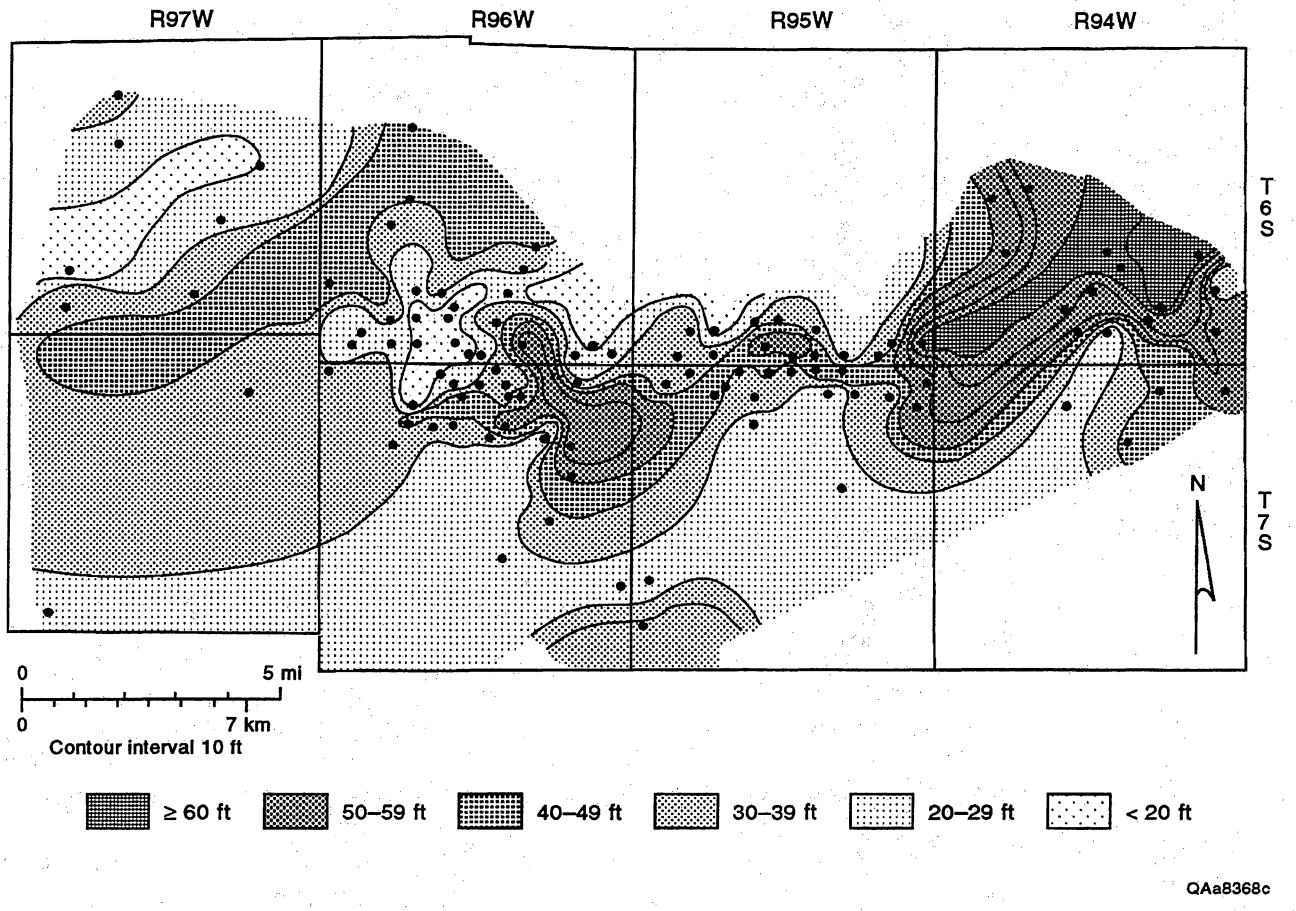

Figure 65. Net coal map of Cameo Coal Group.

the distance between coal depocenters should reflect the distance between respective stable shoreline positions. Thus, the distance between coal depocenters may reflect the distance prograded prior to the next stillstand. In the Grand Valley/Rulison area, the lateral distance, parallel to the eastern shoreline, between the Grand Valley/Parachute and Rulison coal depocenters is 3 to 8 mi, depending on inferred northeast- or north-trending shorelines, respectively.

CAMEO PRODUCTION

Statistics

In the Grand Valley/Rulison area there are 78 wells that produce from Cameo coals or sandstones or jointly from both. Grand Valley field has 41 Cameo wells, and cumulative gas production through June 1994 was 11.69 Bcf (Petroleum Information, 1994). For the same period, Parachute field, with 29 wells, had a cumulative production of 3.91 Bcf and Rulison field, with 8 wells, had a cumulative production of 1.71 Bcf (Petroleum Information, 1994). Most wells in Grand Valley field have produced for 5 yr or more, with peak production generally occurring in the first or second year. Only a few wells show negative production decline. Cumulative production of individual wells is typically less than 300 MMcf. Most wells in Parachute and Rulison fields have produced for 3 to 5 yr, with peak production occurring in the first or second year. No wells show negative decline. Cumulative production from individual wells is typically less than 200 MMcf. Coal and sandstone production are not reported separately by Petroleum Information Corporation (PI).

To compare productivity among wells that have productive lives of variable duration and to minimize the time variable inherent in cumulative production, we examined maximum annual production (MAP) (fig. 66), or production of the well's most productive year, as taken from Petroleum Information's data on CD-ROM. MAP measures a well's highest capacity to produce gas. In the study area, the MAP of gas is typically less than 100 MMcf; 15 wells exceed

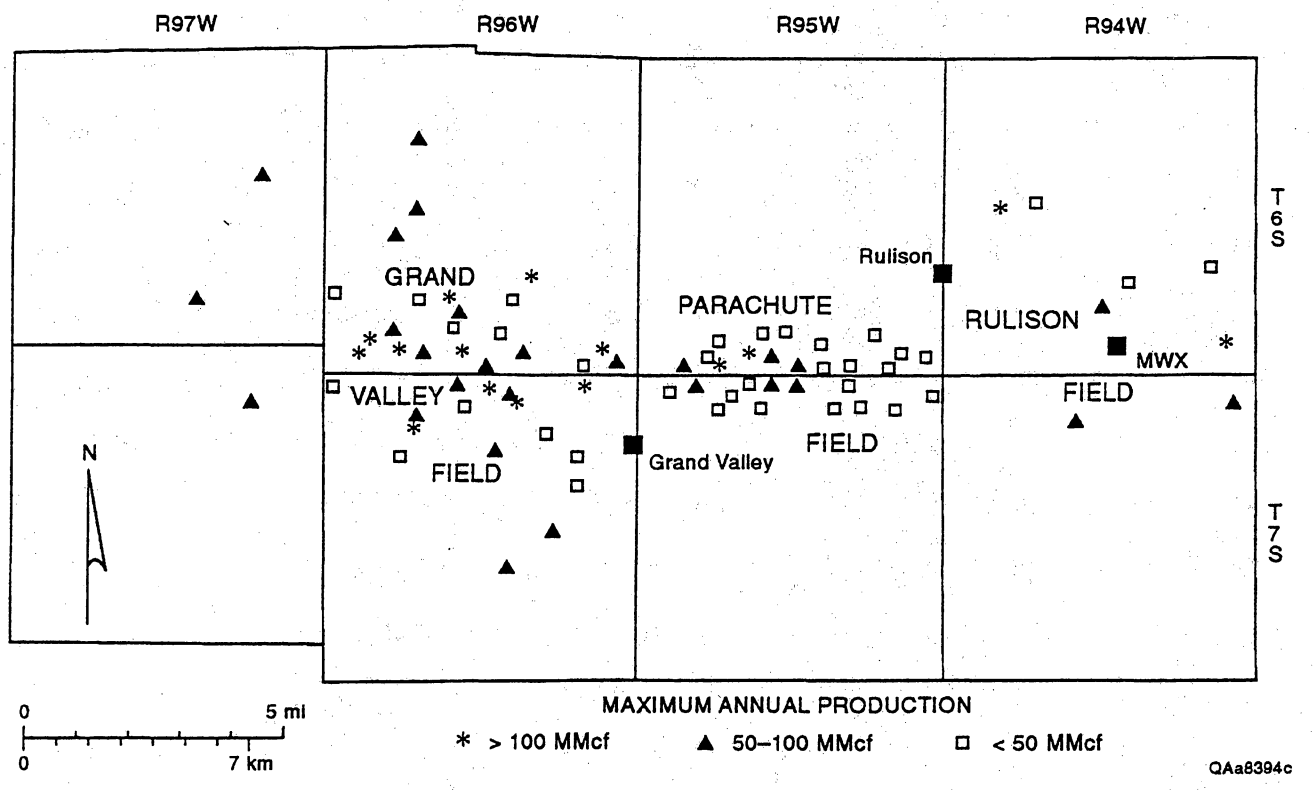

Figure 66. Map of maximum annual production (MAP), Cameo wells, Grand Valley/Rulison area. Better production is west of syndepositional hingeline and shows strongest correspondence to trends of maximum sandstone (fig. 61), locations of structural terraces, and along the axis of the Rulison Anticline (fig. 58).

that rate; among those 15, 5 wells exceed 150 MMcf and 3 exceed 200 MMcf. The MAP of water is typically low, a few 100 bbl, and rarely exceeds 1,000 bbl.

Controls on Production

Permeability is the most important control on production and is very low in the Grand Valley/Rulison area (Reinecke and others, 1991). An investigation of its nature is precluded by lack of data. However, structural and depositional setting were investigated for correlation with production. Maps showing structure, coal occurrence (net coal and maximum coal thickness), and maximum sandstone thickness were compared with gas-productivity trends (MAP) to identify possible geologic controls on production.

There appears to be structural control on production, which is evident from a comparison of MAP and structure on the top of the lower Williams Fork Formation (figs. 56, 58, and 66). In Grand Valley field, the trend of the most productive wells (MPW), or those with MAP exceeding 50 MMcf, is parallel or oblique to strike. A large number of MPW's are associated with a structural terrace, or flattening of regional dip. Perhaps flexure, associated with change of dip, has produced fracture-enhanced permeability. Although new wells in T6S-R97W are being production tested in sandstones, it is too early to assess the presence or absence of correlation with the Crystal Creek Anticline and the possibility of conventional structural trapping of gas. In Parachute field the trend of MPW's is also parallel or oblique to strike. Again, MPW's appear to correlate with a structural terrace that may be related to the terminations of two small converging horsts. Differential compaction may also contribute to dip flattening. In Rulison field, MPW's apparently follow the axis of the small, north-trending Rulison Anticline (nose of the Divide Creek Anticline). Permeability may be fracture enhanced along the fold axis. The combination of enhanced permeability and possible structural trapping may account for better production on the fold.

In Grand Valley and Parachute fields, MPW's follow the trend of maximum sandstones in the lower Williams Fork above the Rollins Sandstone (figs. 56, 61, and 66). This may reflect

better sandstone reservoir development and/or associated differential compaction of coal beds, leading to fracture enhancement of the coals. However, in Rulison field, there is no apparent correlation between MPW's and maximum sandstone thickness. In the three fields, MPW's show no apparent relation to coal occurrence.

Generally, most of the MPW's are to the west of an inferred syndepositional hingeline that crosses Parachute field (fig. 59). This area is dominated by narrow channel–sandstone belts. To the east, however, the lowermost Williams Fork becomes increasingly marine influenced where sandstone bodies become more laterally continuous, or sheetlike. In the Rulison area the lowermost Cameo interval appears to contain abundant marine sandstone. It is possible that local coal anticlines that syndepositionally developed on narrow (average 1,500 ft wide) channel belts in the fluvial environment to the west provide better gas traps (tighter closure) than do the broader folds that formed on marine sheet sands to the east. Differential compactional features similar to those described for the Grand Valley area are highly productive in the Powder River Basin (Oldham, 1994).

Producibility Model

The Grand Valley/Rulison area lies in the Colorado River valley, a presumed regional discharge area, or no-flow boundary, oriented orthogonal to the regional flow direction. It is an area of upward flow located at the termination of regional flow paths (Kaiser, 1994). Coal rank is low-volatile bituminous (R_m 1.5 to 1.9 percent; Reinecke and others, 1991), and significant volumes of thermogenic gas were generated for high gas contents. As predicted (on the regional scale) from our coalbed methane producibility model (Kaiser and others, 1994), the area should be and is productive. Although predictably productive, the area's cumulative production is modest and limited by a very low matrix permeability (microdaries). Low permeability restricts ground-water flow and, when combined with hydrocarbon overpressure, eliminates meteoric circulation. Gas is probably the pressuring fluid because wells produce little or no water. Thus, dynamic ground-water flow is precluded and, by implication from the model, so is extraordinary

coal-gas production. The model requires ground-water flow basinward from recharge through aquifer coal beds, orthogonally toward regional no-flow boundaries. Active flow implies good permeability and promotes generation of secondary biogenic gas and advective gathering and transport of gas, which contribute to fully gas-saturated coals and high productivity.

FUTURE WORK

Future investigations in the Grand Valley/Rulison area will include structural mapping of the most extensive coal bed, net sand mapping of the underlying siliciclastic interval to demonstrate possible reservoir development associated with differential compaction of coal-siliciclastic sequences, analysis of the pressure regime, and disaggregation of the production data to identify coal-gas production and controls on it.

CONCLUSIONS

1. An operational Williams Fork Formation is defined by a maximum flooding surface at the base of the Rollins shale (Mancos Tongue) and a change in sandstone stacking pattern and associated high-conductivity interval at the top. The formation is approximately 1,600 ft thick; it is divided into a lower unit dominated by the Cameo Coal Group and an upper coal-barren unit by a high-conductivity kick in a 100- to 200-ft high-conductivity interval above the Cameo coals. This interval is regionally extensive and correlates with a marine shale to the east separating units 2 and 3 of the Williams Fork.

2. Strata strike northwest across the area and dip regionally 2.7° northeast. The Crystal Creek and Rulison Anticlines are Laramide structures associated with postulated southwest-directed compression. Greater structural complexity on the younger lower Williams Fork than on the Mancos Tongue is thought to reflect detachment in the Mancos Shale and splay faulting into the overlying Williams Fork. The anticlines probably formed above the tip lines of these splay faults. Seismic data indicate northeast-dipping reverse faults, whereas subsurface data

indicate normal faults. Normal motion is inferred to result from relaxation of compression in post-Laramide time.

3. Coal beds display considerable local relief of up to 50 ft over a 1 mi distance or less that results from differential compaction of coals about narrow (0.25 to 1 mi wide) fluvial-channel-sandstone belts. Compactional coal anticlines and synclines are inferred to parallel sandstone belts. Differential compaction may contribute to present-day structural terraces in Grand Valley and Parachute fields.

4. Coals immediately above the Rollins Sandstone in the lower Williams Fork Formation are generally the thickest and most laterally continuous. At least seven coals extend across the study area, becoming thicker eastward and individually attaining thicknesses of 30 ft to the east in Rulison field. Net coal ranges in thickness from 40 to 100 ft and typically exceeds 70 ft in Rulison, central Parachute, and southeastern Grand Valley fields.

5. Laterally extensive coal beds stratigraphically bound genetic siliciclastic sequences. At least seven sequences have been recognized. Equivalence of correlated individual channel-fill sandstones is more apparent than real. Individual sandstones are vertically and laterally amalgamated to form narrow channel-sandstone belts 0.25 to 1 mi wide. Belt width sets an upper limit for correlatability and may be closer to 0.25 mi than 1 mi. The published average width is 1,500 ft (0.28 mi). Commonly, sandstones as close as 1,200 ft are not in pressure communication, reflecting reservoir compartmentalization and very low matrix permeability (microdaries).

6. On the basis of the coincidence of several geologic anomalies, a syndepositional hingeline is inferred to cross Parachute field. Its inferred presence here and possibly basinwide may be very important to exploration strategy. In the San Juan Basin, a hingeline is the site of prolific coal and sandstone gas production.

7. Williams Fork sediment was sourced from the west and transported southeast, east, and northeast across the Grand Valley/Rulison area by a fluvial system that fed a prograding, northerly trending shoreline to the east. Sandstones increase in thickness to the west and

stratigraphically up section. On a coastal plain landward of the shoreline, vast wetlands (mires) developed to accumulate thick, laterally extensive peats (coals). Net coal thicks trend northeast and reflect the regional depositional setting.

8. There are 78 gas wells that produce from Cameo coals or sandstones or jointly from both. Cumulative Cameo production for the area through June 1994 is 17.31 Bcf. Cameo wells typically produced less than 100 MMcf in their most productive year. Cumulative production of individual wells is typically less than 300 MMcf. Negative production decline is rare. Water production rarely exceeds 1,000 bbl annually. Geologic controls on production, besides permeability, the most important control, are structure and sandstone development. The most productive wells (MPW's) are on structural terraces and anticlines and may reflect fracture-enhanced permeability related to flexure or conventional structural trapping of gas. MPW's correspond to Cameo maximum sandstone trends in Grand Valley and Parachute fields west of an inferred syndepositional hingeline. This correlation is attributed to better sandstone reservoirs and/or differential compaction, resulting in fracture-enhanced coal permeability and tighter folding (better closure) of the coals than expected over more sheetlike sands to the east.

Coalbed Methane Producibility in the Williams Fork Formation, White River and Pinyon Ridge Fields, Northern Piceance Basin

Andrew R. Scott

ABSTRACT

The northern Piceance Basin is an area of significant coalbed methane activity. High-conductivity shale markers separating individual genetic units in the Williams Fork Formation, as defined in the Sand Wash Basin, and the Yampa Bentonite marker are correlated in the northern Piceance Basin. Maximum net coal thickness trends for the Williams Fork lower coal-bearing interval (units 1 and 2) are oriented northeastward in both basins, reflecting the accumulation of peat on a coastal plain landward of northeast-trending shoreline sandstones. Coals in the northern Piceance Basin are predominantly high-volatile C and B bituminous ranks, indicating that the coals have not reached the threshold of significant thermogenic methane generation. The coal gases are unusual because they contain significant amounts of wet gas components and carbon dioxide. Chemically wet gases and condensate produced in the northern part of the basin are indigenous to the coals, whereas carbon dioxide probably originated from the decomposition of Paleozoic carbonate rocks and migrated up thrust faults. Isotopic data suggest that as much as 75 percent of the carbon dioxide was derived from outside of the study area.

Coalbed methane occurrence in the northern Piceance Basin is consistent with an evolving coalbed methane producibility model. The complex structural development of the basin locally enhanced permeability through the formation of extensional fractures along the crests of tightly folded anticlines. Normal faults along the crest of the White River Anticline and facies changes are perpendicular to inferred migration pathways, suggesting that significant volumes of gas are conventionally trapped. Migrated and conventionally trapped coal gases

account for approximately 65 to 80 percent of gas production from the White River field. The northwest-trending Danforth Hills thrust fault, along the eastern margin of the basin, separates Williams Fork coals in the elevated outcrop from coals deeper in the basin, effectively preventing meteoric recharge and the possible generation of secondary biogenic gases and basinward transport of dissolved gas for conventional trapping along flow barriers.

INTRODUCTION

Hydrogeologic controls on coalbed methane occurrence and producibility are complex (Kaiser and others, 1994a) and may vary from one part of a basin (or subbasin) to another. Therefore, in addition to regional studies, more detailed subregional studies are often required to fully determine local controls on coalbed methane producibility. The northern Piceance Basin was selected for a detailed evaluation because two coalbed methane fields, the White River and Pinyon Ridge, are located there (fig. 67). Although all of the coalbed methane wells in the northern Piceance Basin are located within the primary study area, the study area was expanded for net coal mapping to include the Sand Wash Basin, which is located immediately to the northeast of the Piceance Basin. The proximity of the basins and similar depositional settings in both areas provided the basis for using net coal thickness trends in the Sand Wash Basin to constrain net coal trends in the northern Piceance Basin. The objectives of this study are to (1) define the occurrence and distribution of coal beds, (2) identify structural features that may enhance coalbed methane producibility, (3) evaluate the composition and origins of coal gases, (4) discuss trends in gas and water production, and (5) summarize the hydrogeologic factors affecting coalbed methane producibility and discuss how these factors compare with the coalbed methane producibility model discussed by Kaiser and others (1994a).

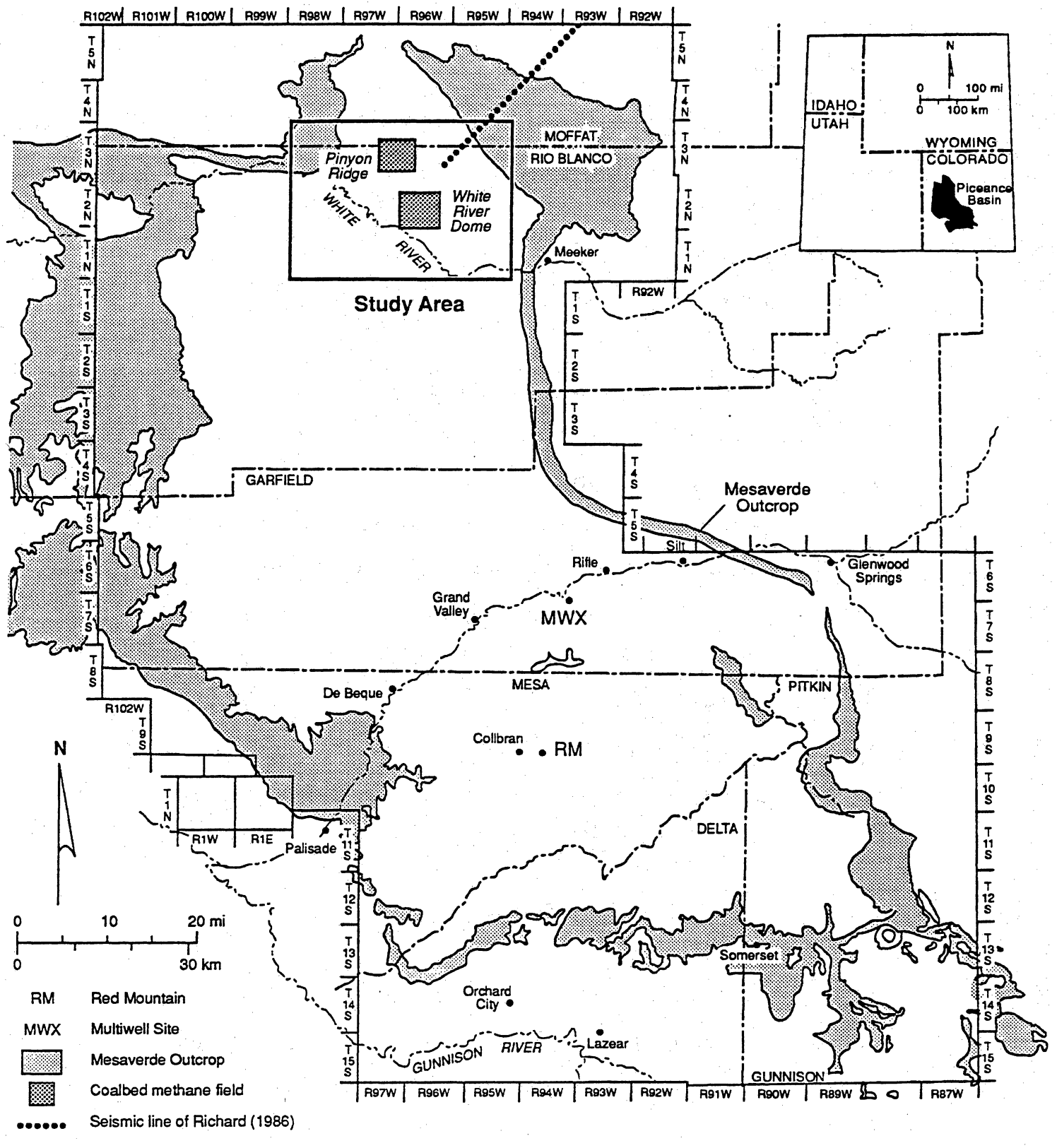

Figure 67. Map showing location of study area and coalbed methane fields in the northern Piceance Basin.

METHODS

Geophysical logs from approximately 40 oil and gas wells were used to define formation tops, genetic boundaries, and net coal trends. Coal density logs were available for most of the wells and were used to identify coal beds, trace coal beds laterally, and determine net coal. Net coal thickness trends in the northern Piceance Basin were constructed from net coal values and constrained, using net coal maps from the Sand Wash Basin upon correlation of the two basins. Net coal maps of units 1 and 2 in the Sand Wash Basin (Hamilton, 1994) were digitized and then converted to grid patterns composed of an evenly spaced node system of 3,000 m (9,840 ft) between nodes. The net coal values at each respective node were summed, and a net coal map for units 1 and 2 was constructed. A structure map was constructed for the top of the Rollins-Trout Creek sandstone rather than the base because not all of the logs in the study area extended to the base of the sandstone. Structure and geologic maps from the Dakota (Barlow and Haun, 1975) and northern Piceance Basin (Hail and Smith, 1994), respectively, were used in addition to log picks to better define and constrain contours. Faults and/or inferred faulting were defined on the basis of data from (1) a missing section in geophysical logs, (2) closely spaced structural contours, (3) surface structures and faulting, and (4) production and/or coal gas compositional trends. Annual precipitation maps were modified from the Colorado Climate Center (1984).

STRUCTURAL FEATURES

The northern part of the Piceance is separated from the rest of the basin by the White River Dome, which is a southeast-plunging anticline. Although the regional compressive stress regime during the Laramide Orogeny was primarily east-west, the northwest trend of the White River and other folds in the Piceance Basin suggest that an episode of northeast-oriented compression also occurred (Tyler and others, 1991). The White River Dome probably started to form at the end of the Cretaceous and continued to develop throughout the Paleocene and

Eocene (Johnson and Nuccio, 1986). Maximum structural dip on Upper Cretaceous rocks on the south side of the White River Dome has been reported to be 45° (Hail, 1974), and thrust faulting has been hypothesized to have occurred beneath the structure (Johnson and Nuccio, 1986). The Danforth Hills thrust fault in the northeast corner of the primary study area (fig. 68) is associated with the Danforth Hills Anticline located immediately northeast of the primary study area. Seismic lines across the northwest-trending Danforth Hills Anticline indicate the presence of the Danforth Hills thrust fault with 9,000 to 10,000 ft of throw (fig. 69) (Richard, 1986). Thrust faulting within and adjacent to the primary study area has significant implications for coalbed methane producibility that will be discussed later.

The Pinyon Ridge and White River fields are both associated with anticlines. The Pinyon Ridge field is located along the crest and south flank of the east-plunging Midland Anticline (fig. 68). The trend of the Midland Anticline on the Dakota (Barlow and Haun, 1975) is located approximately 2 mi north of the anticlinal trend on the Rollins-Trout Creek sandstone, indicating that the Midland Anticline is asymmetric. The east-west-trending fault south of the Midland Anticline probably continues westward from the study area where normal faulting occurs at the surface. Thrust faulting along the Willow Creek Fault also occurs west of the study area in T3N, R103W (Tweto, 1979; Johnson and Nuccio, 1986).

The White River field is associated with a southeast-plunging anticline, herein called the White River Anticline, which becomes a dome on the deeper Dakota horizon (Barlow and Haun, 1975). Structural dip on the northeast flank of the anticline exceeds 500 ft/mi (95 m/km) (>5.4°), and normal faulting is present on the southwest flank, where more than 300 ft (91 m) of missing section has been recognized in one well. These normal faults have been mapped on the surface (Tweto, 1979; Hail and Smith, 1994) and probably affect the northwest-southeast orientation of the White River. Additional faulting probably occurs along the crest and flanks of the anticline but is difficult to document with well control alone, although structural, production, and gas compositional trends are compatible with faulting. Johnson and Nuccio (1986) suggested that a thrust fault paralleling the White River along the crest of an anticline

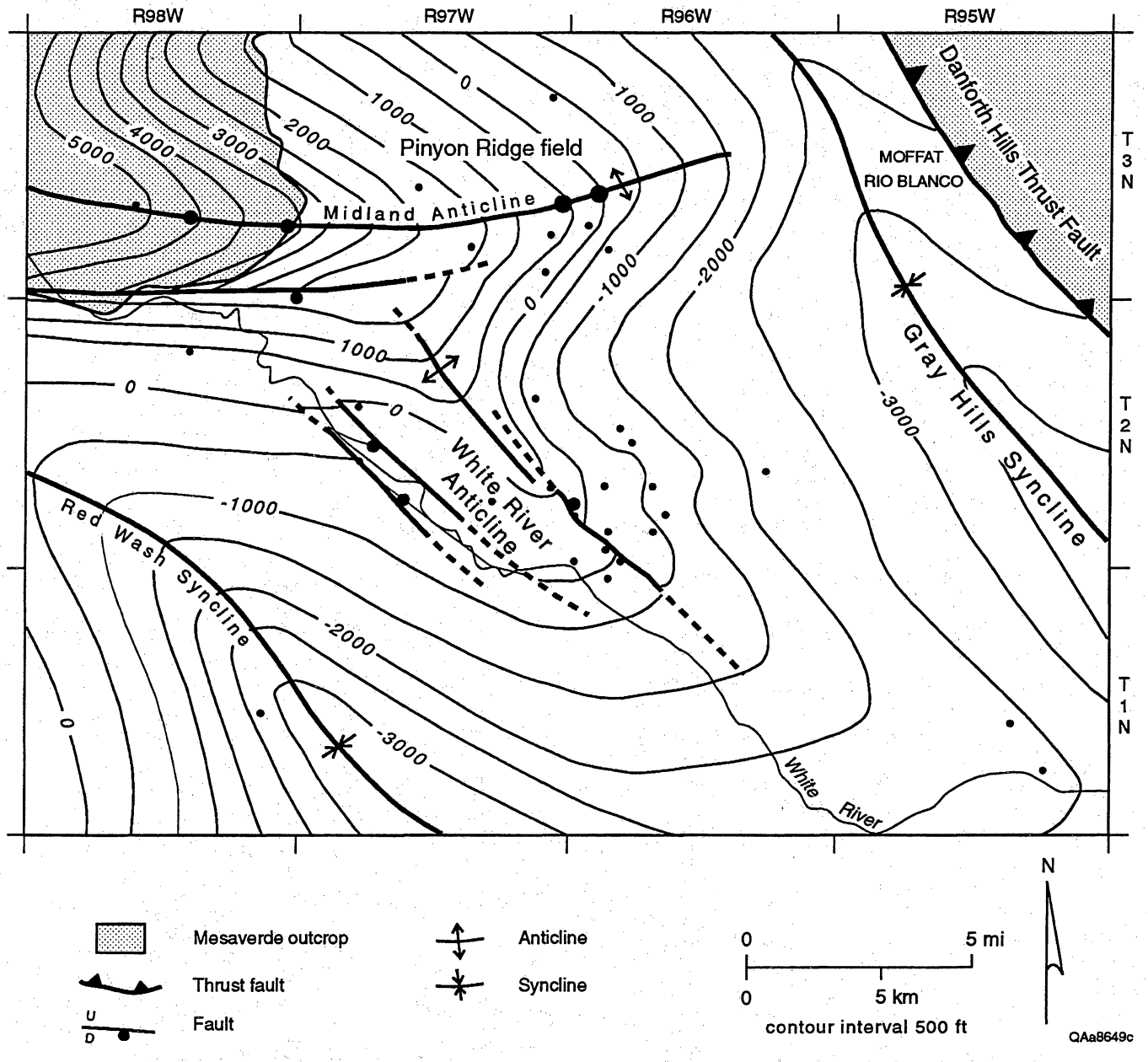

Figure 68. Structure map, top of the Rollins-Trout Creek sandstone. Normal faults along the crest of the southeast-trending White River Anticline are extensional fractures related to possible thrust faulting. The northwest-trending Danforth Hills thrust fault is in the northeast part of the study area.

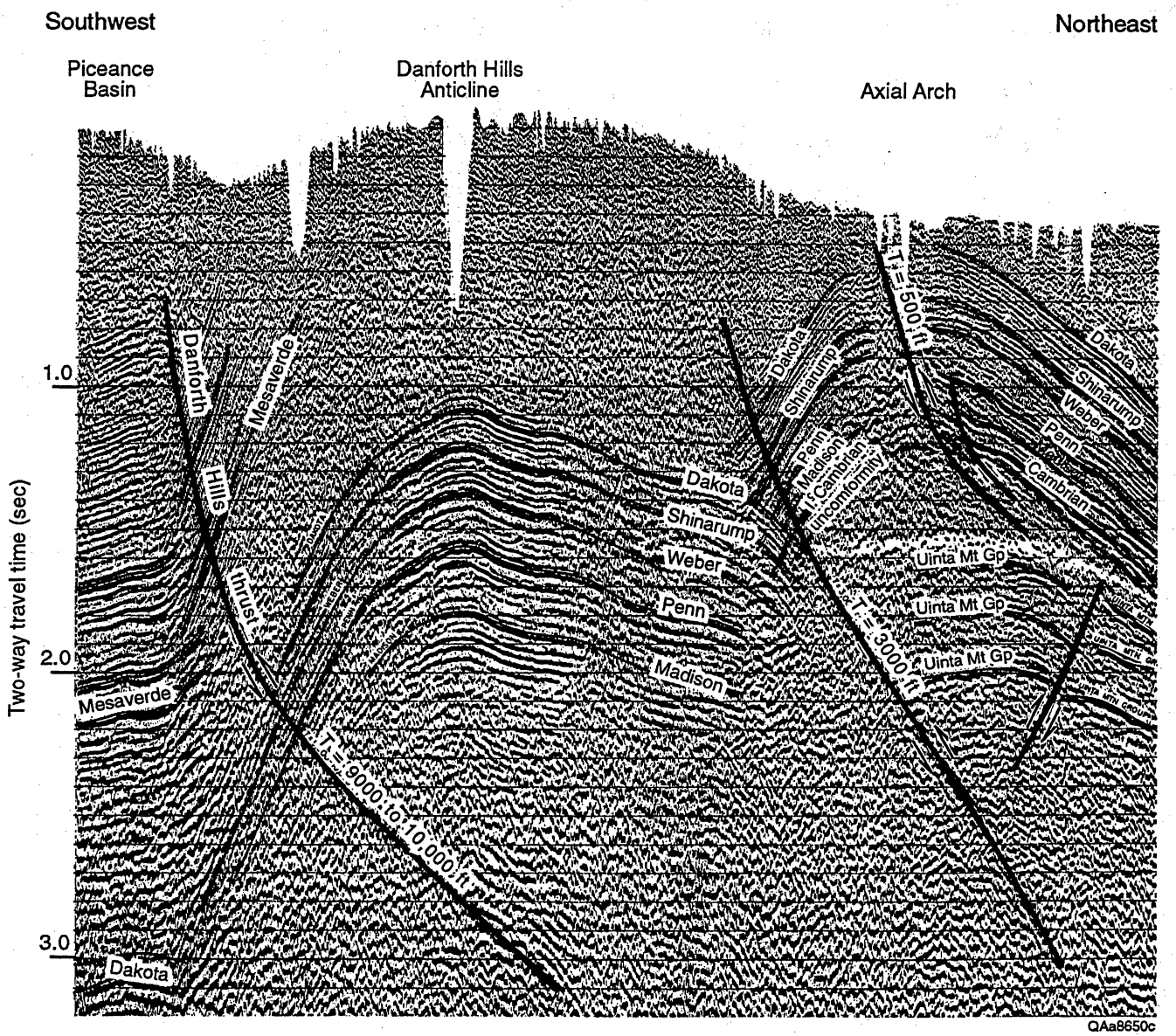

Figure 69. Seismic line across the northeastern part of the study area. There has been approximately 9,000 to 10,000 ft of throw along the Danforth Hills thrust fault. Approximate location of seismic line is shown in figure 67. From Richard (1986).

may exist beneath the White River Anticline. However, if this thrust fault is actually located to the southwest of the White River, then the normal faults along the White River Anticline may represent extensional fractures associated with a thrust-related anticline. Alternatively, normal faulting may have resulted in relaxation of compression in post-Laramide time. Similar thrust faults are present northeast of the study area (fig. 69).

COAL DEPOSITIONAL PATTERNS

The Williams Fork Formation occurs in the upper part of the Mesaverde Group, which is the major coal-bearing unit in the northern Piceance Basin. During the Upper Cretaceous, the northern Piceance and Sand Wash Basins were occupied by the Western Interior Seaway, which received clastic sediments from the rising overthrust belt to the west. Sedimentation patterns were affected by eustatic sea-level fluctuations (Kauffmann, 1977) in addition to cyclic sediment input (Hamilton, 1994).

The genetic stratigraphic framework for the Williams Fork Formation in the Sand Wash Basin, located immediately north of the Piceance Basin, was established by Hamilton (1994), who recognized four genetic units. Genetic units 1 through 4 are identified by low-resistivity shale markers representing discrete depositional episodes. These genetic units have been correlated over the entire Sand Wash Basin and the eastern Greater Green River Basin (Hamilton, 1994; Tyler and Hamilton, 1994). The proximity of the Sand Wash and northern Piceance Basins suggests that genetic units originally described by Hamilton (1994) in the Sand Wash Basin may be correlated in the northern Piceance Basin. Comparison of log patterns from both basins indicates that the low-resistivity shale markers separating units 1 through 4 as well as the Yampa bentonite bed, can be correlated in the northern Piceance Basin (fig. 70). Therefore, the depositional settings and conditions for peat accumulations are similar in both basins.

The thickest coals in the White River and Pinyon Ridge fields occur in unit 1, although thick coals are present in units 2 and 3 as well; thin, laterally discontinuous coal beds occur in

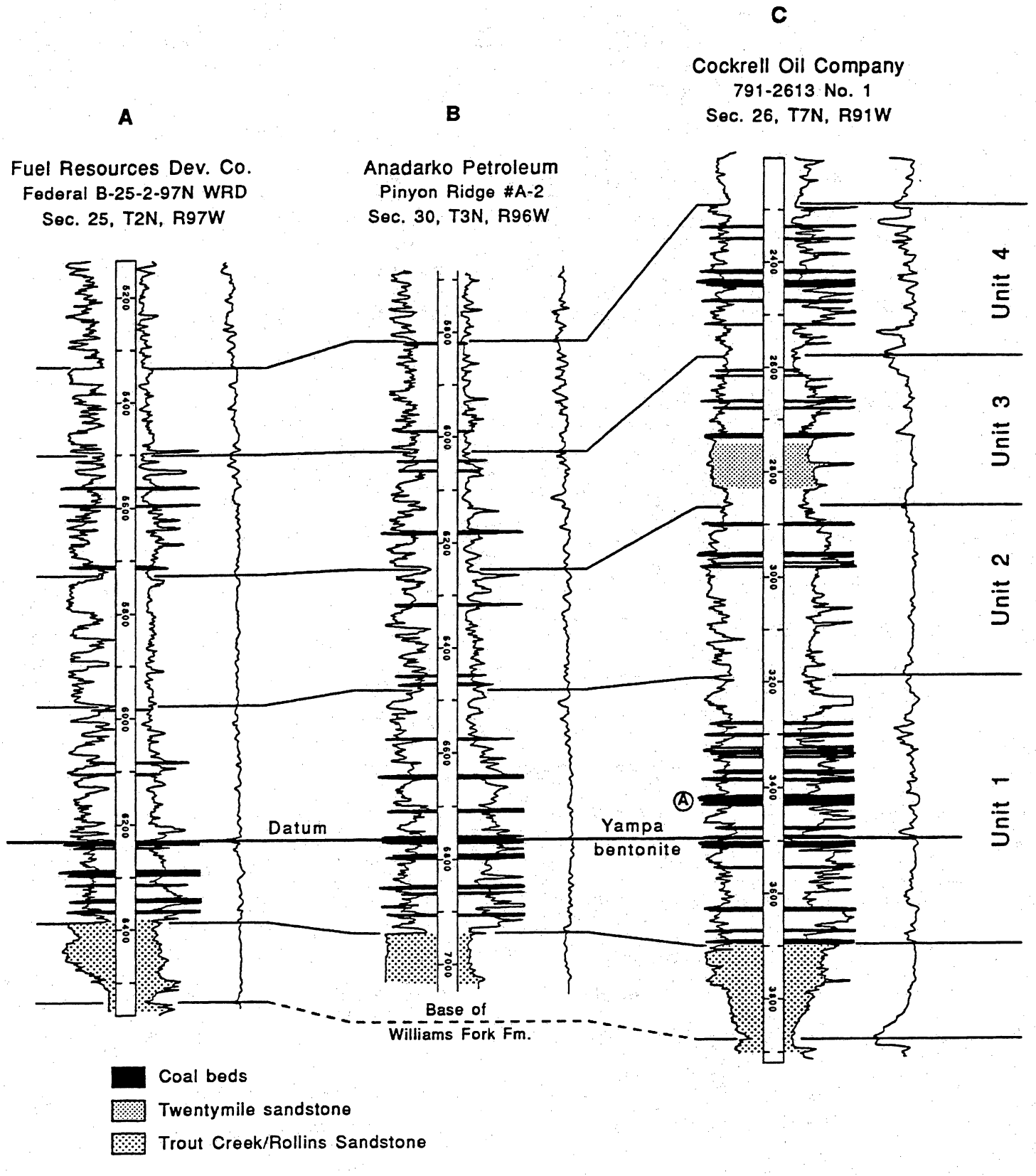

Figure 70. Type logs from the White River Dome (A) and Pinyon Ridge (B) fields in the northern Piceance Basin and from Sand Wash Basin (C). The high-conductivity shale markers described by Hamilton (1994) that separate genetic units 1 through 4 and the Yampa Bentonite are correlated in the northern Piceance Basin. Location of logs is shown in figure 71.

unit 4. Net coal thickness for the lower coal-bearing interval in the study area ranges from less than 20 to nearly 100 ft, and individual seam thickness can exceed 20 ft. However, oil- and gas-well distribution and the number of available logs covering the entire Williams Fork Formation made determination of net coal trends difficult to evaluate in the study area. Therefore, a net coal map of the lower coal-bearing interval (units 1 and 2) in the Sand Wash Basin was combined with net coal data from the northern Piceance Basin, including wells penetrating the Williams Fork in the Mesaverde outcrop, to define net coal trends in the study area (figs. 71 and 72).

The southwest-northeast-oriented net coal thickness trends in the Sand Wash Basin continue into the northern Piceance Basin (fig. 71), suggesting that the conditions for peat accumulation was similar in both basins. On the basis of net coal and sandstone trends in the Sand Wash Basin, Hamilton (1994) determined that ideal conditions for peat accumulation occurred on the coastal plain of units 1 and 2 immediately landward of equivalent shoreline sandstones. Sediment bypass, maintenance of high-water table levels, and optimum subsidence resulted in the maximum accumulation and preservation of peat.

Westward thinning of units 1 and 2 in the Sand Wash Basin corresponds with the transition from the coastal plain to the alluvial plain and subsequent thinning of net coal thickness. Units 1 and 2 are thickest in the southeastern part of the Sand Wash Basin near Craig but thin to the northeast (Hamilton, 1994) and southwest (fig. 70), indicating that maximum basin subsidence occurred in the southeastern Sand Wash Basin. The thinning of the lower coal-bearing unit toward the southwest in the Piceance Basin (fig. 70) and the decrease in net coal thickness to the west and northwest (fig. 72) suggest a transition from a coastal plain to an alluvial plain. Regional net coal trends in the Piceance (Tyler and McMurry, this volume) also show a decrease in net coal thickness in the northwestern part of the basin, indicating that conditions were not favorable for the accumulation and preservation of peat to the west and southwest of the study area.

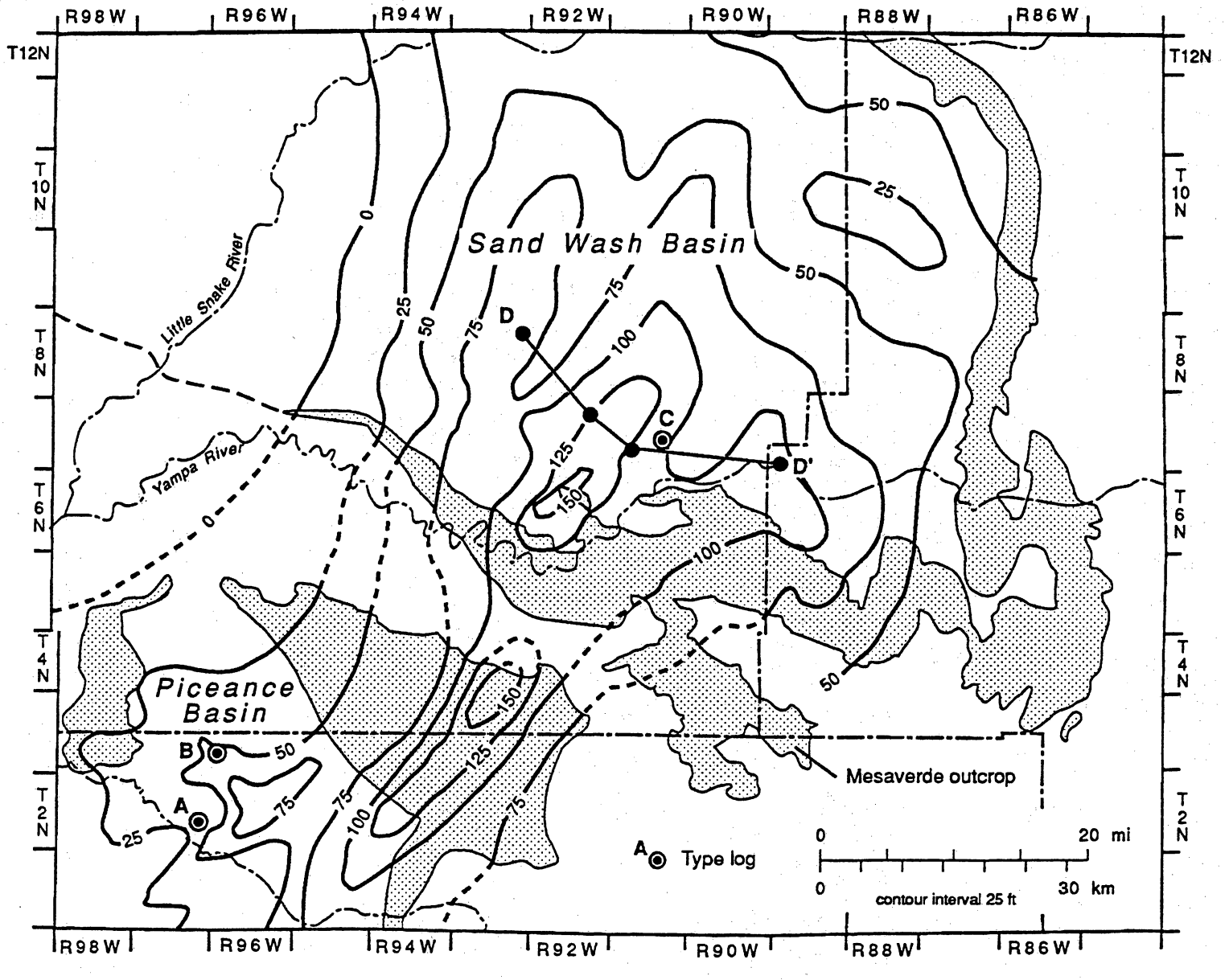

Figure 71. Net coal trends for the lower coal-bearing interval (units 1 and 2) of the Williams Fork Formation in the northern Piceance and Sand Wash Basins. Thick peat accumulated on the coastal plain behind a northeast-trending shoreline. Dashed lines indicate net coal trends where erosion has removed the Williams Fork Formation. Decreasing net coal trends westward are attributed to the coastal plain/alluvial plain transition.

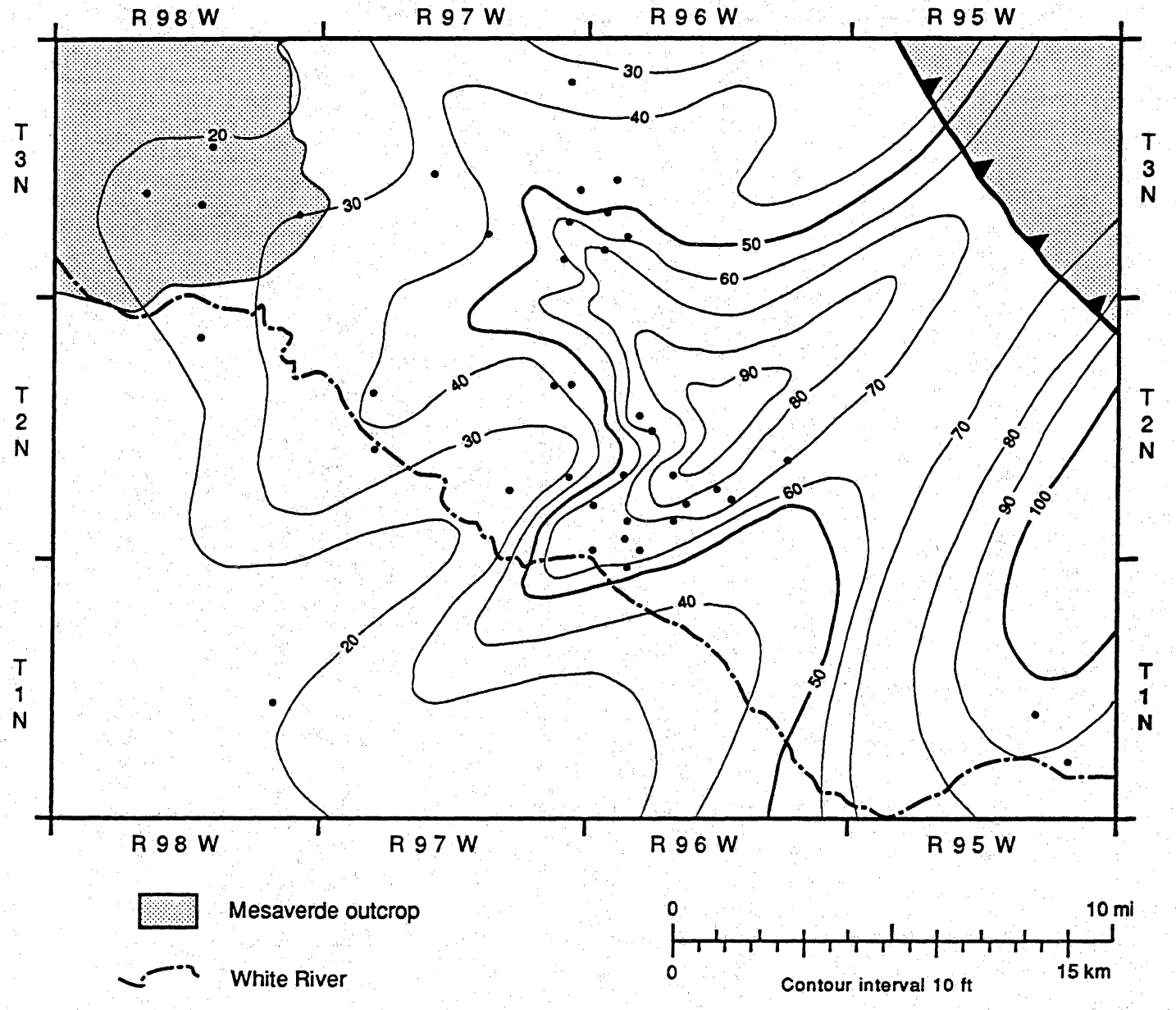

Figure 72. Net coal map for the lower coal-bearing interval (units 1 and 2) of the Williams Fork Formation in the northern Piceance Basin. Net coal thickness ranges from less than 20 to nearly 100 ft in the study area.

COMPOSITION AND ORIGINS OF COAL GASES

Several types of coal gases are generated during stages of coalification (Russell, 1990; Scott, 1993). Primary biogenic methane is generated in the peat swamp but is probably not retained by the peat because of the high moisture content in peat (Levine, 1993). Early thermogenic gases generated at low levels of thermal maturity (lignite to subbituminous) commonly contain relatively minor quantities of wet gases (ethane, propane, butane, etc.). However, with increasing burial and maturation, coals containing sufficient quantities of exinitic (hydrogen-rich) material can generate significant quantities of wet-gas components during the wet-gas-generating stage between vitrinite reflectance (R_m) values of 0.6 to 0.8 percent or high-volatile B and A bituminous ranks (Scott, 1993). Wet-gas generation begins at R_m values of approximately 0.5 percent and the wet-gas-generation rate increases until reaching R_m values of 0.9 to 1.0 percent based on data from Burnham and Sweeney (1989) (fig. 73a).

Significant quantities of methane are not generated until a certain threshold of thermal maturity is reached at vitrinite reflectance values of approximately 0.8 percent, or the high-volatile bituminous rank (Burnham and Sweeney, 1989; Tang and others, 1991) (fig. 73a). The largest increase in the methane-generation rate occurs between vitrinite reflectance values of 0.8 and 1.5 percent (high-volatile A to low-volatile bituminous) and the peak hydrocarbon-generation rate occurs in medium-volatile bituminous coals (fig. 73a). With increasing maturation, wet gases and other hydrocarbons produced during the wet-gas-generating stage are thermally cracked to produce additional methane. Thermal cracking, combined with the generation of additional methane from the coal, results in a decrease in the amount of wet gases and subsequent gradational increase in the gas dryness index (C_1/C_{1-5} value) with increasing rank. The gas dryness index approaches unity in the semianthracite to anthracite coal ranks (Scott, 1993).

Secondary biogenic gases are generated after burial, coalification, and subsequent uplift and erosion along basin margins (Scott and Kaiser, 1991; Scott, 1993). Bacteria transported

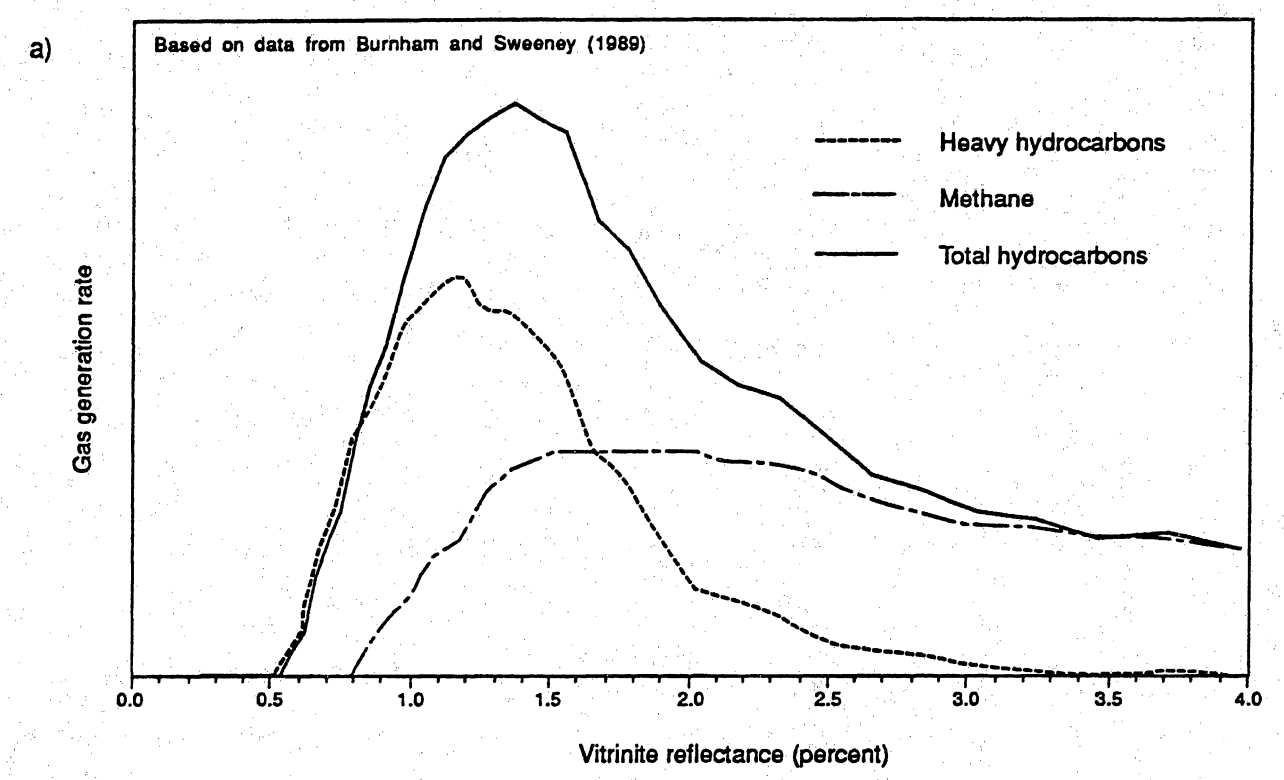

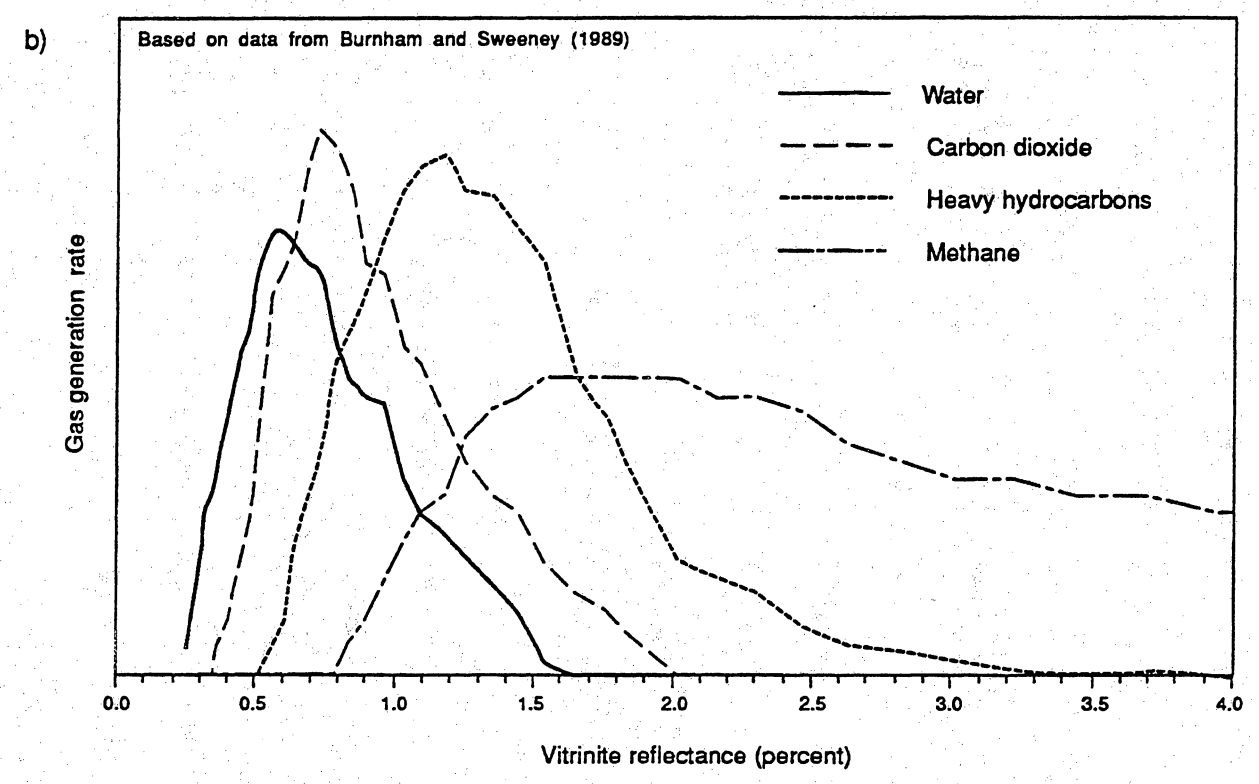

Figure 73. Relation between the coal-gas-generation rate and vitrinite reflectance. (a) Significant methane generation does not occur until vitrinite reflectance values reach approximately 0.8 percent; peak hydrocarbon generation occurs during the medium-volatile and low-volatile bituminous coal ranks (R_m of approximately 1.5 percent). (b) Peak carbon dioxide generation occurs during the wet-gas-generating stage at vitrinite reflectance values between 0.6 and 0.8 percent. Curves were generated from the data of Burnham and Sweeney (1989).

through permeable coals metabolize n-alkanes and wet gases produced during the wet-gas-generation stage to produce secondary biogenic methane and carbon dioxide. Wet gases subjected to bacterial alteration are modified compositionally to resemble thermally mature gases having gas dryness indices near unity (James and Burns, 1984).

Vitrinite reflectance values in the study area range from 0.55 to 0.67 (Nuccio and Johnson, 1983), indicating that coal rank ranges from high-volatile C to high-volatile B bituminous. Therefore, coals in the northern Piceance Basin probably have not entered the threshold of significant methane generation but are within the wet-gas-generating stage. Coal gases from the White River field are wet to very wet, having gas dryness indices ranging from 0.78 to 0.91 and ethane content exceeding 6 percent (Scott, 1993). The presence of significant quantities of wet gases suggests that the coals may be hydrogen rich and that the condensate produced by coalbed methane wells in the northern Piceance Basin probably originated from the coal.

The carbon dioxide content of coal gases from the White River field ranges from 8 to 38 percent and averages 25 percent (Scott, 1993). The carbon dioxide content of Upper Cretaceous sandstone gases ranges from 13.7 to 22.4 percent, whereas Wasatch sandstones contain less than 0.5 percent carbon dioxide (Moore and Sigler, 1987; Johnson and Rice, 1990). Coal-gas carbon dioxide content is highest (≥24 percent) on the northeast flank of the White River Anticline and lowest (<24 percent) on the upthrown side of a southeast-trending fault (fig. 74), suggesting possible carbon dioxide migration from the northeast parallel to net coal thickness trends (fig. 72). Although carbon dioxide does not correlate well with net coal thickness (fig. 75a), carbon dioxide content increases with decreasing maximum coal thickness, or thickness of single thickest coal bed (fig. 75b). Why carbon dioxide content correlates with maximum coal thickness is unknown, although it is possible that maximum coal seam thicknesses simply decrease off the northeast flank of the White River Anticline.

Coal beds in the Sand Wash Basin also contain large amounts of carbon dioxide, based on the composition of desorbed coal gases (Scott, 1994). However, carbon dioxide content varies

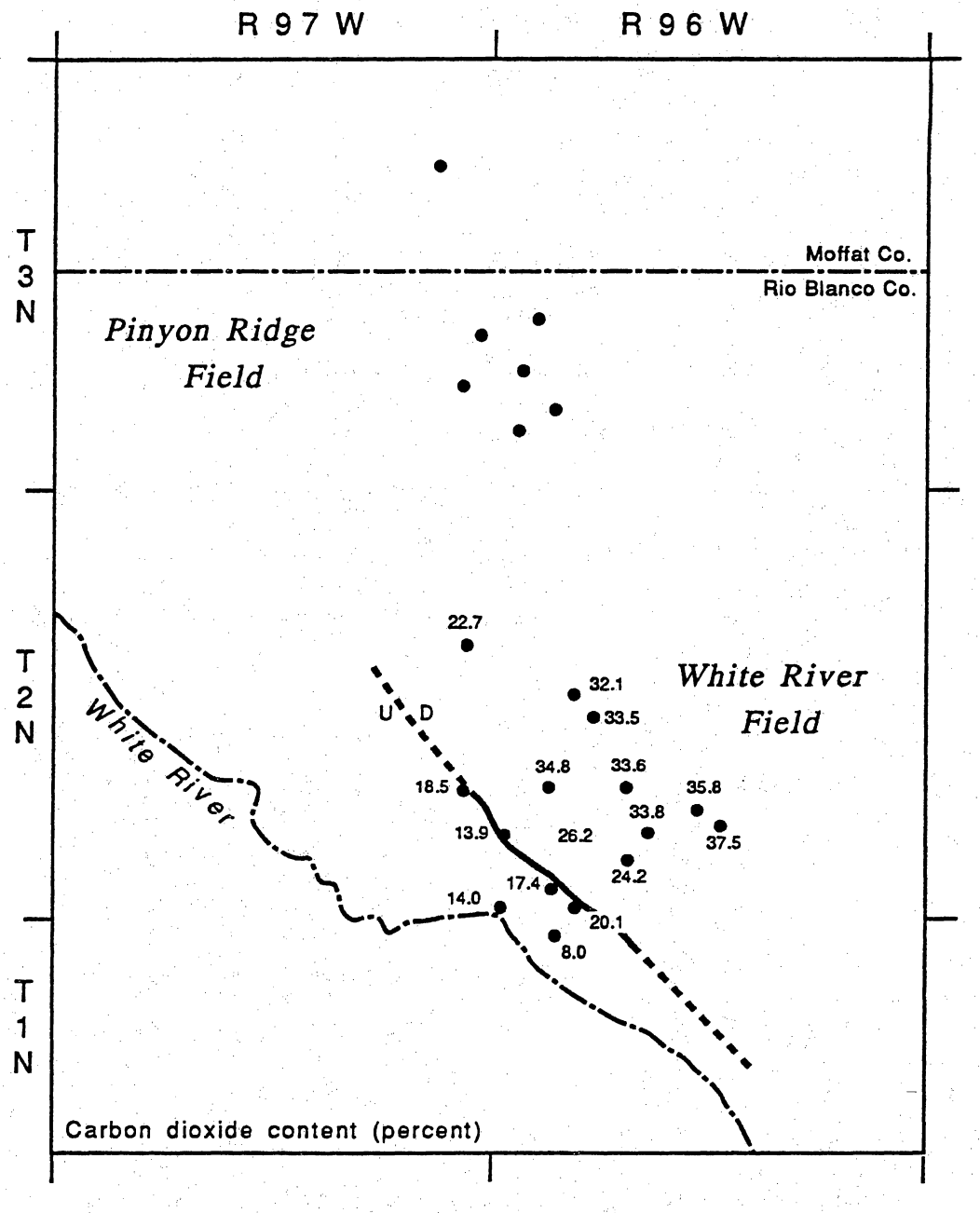

Figure 74. Carbon dioxide content of coal gases in the northern Piceance Basin. Coal gases in the study area are unusual because of the high carbon dioxide content and relatively large amounts of wet gas components and condensate. The highest carbon dioxide contents (>20 percent) occur along, or on the downthrown side of, a northwest-trending fault.

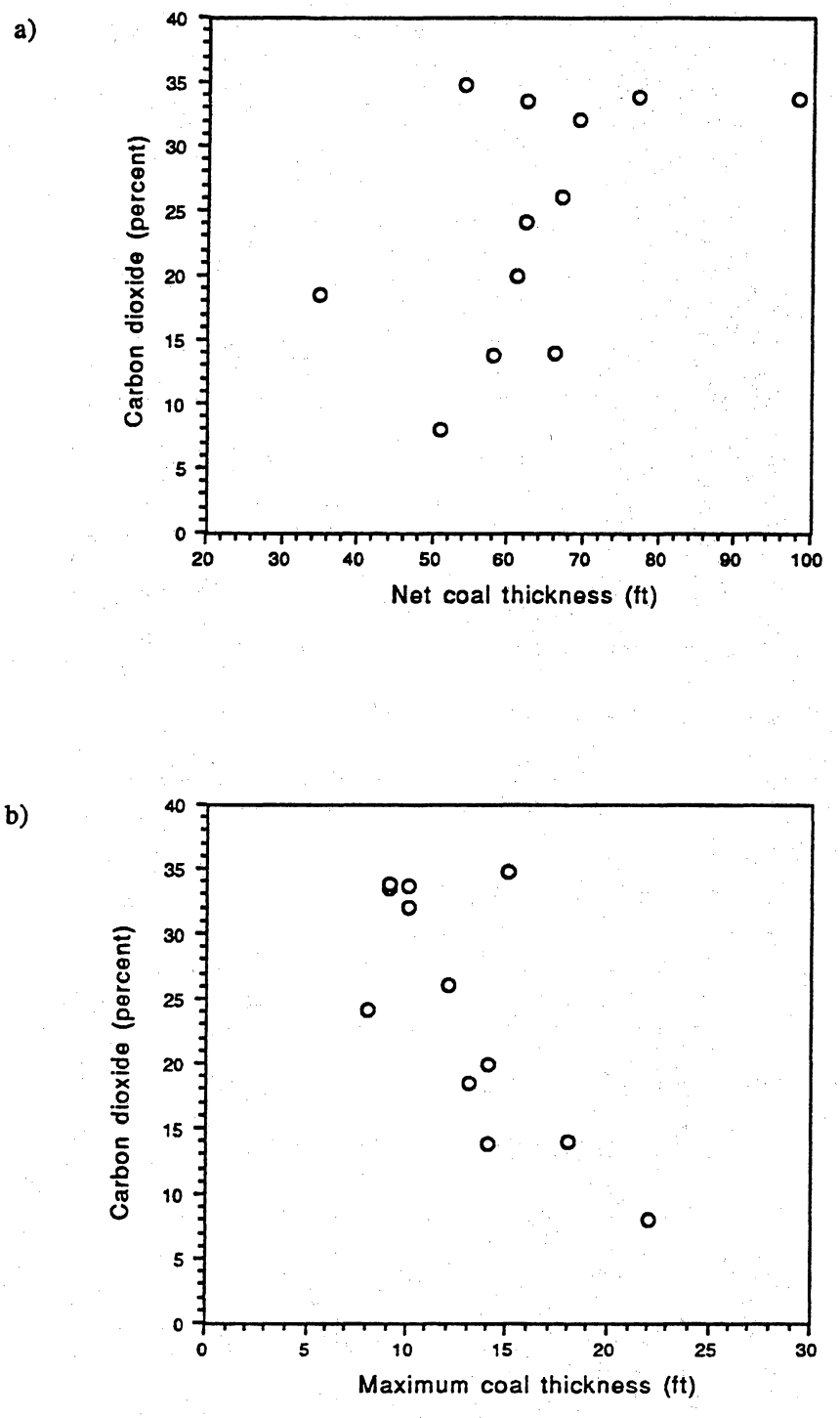

Figure 75. Correlation of coal thickness and carbon dioxide content. (a) Carbon dioxide content does not correlate well with net coal thickness. (b) A correlation exists between maximum coal thickness and carbon dioxide content. Wells with the thickest coal bed tend to have coal gases with a lower carbon dioxide content.

significantly between individual seams and between wells (fig. 76). However, if the same type of carbon dioxide content trends are present in the northern Piceance Basin, then a large part of the carbon dioxide produced during coalbed methane production may be derived predominantly from one or two seams rather than equally from all perforated intervals in the well.

Although coal gases in other basins also have high carbon dioxide contents, the combination of high carbon dioxide and wet gas (ethane) content in the northern Piceance Basin is unusual. The high carbon dioxide content of coal gases from the San Juan Basin is attributed to the generation and migration of secondary biogenic gases (Scott and Kaiser, 1991; Scott and others, 1994). Coal gases with the highest carbon dioxide content have C_1/C_{1-5} values near 1.00 because bacteria have removed the wet-gas components. The high carbon dioxide content of coal gases in the White River field cannot be attributed to secondary biogenic gas generation because the coal gases contain significant quantities of wet gases that normally would be metabolized by the bacteria. Therefore, an alternative origin for the carbon dioxide is required.

Peak carbon dioxide generation occurs during the high-volatile C bituminous ranks at vitrinite reflectance values of approximately 0.75 percent (fig. 73b), suggesting that the carbon dioxide in the northern Piceance Basin could be thermogenic. However, carbon dioxide content in similar rank coals in other western United States basins is usually less than 1 or 2 percent, suggesting that either the coals in the northern Piceance Basin are chemically unique and prone to generating significant quantities of carbon dioxide or the carbon dioxide migrated from an outside source. The isotopic composition of carbon dioxide in the White River ranges from –7.0 to –7.1‰ (Rice, 1993), indicating that the carbon dioxide is not entirely thermogenic because carbon dioxide generated during coalification ranges from –25 to –30‰ (Irwin and others, 1977). Tyler and others (1991a) suggested that the carbon dioxide in the northern Piceance Basin migrated from deeper horizons along thrust faults. Rice (1993) suggested that the carbon dioxide resulted from the thermal decomposition of Paleozoic carbonates or deep-

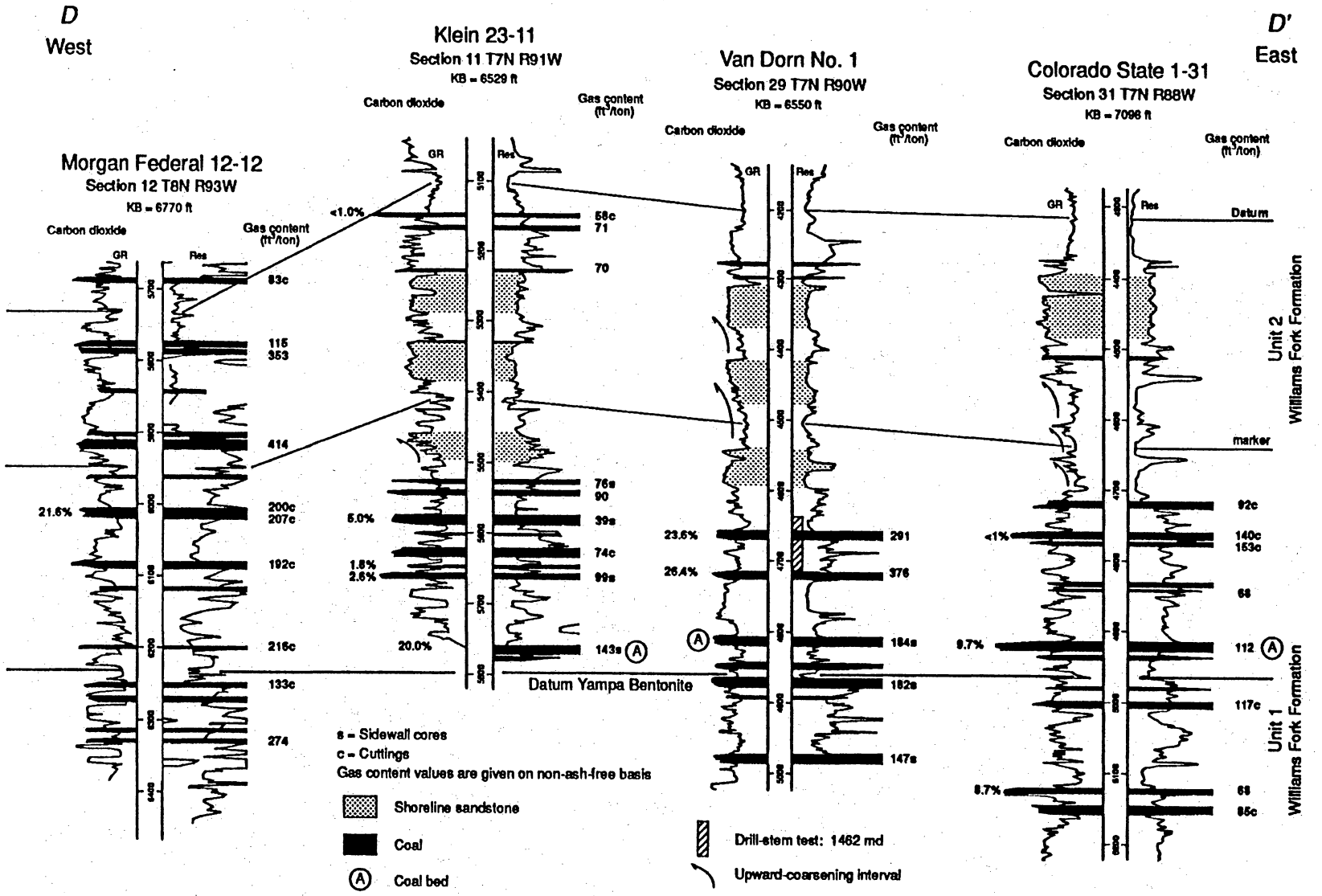

Figure 76. Cross section showing the variability of carbon dioxide and gas content in the Sand Wash Basin. Carbon dioxide varies significantly between Williams Fork coal beds in the Sand Wash Basin. Location of cross section is shown in Figure 71. Modified from Scott (1994).

seated igneous activity. A mixture of 25 percent thermogenic carbon dioxide (–28‰) and 75 percent marine carbonate (0‰) derived from degradation of deeply buried Paleozoic carbonates would yield an average carbon dioxide $\delta^{13}C$ value of –7‰. Alternatively, carbon dioxide derived from igneous sources has $\delta^{13}C$ values ranging from –2 to –8‰ (Sakata, 1991), which is similar to $\delta^{13}C$ values of Williams Fork coal gases. However, if the carbon dioxide was derived from igneous activity, which was relatively minor in the northern Piceance Basin, then nearly all of the carbon dioxide would have migrated to the area and very little thermogenic carbon dioxide would have been generated from the coals, based on isotopic considerations. Therefore, carbon dioxide in the White River area is probably a mixture of thermogenic and migrated gases derived from the degradation of carbonate rocks.

GAS AND WATER PRODUCTION

Two gas wells were drilled on the White River Anticline in 1890 to a depth of approximately 700 ft in sec. 31, T2N, R96W (Rocky Mountain Association of Geologists, 1961). Three additional Wasatch wells drilled in 1918 were followed by a fourth well in 1924; the initial flow of these later wells ranged from 2 to 15 MMcf/d (Heaton, 1929). The Lad No. 1 well (sec. 31, T2N, R96W) was reentered and completed as a coalbed methane well by Fuelco in 1989, with an initial potential (IP) of 1,000 Mcf/d and 38 bbl/d of water. Fuelco subsequently drilled the first coalbed methane well in the field (M-30-2-96) in early 1990. Anadarko Petroleum Corporation drilled the first coalbed methane well in the Pinyon Ridge field in late 1991. The Pinyon Ridge Federal No. B-1 was drilled in sec. 12, T3N, R97W and initially produced water and condensate. The White River field currently has 14 producing coalbed methane wells, and the Pinyon Ridge field has 10 producing coalbed methane wells. The White River field has produced 4,417 MMcf of coal gas, 609,000 bbl of water, and 62,242 bbl of condensate, whereas the Pinyon Ridge has produced 176 MMcf of coal gas, 376,011 bbl of water, and 12,660 bbl of condensate, based on cumulative production data through June 1994.

Production data were integrated with geologic information to assess factors affecting coalbed methane production in the northern Piceance Basin. Coal gas, water, and liquid hydrocarbon production can vary from month to month over the life of the well and different well-completion techniques can greatly affect the quantities of produced fluids and gases. Comparison of monthly or average daily production data can be misleading if length of production and other factors are not considered. Therefore, maximum monthly production data, which record the highest production recorded for that well, were evaluated because maximum monthly production data are assumed to represent the production potential of that well.

Maximum monthly gas production on the White River field ranges from 4.3 to 34.0 MMcf (fig. 77). Wells with the highest maximum monthly gas production (>30 MMcf) are located on the downthrown side of a northwest-trending fault. Maximum monthly gas production is lower on the upthrown side of the fault on the top of the anticline but decreases significantly downdip off structure. Maximum monthly water production is generally lower along the crest of the anticline and increases northeastward off structure (fig. 78). One exception is the B25-2-97-N well (sec. 25, T2N,R97W), which has a maximum monthly water production exceeding 11,000 bbl. This well is located near a fault, which may account for the excessive water production. Maximum monthly hydrocarbon production ranges from 0 to 828 bbl (fig. 79). The distribution of values in the field is highly variable and does not correlate directly with structure or net coal thickness. However, the five wells that have maximum monthly hydrocarbon production greater than 500 bbl correspond with areas that are on the downthrown side of the fault (or near the fault) where net coal thickness thins rapidly, suggesting that a combination of structure and net coal may be factors in hydrocarbon migration and trapping. Wells on the downthrown side of the fault having high liquid hydrocarbon production also have high carbon dioxide contents. Killops and others (1994) suggested that carbon dioxide generation during coalification may assist in oil migration in and from coals because carbon dioxide has a considerable solvating potential for hydrocarbons. Therefore,

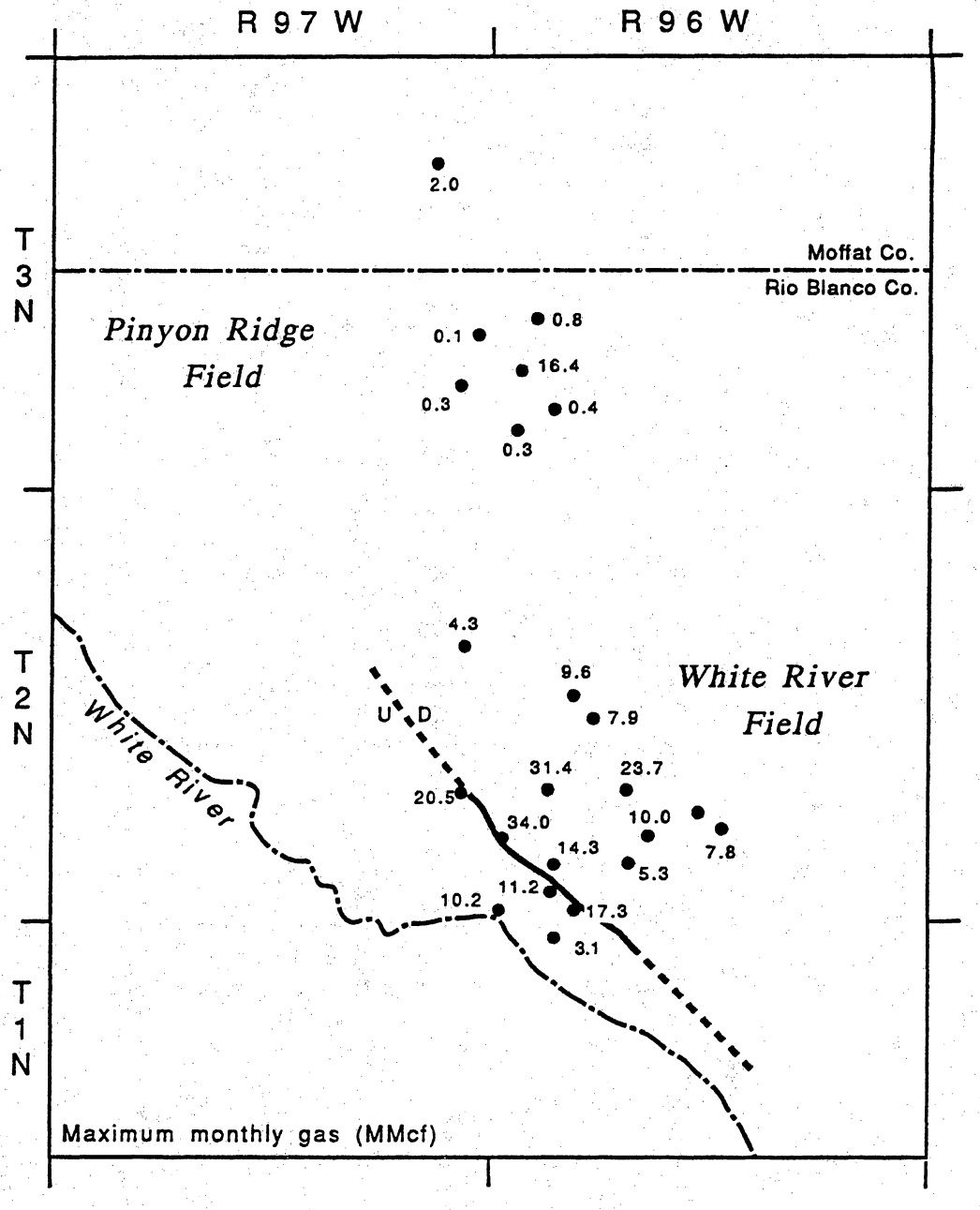

Figure 77. Maximum monthly coal gas production in the study area.

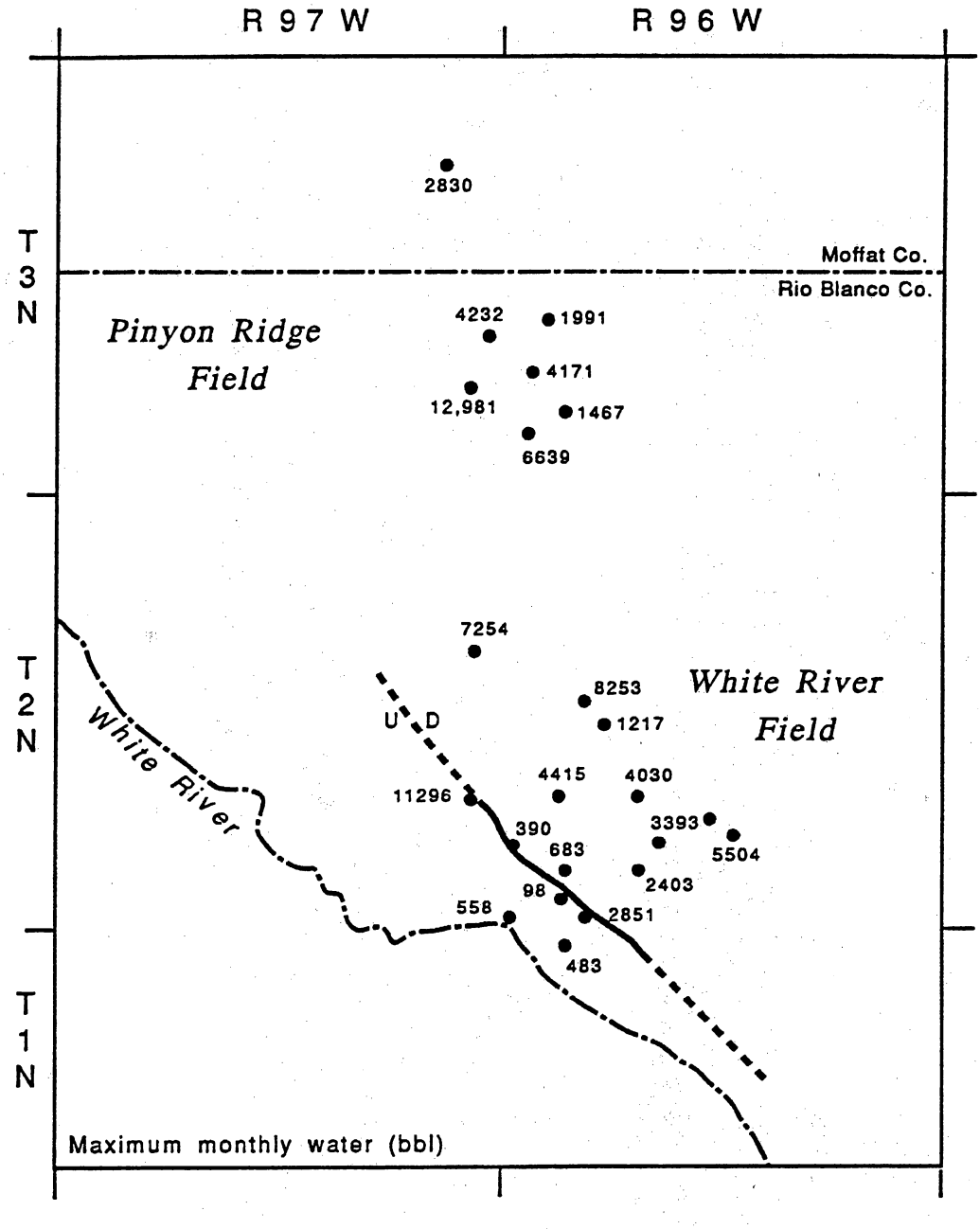

Figure 78. Maximum monthly water production in the study area.

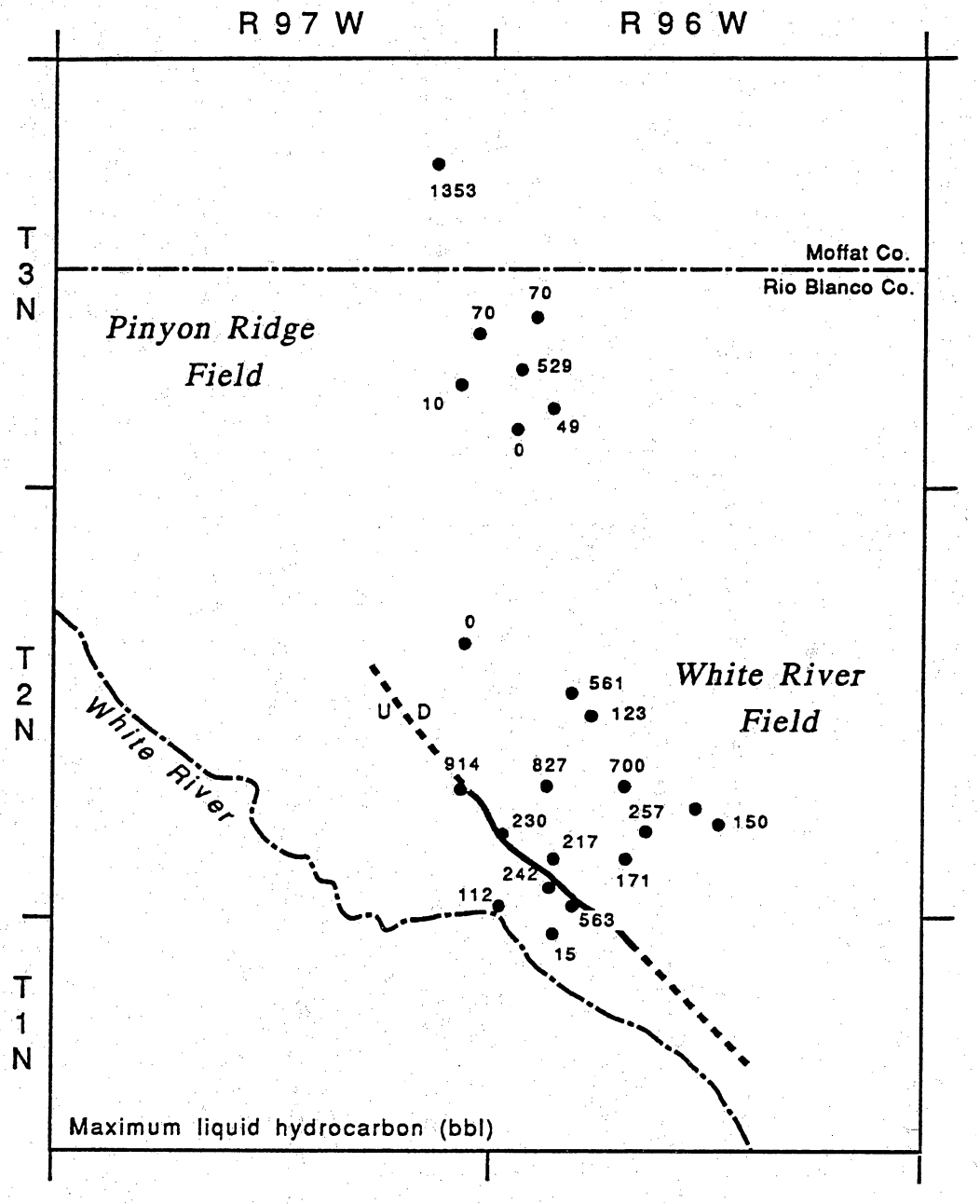

Figure 79. Maximum monthly condensate production in the study area.

carbon dioxide from an outside source may also contribute to oil migration and accumulation in coals. Additional coal and geochemical data and better well control are probably required to fully understand factors affecting liquid hydrocarbon production.

Maximum monthly gas production in the Pinyon Ridge field is highly variable, ranging from 0.1 to 16.4 MMcf (fig. 77); with the exception of two wells, maximum monthly production is less than 1 MMcf. Maximum monthly water production ranges from 1,467 to nearly 13,000 bbl (fig. 78). In general, water production is higher in the Pinyon Ridge field than in the White River field. Liquid hydrocarbon production is similar to the White River field with the exception of one Pinyon Ridge well, which has produced significant quantities of condensate.

HYDROGEOLOGIC FACTORS AFFECTING COALBED METHANE PRODUCIBILITY

Coalbed methane producibility is determined by the complex interplay of coal distribution, coal rank, gas content, permeability, ground-water flow, and depositional and structural setting (Kaiser and others, 1994a). Based on a coalbed methane producibility model discussed by Kaiser and others (1994a), high coalbed methane productivity is typically governed by thick coals of high coal rank, basinward flow of ground water through coals of high rank toward no-flow boundaries (regional hingelines, faults, facies changes, and/or discharge areas) and conventional trapping along those boundaries to provide additional gas beyond that sorbed to the coal surface. The coalbed methane producibility model is used to evaluate hydrogeologic factors controlling coalbed methane production in the northern Piceance Basin. Not all of the key factors required for high coalbed methane producibility are present in the northern Piceance Basin, which explains why the White River and Pinyon Ridge fields are not as productive as the San Juan Basin. However, the synergistic interplay between several factors does account for relatively high coalbed methane production.

Coal rank in the study area ranges from high-volatile C to high-volatile B bituminous, indicating that the coals have not reached the threshold of thermogenic gas generation that occurs at R_m of 0.8 to 1.0 percent (Burnham and Sweeney, 1989; Tang and others, 1991).

However, the hydrogen-rich coals are in the wet-gas-generating stage (R_m between 0.6 and 0.8 percent), which explains the presence of chemically wet gases and condensate production. If these coals are permeable and connected to an elevated outcrop belt with high precipitation, bacteria transported through the coals may generate significant quantities of secondary biogenic gases. Secondary biogenic gases generated from the biodegradation of chemically wet gases and condensate generated during the wet-gas-generating stage, combined with a no-flow boundary (permeability barrier) located downflow, would allow hydrodynamic trapping of thermogenic and secondary biogenic gases as seen in the San Juan Basin (Scott and others, 1994).

The thickest net coal trends are oriented northeastward for intersection with the Mesaverde outcrop belt. Annual precipitation exceeds 16 inches per year in the outcrop belt (figs. 72 and 80), which is favorable for recharge and subsequent generation of secondary biogenic gases, assuming a regionally continuous aquifer. The presence of coals that have generated wet gases and heavier hydrocarbons, the decrease in net coal thickness southwestward (fig. 72), and the presence of faults along the White River Anticline that are orthogonal to flow direction (fig. 68) all indicate favorable conditions for the generation and accumulation of thermogenic and secondary biogenic gases in the northern Piceance Basin. However, the northwestward-trending Danforth Hills thrust (figs. 69 and 72) isolates the coal interval in the outcrop belt from coals basinward in the northern Piceance Basin. In other words, the Mesaverde is a fault-severed aquifer. Therefore, the movement of meteoric water and subsequent generation of secondary biogenic gases seen in the San Juan Basin probably did not occur or is minimized in the northern Piceance Basin. If the Danforth Hills thrust fault did not reach the surface and instead formed a blind thrust fault, the outcrop belt would have been elevated for meteoric recharge similar to that of the San Juan Basin (fig. 81).

Although thrust fault development along the northeastern margin of the basin prevented meteoric recharge into the basin, the structural evolution of the basin proved to be an important aspect of coalbed methane producibility in the northern Piceance Basin. One key factor affecting coalbed methane producibility is permeability (Kaiser and others, 1994a). Both

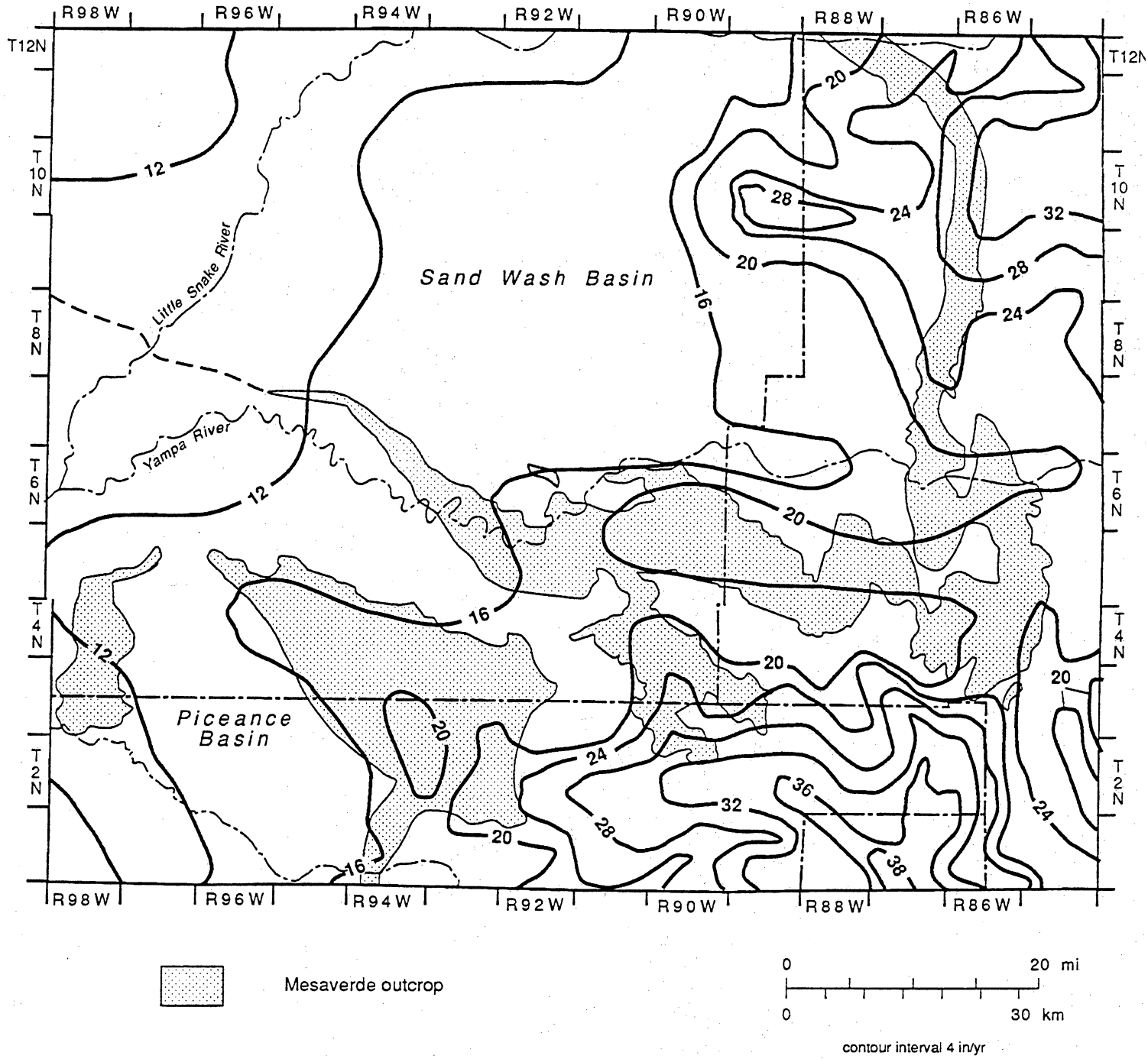

Figure 80. Mean annual precipitation for the northern Piceance and Sand Wash Basins. Data from Colorado Climate Center (1984). Precipitation along the Danforth Hills Anticline in the northern Piceance Basin exceeds 20 inches per year.

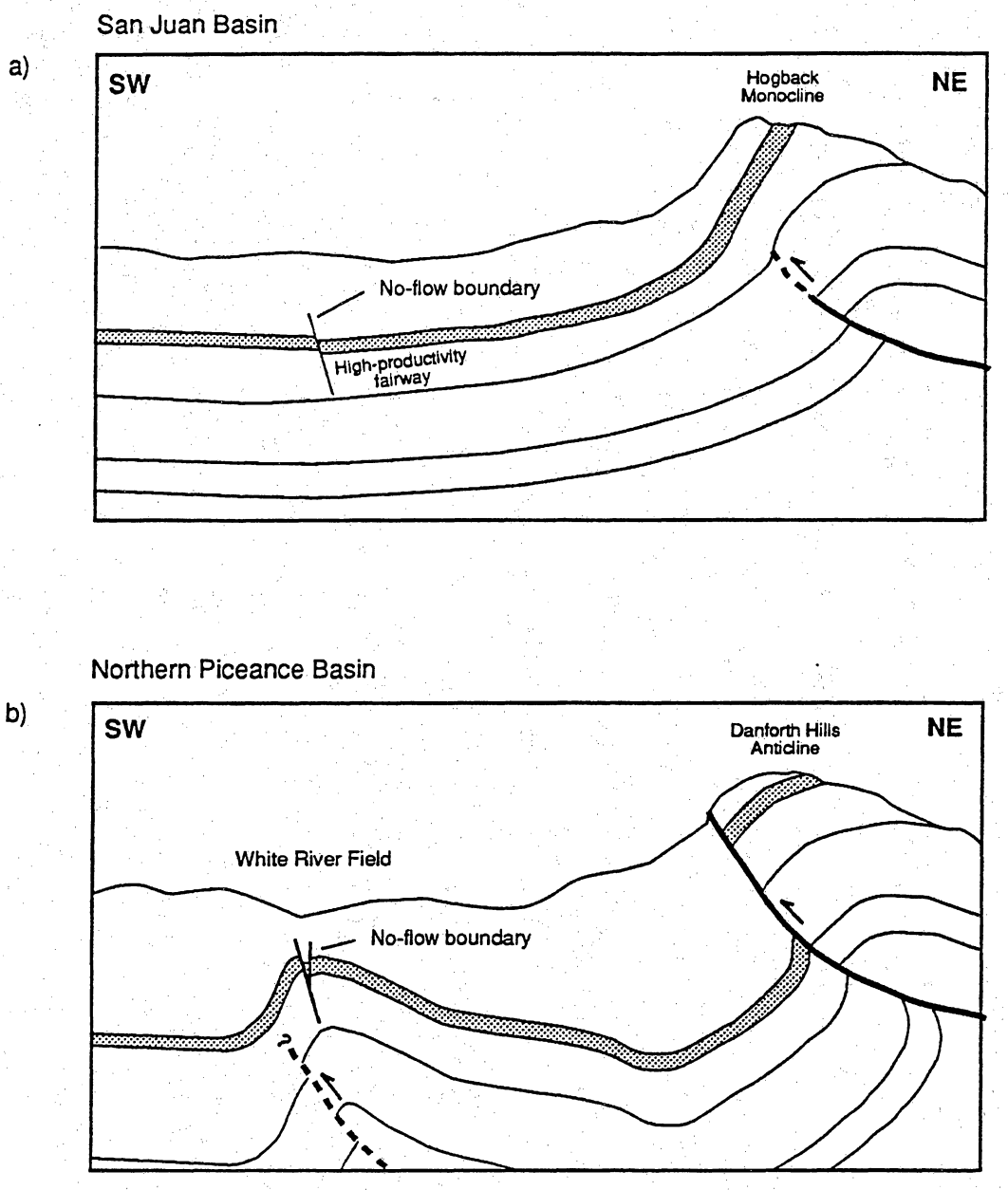

Figure 81. Schematic diagram showing the importance of thrust faulting to regional hydrogeology. (a) Blind thrust faults may elevate permeable coal-bearing units for possible recharge along basin margins so that in the San Juan Basin thermogenic secondary biogenic gases are swept basinward for conventional trapping at no-flow boundaries. (b) A no-flow boundary (faults and facies change) orthogonal to meteoric recharge and gas migration is present in the northern Piceance Basin; however, the Danforth Hills thrust fault prevents meteoric recharge by isolating or severing coals at the outcrop from those deeper in the basin.

coalbed methane fields are associated with anticlines. Extensional fracture and/or cleat development along the crest of these anticlines (fig. 69) probably contributed to enhanced coal permeability in the northern Piceance Basin. Therefore, the importance of structural evolution and cleat development discussed by Kaiser and others (1994a) applies to the northern Piceance Basin.

In addition to permeability requirements, Kaiser and others (1994a) also stressed the importance of conventional trapping of coal gases. Scott and others (1994) suggested that 50 to 75 percent of the coal gas produced from the high-productivity fairway in the San Juan Basin was derived from conventional trapping of thermogenic and secondary biogenic gases. As discussed previously, a significant part of the carbon dioxide produced from Williams Fork coals in the northern Piceance basin probably migrated from deeper Paleozoic sources, based on isotopic evidence. The presence of abnormally high gas contents in lower rank coals also indicates gas migration (Scott and Ambrose, 1992). On the basis of experimental data of Tang and others (1991) and observations in other coal basins, high-volatile C and B bituminous coals should have ash-free gas contents less than 200 scf/ton. However, gas contents of Williams Fork coals range between 561 to 607 scf/ton in one coalbed methane well and would be higher if corrected to an ash-free basis. Therefore, coal rank, coal gas composition, and gas content data suggest that migrating gases were conventionally trapped in the northern Piceance Basin.

Arri and others (1992) evaluated the correlation between the amount of a coal gas component sorbed on the coal surface and the amount of that gas component in the produced coal gas and determined much more carbon dioxide is sorbed to the coal surface than is present in the produced coal gas. Therefore, assuming an average produced gas composition of 75 percent methane and 25 percent carbon dioxide, approximately 50 to 55 percent of the gases sorbed on the Williams Fork coals in the northern Piceance Basin are hydrocarbons (methane, ethane, butane, etc.), whereas the remaining gases, composed predominantly of carbon dioxide, account for 45 to 50 percent of the total gas content. Methane gas contents therefore probably range from 280 to 334 scf/ton, whereas carbon dioxide gas contents are estimated to

range from 252 to 303 scf/ton. Assuming that coals on the White River Dome are between R_m values of 0.60 and 0.75 percent, then approximately 50 to 150 scf/ton of coal gases (methane and wet gas components) were generated by the coals during coalification, according to the data of Tang and others (1991). Therefore, approximately 60 to 80 percent of the hydrocarbon gases migrated to the White River field, whereas only 20 to 40 percent were generated in-place. Combining this data with carbon dioxide migration estimates based on isotopic evidence discussed earlier, migration and conventional trapping of coal gases account for approximately 65 to 80 percent of the gas production from the White River field.

CONCLUSIONS

1. Williams Fork genetic units identified in the Sand Wash Basin by Hamilton (1994) are correlated in the northern Piceance Basin.

2. Net coal thickness for units 1 and 2 in the northern Piceance Basin ranges from less than 20 to nearly 100 ft. Net coal maps for the lower coal-bearing interval (units 1 and 2) constructed for the northern Piceance and Sand Wash Basins indicate a northeastward orientation of thicker net coal formed on a coastal plain behind the marine shoreline.

3. Although net coal trends are oriented favorably for meteoric recharge and secondary biogenic gas generation, the Danforth Hills thrust fault separates the lower coal-bearing interval in the outcrop belt from subsurface coals. Therefore, a dynamic meteoric flow regime similar to that of the San Juan Basin is probably absent in the northern Piceance Basin.

4. Williams Fork coals are predominantly high-volatile C and B bituminous and have not entered the threshold of significant thermogenic methane generation in the northern Piceance Basin. The coals have reached the wet-gas-generating stage, suggesting that wet gases and condensate produced from coalbed methane wells are probably indigenous to the coals. The gas dryness index (C_1/C_{1-5} value) ranges between 0.78 and 0.91.

5. Carbon dioxide content in the White River field ranges between 8 and 34 percent and averages 25 percent. The combination of wet coal gases and high-carbon dioxide content

components in the study area is unusual compared to that in other coal basins. Although the wet gases were generated during coalification, the carbon dioxide was probably sourced from outside the study area and migrated up thrust faults. According to isotopic data, as much as 75 percent of the carbon dioxide in the coal gases may have been derived from the decomposition of Paleozoic carbonates, whereas 25 percent was generated during coalification.

6. The White River and Pinyon Ridge coalbed methane fields are located on anticlines. Extensional fracture and/or cleat development along the crest of these anticlines probably contributed to enhanced coal permeability in the northern Piceance Basin.

7. Normal faulting on the White River Anticline, associated with a possible thrust fault located southwest of the structure, acts as a no-flow boundary and a permeability barrier. Faults and facies changes are perpendicular to gas migration pathways, which is consistent with conventional trapping of gas as predicted from the coalbed methane producibility model of Kaiser and others (1994a).

8. Evidence of gas migration and conventional trapping include the presence of abnormally high gas content in relatively low-rank coals and the isotopic composition of carbon dioxide. Migrated and conventionally trapped coal gases account for approximately 65 to 80 percent of gas production from the White River field. The presence of higher carbon dioxide contents on the northeast side of the White River suggests possible migration from that direction.

FUTURE WORK

Net sandstone mapping, coal seam continuity, initial potential data, coal gas compositional variability in the Pinyon Ridge field, hydrologic data, and the distribution of gas contents will be used to enhance understanding of the hydrogeologic factors affecting coalbed methane producibility in the northern Piceance Basin.

CONCLUSIONS

Roger Tyler, William R. Kaiser, Carol M. Tremain, Andrew R. Scott, H. Seay Nance, Ronald G. McMurry, and Naijiang Zhou

GENETIC STRATIGRAPHY

1. The Piceance Basin has a single major coalbed methane target, the Cameo-Wheeler-Fairfield coal zone (Williams Fork Formation, Mesaverde Group), that ranges from 300 to 600 ft (91 to 183 m) in thickness and lies at an average depth of approximately 6,000 ft (~1,800 m). The most continuous and thickest coal beds (individual seams from 20 to 35 ft [6 to 11 m] thick) formed in coastal plain environments landward (westward) of the progradational strandplain/delta plain deposits of the Rollins-Trout Creek sandstone. Net coal thickness of the Williams Fork Formation averages 80 to 150 ft (24 to 45 m).

2. The Williams Fork Formation can be divided into several genetic depositional sequences. Genetic unit 1 is a progradational/aggradational couplet that extended coal-bearing coastal plain deposits beyond the present-day basin margin. Genetic units 2 and 3 are clastic wedges displaying a similar arrangement of depositional systems. Three depositional systems are recognized in each genetic unit. A north- to northeast-oriented linear shoreline system dominated the easternmost part of the basin and was backed landward by a coastal plain system, which in turn graded westward into an alluvial plain system. Coal beds pinch out against and/or override the shoreline sandstone to the east, and their ultimate lateral extent is limited by the final shoreline position beyond which marine conditions prevail.

3. Continuity of the Williams Fork coals is variable. Some individual seams, particularly in genetic unit 1, are correlatable for up to 30 mi (48 km) in the southeastern half of the basin. Other seams could be correlated only when grouped within coal packages. Coals that reach

outcrop are reduced in number and total thickness and, consequently, their ability to receive and transmit ground water recharge basinward is reduced.

4. Limited recharge may have implications for the producibility of coal gas. In the absence of dynamic ground-water flow, less gas is dissolved and swept basinward for eventual resorption and conventional trapping along potential no-flow boundaries. Thus, high coal-gas productivity may be precluded; conventional traps have the best potential for coal-gas production.

FRACTURES

1. Regional mapping of fracture (cleat) sets in coal beds and sandstones shows that face-cleat strike domains are oriented normal to the basin-fold axis and Grand Hogback thrust front and parallel to the maximum horizontal compressive paleostresses. Upper Cretaceous face-cleat domains correlate with prominent joints in clastic rocks whose strikes are east-northeast in the southern Piceance Basin and west-northwest in the northern Piceance Basin.

2. East-northeast-trending face-cleat domains in the southeast part of the basin are oblique to current maximum stress directions, whereas face-cleat domains in the north half of the basin are parallel to current maximum stress directions. Therefore, face cleats in the north half of the basin may provide more permeable pathways for gas production.

LINEAMENTS

1. Lineaments are neither reliable indicators of regional geologic structure nor predictors of gas production.

2. Two lineament azimuths, 280°–310° and 20°–40°, have orientations similar to those of the cleat domains. The density of lineaments mapped in this study does not delineate geologic structures in the subsurface.

GRAND VALLEY, PARACHUTE, AND RULISON FIELD STUDIES

1. The Crystal Creek and Rulison Anticlines are Laramide structures associated with southwest-directed compression. Greater structural complexity in the Williams Fork Formation is thought to reflect splay faulting and thrust detachment in the Mancos Shale. Differential compaction may also contribute to structural complexity.

2. Net coal thicknesses range from 40 to 100 ft (12 to 30 m) and typically exceed 70 ft (21 m).

3. Channel-fill sandstones are not in pressure communication, reflecting reservoir compartmentalization and very low matrix permeability (microdaries). The average width of channel-sandstone belts is 1,500 ft (460 m).

4. A syndepositional hingeline, inferred to cross Parachute field and possibly basinwide, may be important to exploration strategy. The most productive gas wells are in Rulison field to the east. In the San Juan Basin, a hingeline is the site of prolific coal- and sandstone-gas production.

5. Cumulative Cameo production in the study area through June 1994 was 17.31 Bcf (490 MMm^3). Cameo wells typically produced less than 100 MMcf (2.8 MMm^3) of gas per year. Water production rarely exceeds 1,000 bbl (160 m^3) annually.

6. The most productive wells are on structural terraces and anticlines and may reflect fracture-enhanced permeability related to flexure or conventional structural trapping of gas.

WHITE RIVER AND PINYON RIDGE FIELD STUDIES

1. Although net coal trends are oriented favorably for meteoric recharge and secondary biogenic gas generation, northwest-trending thrust faults separate the lower coal-bearing interval in the outcrop belt from subsurface coals. Therefore, a dynamic meteoric flow regime is probably absent.

2. Williams Fork coals are predominantly high-volatile C and B bituminous and have not entered the threshold of significant thermogenic methane generation. The coals have reached the wet-gas-generating stage, suggesting that wet gases and condensate produced from coalbed methane wells are probably indigenous to the coals.

3. Carbon dioxide content, ranging between 8 and 34 percent and averaging 25 percent, was probably sourced from outside the study area and migrated up thrust faults. According to isotopic data, as much as 75 percent of the carbon dioxide in the coal gases may have been derived from the decomposition of Paleozoic carbonates, whereas 25 percent was generated during coalification.

4. Extensional fracture and/or cleat development along the crest of anticlines probably contributed to enhanced coal permeability.

5. Evidence of gas migration and of conventional trapping includes the presence of abnormally high gas content in relatively low rank coals and the isotopic composition of carbon dioxide.

PRODUCIBILITY MODEL

The Grand Valley/Rulison area lies in the Colorado River valley, a presumed regional discharge area, or no-flow boundary, oriented orthogonal to the regional flow direction. It is an area of upward flow located at the termination of regional flow paths. Coal rank is low-volatile bituminous, and significant volumes of thermogenic gas were generated for high gas contents. The area's cumulative production is modest and limited by a very low matrix permeability (microdaries). Low permeability restricts ground-water flow and, when combined with hydrocarbon overpressure, eliminates meteoric circulation. Gas is probably the pressuring fluid because wells produce little or no water. Thus, dynamic ground-water flow is precluded and, by implication from the model producibility, so is extraordinary coal-gas production. In the northern Piceance Basin, coalbed methane occurrence is consistent with the producibility model. The complex structural development of the basin locally enhanced permeability

through the formation of extensional fractures along the crests of tightly folded anticlines. Normal faults along the crest of the White River Anticline and trend of coal pinch-out are perpendicular to inferred migration pathways and are probable flow barriers, suggesting that significant volumes of gas are conventionally trapped, as they are in the San Juan Basin.

Net coal thicks are oriented northeastward for intersection with the Mesaverde outcrop belt. Annual precipitation exceeds 16 inches per year at outcrop, which is favorable for recharge and subsequent generation of secondary biogenic gases, assuming a regionally continuous aquifer. The presence of coals that have generated chemically wet gases and heavier hydrocarbons, the decrease in net coal thickness southwestward, and the presence of faults along the White River Anticline orthogonal to flow direction all indicate favorable conditions for the generation and accumulation of thermogenic and secondary biogenic gases in the northern Piceance Basin. Because the northwestward-trending Danforth Hills thrust fault isolates coals at outcrop from those basinward, the Mesaverde is a fault-severed aquifer. Therefore, the movement of meteoric water and subsequent generation of secondary biogenic gases seen in the San Juan Basin probably did not occur or were minimal in the northern Piceance Basin. If the Danforth Hills thrust fault were a blind thrust, the outcrop belt would be elevated for meteoric recharge similar to that observed in the San Juan Basin, resulting in hydrogeologic conditions favorable to exceptionally high coalbed methane production. In summary, new data from the Piceance Basin supports the model that required ground-water flow basinward from recharge through aquifer coal beds orthogonally toward regional flow barriers and conventional trapping along those barriers. Active flow implies good permeability and promotes generation of secondary biogenic gas and advective gathering and transport of gas, which contribute to fully gas-saturated coals and high productivity. The best potential for coal-gas production may lie in conventional traps basinward of where outcrop and subsurface coals are in good hydraulic communication.

FUTURE WORK

The authors are currently compiling additional geologic and hydrologic data in evaluating the coalbed methane producibility model. Future work will include access and interpretation of geophysical seismic lines, additional field study, and interpretation and description of Mesaverde Group coalbed cores. Net sandstone mapping, coal seam continuity, initial potential data, coal gas compositional variability, hydrologic data, and the distribution of gas contents will be used to enhance understanding of the hydrogeologic factors affecting coalbed methane producibility in the Piceance Basin.

To complete the lineament analysis, a statistical analysis will be undertaken to correlate lineament attributes with production data from Mesaverde Group wells. We will establish the relationship between producing wells on lineaments with those not on lineaments, therefore testing the utility of lineaments in identifying highly productive coalbed methane trends in the Mesaverde Group.

Future investigations in the Grand Valley/Rulison and Pinyon Ridge/White River area will include structural mapping of the most extensive coal beds, net sand mapping of the underlying siliciclastic interval to demonstrate possible reservoir development associated with differential compaction of coal-siliciclastic sequences, analysis of the pressure regime, and disaggregation of the production data to identify coal-gas production and controls on it.

ACKNOWLEDGMENTS

This research was funded by the Gas Research Institute under contract no. 5091-214-2261. Several operators, including Barrett Resources Corporation and OXY USA Inc., supplied data that greatly enhanced the quality of the study; these contributions are gratefully acknowledged.

The computing staff of the Bureau of Economic Geology, managed by Gerry White, provided guidance in data processing and computer-assisted mapping. Drafting was by the cartographic staff of the Bureau under the direction of Richard L. Dillon, chief cartographer. Word processing was by Susan Lloyd, design by Jamie H. Coggin, and editing by Bobby Duncan.

CONVERSION CHART

Nonmetric unit		Conversion factor		Metric unit
feet (ft)	×	0.3048	=	meters (m)
inches (inch)	×	2.540	=	centimeters (cm)
miles (mi)	×	1.609	=	kilometers (km)
feet/mile (ft/mi)	×	0.1894	=	meters/kilometer (m/km)
square miles (mi^2)	×	2.589	=	square kilometers (km^2)
cubic feet (cf)	×	0.02832	=	cubic meters (m^3)
short tons	×	0.9072	=	metric tons (t)
pounds per square inch (psi)	×	6.895	=	kilopascals (kPa)
psi/ft	×	22.62	=	(kPa/m)

References

Ammosov, I. I., and Eremin, I. V., 1960, Fracturing in coal: Moscow, IZDAT Publishers (translated from Russian), 109 p. (Available from the Office of Technical Services, Washington, D.C.)

Amuedo, C. L., and Ivey, J., 1978, Detailed geologic mapping, U.S. Bureau of Mines tract, Piceance Creek Basin, Rio Blanco County, Colorado: Report prepared for the U.S. Bureau of Mines, Denver Federal Center, under contract no. S0271034, 35 p.

Arri, L. E., Yee, Dan, Morgan, W. D., and Jeansonne, M. W., 1992, Modeling coalbed methane production with binary gas sorption: Society of Petroleum Engineers paper SPE 24363, presented at the SPE Rocky Mountain Regional Meeting, Casper, Wyoming, May 18–21, 1992.

Ayers, W. B., Jr., and Kaiser, W. R., eds., 1994, Coalbed methane in the Upper Cretaceous Fruitland Formation, San Juan Basin, New Mexico and Colorado: The University of Texas at Austin, Bureau of Economic Geology, Report of Investigations No. 218, Colorado Geologic Survey, Department of Natural Resources, Resource Series 31, and New Mexico Bureau of Mines and Mineral Resources Bulletin 146, 216 p.

Ayers, W. B., Jr., Kaiser, W. R., Laubach, S. E., Ambrose, W. A., Baumgardner, R. W., Jr., Scott, A. R., Tyler, Roger, Yeh, Joseph, Hawkins, G. J., Swartz, T. E., Schultz-Ela, D. D., Zellers, S. D., Tremain, C. M., and Whitehead, N. H., III, 1991, Geologic and hydrologic controls on the occurrence and producibility of coalbed methane, Fruitland Formation, San Juan Basin: The University of Texas at Austin, Bureau of Economic Geology, topical report prepared for the Gas Research Institute under contract no. 5087-214-1544 (GRI-91/0072), 314 p.

Baars, D. L., Bartleson, B. L., Chapin, C. E., Curtis, B. F., De Voto, R. H., Everett, J. R., Johnson, R. C., Molenaar, C. M., Peterson, F., Schenk, C. J., Love, J. D., Merin, I. S., Rose, P. R., Ryder, R. T., Waechter, N. B., and Woodward, L. A., 1988, Basins of the Rocky Mountain Region, *in* Sloss, L. L., ed., Sedimentary cover—North American Craton, U.S.: Geological Society of America, Decade of North American Geology, v. D-2, p. 109–220.

Barlow, J. A., Jr., and Haun, J. D., 1975, Structure contour map, N 1/2 Piceance Basin, Douglas Creek Arch: Barlow & Haun Inc. Geologists, Pomco Energy Map Services; scale 1:125,000.

Baumgardner, R. W., Jr., 1987, Landsat-based lineament analysis, East Texas Basin and Sabine Uplift area: The University of Texas at Austin, Bureau of Economic Geology Report of Investigations No. 167, 26 p.

Baumgardner, R. W., Jr., 1991, Comparative lineament analysis of the San Juan Basin: Relationships between lineament attributes and coalbed methane production, *in* Ayers, W. B., Jr., Kaiser, W. R., Laubach, S. E., Ambrose, W. A., Baumgardner, R. W., Jr., Scott, A. R., Tyler, R., Yeh, J. S., Hawkins, G. J., Swartz, T. E., Schultz-Ela, D. D., Zellers, S. D., Tremain, C. M., and Whitehead, N. H., III, eds., Geologic and hydrologic controls on the occurrence and producibility of coalbed methane, Fruitland Formation, San Juan Basin:

The University of Texas at Austin, Bureau of Economic Geology, topical report prepared for the Gas Research Institute under contract no. 5087-214-1544 (GRI-91/0072), p. 153–179.

Baumgardner, R. W., Jr., 1994, Use of lineament attributes to predict coalbed methane production in the northern San Juan Basin, *in* Ayers, W. B., Jr., and Kaiser, W. R., eds., Coalbed methane in the Upper Cretaceous Fruitland Formation, San Juan Basin, New Mexico and Colorado: The University of Texas at Austin, Bureau of Economic Geology, Report of Investigations No. 218, Colorado Geologic Survey, Department of Natural Resources, Resource Series 31, and New Mexico Bureau of Mines and Mineral Resources Bulletin 146, p. 119–132.

Bell, G. J., and Wiman, S. K., 1985, Second Deep Seam Project well in western Colorado tests drilling and fracturing techniques in deep seams: Gas Research Institute Quarterly Review of Methane from Coal Seams Technology, v. 3, no. 1, p. 23–34.

Berry, G. W., 1959, Divide Creek field, Garfield and Mesa Counties, Colorado, *in* Huan, J. D., and Weimer, R. J., eds., Cretaceous rocks of Colorado and adjacent areas: Rocky Mountain Association of Geologists Symposium, p. 89–91.

Boreck, D. L., and Strever, M. T., 1980, Conservation of methane from Colorado's mined/minable coal beds: a feasibility study: Colorado Geological Survey Open-File Report 80-5, 95 p.

Boreck, D. L., Jones, D. C., Murray, D. K., Schultz, J. E., and Suek, D. C., 1977, Colorado coal analyses, 1975 (analyses of 64 samples collected in 1975): Colorado Geological Survey Information Series 7, 112 p.

Bostick, N. H., and Freeman, V. L., 1984, Tests of vitrinite reflectance and paleotemperature models at the mutiwell experiment site, Piceance Creek Basin, Colorado, *in* Spencer, C. W., and Keighin, C. W., eds., Geological studies in support of the U.S. Department of Energy multiwell experiment, Garfield County, Colorado: U.S. Geological Survey Open-File Report 84-757, p. 110–120.

Branagan, P. T., Cipolla, C. L., Lee, S. J., and Yan, L., 1987, Case history of hydraulic fracture performance in the naturally fractured paludal zone: the transitory effects of damage: Society of Petroleum Engineers, SPE paper 16397, p. 61–71.

Branagan, P., Hill, R., Kukal, G., Middlebrook, M. L., and Peterson, R., 1992, Geological, petrophysical and engineering analysis of the Mancos B: Chandler & Associates, Topical Report, June 1992: Chicago, Illinois, Gas Research Institute, 56 p.

Bredehoeft, J. D., Wolff, R. G., Keys, W. S., and Shuter, Eugene, 1976, Hydraulic fracturing to determine the regional in situ stress field, Piceance Basin, Colorado: Geological Society of America Bulletin, v. 87, no. 2, p. 250–258.

Burnham, A. K., and Sweeney, J. J., 1989, A chemical kinetic model of vitrinite reflectance maturation and reflectance: Geochemica et Cosmochimica Acta, v. 53, p. 2649–2657.

CER Corporation, 1985, Summary of data acquisition and field operations, Barrett Energy Company, Grand Valley No. 2 Federal, Garfield County, Colorado: Chicago, Illinois, Gas Research Institute, 66 p.

Chapin, C. E., and Cather, S. M., 1983, Eocene tectonics and sedimentation in the Colorado Plateau—Rocky Mountain area, *in* Lowell, J. D., ed., 1983, Rocky Mountain Foreland Basins and Uplifts: Denver, Colorado, Rocky Mountain Association of Geologists, p. 33–36.

Choate, Raoul, Jurich, D., Saulnier, G. J., 1984, Geologic overview, coal deposits and potential for methane recovery from coalbeds, Piceance Basin, Colorado, *in* Rightmire, C. T., Eddy, G. E., and Kirr, J. N., eds., Coalbed methane resources of the United States: American Association of Petroleum Geologists Studies in Geology 17, p. 223–251.

Clark, J. A., 1983, The prediction of hydraulic fracture azimuth through geological, core, and analytical studies: Society of Petroleum Engineers/U.S. Department of Energy Symposium on Low Permeability Gas Reservoirs, Denver, Colorado, 1983, Proceedings 11616, p. 107–114.

Close, J. C., Pratt, T. J., Logan, T. L., and Mavor, M. J., 1993, Western cretaceous coal seam project, summary of the Conquest Oil Company South Shale Ridge #11-15 well, Piceance Basin, western Colorado: Resource Enterprises, Inc., report prepared for the Gas Research Institute under contract no. 5088-214-1657, 65 p.

Colorado Climate Center, 1984, Colorado average annual precipitation 1951–1980: Fort Collins, Colorado State University, Department of Atmospheric Science, Colorado Climate Center, scale 1:500,000.

Collins, B. A., 1970, Geology of the coal-bearing Mesaverde Formation (Cretaceous), Coal Basin area, Pitkin County, Colorado: Colorado School of Mines, Master's thesis, 116 p.

Collins, B. A., 1976, Coal deposits of the Carbondale, Grand Hogback, and Southern Danforth Hills coal fields, eastern Piceance Basin, Colorado: Quarterly of the Colorado School of Mines, v. 71, no. 1, 138 p.

DeVoto, R. H., 1980, Pennsylvanian stratigraphy and history of Colorado, *in* H. C. Kent and K. W. Porter, eds., Colorado geology: Rocky Mountain Association of Geologists, p. 71–102.

Dickinson, W. R., and Snyder, W. S., 1978, Plate tectonics of the Laramide orogeny, *in* Matthews, Vincent, III, ed., Laramide folding associated with basement block faulting in the western United States: Geological Society of America Memoir 151, p. 355–366.

Dix, O. R., and Jackson, M. P. A., 1981, Statistical analysis of lineaments and their relation to fracturing, faulting, and halokinesis in the East Texas Basin: The University of Texas at Austin, Bureau of Economic Geology Report of Investigations No. 110, 30 p.

Dula, William F., Jr., 1981, Correlation between deformation lamellae, microfractures, macrofractures, and in situ stress measurements, White River Uplift, Colorado: Geological Society of America Bulletin, pt. I, v. 92, no. 1, p. 37–46.

Dunn, H., and Irwin, D., 1977, Subsurface correlation of upper Cretaceous rocks, Sand Wash and Piceance Basins, *in* Irwin, D. (chairman), Subsurface cross sections of Colorado: Rocky Mountain Association of Geologists Special Publication No. 2, plate 15.

Epis, R. C., and Chapin, C. E., 1975, Geomorphic and tectonic implications of the post-Laramide, late Eocene erosion surface in the southern Rocky Mountains, *in* Curtis, B. F., ed., Cenozoic history of the southern Rocky Mountains: Geological Society of America, Memoir 144, p. 45–74.

Fender, H. B., and Murray, D. K., 1978, Data accumulation on the methane potential of the coal beds of Colorado: Colorado Geological Survey Open-File Report 78-2, 25 p.

Finley, R. J., 1984, Geology and engineering characteristics of selected low-permeability gas sandstones: a national survey: The University of Texas at Austin, Bureau of Economic Geology Report of Investigations No. 138, 220 p.

Finley, R. J., 1985, Reservoir properties and gas productivity of the Corcoran and Cozzette tight sandstones, Colorado: Society of Petroleum Engineers, Society of Petroleum Engineers/Department of Energy paper 13852, p. 33–39.

Finley, R. J., and Ladwig, L. R., 1985, Depositional systems of a tight gas-productive barrier-strandplain sequence: Corcoran and Cozzette Sandstones, northwest Colorado (abs.): American Association of Petroleum Geologists Bulletin, v. 69, no. 2, p. 255.

Finley, R. J., Garrett, C. M., Han, J. H., Lin, Z.-S., Seni, S. J., Saucier, A. E., and Tyler, Noel, 1983, Geologic analysis of primary and secondary tight gas sand objectives: The University of Texas at Austin, Bureau of Economic Geology, annual report prepared for the Gas Research Institute under contract no. 5082-211-0708, 334 p.

Finley, S. J., and Lorenz, J. C., 1988, Characterization of natural fractures in Mesaverde core from the Multiwell experiment: Sandia National Laboratories, A report for the U.S. Department of Energy, under contract no. DE-AC04-76DP00789, SAND88-1800•UC-92, 90 p.

Fouch, T. D., Lawton, T. F., Nichols, D. J., Cashion, W. B., and Cobban, W. A., 1983, Patterns and timing of synorogenic sedimentation in Upper Cretaceous rocks of central and northeast Utah, in Reynolds, M. W., and Dolly, E. D., eds., Mesozoic paleogeography of the west-central United States: Rocky Mountain Section, Society of Paleontologists and Mineralogists, Rocky Mountain Paleogeography Symposium 2, p. 305–336.

Galloway, W. E., 1989, Genetic stratigraphic sequences in basin analysis I: architecture and genesis of flooding-surface bounded depositional units: American Association of Petroleum Geologists, v. 73, no. 2, p. 125–142.

Geological Services of Tulsa, Inc., 1980, Geologic framework and potential structural control of methane in coalbeds of southeastern Piceance Creek Basin, Colorado: U.S. Department of Energy contracted report, 34 p., 8 sheets.

Gualtieri, J. L., 1979, Preliminary results of coal exploratory drilling in the Book Cliffs Coal Region, Garfield County, Colorado and Grand County, Utah: U.S. Geological Survey Open-File Report 79–999, 53 p.

Gill, J. R., and Cobban, W. A., 1969, Paleogeographic maps, Western Interior: U.S. Geological Survey Open File Report, 6 sheets.

Gill, J. R., and Cobban, W. A., 1966, Regional unconformity in Late Cretaceous, Wyoming: U.S. Geological Survey Professional Paper 550-B, p. B20–B27.

Gill, J. R., and Hail, W. J., 1975, Stratigraphic sections across Upper Cretaceous Mancos Shale-Mesaverde Group boundary, eastern Utah and western Colorado: U.S. Geological Survey Oil and Gas Investigation Chart OC-68.

Gries, R. R., 1983, North-south compression of Rocky Mountain foreland structures, *in* Lowell, J. D., ed., Rocky Mountain foreland basins and uplifts: Rocky Mountain Association of Geologists, p. 9–32.

Grout, M. A., 1991, Coal cleats in the southern Piceance Basin, Colorado: correlation with regional and local fracture sets in associated clastic rocks, *in* Schwochow, S. D., ed., Coalbed methane of western North America: U.S. Geological Survey, Rocky Mountain Association of Geologists Guidebook, p. 35–38.

Grout, M. A., Abrams, G. A., Tang, R. L., Hainsworth, T. J., and Verbeek, E. R., 1991, Late Laramide thrust-related and evaporite-domed anticlines in the southern Piceance Basin, northeastern Colorado: American Association of Petroleum Geologists Bulletin, v. 75, no. 2, p. 205–218.

Grout, M. A., and Verbeek, E. R., 1983, Field studies of joints—insufficiencies and solutions, with examples from the Piceance Creek Basin, Colorado, *in* Gary, J. H., ed., Proceedings of the 16th Oil Shale Symposium: Colorado School of Mines, p. 68–80.

Grout, M. A., and Verbeek, E. R., 1985, Fracture history of the Plateau Creek and adjacent Colorado River Valleys, southern Piceance Basin—implications for predicting joint patterns at depth: U.S. Geological Survey Open-File Report 85-744, 17 p.

Grout, M. A., and Verbeek, E. R., 1987, Regional joint sets unrelated to major folds—example from the Piceance Basin, northeastern Colorado Plateau: Geological Society of America Abstracts with Programs, v. 19, no. 5, p. 279.

Grout, M. A., and Verbeek, E. R., 1992, Fracture history of the Divide Creek and Wolf Creek anticlines and its relation to Laramide basin-margin tectonism, southern Piceance Basin, northwestern Colorado: U.S. Geological Survey Bulletin 1787-Z, 32 p.

Gunneson, B. G., Wilson, M. S., and Labo, Jim, 1994, A structural history of Divide Creek Anticline, Piceance Basin, northwest Colorado: 1994 American Association of Petroleum Geologists Annual Convention, Official Program, v. 3, p. 160.

Gunter, C. E., 1962, Oil and gas potential of Upper Cretaceous sediments, southern Piceance Creek Basin, *in* Bolyard, D. W., ed., Deep drilling frontiers in the central Rocky Mountains: Rocky Mountain Association of Geologists, p. 114–118.

Hail, W. J., Jr., 1974, Geologic map of the Rough Gulch quadrangle, Rio Blanco and Moffat Counties, Colorado: U.S. Geological Survey Geologic Quadrangle Map GQ-1195, scale 1:24,000.

Hail, W. J., Jr., and Smith, M. C., 1994, Geologic map of the northern part of the northern Piceance Creek Basin, northwestern Colorado: U.S. Geological Survey, Miscellaneous Investigations Series Map 1-2400; scale, 1:100,000.

Hamilton, D. S., 1993, Stratigraphy and coal occurrence of the Upper Cretaceous Mesaverde Group, Sand Wash Basin, *in* Kaiser, W. R., Scott, A. R., Hamilton, D. S., Tyler, Roger, McMurry, R. G., Zhou, Naijiang, and Tremain, C. M., 1993, Geologic and hydrologic controls on coalbed methane: Sand Wash Basin, Colorado and Wyoming: The University of Texas at Austin, Bureau of Economic Geology, annual report prepared for the Gas Research Institute under contract number 5091-214-2261, p. 23–49.

Hamilton, D. S., 1994, Stratigraphy and coal occurrence of the Upper Cretaceous Mesaverde Group, Sand Wash Basin, *in* Kaiser, W. R., Scott, A. R., Hamilton, D. S., Tyler, Roger, McMurry, R. G., Zhou, Naijiang, and Tremain, C. M., 1994, Geologic and hydrologic controls on coalbed methane: Sand Wash Basin, Colorado and Wyoming: The University of Texas at Austin, Bureau of Economic Geology Report of Investigations No. 220, and Colorado Geologic Survey, Department of Natural Resources, Resource Series 30, p. 23–49.

Hancock, E. T., 1925, Geology and coal resources of the Axial and Monument Butte quadrangles, Moffat County, Colorado: U.S. Geological Survey Bulletin 757, 134 p.

Hancock, P. L., 1985, Brittle microtectonics: principles and practice: Journal of Structural Geology, v. 7, no. 3/4, p. 437–459.

Hancock, P. L., and Bevan, T. G., 1987, Brittle modes of foreland extension, *in* Coward, M. P., Dewey, J. F., and Hancock, P. L., eds., Continental extensional tectonics: Geological Society of London Special Publications No. 28, p. 127–138.

Heaton, R. L., 1929, White River Dome: American Association of Petroleum Geologists Structure of Typical American Oil Fields, v. II, p. 111–112.

Henkle, W. R., Jr., Muhm, J. R., and DeBuly, H. F., 1978, Cleat orientation in some subbituminous coals of the Powder River and Hanna Basins, Wyoming, *in* Hodgson, H. E., ed., 1978, Proceedings of the Second Symposium on the Geology of Rocky Mountain Coal—1977: Colorado Geological Survey Resource Series 4, p. 129–141.

Hobbs, R. G., Gualtieri, J. L., and Babcock, R. N., 1982, Carbonera coal geophysical logging research hole core descriptions and coal analysis: U.S. Geological Survey Open-File Report 82-827, 46 p.

Holmes, W. H., 1877, Report on the San Juan district, *in* 9th Annual Report, U.S. Geological and Geographical Survey of Territories, p. 237–276.

Horn, G. H., and Gere, W. C., 1959, Geology of the Rifle Gap coal district, Garfield County, Colorado: U.S. Geological Survey Open-File Report 59-63.

Hucka, Brigitte, Sommer, S. N., and Keith, A. C., 1990, Cleat and joint system evaluation and coal characterization of the B-bed coal Dutch Creek Mine, Pitkin County, Colorado: Utah Geological and Mineral Survey Open-File Report 171, 31 p.

Irwin, Hilary, Curtis, C. D., and Coleman, M., 1977, Isotopic evidence for source of diagenetic carbonates formed during burial of organic-rich sediments: Nature, v. 269, p. 209–213.

James, T. A., and Burns, B. J., 1984, Microbial alteration of subsurface natural gas accumulations: American Association of Petroleum Geologists Bulletin, v. 68, p. 957–960.

Jamison, W. R., and Stearns, D. W., 1982, Tectonic deformation of Wingate Sandstone, Colorado National Monument: American Association of Petroleum Geologists Bulletin, v. 66, no. 12, p. 2584–2608.

Jeu, S. J., Logan, T. L., Decker, A. D., and Counsil, J., 1988, Development and evaluation of the technology for methane production from a deep coal seam in the Piceance Basin: Resource Enterprises, Inc., final report prepared for the Gas Research Institute under contract no. 5083-214-0844, 35 p.

Johnson, R. C., 1985, Early Cenozoic history of the Uinta and Piceance Creek Basins, Utah and Colorado, with special reference to the development of Eocene Lake Uinta, *in* Flores, R. M., and Kaplin, S. S., eds., Cenozoic paleogeography of the west-central United States: Rocky Mountain Section, Society of Economic Paleontologists and Mineralogists, Rocky Mountain Paleogeography Symposium 3, p. 247–276.

Johnson, R. C., 1986, Structure contour map of the top of the Castlegate sandstones, eastern part of the Uinta Basin and western part of the Piceance Creek Basin, Utah and Colorado: U.S. Geological Survey Miscellaneous Field Studies Map Series MF-1826, scale 1:233,440.

Johnson, R. C., 1987, Geologic history and hydrocarbon potential of Late Cretaceous-age, low-permeability reservoirs, Piceance Basin, western Colorado: U.S. Geological Survey, final report prepared for the U.S. Department of Energy, Office of Fossil Energy, under contract no. DE-AC21-83MC20422, 97 p.

Johnson, R. C., 1989, Geologic history and hydrocarbon potential of Late Cretaceous-age, low-permeability reservoirs, Piceance Basin, western Colorado: U.S. Geological Survey Bulletin 1787-E, 51 p.

Johnson, R. C., Crovelli, R. A., Spencer, C. W., and Mast, R. F., 1987, An assessment of gas resources in low permeability sandstones of the Upper Cretaceous Mesaverde group, Piceance Basin, Colorado: U.S. Geological Survey Open-File Report 87-357, unpaginated.

Johnson, R. C., and Finn, T. M., 1986, Cretaceous through Holocene history of the Douglas Creek arch, Colorado and Utah, *in* Stone, D. S., ed., New interpretations of northwest Colorado geology: Rocky Mountain Association of Geologists, p. 77–95.

Johnson, R. C., and Keighin, C. W., 1981, Creataceous and Tertiary history and resources of the Piceance Creek Basin, western Colorado: New Mexico Geological Society Field Conference, 32nd, Western Slope, Colorado, 1981, Guidebook, p. 199–210.

Johnson, R. C., and Nuccio, V. F., 1983, Structural and thermal history of the Piceance Creek Basin, western Colorado, in relation to hydrocarbon occurrence in the Mesaverde Group: American Association of Petroleum Geologists Bulletin, v. 67, no. 3, p. 490–491.

Johnson, R. C., and Nuccio, V. F., 1986, Structural and thermal history of the Piceance Creek Basin, western Colorado, in relation to hydrocarbon occurrence in the Mesaverde Group, *in* Spencer, C. W., and Mast, R. F., eds., Geology of tight gas reservoirs: American Association of Petroleum Geologists Studies in Geology 24, p. 165–205.

Johnson, R. C., and Rice, D. D., 1990, Occurrence and geochemistry of natural gases, Piceance Basin, northwest Colorado: American Association of Petroleum Geologists Bulletin, v. 74, no. 6, p. 805–829.

Johnson, V. H., 1948, Geology of the Paonia [sic] coal field, Delta and Gunnison Counties, Colorado: U.S. Geological Survey coal inventory map.

Johnston, D. J., and Scholes, P. L., 1991, Predicting cleats in coal seams from mineral and maceral composition with wireline logs, *in* Schwochow, S. D., Murray, D. K., and Fahy, M. F., eds., 1991, Coalbed methane of western North America: Guidebook for the Rocky Mountain Association of Geologists Fall Conference and Field Trip, September 17–20, 1991, Glenwood Springs, Colorado: Denver, Colorado, Rocky Mountain Association of Geologists, p. 123–136.

Kaiser, W. R., 1994, Development and evaluation of a basin-scale coalbed methane producibility model: In Focus—Tight Gas Sands, v. 10, no. 1, p. 47–52.

Kaiser, W. R., Hamilton, D. S., Scott, A. R., and Tyler, Roger, 1994a, Geological and hydrological controls on the producibility of coalbed methane: Journal of the Geological Society of London, v. 151, p. 417–420.

Kaiser, W. R., Scott, A. R., Hamilton, D. S., Tyler, Roger, McMurry, R. G., Zhou, Naijiang, and Tremain, C. M., 1993, Geologic and hydrologic controls on coalbed methane: Sand Wash Basin, Colorado and Wyoming: The University of Texas at Austin, Bureau of Economic Geology, topical report prepared for the Gas Research Institute under contract no. 5091-214-2261 (GRI-92/0420), 151 p.

Kaiser, W. R., Scott, A. R., Hamilton, D. S., Tyler, Roger, McMurry, R. G., Zhou, Naijiang, and Tremain, C. M., 1994b, Geologic and hydrologic controls on coalbed methane: Sand Wash Basin, Colorado and Wyoming: The University of Texas at Austin, Bureau of Economic Geology Report of Investigations No. 220, and Colorado Geologic Survey, Department of Natural Resources, Resource Series 30, 151 p.

Kauffman, E. G., 1977, Geological and biological overview—Western Interior Cretaceous basin, *in* Kauffman, E. G., ed., Cretaceous facies, faunas, and paleoenvironments across the Western Interior basin: The Mountain Geologist, v. 6, p. 227–245.

Kelley, V. C., and Clinton, N. J., 1960, Fracture systems and tectonic elements of the Colorado Plateau: University of New Mexico Publications in Geology, no. 6, 104 p.

Kent, B. H., and Arndt, H. H., 1980, Geology of the Carbondale coal mining area, Garfield and Pitkin Counties, Colorado, as related to subsurface hydraulic mining potential: U.S. Geological Survey Open-File Report 80-709, 94 p.

Khalsa, N. S., and Ladwig, L. R., 1981, Colorado coal analyses 1976–1979: Colorado Geological Survey Information Series 10, 364 p.

Killops, S. D., Woolhouse, A. D., Weston, R. J., and Cook, R. A., 1994, A geochemical appraisal of oil generation in the Taranaki Basin, New Zealand: American Association of Petroleum Geologists Bulletin, v. 78, p. 1560–1585.

Kukal, G. C., Price, E. H., Hill, R. E., and Monson, E. R., 1992, Results of field verification tests in the tight Mesaverde Group: Piceance Basin, Colorado: CER Corporation: U.S. Department of Energy, DOE/MC/24120-312 (DE93000201),153 p.

Larsen, E. E., Ozima, M., and Bradley, W. D., 1975, Late Cenozoic basic volcanism in northwestern Colorado and its implications concerning tectonism and the origin of the Colorado River system: Geological Society of America Memoir 144, p. 155–178.

Laubach, S. E., and Tremain, C. M., 1994, Fracture swarms: potential targets for methane exploration in Upper Cretaceous sandstone and coal, northern San Juan Basin, Colorado, *in* Ayers, W. B., Jr., and Kaiser, W. R., eds., Coalbed methane in the Upper Cretaceous Fruitland Formation, San Juan Basin, New Mexico and Colorado: The University of Texas at Austin, Bureau of Economic Geology, Report of Investigations No. 218, Colorado Geological Survey, Department of Natural Resources, Resource Series 31, and New Mexico Bureau of Mines and Mineral Resources Bulletin 146, p. 103–118.

Laubach, S. E., Tyler, Roger, Ambrose, W. A., and Tremain, C. M., 1992a, Preliminary map of fracture patterns in coal in the western United States, *in* Fractured and jointed rock masses, June 3–5: International Society for Rock Mechanics, prepared for the U.S. Department of Energy under contract no. DE-AC03-76SF00098, v. 1, p. 183–190.

Laubach, S. E., Tyler, Roger, Ambrose, W. A., Tremain, C. M., and Grout, M. A., 1992b, Preliminary map of fracture patterns in coal in the western United States, *in* Mullen, C. E., ed., Rediscover the Rockies: Wyoming Geological Association Forty-Third Field Conference Guidebook, p. 253–267.

Law, B. E., 1993, The relationship between coal rank and cleat spacing: implications for the prediction of permeability in coal, *in* Proceedings, the 1993 International Coalbed Methane Symposium, May 17–21, 1993, Birmingham, Alabama, p. 435–441.

Law, B. E., and Johnson, R. C., 1989, Structural and stratigraphic framework of the Pinedale Anticline area, Wyoming, and at the Multiwell Experiment site, Colorado, *in* Law, B. E., and Spencer, C. W., eds., Geology of tight gas reservoirs in the Pinedale Anticline area, Wyoming, and at the Multiwell Experiment site, Colorado: U.S. Geological Survey Bulletin 1886, p. B1–B11.

Lee, W. T., 1909, The Grand Mesa coal field, Colorado: U.S. Geological Survey Bulletin 341, pt. 2, p. 316–334.

Lee, W. T., 1912, Coal fields of Grand Mesa and the West Elk Mountains, Colorado: U.S. Geological Survey Bulletin 510, 237 p.

Levine, J. R., 1993, Coalification: the evolution of coal as source rock and reservoir rock for oil and gas, *in* Law, B. E., and Rice, D. D., eds., Hydrocarbons from coal: American Association of Petroleum Geologists Studies in Geology, Series No. 38, Chapter 3, p. 39–77.

Lin, W., and Heuze, F. E., 1987, Comparison of in situ dynamic moduli and laboratory moduli of Mesaverde rocks: International Journal of Rock Mechanics and Mining Sciences, v. 24, no. 4, p. 257–263.

Logan, T. L., Seccombe, J. C., and Jones, A. H., 1986, Hydraulic fracture stimulation and openhole testing of a deeply buried coal seam in the Piceance Basin, Colorado: Unconventional Gas Technology Symposium of the Society of Petroleum Engineers, Louisville, Kentucky, May 18–21, 1986, SPE paper 15251, p. 501–512.

Lorenz, J. C., 1983a, Lateral variability in the Corcoran and Cozzette blanket sandstones and associated Mesaverde rocks, Piceance Creek Basin, northwestern Colorado: Society of Petroleum Engineers, SPE/DOE paper 11608, p. 81–86.

Lorenz, J. C., 1983b, Reservoir sedimentology in Mesaverde rocks at the multi-well experiment site: Sandia National Laboratories report SAND83-1078, 38 p.

Lorenz, J. C., 1985, Tectonic and stress histories of the Piceance Creek Basin and the MWX site, from 75 m.y.a. to the present: Sandia National Laboratories report SAND84-2603, UC-92, 48 p.

Lorenz, J. C., 1989, Reservoir sedimentology of rocks of the Mesaverde Group, multiwell experiment site and east-central Piceance Basin, northwest Colorado, *in* Law, B. E., and Spencer, C. W., eds., Geology of tight gas reservoirs in the Pinedale Anticline area, Wyoming, and at the multiwell experiment site, Colorado: U.S. Geological Survey Bulletin 1886, p. K1–K24.

Lorenz, J. C., 1991, Subsurface fracture spacing: comparison of influences from slant/horizontal core and vertical core in Mesaverde reservoirs: Rocky Mountain Region, Society of Petroleum Engineers, Proceedings, Low Permeability Reservoirs Symposium and Exhibition, p. 705–716.

Lorenz, J. C., and Finley, S. J., 1987a, Differences in fracture characteristics and related production of natural gas in different zones of the Mesaverde Formation, northwestern Colorado: Society of Petroleum Engineers, SPE paper 16809, p. 589–596.

Lorenz, J. C., and Finley, S. J., 1987b, Significance of drilling and coring-induced fractures of Mesaverde core, northwestern Colorado: Sandia National Laboratories report SAND 87-1111, 29 p.

Lorenz, J. C., and Finley, S. J., 1991, Regional fractures II: fracturing of Mesaverde reservoirs in the Piceance Basin, Colorado: The American Association of Petroleum Geologists Bulletin, v. 75, no. 11, p. 1738–1757.

Lorenz, J. C., Heinze, D. M., Clark, J. A., and Searles, C. A., 1985, Determination of widths of meander belt sandstone reservoirs from vertical down-hole data, Mesaverde Group, Piceance Creek basin, Colorado: American Association of Petroleum Geologists Bulletin, v. 69, p. 710–721.

Lorenz, J. C., and Hill, R. E., 1991, Subsurface fracture spacing: comparison of inferences from slant/horizontal core and vertical core in Mesaverde reservoirs: SPE 21877, p. 705–716.

Lorenz, J. C., and Hill, R. E., 1994, Subsurface fracture spacing: comparison of inferences from slant/horizontal and vertical cores: SPE Formation Evaluation, March 1994, p. 66–72.

Lorenz, J. C., Branagan, P., Warpinski, N. R., and Sattler, A. R., 1986, Fracture characteristics and reservoir behavior of stress-sensitive fracture systems in flat-lying lenticular formations: Society of Petroleum Engineers, SPE paper 15244, p. 423–436.

Lorenz, J. C., and Laubach, S E., 1994, Description and interpretation of natural fracture patterns in sandstones of the Frontier Formation along the Hogsback, southwestern Wyoming: Gas Research Institute topical report GRI-94/0020, 89 p.

Lorenz, J. C., and Rutledge, A. K., 1985, Facies relationships and reservoir potential of Ohio Creek interval across Piceance Creek Basin, northwest Colorado: Albuquerque, New Mexico, Sandia National Laboratories Report SAND-84-2610. 52p.

Lorenz, J. C., Warpinski, N. R., and Teufel, L. W., 1993, Rationale for finding and exploiting fractured reservoirs, based on the MWX/SHCT–Piceance Basin experience: Sandia National Laboratories Report SAND93-1342/UC-132, U.S. Department of Energy: National Technical Information Service, U.S. Department of Commerce, 147 p.

Madden, D. J., 1985, Description and origin of the lower part of the Mesaverde Group in Rifle Gap, Garfield County, Colorado: Mountain Geologist, v. 22, no. 3, p. 128–138.

Mann, R. L., 1993, Slant hole completion test, final report: CER Corporation: U.S. Department of Energy, 87 p.

McFall, K. S., Wicks, D. E., Kuuskraa, V. A., and Sedwick, K. B., 1986, A geologic assessment of natural gas from coal seams in the Piceance Basin, Colorado: ICF Resources–Lewin and Associates and Colorado Geological Survey, topical report prepared for the Gas Research Institute under contract no. 5084-214-1066, 75 p.

McLellan, R. R., 1965, Description of geology and results of work accomplished to date at the Bear coal mine, Gunnison County, Colorado: unpublished memorandum to Bryan C. Parks, Pittsburgh Mining Research Center, November 4, 1965, 8 p.

Moore, B. J., and Sigler, Stella, 1987, Analysis of natural gases, 1917–85: Bureau of Mines Information Circular 9129, 1,197 p.

Murray, D. K., Fender, H. B., and Jones, D. C., 1977, Coal and methane gas in the southeastern part of the Piceance Creek Basin, Colorado, *in* Veal, H. K., ed., Exploration frontiers of the central and southern Rockies, Rocky Mountain Association of Geologists Symposium, p. 379–405.

Murray, F. N., 1967, Jointing in sedimentary rocks along the Grand Hogback monocline, Colorado: Journal of Geology, v. 75, no. 3, 340–350.

Myal, F. R., Price, E. H., Hill, R. E., Kukal, G. C., Abadie, P. A., Riecken, C. C., 1989, Geologic and production characteristics of the tight Mesaverde Group: Piceance Basin, Colorado: CER Corporation: U.S. Department of Energy, DOE/MC/24102-2769 (DE90000415), 126 p.

Newman, K. R., 1961, Micropaleontology and stratigraphy of Late Cretaceous and Paleocene Formations, northwest Colorado, Ph.D. dissertation, University of Colorado.

Newman, K. R., 1964, Palynologic correlations of Late Cretaceous and Paleocene Formations, northwestern Colorado, *in* Cross, A. T., ed., Palynology in oil exploration: Society of Economic Paleontologists and Mineralogists Special Publications 11, p. 169–180.

Newman, K. R., 1965, Mancos to Wasatch measured section in the Meeker–Rio Blanco area, northwestern Colorado: Mountain Geologist, v. 2, no. 3, p. 135–139.

Nowak, H. C., 1990, Stratigraphy of the coal-bearing part of the Mesaverde Formation, and application to coal bed methane exploration, southeast Piceance Creek Basin, Colorado: Master's thesis, The Colorado School of Mines, 124 p.

Nowak, H. C., 1991, Depositional environments and stratigraphy of Mesaverde Formation, southeastern Piceance Basin, Colorado–implications for coalbed methane exploration, *in* Schwochow, S. D., ed., Coalbed methane of Western North America: Rocky Mountain Association of Geologists, p. 1–20.

Nuccio, V. F., and Johnson, R. C., 1981, Map showing drill stem test and perforation recoveries of the Upper Cretaceous Mesaverde Group, Piceance Creek Basin, Colorado: U.S. Geological Society Miscellaneous Field Studies Map MF-1359, scale 1:250,000.

Nuccio, V. F., and Johnson, R. C., 1983, Preliminary thermal maturity map of the Cameo-Fairfield or equivalent coal zone in the Piceance Creek Basin, Colorado: U.S. Geological Survey Miscellaneous Investigations Series Map MF-1575, scale 1:253,440.

Oldham, D. W., 1994, Shallow gas production from sandstone reservoirs of the Fort Union Formation, Powder River Basin, Wyoming, *in* Sonnenberg, S. A., compiler, Natural gas in the western United States, First Biennial Conference, Extended Abstracts: Rocky Mountain Association of Geologists and Colorado Oil and Gas Association, 4 p.

Payne, J. B., and Scott, A. J., 1982, Late Cretaceous anastomosing fluvial systems, northwestern Colorado (abs.): American Association of Petroleum Geologists Bulletin, v. 66, no. 5, p. 616.

Petroleum Information, 1994, Rocky Mountain Coalbed Methane Report, November 1994, v. 5, no. 11, variously paginated.

Pipiringos, G. N., and Rosenlund, G. C., 1977, Preliminary geological map of the White Rock Quadrangle, Rio Blanco and Moffat Counties, Colorado: U.S. Geological Survey Miscellaneous Field Studies Map MF-837, scale 1:24,000

Pollard, D. D., and Aydin, A., 1988, Progress in understanding jointing over the past century: Geological Society of America Bulletin, v. 100, no. 8, p. 1181–1204.

Quigley, M. D., 1965, Geologic history of Piceance Creek–Eagle Basins: American Association of Petroleum Geologists Bulletin, v. 49, no. 11, p. 1974–1996.

Raleigh, C. B., Healy, J. H., and Bredehoeft, J. D., 1972, Faulting and crustal stress at Rangely, Colorado: American Geophysical Union Geophysical Monograph 16, p. 175–284.

Reheis, M. J., 1978, Drilling during 1978 in the Danforth Hills Coal Field, Easton Gulch, Devils Hole Gulch, Axial, and Ninemile Gap Quadrangles, Moffat and Rio Blanco Counties, Colorado: U.S. Geological Survey Open-File Report 78-1031, 38 p.

Reinecke, K. M., Rice, D. D., and Johnson, R. C., 1991, Characteristics and development of fluvial sandstone and coalbed reservoirs of Upper Cretaceous Mesaverde Group, Grand Valley field, Colorado, *in* Schwochow, S. D., Murray, D. K., and Fahy, M. F., eds., Coalbed methane of Western North America: Rocky Mountain Association of Geologists, p. 209–225.

Rice, D. D., 1993, Composition and origins of coalbed gas, *in* Law, B. E., and Rice, D. D., eds., Hydrocarbons from coal: American Association of Petroleum Geologists Studies in Geology No. 38, p. 159–184.

Richard, J. J., 1986, Interpretation of a seismic section across the Danforth Hills Anticline (Maudlin Gulch) and Axial Arch in northwest Colorado, *in* Stone, D. S., and Johnson, K. S., eds., New Interpretations of northwest Colorado Geology: Rocky Mountain Association of Geologists, p. 191–193.

Richardson, G. B., 1909, Reconnaissance of the Book Cliffs Coal Field between Grand River, Colorado and Sunnyside, Utah: U.S. Geological Survey Bulletin 371, 54 p.

Rocky Mountain Association of Geologists, 1961, White River Dome field: Oil & Gas Field Volume, Colorado–Nebraska, 1961, p. 257–258.

Rocky Mountain Association of Geologists, Research Committee, 1977, Subsurface cross sections of Colorado: Rocky Mountain Association of Geologists Special Publication 2, 39 p.

Russell, N. J., 1990, The vitrinite reflectance reflectivity and thermal maturation of coal, *in* Peterson, Lincoln, ed., Methane drainage from coal: Commonwealth Scientific and Industrial Research Organization, Australia, p. 19–26.

Sakata, S., 1991, Carbon isotope geochemistry of natural gases from the Green Tuff Basin, Japan: Geochemica et Cosmochimica Acta, v. 55, p. 1395–1405.

Sandia National Laboratories, and CER Corp., 1987, Multiwell experiment final report: I. The marine interval of the Mesaverde Formation: A report for the U.S. Department of Energy, under contract no. DE-AC04-76DP00789, SAND87-0327•UC92a.

Sandia National Laboratories, and CER Corp., 1988, Multiwell experiment report: II. The paludal interval of the Mesaverde Formation: A report for the U.S. Department of Energy, under contract no. DE-AC04-76DP00789, SAND88-1008•UC-92.

Sandia National Laboratories, and CER Corp., 1989, Multiwell experiment report: III. The coastal interval of the Mesaverde Formation: A report for the U.S. Department of Energy, under contract no. DE-AC04-76DP00789, SAND88-3284•UC-92.

Sandia National Laboratories, and CER Corp., 1990, Multiwell experiment final report: IV. The fluvial interval of the Mesaverde Formation: A report for the U.S. Department of Energy, under contract no. DE-AC04-76DP00789, SAND89-2612/A•UC-132.

Scott, A. R., 1993, Composition and origin of coalbed gases from selected basins in the United States, *in* Thompson, D. A., ed., Proceedings from the 1993 International Coalbed Methane Symposium, Birmingham, Alabama, May 17–24: Paper 9370, v. 1, p. 207–222.

Scott, A. R., 1994, Coal rank, gas content, and composition and origin of coalbed gases, Mesaverde Group, Sand Wash Basin, Colorado and Wyoming, *in* Kaiser, W. R., Scott, A. R., Hamilton, D. S., Tyler, Roger, McMurry, R. G., Zhou, Naijiang, and Tremain, C. M., 1994, Geologic and hydrologic controls on coalbed methane: Sand Wash Basin, Colorado and Wyoming: The University of Texas at Austin, Bureau of Economic Geology Report of Investigations No. 220, and Colorado Geologic Survey, Department of Natural Resources, Resource Series 30, p. 51–62

Scott, A. R., and Ambrose, W. A., 1992, Thermal maturity and coalbed methane potential of the Greater Green River, Piceance, Powder River, and Raton Basins (abs.), *in* Calgary: American Association of Petroleum Geologists 1992 annual convention official program: American Association of Petroleum Geologists, p. 116.

Scott, A. R., and Kaiser, W. R., 1991, Relation between basin hydrology and Fruitland gas composition, San Juan Basin, Colorado and New Mexico: Quarterly Review of Methane from Coal Seams Technology, v. 9, no. 1, p. 10–18.

Scott, A. R., Kaiser, W. R., and Ayers, W. B., Jr., 1994, Thermogenic and secondary biogenic gases, San Juan basin, Colorado and New Mexico–implications for coalbed gas producibility: American Association of Petroleum Geologists Bulletin, v. 78, no. 8, p. 1186–1209.

Seccembe, J. C., Schwoebel, J. J., Logan, T. L., Decker, A. D., and Cooper, J. D., 1986, Development and evaluation of technology for methane production, from a deep coal

seam in the Piceance Basin: Resource Enterprises, annual report prepared for Gas Research Institute, 101 p.

Siegel, Sidney, 1956, Nonparametric statistics of the behavioral sciences: New York, McGraw-Hill, 312 p.

Siepman, B. R., 1985, Stratigraphy and petroleum potential of Trout Creek and Twentymile Sandstones (Upper Cretaceous), Sand Wash Basin, Colorado: Colorado School of Mines Quarterly, v. 80, no. 2, 59 p.

Smith, R. S., 1980, A regional study of joints in the northern Piceance Basin, northwestern Colorado: Colorado School of Mines, Master's thesis, 126 p.

Smith, R. S., and Whitney, J. W., 1979, Map of joint sets and airphoto lineaments of the Piceance Creek Basin, northwestern Colorado: U.S. Geological Survey Miscellaneous Field Studies Map MF-1128, scale 1:100,000.

Spieker, E. M., 1949, Sedimentary facies and associated diastrophism in the Upper Cretaceous of central and eastern Utah: Geological Society of America Memoir 39, p. 55–81.

Stone, D. S., 1975, A dynamic analysis of subsurface structure in northwestern Colorado, *in* Bolyard, D. W., ed., Deep drilling frontiers in the central Rocky Mountains: Rocky Mountain Association of Geologists, p. 33–40.

Stone, D. S., 1986, Seismic and borehole evidence for important pre-Laramide faulting along the Axial Arch in northwest Colorado, *in* Stone, D. S., ed., New interpretations of northwest Colorado geology, p. 19–36.

Stone, D. S., 1977, Tectonic history of the Uncompahgre Uplift, *in* Veal, H. K., ed., Exploration frontiers of the central and southern Rockies: Rocky Mountain Association of Geologists, p. 23–30.

Tang, Y., Jenden, P. D., and Teerman, S. C., 1991, Thermogenic methane formation in low-rank coals—published models and results from laboratory pyrolysis of lignite, *in* Manning, D. A. C., ed., Organic geochemistry—advances and applications in the natural environment: Manchester, Manchester University Press, p. 329–331.

Ting, F. T. C., 1977, Origin and spacing of cleats in coal beds: Journal of Pressure Vessel Technology (Transactions of the ASME), November 1977, p. 624–626.

Towse, D. F., and Heuze, F. E., 1983, Estimating in situ stresses and rockmass properties from geological and geophysical data: applications in the hydraulic fracturing of tight gas reservoirs: Lawrence Livermore National Laboratory, report UCRL-53443, 33 p.

Tremain, C. M., 1982, Coal bed methane potential of the Piceance Basin, Colorado: Colorado Geological Survey Open-File Report 82-1, 49 p., 5 sheets.

Tremain, C.M., 1989, Fracture occurrence in tight Mesaverde sandstones, Piceance Basin, Colorado: Colorado Geological Survey unpublished report, 25 p.

Tremain, C. M., Laubach, S. E., and Whitehead, N. H., III, 1991a, Coal fracture (cleat) patterns in Upper Cretaceous Fruitland Formation, San Juan Basin, Colorado and New Mexico: implications for coalbed methane exploration and development, *in* Ayers, W. B., Jr., Kaiser, W. R., Laubach, S. E., Ambrose, W. A., Baumgardner, R. W., Jr., Scott, A. R., Tyler, Roger, Yeh, J. S., Hawkins, G. J., Swartz, T. E., Schultz-Ela, D. D., Zellers, S. D., Tremain, C. M., and Whitehead, N. H., III, eds., Geologic and hydrologic controls on the occurrence and producibility of coalbed methane, Fruitland Formation, San Juan Basin: The University of Texas at Austin, Bureau of Economic Geology, topical report prepared for the Gas Research Institute under contract no. 5087-214-1544 (GRI-91/0072), p. 97–117.

Tremain, C. M., Laubach, S. E., and Whitehead, N. H., III, 1991b, Coal fracture (cleat) patterns in Upper Cretaceous Fruitland Formation, San Juan Basin, Colorado and New Mexico—implications for coalbed methane exploration and development, *in* Schwochow, S. D., Murray, D. K., and Fahy, M. F., eds., Coalbed methane of western North America: guidebook for Rocky Mountain Association of Geologists fall conference and field trip: Rocky Mountain Association of Geologists, p. 49–59.

Tremain, C. M., Laubach, S. E., and Whitehead, N. H., III, 1994, Coal fracture (cleat) patterns in Upper Cretaceous Fruitland Formation coal seams, San Juan Basin, *in* Ayers, W. B., Jr., and Kaiser, W. R., eds., Coalbed methane in the Upper Cretaceous Fruitland Formation, San Juan Basin, New Mexico and Colorado: The University of Texas at Austin, Bureau of Economic Geology Report of Investigations No. 218, Colorado Geologic Survey, Department of Natural Resources, Resource Series 31, and New Mexico Bureau of Mines and Mineral Resources Bulletin 146, p. 87–102.

TRW, 1980, Geologic framework and potential structural control of methane in coal beds of southeastern Piceance Creek basin, Colorado: prepared by Geological Services of Tulsa, Inc., for TRW Energy Systems Group (under TRW subcontract no. J44432JJOE, DOE contract no. DE-AC-21-78MCO8089) for U.S. Department of Energy, Morgantown Energy Technology Center, 34 p.

Tweto, Ogden, 1979, Geologic map of Colorado: U.S. Geological Survey, scale 1:500,000.

Tweto, Ogden, 1980, Tectonic history of Colorado, *in* Kent, H. C., and Porter, K. W., eds., Colorado geology: summary of Laramide orogeny in Colorado: Denver, Rocky Mountain Association of Geologists Symposium, p. 129–134.

Tyler, Roger, Ambrose, W. A., Scott, A. R., and Kaiser, W. R., 1991a, Coalbed methane potential of the Greater Green River, Piceance, Powder River and Raton Basins: The University of Texas at Austin, Bureau of Economic Geology, topical report prepared for the Gas Research Institute under contract no. 5087-214-1544 (GRI-91/0315), 244 p.

Tyler, Roger, Ambrose, W. A., Scott, A. R., and Kaiser, W. R., 1992, Evaluation of the coalbed methane potential in the Greater Green River, Piceance, Powder River, and Raton Basins, *in* Mullen, C. E., ed., Rediscover the Rockies: Wyoming Geological Association, Forty-Third Field Conference Guidebook, p. 269–302.

Tyler, Roger, and Hamilton, D. S., 1994, Tectonic and stratigraphic setting and coal occurrence of the Upper Cretaceous Mesaverde Group and Lower Tertiary Fort Union Formation, Greater Green River Basin, *in* Tyler, Roger, Kaiser, W. R., Scott, A. R., Hamilton, D. S., McMurry, R. G., and Zhou, Naijiang, Geologic and hydrologic assessment of natural gas from coal seams in the Mesaverde Group and Fort Union Formation, Greater Green River Basin, Wyoming and Colorado: The University of Texas at Austin, Bureau of Economic Geology, topical report prepared for the Gas Research Institute under contract no. 5091-214-2261 (GRI-93/0320), p. 8–68.

Tyler, Roger, and McMurry, R. G., 1994, Stratigraphy and coal occurrence of the Paleocene Fort Union Formation, Sand Wash Basin, *in* Kaiser, W. R., Scott, A. R., Hamilton, D. S., Tyler, Roger, McMurry, R. G., Zhou, Naijiang, and Tremain, C. M., 1994, Geologic and hydrologic controls on coalbed methane: Sand Wash Basin, Colorado and Wyoming: The University of Texas at Austin, Bureau of Economic Geology Report of Investigations No. 220, and Colorado Geologic Survey, Department of Natural Resources, Resource Series 30, p. 79–106.

Tyler, Roger, and Tremain, C. M., 1994, Tectonic evolution, stratigraphic setting, and coal fracture patterns of the Sand Wash Basin, *in* Kaiser, W. R., Scott, A. R., Hamilton, D. S., Tyler, Roger, McMurry, R. G., Zhou, Naijiang, and Tremain, C. M., 1994, Geologic and hydrologic controls on coalbed methane: Sand Wash Basin, Colorado and Wyoming: The University of Texas at Austin, Bureau of Economic Geology Report of Investigations No. 220, and Colorado Geologic Survey, Department of Natural Resources, Resource Series 30, p. 3–19.

Tyler, Roger, Kaiser, W. R., Ambrose, W. A., Scott, A. R., Laubach, S. E., and Ayers, W. B., Jr., 1992, Coalbed methane characteristics in the foreland of the Cordilleran thrust belt, western United States, *in* Symposium on coalbed methane research and development in Australia: Australia's new energy source: Coalseam Gas Research Institute, James Cook University of New Queensland, Australia, p. 11–32.

Tyler, Roger, Kaiser, W. R., Scott, A. R., Hamilton, D. S., McMurry, R. G., and Zhou, Naijiang, 1994, Geologic and hydrologic assessment of natural gas from coal seams in the Mesaverde Group and Fort Union Formation, Greater Green River Basin, Wyoming and Colorado: The University of Texas at Austin, Bureau of Economic Geology, topical report prepared for the Gas Research Institute under contract no. 5091-214-2261 (GRI-93/0320), 120 p.

Tyler, Roger, Laubach, S. E., Ambrose, W. A., Tremain, C. M., and Grout, M. A., 1993, Coal fracture patterns in the foreland of the Cordilleran Thrust Belt, Western United States, *in* Proceedings of the 1993 International Coalbed Methane Symposium, The University of Alabama/Tuscaloosa, May 17–21, 1993, p. 695–704.

Tyler, Roger, Laubach, S. E., and Ambrose, W. A., 1991b, Effects of compaction on cleat characteristics: preliminary observations, *in* Ayers, W. B., Jr., Kaiser, W. R., Laubach, S. E., Ambrose, W. A., Baumgardner, R. W., Jr., Scott, A. R., Tyler, R., Yeh, Joseph, Hawkins,

G. J., Swartz, T. E., Schultz-Ela, D. D., Zellers, S. D., Tremain, C. M., and Whitehead, N. H., III, eds., Geologic and hydrologic controls on the occurrence and producibility of coalbed methane, Fruitland Formation, San Juan Basin: The University of Texas at Austin, Bureau of Economic Geology, topical report prepared for the Gas Research Institute under contract no. 5087-214-1544 (GRI-91/0072), p. 141–152.

Vail, P. R., 1987, Seismic stratigraphy interpretation procedure, part 1, *in* Bally, A. W., ed., Atlas of seismic stratigraphy: American Association of Petroleum Geologists Studies in Geology No. 27, v. 1, p. 1–10.

Verbeek, E. R., and Grout, M. A., 1983, Fracture history of the northern Piceance Creek Basin, northwestern Colorado, *in* Gary, J. H., ed., Proceedings, 16th Oil Shale Symposium, p. 29–44.

Verbeek, E. R., and Grout, M. A., 1984a, Fracture studies in Cretaceous and Paleocene strata in and around the Piceance Basin, Colorado: Preliminary results and their bearing on a fracture-controlled natural-gas reservoir at the MWX site: U.S. Geological Survey Open-File Report 84-156, 32 p.

Verbeek, E. R., and Grout, M. A., 1984b, Prediction of subsurface fracture patterns from surface studies of joints—an example from the Piceance Creek Basin, Colorado, *in* Spencer, C. W., and Keighin, C. W., eds., Geological studies in support of the U.S. Department of Energy multiwell experiment, Garfield County, Colorado: U.S. Geological Survey Open-File Report 84-757, p. 84–757.

Verbeek, E. R., and Grout, M. A., 1986, Cenozoic stress rotation, northeastern Colorado Plateau, *in* Stone, D. S., and Johnson, K. S., eds., New interpretations of northwest Colorado geology: Denver, Rocky Mountain Association of Geologists, p. 97.

Vistelius, A. B., 1966, Structural diagrams: New York, Pergamon, 178 p.

Waechter, N. B., and De Voto, R. H., 1989, Tectonic-stratigraphic framework and petroleum potential of the Late Paleozoic central Colorado Trough, northwestern Colorado, *in* Lorenz, J. C., and Lucas, S. G., eds., 1989, Energy frontiers in the Rockies: Companion volume for the 1989 meeting of the Rocky Mountain Section of the American Association of Petroleum Geologists, Albuquerque Geological Society, p. 91–100.

Warner, D. L., 1964, Stratigraphy of Mancos-Mesaverde (Upper Cretaceous) intertonguing relations, southeast Piceance Basin, Colorado: American Association of Petroleum Geologists Bulletin, v. 48, no. 7, p. 1091–1107.

Warpinski, N. R., 1986, Elastic and viscoelastic calculations of stresses in sedimentary basins: Society of Petroleum Engineers, SPE paper 15243, p. 409–417.

Warpinski, N. R., 1989, Elastic and viscoelastic calculations of stresses in sedimentary basins: Society of Petroleum Engineers–Formation Evaluation, v. 4, p. 522-530.

Warpinski, N. R., and Teufel, L. W., 1987, In situ stress in low-permeability, nonmarine rocks: Society of Petroleum Engineers, SPE paper 16402, p. 125–138.

Weimer, R. J., 1960, Upper Cretaceous stratigraphy, Rocky Mountain area: American Association of Petroleum Geologists Bulletin, v. 44, no. 1, p. 1–20.

Welder, F. A., 1970, Map showing joint patterns inferred from aerial photographs (unpublished map—U. S. Geological Survey), scale 1:25,000.

Wood, G. H., Jr., and Bour, W. V., III, 1988, Coal map of North America: U.S. Geological Survey Special Geologic Map, scale 1:500,000.

Wolff, R. G., Bredehoeft, J. D., Keys, W. S., and Shuter, E., 1974, Tectonic stress determinations, northern Piceance Creek Basin, Colorado, *in* Murray, D. K., ed., 1974, Energy resources of the Piceance Creek Basin, Colorado: Twenty-Fifth Field Conference 1974, Rocky Mountain Association of Geologists, Denver, Colorado, p. 193–198.

Wong, I. G., and Humphrey, J. R., 1989, Contemporary seismicity, faulting, and the state of stress in the Colorado Plateau: Geological Society of America Bulletin, v. 101, p. 1127–1146.

Young, R. G., 1955, Sedimentary facies and intertonguing in the Upper Cretaceous of the Book Cliffs, Utah–Colorado: Geological Society of America Bulletin, v. 66, no. 2, p. 177–202.

Young, R. G., 1966, Stratigraphy of coal-bearing rocks of the Book Cliffs, Utah–Colorado: Utah Geological and Mineralogical Survey Bulletin 80, p. 7–20.

Zapp, A. D., and Cobban, W. A., 1960, Some Late Creatceous strand lines in northwestern Colorado and northeastern Utah: U.S. Geological Survey Professional Paper 400-B, p. B246–B249.

Zoback, M. L., and Zoback, M. D., 1980, State of stress in the conterminous United States: Journal of Geophysical Research, v. 85, no. B11, p. 6113–6156.

Zoback, M. L., and Zoback, M. D., 1989, Tectonic stress field of the continental United States, *in* Pakiser, L. C., and Mooney, W. D., Geophysical framework of the continental United States: Geological Society of America Memoir 172, p. 523–539.